RESEARCH & REVIEWS IN SCIENCE AND MATHEMATICS - II

DECEMBER, 2021

EDITORS

PROF. DR. HASAN AKGÜL
PROF. DR. AHMET AKSOY

Research & Reviews in Science and Mathematics - II

December, 2021

Editors

Prof. Dr. Hasan AKGÜL
Prof. Dr. Ahmet AKSOY

CONTENTS

Chapter 1

APPLICATION OF DİJKSTRA ALGORITHM WITH SEQUENCE F_m IN $F_{u,N}$

İbrahim GÖKCAN[1]

1 Dr., Artvin Çoruh University, ORCID: 0000-0002-6933-8494, gokcan@artvin.edu.tr.

INTRODUCTION

The subjects studied on Euclidean geometry had the chance to be studied in many different fields with the discovery of non-Euclidean geometries. In recent years, there has been an increasing amount of literature on Graph theory. These studies have provided important advances in science,both in theory and in practice.

Algorithms underlying computer and network technology are of increasing importance. Problems that took a long time to solve in previously can be solved in a very short time thanks to algorithms. The search for algorithms that provide solutions for different problems and the process of developing previously obtained algorithms are continuous. In this study, the algorithm defined by Dijkstra (1959) was examined. Dijkstra's algorithm focused on two main problems. The first of these is to obtain the minimum length between two points in a graph, and the second is to obtain the minimum length tree.

In this study, the graph theory defined on hyperbolic geometry was examined. An example of graph was studied by examining the Dijkstra algorithm. The minimum number of steps to the vertices was obtained with the help of continued fractions by Jones etc (1991).Unlike this, in my doctoral thesis, which I submitted in 2021, I studied the Dijkstra algorithm in Farey graphs consisting of a finite number of elements, and associated the minimum number of edges to the vertices with the number of steps. In this thesis, I proposed a work with related obtaining minimum number of steps to vertices of F_m of defined in $F_{u,N}$ under Dijkstra algorithm. Accordingly,the aim of this article is to explore the minimum number of steps to the vertices and a graph tree formed by the elements of the generalized Fm sequence, starting from the ∞ vertex in $F_{u,N}$ with the help of Dijkstra's algorithm, which gives the minimum length between two points.

Definition 1. A simple graph is a graph that consists of vertices and the edges connecting these vertices and does not give any geometrical information.

Definition 2. The element located at both ends of an edge is called a vertex.

Definiton 3. The element between two vertices in a graph is called an edge.

Definition 4. Graphs whose edges contain direction information are called directional graphs. All or none of the edges in a graph have direction information.

Definition 5. The sum of the edges to be traced in a graph while going from one vertex to another is called a path. If the graph is simple, the total path is equal to the number of edges traversed.

Definition 6. A path that starts from a vertex and returns to the same vertex and does not pass through a vertex twice is called a loop. In a graph, if the number of edges is equal to the number of vertices or the number of edges is more than the number of vertices, there is at least one loop in the graph.

Definition 7. A graph without loops is called a tree. If an edge is added to this graph, a loop occurs and the number of edges in the graph is one less than the number of vertices.

Definition 8. A graph that is not connected and does not contain loops is called a forest. A forest is made up of trees, and a tree by itself is a forest.

Definition 9. In a graph, the edges can take values and these values are included in the graph's structure. Graphs in which all edges have different values are called cost graphs. The sum of all values in a cost graph gives the graph's total cost. Graphs where all edges have equal value are considered as simple graphs.

Definition 10. After calculating the least cost path (tree) for any vertex in a graph, the sum of the costs on the path gives the total cost of the tree. It is more central, which costs less than the two

vertices. The least costly vertex in a graph is called the central vertex of the graph.

Definition 11. A tree that covers all the vertices in a graph is called a spanning tree.

Examining of Modular Group, $G_{u,N}$ and $F_{u,N}$

In hyperbolic geometry, starting from ∞, the values taken in $\bar{\mathbb{R}} = \mathbb{R} \cup \{\mp\infty\}$ are vertices; Hyperbolic geodesics, consisting of lines perpendicular to $\bar{\mathbb{R}}$ between vertices and semi-circles with a center on R, are the elements of graph theory as edges. Schoeneberg (1974), Ratcliffe (1994) and Anderson (2005) can be examined for applications of Graph theory in Hyperbolic plane .

The act of G in Ω, orbits of G, definitions of vertex and edge were first introduced in Sims [13],and then included in studies of Neumann (1977) and Tsukuzu (1979) for finite groups.

In later studies, Γ- Modular group is taken as G and $\widehat{\mathbb{Q}}$ is taken as Ω. Then act of Γ- Modular group on $\widehat{\mathbb{Q}}$ is examined. The Modular group and its equivalent subgroups, which have an important place in Fermat's last theorem, which he proved in 1639, have been studied extensively in the literature. Elements of Modular group are known for Mobiüs transforms. Modular group is defined as follows:

$$\Gamma = PSL(2,\mathbb{Z}) \cong {SL(2,\mathbb{Z})}\Big/{\{\mp I\}}$$

$$= \left\{ \mp \begin{pmatrix} a & b \\ c & d \end{pmatrix} | a, b, c, d \in \mathbb{Z} \, vead - bc = 1 \right\}.$$

Biggs and White (1979) and Jones vd.(1991) can be examined for more detailed information.

The movement of Γ on $\widehat{\mathbb{Q}}$ is transitive, so for $v \in \widehat{\mathbb{Q}}$, each suborbit contains the (∞, v) pair. If $v = \frac{u}{N}$ for $N \geq 0$ and (u,N)=1, this suborbital is denoted by $O_{u,N}$ and the suborbital graph $G(\infty, v)$ corresponding to the suborbital is also denoted by $G_{u,N}$. $F_{u,N}$ is the

subgraph of $G_{u,N}$ consisting of the $[\infty] = \left\{ x, y \in \widehat{\mathbb{Q}} \mid y \equiv 0 \ (mod \ N) \right\}$ block whose vertices contain ∞. $G_{u,N}$ consists of $F_{u,N}$ discrete copies. Jones et al. (1991) showed that for two vertices defined in $F_{u,N}$ to be neighbors, they must satisfy the "$\frac{r}{s} \rightarrow \frac{x}{y} \in F_{u,N} \Leftrightarrow$ i) $x \equiv ur \ (mod \ N)$ and $ry - sx = N$, ii)$x \equiv -ur \ (mod \ N)$ and $ry - sx = -N$" condition. Sims (1967), Jones et al. (1991) and Akbaş (2001) can be given for $F_{u,N}$ and releated studies as references.

Farey Diagram

The related diagram is called Farey diagram because of its relationship with Farey sequences. To draw a Farey diagram, a diameter is first drawn on an empty circle. Four curved triangles are drawn with one vertex common to this diameter. Then, eight curved triangles are drawn, with one vertex of the four in common with the diameter. Continuing in this way, an infinite number of curved triangles are drawn, gradually approaching the circle. The vertices at the top of the diagram are positive, and the vertices at the bottom are negative. The symmetry of a vertex in the upper half-plane is its inverse negative. In the Farey diagram, the vertex between two vertices is found with the median. Median is $\frac{r}{s} \oplus \frac{x}{y} = \frac{r+x}{s+y}$, where $\frac{r}{s}$ and $\frac{x}{y}$ are two vertices in Farey diagram. Farey sequences with vertices $\frac{0}{1}$ and $\frac{1}{1}$ are as follows:

$$F_1 = \left\{ \frac{0}{1}, \frac{1}{1} \right\}, F_2 = \left\{ \frac{0}{1}, \frac{1}{2}, \frac{1}{1} \right\}, F_3 = \left\{ \frac{0}{1}, \frac{1}{3}, \frac{1}{2}, \frac{2}{3}, \frac{1}{1} \right\}, F_4$$
$$= \left\{ \frac{0}{1}, \frac{1}{4}, \frac{1}{3}, \frac{2}{5}, \frac{1}{2}, \frac{3}{5}, \frac{2}{3}, \frac{3}{4}, \frac{1}{1} \right\}, \dots$$

Dijkstra Algorithm

Today, thanks to computer technology, many events that took a long time in the past take place in a very short time and our life becomes easier. Computers can store large amounts of information in an organized manner, and can calculate a problem that would

take a long time to solve with paper and pen in a very short time. The combination of internet technology and computer technology has offered many different fields and has been put at the disposal of humanity. For example, the presence of an e-mail system is an important stage in communication, and social media is also an important stage in communication. The fact that scientists working in different fields have the opportunity to have access to the online resources at libraries, and the online access to the journals and books which the studies are published in has brought along a tremendous speed of information production. However, the fact that should not be forgotten is that algorithms are the basis of all computer technologies and programs that provide these conveniences. Algorithms are chains of commands defined to computers. Algorithms are not the solution to a particular problem, but the way to that solution. The search for algorithms for different problems continues. In addition to this, algorithm studies are also continuing in order for an improved algorithm to give a shorter and clearer solution. Ahuja et al.(1993), Dreyfus (1969) and Ruohonen (2008) can be given as references for further information.

Dijkstra (1959) and Whiting and Hillier (1960)have worked on calculating the minimum length between two points through algorithms. The algorithm to be used differs depending on whether the edges of the graph are positively or negatively charged. For example, Dijkstra's algorithm does not work on negatively charged graphs, in such cases it is necessary to work with algorithms such as Bellman-Ford or Floyd. In this study, the Dijkstra algorithm which is one of the algorithms that gives the minimum path to the vertices defined in the graph,starting from any source point will be used. Dijkstra algorithm was defined by Edger Dijkstra (1959). In this study, Dijkstra focused on two problems. These find the minimum length between two points in the graph, and the other obtains the minimum length tree in a given graph.

Dijkstra's algorithm basically has temporary and permanent labels. The algorithm starts working from a source vertex. The value of the source vertex is taken as 0, since a path is not required to go to the

first vertex, the source vertex. Let assume that one of the second vertices neighboring the source vertex is visited. The length value between two neighboring vertices is assigned as the value for the second vertex. For other situations, the sum of minimum value of previous vertex and the length between the neighboring vertices is assigned as value of next vertex. For $i \in \mathbb{N}$, let α_i be the vertices, $\gamma(\alpha_i)$ the minimum values assigned to the corresponding vertices, and $\beta(\alpha_i, \alpha_{i+1})$ the length between the two neighboring vertices. From here, $\gamma(\alpha_1) = 0$ and $\gamma(\alpha_2) = \gamma(\alpha_1) + \beta(\alpha_1, \alpha_2)$. Similarly, $\gamma(\alpha_3) = \gamma(\alpha_2) + \beta(\alpha_2, \alpha_3)$. More generally, $\gamma(\alpha_{i+1}) = \gamma(\alpha_i) + \beta(\alpha_i, \alpha_{i+1})$ can be obtained. With the help of Dijkstra's algorithm, the previously valued vertex can be reached again in calculating the minimum length for the vertices. In this case, a comparison is made between the newly found value and the previously found value. The smaller value is assigned as the value of the vertex.

Dijkstra's algorithm basically has temporary and permanent labels. The algorithm starts working from a source vertex. The value of the source vertex is taken as 0, since a path is not required to go to the first vertex, the source vertex. Let's assume that one of the second vertices adjacent to the source vertex is visited. The length value between two adjacent vertices is assigned as the value for the second vertex. For $i \in \mathbb{N}$, let α_i be the vertices, $\gamma(\alpha_i)$ the minimum values assigned to the corresponding vertices, and $\beta(\alpha_i, \alpha_{i+1})$ the length between the two vertices. From here, $\gamma(\alpha_1) = 0$ and $\gamma(\alpha_2) = \gamma(\alpha_1) + \beta(\alpha_1, \alpha_2)$. Similarly, $\gamma(\alpha_3) = \gamma(\alpha_2) + \beta(\alpha_2, \alpha_3)$. More generally, $\gamma(\alpha_{i+1}) = \gamma(\alpha_i) + \beta(\alpha_i, \alpha_{i+1})$ can be obtained. With the help of Dijkstra's algorithm, the previously valued vertex can be reached again in calculating the minimum length for the vertices. In this case, a comparison is made between the newly found value and the previously found value. The smaller value is assigned as the value of the vertex.

The flow chart of Dijkstra's algorithm is given.

Let $\beta(\alpha_{j-1}, \alpha_j)$ be the length of the (α_{j-1}, α_j) edge. Dijkstra's algorithm labels vertices temporarily or permanently.

$$\omega(\alpha_{j-1}) = \begin{cases} 1, & \text{Permanent Label} \\ 0, & \text{Temporarily Label} \end{cases}$$

where $\gamma(\alpha_{j-1})$ is value of α_{j-1} vertex. Temporary $\gamma(\alpha_{j-1})$ values are taken as ∞, where $\gamma(\alpha_{j-1})$ is permanent label that the smallest value of length $\alpha_{j-2} - \alpha_{j-1}$. Let the premise of α_j be

$$\vartheta(\alpha_{j-1}) = \begin{cases} \text{If any} \\ 0, & \text{Or} \end{cases}$$

on the least-valued path of length $\alpha_{j-2} - \alpha_{j-1}$.

The steps of the algorithm are implemented as follows:

For α_i source vertex,

1. Step: $\gamma(\alpha_{j-2}) \to 0$ and $\omega(\alpha_{j-2}) = 1$. For other vertices $\alpha_{j-1}, \gamma(\alpha_j) \to \infty$. For all vertices $\alpha_{j-1}, \vartheta(\alpha_j) \to 0$. Additionally $\alpha_{j-2} \to \alpha_{j-3}$.

2. Step: Let $(\alpha_{j-1}) > \gamma(\alpha_{j-3}) + \beta(\alpha_{j-3}, \alpha_{j-1})$ and $\gamma(\alpha_{j-1}) = 0$ for $\forall(\alpha_{j-3}, \alpha_{j-1})$ length. So, $\gamma(\alpha_{j-3}) + \beta(\alpha_{j-3}, \alpha_{j-1}) \to \gamma(\alpha_{j-1})$, $\vartheta(\alpha_{j-1}) \to \alpha_{j-3}$.

3. Step: Let's find α_{j-1}^* to be $\omega(\alpha_{j-1}^*) = 0$, $\gamma(\alpha_{j-1}^*) < \infty$ and $\gamma(\alpha_{j-1}^*) = \min_{\omega(\alpha_{j-1})=0}\{\gamma(\alpha_{j-1})\}$. Then $\gamma(\alpha_{j-1}^*) \to 1$ ve $\alpha_{j-1}^* \to w$ olur.

If there is no such vertex α_{j-1}^*, there is no directional length $\alpha_{j-2} - \alpha_{j-4}$ and the algorithm stops.

4. Step: If $\alpha_{j-3} \neq \alpha_{j-4}$, go to 2. step.

5. Step: Stop(Ruohonen, 2008).

An example of applying this algorithm on a suborbital graph is given below. In this example, the edges are taken as unloaded, the length between the two vertices is matched to the number of steps. As given in (Gökcan, 2021), let's find the minimum number of steps between two points and obtain the tree graph in the Farey graph given below.
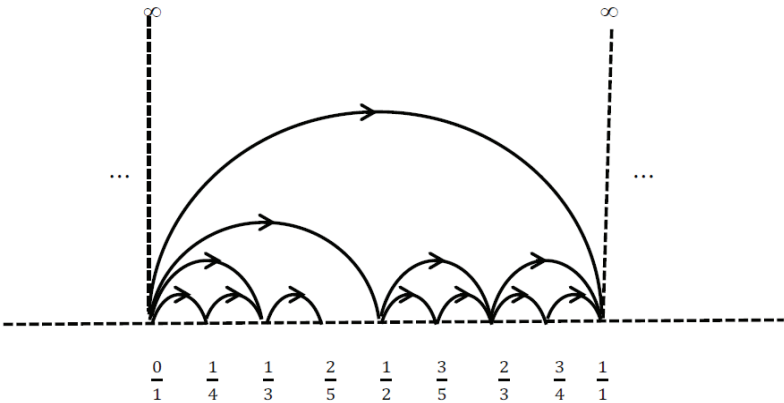
Figure 1: Farey sequence graph

Firstly, we take ∞ as source vertex.

1.Step:Since the source vertex is taken as ∞ and no steps are required to go to the ∞ vertex, the step number of the ∞ vertex is 0, and the others are uncertain, so other vertices take the value ∞.

Vertex	∞	$\frac{0}{1}$	$\frac{1}{4}$	$\frac{1}{3}$	$\frac{2}{5}$	$\frac{1}{2}$	$\frac{3}{5}$	$\frac{2}{3}$	$\frac{3}{4}$	$\frac{1}{1}$
Number of Steps	0	∞	∞	∞	∞	∞	∞	∞	∞	∞

Table 1. Table of the number of steps of 1. step

2. Step: The only vertex that can be reached from the ∞ vertex is $\frac{0}{1}$. Then, number of step of $\frac{0}{1}$ vertex is 1. Other verties take the value of ∞ since the others are indefinite.

Vertex	∞	$\frac{0}{1}$	$\frac{1}{4}$	$\frac{1}{3}$	$\frac{2}{5}$	$\frac{1}{2}$	$\frac{3}{5}$	$\frac{2}{3}$	$\frac{3}{4}$	$\frac{1}{1}$
Number of Steps	0	1	∞	∞	∞	∞	∞	∞	∞	∞

Table 2. Table of the number of steps of 2. step

3.Step:The vertices that can be reached from the $\frac{0}{1}$ vertex are $\frac{1}{4}, \frac{1}{3}, \frac{1}{2}$ and $\frac{1}{1}$. Then, the number of steps of these vertices is 2, and the others are uncertain, so they take the value of ∞.

Vertex	∞	$\frac{0}{1}$	$\frac{1}{4}$	$\frac{1}{3}$	$\frac{2}{5}$	$\frac{1}{2}$	$\frac{3}{5}$	$\frac{2}{3}$	$\frac{3}{4}$	$\frac{1}{1}$
umber of Steps	0	1	2	2	∞	2	∞	∞	∞	2

Table 3. Table of the number of steps of 3. step

4.Step:Let assume that we went from the $\frac{0}{1}$ vertex to the $\frac{1}{4}$ vertex. The only vertex that can be reached from the $\frac{1}{4}$ vertex is $\frac{1}{3}$. So, number of steps of $\frac{1}{3}$ vertex is 3. In this case, the number of steps of the $\frac{1}{3}$ vertex increases, so there is no change in the number of steps.

Vertex	∞	$\frac{0}{1}$	$\frac{1}{4}$	$\frac{1}{3}$	$\frac{2}{5}$	$\frac{1}{2}$	$\frac{3}{5}$	$\frac{2}{3}$	$\frac{3}{4}$	$\frac{1}{1}$
umber of Steps	0	1	2	2	∞	2	∞	∞	∞	2

Table 4. Table of the number of steps of 4. step

5.Step:Let assume that we went from the $\frac{1}{4}$ vertex to the $\frac{1}{3}$ vertex. The only vertex that can be reached from the $\frac{1}{3}$ vertex is $\frac{2}{5}$. So, number of steps of $\frac{2}{5}$ vertex is 3.

Vertex	∞	$\frac{0}{1}$	$\frac{1}{4}$	$\frac{1}{3}$	$\frac{2}{5}$	$\frac{1}{2}$	$\frac{3}{5}$	$\frac{2}{3}$	$\frac{3}{4}$	$\frac{1}{1}$
umber of Steps	0	1	2	2	3	2	∞	∞	∞	2

Table 5. Table of the number of steps of 5. step

6.Step:Let assume that we went from the $\frac{0}{1}$ vertex to the $\frac{1}{2}$ vertex. $\frac{3}{5}$ and $\frac{2}{3}$ vertices can be reached from $\frac{1}{2}$ vertex. In this case, number of steps of $\frac{3}{5}$ and $\frac{2}{3}$ is 3.

Vertex	∞	$\frac{0}{1}$	$\frac{1}{4}$	$\frac{1}{3}$	$\frac{2}{5}$	$\frac{1}{2}$	$\frac{3}{5}$	$\frac{2}{3}$	$\frac{3}{4}$	$\frac{1}{1}$
umber of Steps	0	1	2	2	3	2	3	3	∞	2

Table 6. Table of the number of steps of 6. step

7.Step:Let assume that we went from the $\frac{1}{2}$ vertex to the $\frac{3}{5}$ vertex. The only vertex that can be reached from the $\frac{3}{5}$ vertex is $\frac{2}{3}$. So, number of steps of $\frac{2}{3}$ vertex is 4. In this case, the number of steps of the $\frac{2}{3}$ vertex increases, so there is no change in the number of steps.

Vertex	∞	$\frac{0}{1}$	$\frac{1}{4}$	$\frac{1}{3}$	$\frac{2}{5}$	$\frac{1}{2}$	$\frac{3}{5}$	$\frac{2}{3}$	$\frac{3}{4}$	$\frac{1}{1}$
umber of Steps	0	1	2	2	3	2	3	3	∞	2

Table 7. Table of the number of steps of 7. step

8.Step:Let assume that we went from the $\frac{1}{2}$ vertex to the $\frac{2}{3}$ vertex. $\frac{3}{4}$ and $\frac{1}{1}$ vertices are reached from $\frac{2}{3}$ vertex. Then, number of steps of $\frac{3}{4}$ and $\frac{1}{1}$ vertices are 4. So, the number of steps of the $\frac{1}{1}$ vertex increases, so there is no change in the number of steps.

Vertex	∞	$\frac{0}{1}$	$\frac{1}{4}$	$\frac{1}{3}$	$\frac{2}{5}$	$\frac{1}{2}$	$\frac{3}{5}$	$\frac{2}{3}$	$\frac{3}{4}$	$\frac{1}{1}$
Number of Steps	0	1	2	2	3	2	3	3	4	2

Table 8. Table of the number of steps of 8. step

9.Step:: Let assume that we went from the $\frac{2}{3}$ vertex to the $\frac{3}{4}$ vertex. The only vertex that can be reached from the $\frac{3}{4}$ vertex is $\frac{1}{1}$. Then, number of steps of $\frac{1}{1}$ vertex are 5. So, the number of steps of the $\frac{1}{1}$ vertex increases, so there is no change in the number of steps.

Vertex	∞	$\frac{0}{1}$	$\frac{1}{4}$	$\frac{1}{3}$	$\frac{2}{5}$	$\frac{1}{2}$	$\frac{3}{5}$	$\frac{2}{3}$	$\frac{3}{4}$	$\frac{1}{1}$
Number of Steps	0	1	2	2	3	2	3	3	4	2

Table 9. Table of the number of steps of 9. step

From here, the tree graph is obtained as follows.
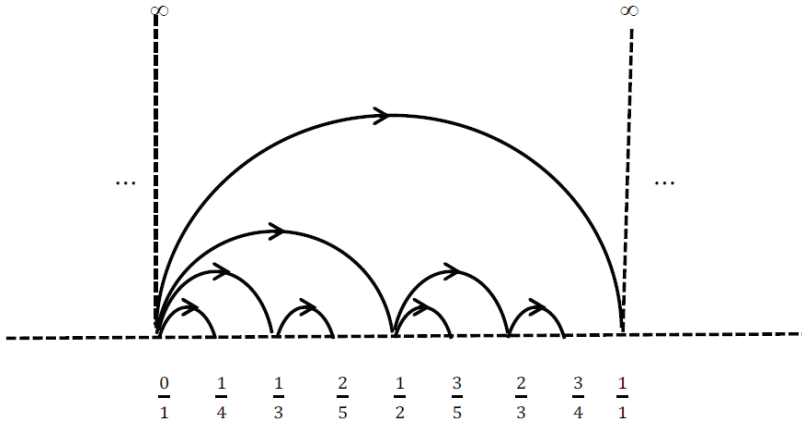
Figure 2: Farey sequence tree graph

Obtaining Number of Minimum Steps with Help of Dijkstra Algortihm with F_m Sequence in $F_{u,N}$

Let $\frac{r}{s}$ and $\frac{x}{y}$ be two consecutive vertices with neighboring vertex conditions in $F_{u,N}$. Farey sequences with vertices $\frac{r}{s}$ and $\frac{x}{y}$ are as follows:

$$F_1 = \left\{ \frac{r}{s}, \frac{x}{y} \right\}$$

$$F_2 = \left\{ \frac{r}{s}, \frac{r+x}{s+y}, \frac{x}{y} \right\}$$

$$F_3 = \left\{ \frac{r}{s}, \frac{2r+x}{2s+y}, \frac{r+x}{s+y}, \frac{r+2x}{s+2y}, \frac{x}{y} \right\}$$

$$F_4$$
$$= \left\{ \frac{r}{s}, \frac{3r+x}{3s+y}, \frac{2r+x}{2s+y}, \frac{3r+2x}{3s+2y}, \frac{r+x}{s+y}, \frac{2r+3x}{2s+3y}, \frac{r+2x}{s+2y}, \frac{r+3x}{s+3y}, \frac{x}{y} \right\}$$

$$\vdots$$

Similarly, using the median, the sequence F_m is obtained. Number of steps for F_4 were found in the Farey graph example below. Attempts were made to generalize numbers of step for F_m.
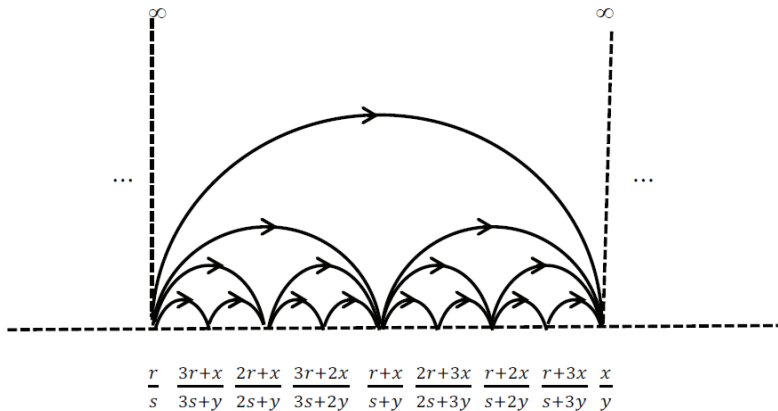
Figure 3: Farey sequence F_4 graph

The edges, vertices and median values given in the Farey graph F_4 are given in the table below for convenience in the next parts of our study.

Name of Hyperbolic Line	Starting Vertex	End Vertex	Median Value
D_1	$\dfrac{r}{s}$	$\dfrac{x}{y}$	$\dfrac{r+x}{s+y}$
D_2	$\dfrac{r}{s}$	$\dfrac{r+x}{s+y}$	$\dfrac{2r+x}{2s+y}$
D_3	$\dfrac{r+x}{s+y}$	$\dfrac{x}{y}$	$\dfrac{r+2x}{s+2y}$
D_4	$\dfrac{r}{s}$	$\dfrac{2r+x}{2s+y}$	$\dfrac{3r+x}{3s+y}$
D_5	$\dfrac{2r+x}{2s+y}$	$\dfrac{r+x}{s+y}$	$\dfrac{3r+2x}{3s+2y}$
D_6	$\dfrac{r+x}{s+y}$	$\dfrac{r+2x}{s+2y}$	$\dfrac{2r+3x}{2s+3y}$
D_7	$\dfrac{r+2x}{s+2y}$	$\dfrac{x}{y}$	$\dfrac{r+3x}{s+3y}$
D_8	$\dfrac{r}{s}$	$\dfrac{3r+x}{3s+y}$	$\dfrac{4r+x}{4s+y}$
D_9	$\dfrac{3r+x}{3s+y}$	$\dfrac{2r+x}{2s+y}$	$\dfrac{5r+2x}{5s+2y}$
D_{10}	$\dfrac{2r+x}{2s+y}$	$\dfrac{3r+2x}{3s+2y}$	$\dfrac{5r+3x}{5s+3y}$
D_{11}	$\dfrac{3r+2x}{3s+2y}$	$\dfrac{r+x}{s+y}$	$\dfrac{4r+3x}{4s+3y}$
D_{12}	$\dfrac{r+x}{s+y}$	$\dfrac{2r+3x}{2s+3y}$	$\dfrac{3r+4x}{3s+4y}$
D_{13}	$\dfrac{2r+3x}{2s+3y}$	$\dfrac{r+2x}{s+2y}$	$\dfrac{3r+5x}{3s+5y}$
D_{14}	$\dfrac{r+2x}{s+2y}$	$\dfrac{r+3x}{s+3y}$	$\dfrac{2r+5x}{2s+5y}$
D_{15}	$\dfrac{r+3x}{s+3y}$	$\dfrac{x}{y}$	$\dfrac{r+4x}{s+4y}$

Table 10. Edge names of F_4 Farey graph

Now let's apply Dijkstra's algorithm to $F_{u,N}$. ∞ is a vertex in $F_{u,N}$ and vertices are orbital of ∞. Let the elements of the Farey sequences F_4 on $\bar{\mathbb{Q}}$ and the vertex ∞ be taken as vertices. In addition, let edges between two vertices be taken as steps. ∞ is taken as source vertex. Since no steps are required to go to the ∞ vertex, the step number of the ∞ vertex is 0, and the others are uncertain, so other vertices take the value ∞. Then, number of step of $\frac{r}{s}$ vertex is 1.

However, number of steps of all vertices that neigbour $\frac{r}{s}$ is 2. Among the vertices with 2 steps, the farthest vertex from the $\frac{r}{s}$ vertex is $\frac{x}{y}$. With the help of the median, an infinite number of vertices with two steps can be obtained approaching to $\frac{r}{s}$ vertex. Vertices can be arranged as follows for $n \in \mathbb{N}$. The order of the vertices is not random, but according to the order of placement in the Farey graph.

$$\ldots, \frac{nr + x}{ns + y}, \frac{(n-1)r + x}{(n-1)s + y}, \ldots, \frac{3r + x}{3s + y}, \frac{2r + x}{2s + y}, \frac{r + x}{s + y}, \frac{x}{y}$$

All vertices satisfying the neighbor vertex condition in $F_{u,N}$ with vertices with 2 steps have 3 steps. In finding the biggest vertex with 3 steps, $\frac{x}{y}$ vertex with 2 steps is not taken into account since the graph is unidirectional and limited between $\frac{r}{s}$ and $\frac{x}{y}$ vertices. After $\frac{x}{y}$ vertex, the biggest vertex with 2 steps is $\frac{r+x}{s+y}$. So, median of $\frac{r+x}{s+y}$ and $\frac{x}{y}$ is the biggest vertex with 3 steps. Value of this vertex is $\frac{r+x}{s+y} \oplus \frac{x}{y} = \frac{r+2x}{s+2y}$. The vertex with the next step number 3 is the median of $\frac{r+x}{s+y}$ and $\frac{r+2x}{s+2y}$. This vertex is $\frac{r+x}{s+y} \oplus \frac{r+2x}{s+2y} = \frac{2r+3x}{2s+3y}$. Accordingly, median of each new value found with $\frac{r+x}{s+y}$ gives the vertices with step number of 3, and there are infinite vertices approaching the $\frac{r+x}{s+y}$ vertex. To generalize the vertex value, for $n \in \mathbb{N}$, consider the $\frac{(n-1)r+nx}{(n-1)s+ny}$ vertex as a vertex with 3 steps and

approaching the $\frac{r+x}{s+y}$ vertex. $\frac{r+x}{s+y} \oplus \frac{(n-1)r+nx}{(n-1)s+ny} = \frac{nr+(n+1)x}{ns+(n+1)y}$ is obtained from medians of vertices. In that case, between vertices with 3 steps $\frac{r+x}{s+y}$ vertex with 2 steps and $\frac{r+2x}{s+2y}$ vertex with 3 steps are be arranged as follows for $n \in \mathbb{N}$.

$$\dots, \frac{nr+(n+1)x}{ns+(n+1)y}, \frac{(n-1)r+nx}{(n-1)s+ny}, \dots, \frac{2r+3x}{2s+3y}, \frac{r+2x}{s+2y}$$

Only vertices with 3 steps between $\frac{r+x}{s+y}$ and $\frac{x}{y}$ were found here. Similarly, there can be an infinite number of vertices with 3 steps between all vertices with 2 steps and the vertices satisfying the neighboring vertex condition in $F_{u,N}$. With vertices with 3 steps, the number of steps of all vertices satisfying the neighboring vertex condition in $F_{u,N}$ is 4. Median of $\frac{r+2x}{s+2y}$ and $\frac{x}{y}$ is the biggest vertex that with 4 steps. Value of this vertex is $\frac{r+2x}{s+2y} \oplus \frac{r+3x}{s+3y} = \frac{2r+5x}{2s+5y}$. From here, the next vertex with step number 4 is the median of $\frac{r+2x}{s+2y}$ and $\frac{r+3x}{s+3y}$. This vertex is $\frac{r+2x}{s+2y} \oplus \frac{x}{y} = \frac{r+3x}{s+3y}$. Consequently, median of each new value found with $\frac{r+2x}{s+2y}$ gives the vertices with 4 steps, and there is an infinite number of vertices approaching the $\frac{r+2x}{s+2y}$ vertex. To generalize the vertex value, for $n \in \mathbb{N}$, consider the $\frac{nr+(2n+1)x}{ns+(2n+1)y}$ vertex as a vertex with 4 steps and approaching the $\frac{r+2x}{s+2y}$ vertex. $\frac{r+2x}{s+2y} \oplus \frac{nr+(2n+1)x}{ns+(2n+1)y} = \frac{(n+1)r+(2n+3)x}{(n+1)s+(2n+3)y}$ are obtained from medians of vertices. Then, vertices between $\frac{r+2x}{s+2y}$ vertex that 3 steps and $\frac{r+3x}{s+3y}$ vertex that 4 steps are arranged as follows for $n \in \mathbb{N}$.

$$\dots, \frac{(n+1)r+(2n+3)x}{(n+1)s+(2n+3)y}, \frac{nr+(2n+1)x}{ns+(2n+1)y}, \dots, \frac{2r+5x}{2s+5y}, \frac{r+3x}{s+3y}$$

Only vertices with 4 steps between $\frac{r+3x}{s+3y}$ and $\frac{r+2x}{s+2y}$ are found here. Similarly, there can be an infinite number of vertices with 4 steps

between all vertices with 3 steps and the vertices satisfying the neighboring vertex condition in $F_{u,N}$.

With the help of the information given above, there can be an infinite number of vertices with 5 steps between all vertices with 4 steps and the vertices satisfying the neighboring vertex condition in $F_{u,N}$.

Let's generalize the situation by continuing in a similar way. For $m, n \in \mathbb{N}$, if number of steps of vertex α_m is t, number of steps of vertex α_n satisfying the neighboring vertex condition in $F_{u,N}$ is $t + 1$.

The number of steps of any vertex is the minimum number of steps that can be reached, starting from the ∞ vertex. Any vertex in the Farey graph can be reached in different ways than the one that gives the minimum number of steps. However, this increases the number of steps. It contradicts the concept of minimum principle of Dijkstra's algorithm. For example, edge D_1 connects $\frac{r}{s}$ to $\frac{x}{y}$. Using the other edges, $\frac{r}{s}$ to $\frac{x}{y}$ can be achieved, but the number of steps increases. The number of steps of the vertices found with the median rule between the vertices that can be reached with the minimum number of steps and the neighboring vertices is 1 more than the previous vertices. Connecting two neighboring vertices using the median increases the number of steps. As a result, the edges connecting the median to the next vertex according to the direction of the graph are not taken into account in the Dijkstra algorithm. For example, the minimum number of steps of vertex $\frac{x}{y}$ with D_1 edge is 2. However, if $\frac{r}{s}$ and $\frac{x}{y}$ are connected using the $\frac{r+x}{s+y}$ median, the number of steps of x y is 3. The edges that are ignored by the Dijkstra algorithm are shown in red in the graph below.
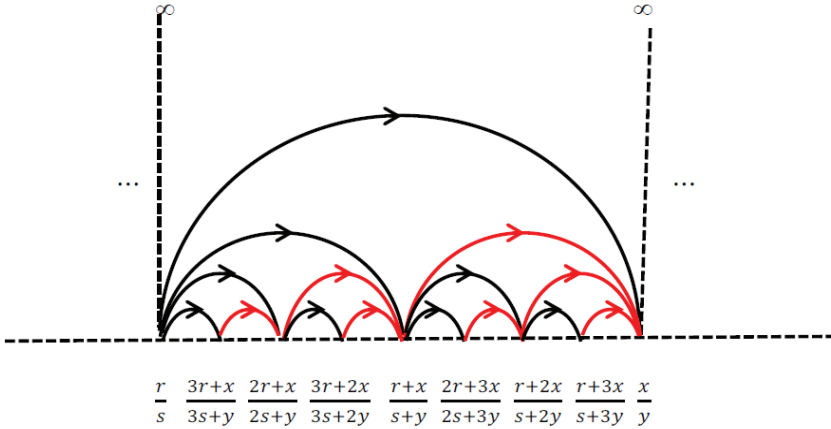
Figure 4: Farey sequence F_4 graph

As seen in Figure 4; D_9, D_5, D_{11}, D_3, D_{13}, D_7 and D_{15} edges are not needed to obtain the minimum number of steps to the vertices of the F_4 Farey graph.

Conclusion

In this article, obtaining minimum number of steps to reach vertices of F_m were examined. There is a one vertex that have with 1 step. Howewer, there are number of infinetly vertices that with 2 steps, with 3 steps, $\cdots$. The median between two vertices is vertex that have minimum number of step. In addition to this, edge located after median, increases the number of step. This study is important because of be an application of algorithm on hyperbolyc geometry which non-euclidiean geometry. In addition to this study, different algorithms can be studied on loaded graphs with different directions.

References

Ahuja, R.K., Magnanti TL., Orlin JB. (1993).*Network Flows*.Prentice-Hall, New Jersey.

Akbaş, M. (2001).*On Suborbital Graphs for Modular Group*. Bull. London Math. Soc.,33, 647-652.

Anderson, J.W. (2005).*Hyperbolic Geometry*. Second Edition,Southampton: Springer

Biggs, N.L., White, A.T.(1979). *Permutation Groups and Combinatorial Structures*. London Math. Soc. Lecture Notes 33,Cambridge: Cambridge University Press.

Dijkstra, E.W. (1959). A Note on Two Problems in Connexion with Graphs. *Numerische mathematik*, 1, 269-271.

Dreyfus, S.E.(1969). An Appraisel of Some Shortest-Path Algorithms. *Operations Research*, 17, 395-412.

Jones, G.A., Singerman, D., Wicks, K.(1991). The Modular Group and Generalized Farey Graphs. *London Math. Soc. Lecture Note Ser*., 160, 316-338.

Gökcan, İ.(2021). Some Relations Between Special Vertex Values of Suborbital Graphs and Special Number Sequences, PhD. Thesis, Trabzon: Karadeniz Technical University.

Neumann, P.M.(1977).*Finite Permutation Groups, Edge Coloured Graphs and Matrices, Topics in Group Theory and Computation*.Curran M.P.J. (eds.),London: Academic Press.

Ratcliffe, J.G.(1994).*Foundations of Hyperbolic Manifolds*. New York: Springer-Verlag.

Ruohonen, K.(2008).*Graph Theory*. Tampere University of Technology.

Schoeneberg, B.(1974).*Elliptic Modular Functions*. New York: Springer-Verlag.

Sims, C.C.(1967). Graphs and Finite Permutation Groups. *Mathematische. Zeitschrift*. ,95, 76-86.

Tsukuzu, T.(1982). *Finite Groups and Finite Geometrie*. Cambridge: Cambridge University Press.

Whiting, P.D., Hillier, J.A.(1960). A Method for Finding the Shortest Route Trough a Road Network. *Operations Research Quarterly*,11, 37-40.

Chapter 2

AN OVERVIEW OF PROGRESSIVE ADDITION LENSES (PALS)

Tuba ÖZDEMİR ÖGE[1]

1 **Assoc. Prof. Dr.,** Bartın University, Vocational School of Health Services, Bartın, Turkey, 74100, E-mail: tozdemir@bartin.edu.tr, ORCID ID, https://orcid.org/0000-0001-6690-7199

1. PROGRESSIVE ADDITION LENSES (PALs)

Progressive addition lenses (PALs) refer to a type of multifocal lens which do not have visible lines on the lens as opposed to bifocal and trifocal lenses (McCleary, 2018). The dioptric power on PAL surfaces with specific geometric shapes increases smoothly downward. There is a power change in the base curve of the lens (Aksak and Küçüker 2005). Side and skewed gaze reduce vision or even make it impossible due to peripheral "dead zones". This peripheral distortion, which is evident in the lower inner and outer corners, occurs with astigmatism caused by the change of aspheric folds (Büyükyıldız, 2011). Progressive lenses are classified based on the distribution of astigmatism as "hard" and "soft" design (Meister, 2006). PALs provide the user with distance, intermediate and near vision. The upper sides of eyeglasses allow distance vision. There is a small transition area between the upper part and the lower part, and this area is called as the progressive corridor.

There are several studies on the main principles, specifications and fitting and dispensary of ophthalmic optics lenses (Özdemir, 2016; Özdemir and Özdemir, 2016; Özdemir et al, 2016; Özdemir Öge, 2019; Özdemir Öge, 2020; Özdemir et al, 2021). In this book chapter, the general features of PALs are explained on the figures. The aim of this study is to summarize the features of PALs and to give detailed information about their fitting.

2. THE STRUCTURE OF PROGRESSIVE ADDITION LENSES

PALs are preferred by patients who need corrective lenses for clear vision (farsightedness, nearsightedness and/or astigmatism) and is also preferred by patients with presbyopia. Progressive lenses fall into the group of multifocal lenses or varifocal lenses. There is no transition between the far and near regions when viewed from the outside with progressive lenses and there is also no "image jump" as bifocal and trifocal lenses. These lenses provide vision at all distances (distance-intermediate-near) through distance vision region on the upper side of the lenses, progressive transition region (progressive corridor) in the middle, near vision zone at the bottom and blending region on peripheral distortion as shown in Figure 1 and Figure 2.

PALs are ordered according to the patient's prescription information and the measurements of the preferred frame. Progressive lenses have a '+' sign to be placed on the pupil and a round sign symbolizing the reading area section. The '+' sign on the progressive lens is superimposed with the '+' sign marked on the template (marked on the pupils). Here, it is ensured that the reading area mark remains within the lens to be cut. It should

be also ensured that the near reference circle is retained in the lens after edging (Şen 2017).
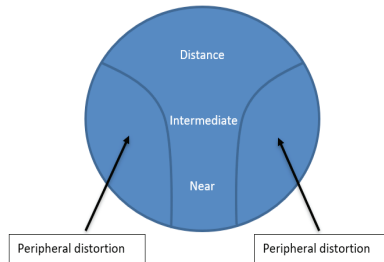
Figure 1. *The illustration of optical regions on a PAL.*

The upper areas of PAL are for the distance vision. The area for the distance Rx power is the distance reference point. The distance reference point is approximately 4 mm above of the fitting point. The area for reading Rx power is the near reference point. A PAL has major reference point (MRP) called as a prism reference point (PRP). Distance reference circle, near reference circle, fitting cross, micro-etching, prism reference circle, add power of progressive addition lens are shown in Figure 2.
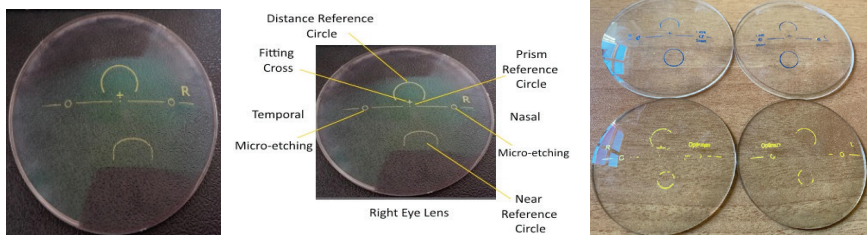
Figure 2. *Progressive addition lens*
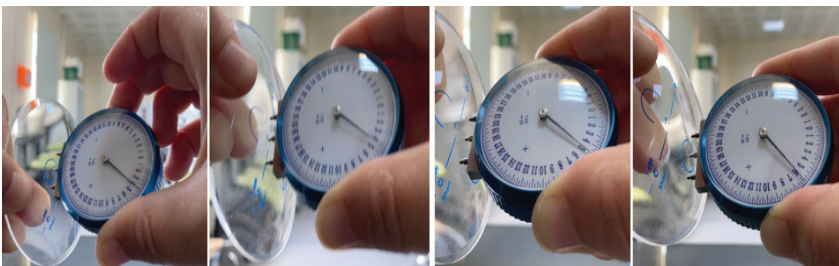
Figure 3. *Base curve measurement of progressive addition lenses from far to near region*

Spherometers are used to measure the surface curvature of lenses. It is also used to measure the dioptric power of front and rear lens surfaces. Figure 3 shows the base curve measurement of PALs from far to near region. The surface curvatures of PALs vary such that they are minimum in the distance zone and maximum in the near zone.
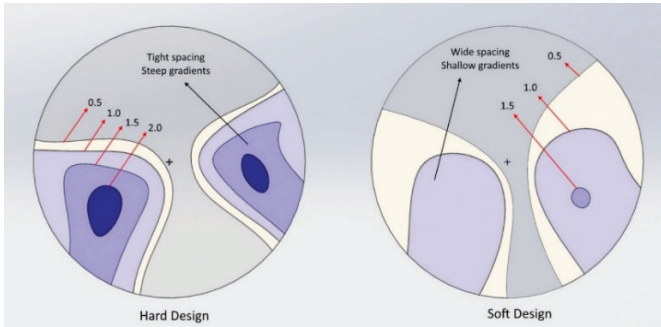
Figure 4. *a) Hard and b) soft design PALs (Meister, 2006)*

The distribution of the distorted vision area on the lens surface determines whether it is a hard or soft design. Soft design PALs are characterized with smooth transitions of optical blur at the peripheral region with a narrower clear vision area, also referred to as progressive corridor (Figure 4). Hard design lenses, on the other hand, provide a wider progressive corridor at the expense of more abrupt refractive power transitions (or unwanted cylinder power) at the peripheral region, thus leading to higher levels of distorted vision when the patient looks through the peripheral regions (Figure 4) (Lestrange-Anginieur and Kee, 2021; Meister, 2006).

3. THE FITTING STEPS OF PAL

a) Prescription Analysis

\- This is an important initial step to compare a patient's new prescription with the older prescription and to perform its analysis. Analyzing a patient's older prescription (with the following steps) before dispensing his/her new eyeglasses holds importance.

\- Measuring the patient's older lenses' values (spherical, cylindrical, axis, addition, and prism if available, the add value as well if available).

\- Checking the dispensing date of the patient's previous eyeglasses.

\- Checking the characteristics and coating of the patient's previous lenses.

\- Comparing these values with the values in the new prescription.

\- Performing the proper fitting according to the new prescription following the above steps.

b) Frame Selection and Adjustment

\- Frame shape, frame depth and frame size is important to select the suitable frame.

- The frame suitable for the face shape of the patient should be selected, such that, it should be adjusted to fit the patient's face perfectly. Large frames should be preferred for PALs.

- Adjustment of the front of the frame (frame-face distance, tilt, balance) and adjustment of the temples (angle, length and alignment, proper curvature of temples, and the form of temples) should be performed. Frame adjustments should always be performed before performing the measurement (Essilor, 2021).

c) Ordering the lens

- PALs should be ordered in accordance with the prescription. During the progressive lens fitting, providing patients with sufficient visibility and field of view holds importance.

- Before the fitting of a progressive lens, the lens' diopter, addition, axis, near and far regions should be carefully controlled by an optician using a lensometer. Progressive addition lenses that fail to comply to the values in the prescription should not be fitted and should be returned (Demir, 2002).

- Freeform surfacing refers to a lens manufacturing process by which complex lens surfaces such as PAL surfaces can be generated using computer numerical controlled (CNC) machines that can operate in three axes which have the capability to generate any surface with the aid of single point cutting tools (Meister, 2008). When compared to traditionally manufactured lenses, that are processed from pre-molded semi-finished blanks, the lenses manufactured with digital freeform technology provide better vision by providing total control on light distribution. Also their reduced mass and fewer surfaces minimize the difficulties during the assembly by simplifying the optical system (Wang, et al., 2016; Rx-safety. com, 2021) Other advantages of freeform PALs over conventional PALs include a significantly wider field of view as the technique is based on application of visual correction on the back of the lens, thus eliminating the key-hole effect encountered in traditional PALs. Moreover, peripheral distortion commonly encountered in traditional PALs are eliminated by using surface designer software (Overnightglasses, 2021).

d) Pupillary Distance Measurement

- Pupillary distance (PD) is the distance between the centers of a person's right and left pupils. PD measurement should be carried out before the fitting of lenses on the frame.

- PD should be determined before prescription lenses are ordered or a visual examination is performed (Brooks and Borish, 2007).

- The device that measures the distance between the pupils of the two eyes or the distance from the center of the pupil to the middle of the center of the nose is called a pupillometer (PD meter).

- Monocular PD distance should be measured for the right and left eyes before the fitting of PALs (Figure 5).
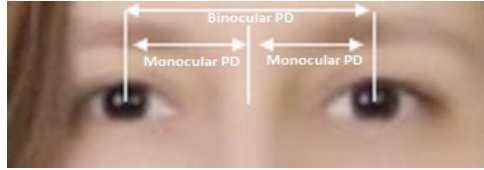
Figure 5. *PD measurement (monocular and binocular PD)*

e) Fitting Height

- Height Measuring System (HMS) is used to measure the segment heights in the boxing system (Essilor, 2021). The distance between the lens' fitting cross and the lower point of the near sight reference circle is the minimum height required for fitting. For a standard progressive lens, this distance is generally in the range of 18-22 mm. Far pupillary points and near sight circles are marked on each lens using the centering chart. This should be performed after the patient puts on the eyeglasses. The centering for far and near sights is then checked (Essilor, 2021).

- During the fitting, the near reference circle should not be trimmed. Therefore, the minimum fitting height required for fitting of the progressive lens should be taken into account during the frame selection step (Demir, 2002).
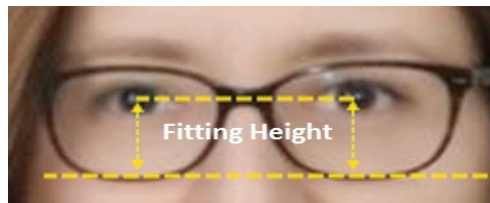
Figure 6. *Fitting height*

- Fitting height, corresponding to the distance between the center of the pupil and the bottom of the left and right lenses for each eye, is shown in Figure 6.

- Apart from pupillary measurement, the distance of both pupils to the lowest point of the frame (mounting height) should be measured separately. After carefully making these measurements, the fitting cross

is superimposed with the pupillary center of the wearer (Figure 7) and the lens is then fitted accordingly.

f) Fitting and Dispensing

-    The presence of diverse dioptric fields on PAL surfaces requires performing the measurement step with utmost care (Figure 4).

-    PAL manufacturers put permanent marks on lenses using laser technology for fitting purposes in order to minimize the fitting errors. Among these marks, fitting cross is superposed with the pupilla center. The far sight optical center is located 4 mm below the fitting cross. When measuring with a lensometer, the diopter value of the far region should be measured inside the reference circle of the far region. The axis should also be controlled by checking the alignment of marker points with fitting reference lines. Afterwards, addition check should be performed (Demir, 2002).

-    Both the centering and fitting steps should be performed in accordance with the boxing system.

-    The frame should be adjusted for the wearer's face ensuring that fitting crosses for far sight are superimposed with the right and left pupilla centers (Figure 7).
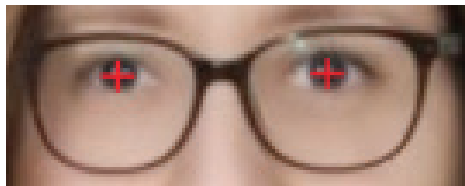
Figure 7. *The fitting cross should be superimposed with the patient's pupilla on the PAL.*

-    The angle between the vertical plane of the face and the frame position is called pantoscopic angle or frame tilt (Figure 8). Pantoscopic angle should be adjusted between 8 and 12 degrees.
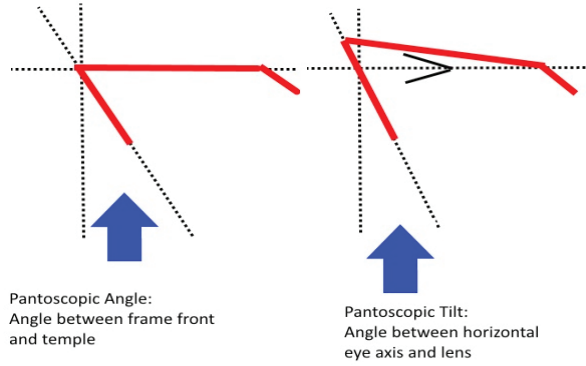
Figure 8. *Pantoscopic angle and pantoscopic tilt (Santini, 2015)*

- The distance between the rear vertex point of the lens and the cornea's vertex point is known as the vertex distance (Figure 9). Vertex distance should be nearly between 12-14 mm. However, following the frame selection, this distance should be checked again by the optician.
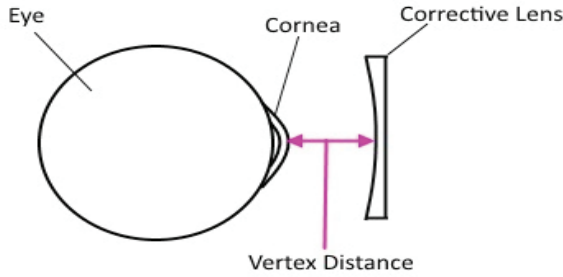
Figure 9. *Vertex distance*

Figure 10. *Facial Wrap (Eyeglasses, 2021).*

- The frame front should follow the line of the face to a great extent. Also, facial wrap should not be too straight (Figure 10). The wrap angle of the frame should be adjusted so as not to let the frame contact with cheeks (Aksak and Küçüker 2005).

g) Verification

- After clearing the markings on the lens, far, intermediate and near regions should be checked and verified with the wearer.

- After the fitting stage, the frame should be checked on the wearer's face.

- Then the fitting measurements should be checked.

Adaptation Problems: Patients may encounter certain adaptation problems when using PALs. One of them is the adaptation problem after the initial use of the progressive lens. It can be difficult for patients to get used to the progressive lens and it can take a long time. Opticians should make recommendations for getting over the adaptation problem. It is also important to provide the wearer with information about overcoming adaptation problems.

The measurement of the dioptric power of PALs is shown in Figure 11. The PAL with suction cup, fitted on the frame after the edging process is shown in Figure 12. Figure 13 shows the final form of the progressive eyeglasses which is ready for final checks on the patient.

Note: The marks on the lens should not be cleared until the eyeglasses are dispensed to the wearer (Figure 13).
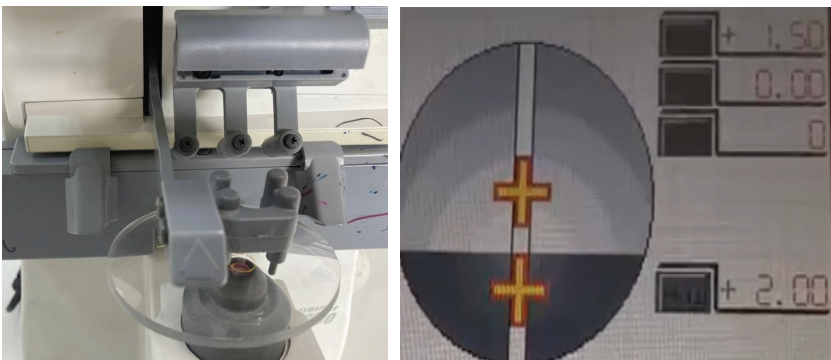
Figure 11. Diopter measurement of progressive addition lenses
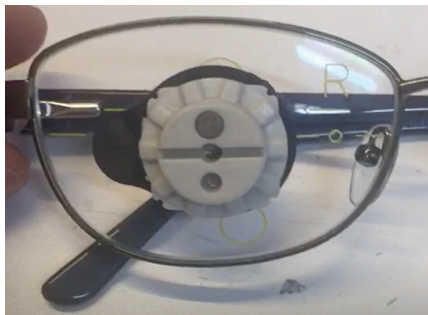
Figure 12. *PAL attached with suction cup*
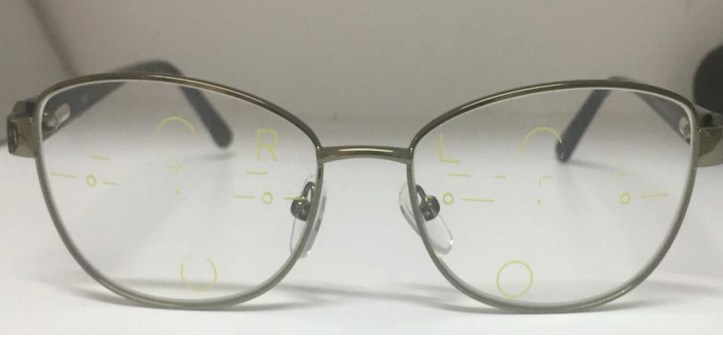
Figure 13. *Fitting of progressive addition lenses on the frame*

4. CONCLUSION

This study explains the specific properties of progressive addition lenses (PAL) and the fitting and dispensing steps of PALs. The patient's visual needs and refractive status are important in choosing PAL.

The main requirements during the dispensing step of progressive addition lenses are correct prescription analysis, correct frame selection, correct measurements (pupillary distance measurement, determination of fitting height, pantoscopic angle, vertex distance, facial wrap), correct lens ordering, correct fitting and dispensing of progressive addition lenses and verification.

Acknowledgements

REFERENCES

Aksak, E., Küçüker, T. (2005). Gözlükçülük, Tüm Optik ve Optometrik Meslekler Birliği Derneği. İstanbul: Esen Ofset Matbaacılık San. ve Tic. A.Ş.

Brooks, C.W., Borish, I. M. (2007). System for Ophthalmic Dispensing. Third Edition, Oxford: Butterworth-Heinemann.

Büyükyıldız, H. Z. (2011). Gözlük Camları, Cam Materyalleri ve Kişiye Özel Gözlük Camları. TJ O 41; 1: 2011, DOI: 10.4274/tjo.41.06.

Demir, F.M. (2002). Opticianry Practices - III Course Laboratory Practicing Guidelines. Muğla Sıtkı Koçman University Health Sciences Vocational School, Opticianry Program.

Essilor, (2021). https://www.essiloracademy.eu/en/publications-progressive-lenses-fitting-guide, Accessed 01.11.2021.

Eyeglasses, (2021). https://www.3dcontentcentral.com/, Accessed 01.11.2021.

Free Form Digital Progressive Lenses (2021). https://www.overnightglasses.com/free-form-digital-progressive-lenses/ Accessed 05.12.2021.

Lestrange-Anginieur, E De., Kee, C. S. (2021). Optical performance of progressive addition lenses (PALs) with astigmatic prescription, Nature Scientific Reports, 11, 2984.

McCleary, D.S. (2018). The Optician Training Manual, Simple Steps to Becoming a Great Optician". 2. Edition. Santa Rosa: Santa Rosa Publishing.

Meister, D. (2006). Fundamentals of Progressive Lens Design, VisionCare Product News, Volume 6, Number 9, September 2006, http://www.laramyk.com/wp-content/uploads/2010/05/Fundamentals-of-Progressive-Lenses.pdf.

Özdemir, T. (2016). A Theoretical Research on CR-39 (Allyl Diglycol Carbonate) Plastic Polymer. International Conference on Material Science and Technology in Cappadocia (IMSTEC'16), April 6-8, 2016, Nevşehir, Turkey.

Özdemir, T., Özdemir, F. B. (2016). The Spectral Light Transmittance of Ophthalmic Optical Lenses. International Conference on Material Science and Technology in Cappadocia (IMSTEC'16), April 6-8, Nevşehir, Turkey.

Özdemir, T., Sağlam, A., Özdemir, F. B., Keskiner, A. Ü., (2016). The evaluation of spectral transmittance of optical eye-lenses. Optik, 127, 2062–2068.

Özdemir Öge, T. (2019) Optical Lenses and Ophthalmic Lens Assembly Steps. International Conference on Materials Science, Mechanical and Automative Engineerings and Technology in Cappadocia/Turkey (IMSMATEC'19), June 21-23.

Özdemir Öge, T. (2020). Ophthalmic Optics Lenses, Fitting Applications And Dispensing Optical Prescription: A Review of Opticianry. Theory and

Research in Health Sciences II, Volume 1, Birinci Basım / First Edition, Aralık.

Özdemir Öge, T., Ozdemir, F.B., Öge, M., Çiçek, O. (2021). Fundamentals of Ophtalmic Lens Decentration, in: Physics Studies, Edited by Emek, M. İksad Publishing House.

Santini, B. (2015). The Real Details of Vertex, Tilt and Wrap. https://www.2020mag.com/ce/the-real-details-of-vertex-5E16F Accessed 01.11.2021.

Şen, F. (2017). Gözlük Camlarının Montajı. İstanbul: Güneş Tıp Kitabevleri.

Meister, D. (2008). The Optics of Free-Form Progressive Lenses, 2021. https://www.2020mag.com/ce/the-optics-of-free-form Accessed 05.12.2021.

Wang, X., Liu, H., Juschkin, L., Li, Y., Xu, J., Quan, X., Lu, Z., Freeform lens collimating spectrum-folded Hadamard transform near-infrared spectrometer, Optics Communications, Volume 380, 1 December 2016, Pages 161-167.

What Are The Advantages of Free Form Progressive Lenses? https://rx-safety.com/2015/09/what-are-the-advantages-of-free-form-progressive-lenses/ Accessed 05.12.2021.

Chapter 3

NUTRIENT CONCENTRATIONS OF SOME MEDICINAL AND AROMATIC PLANTS CONSUMED AS FUNCTIONAL FOOD

Handan Sarac[1]

Hasan Durukan[2]

Ahmet Demirbas[3]

---

1   Assistant Professor, Department of Plant and Animal Production, Sivas Technical Sciences Vocational School, Sivas Cumhuriyet University, Sivas, Turkey. ORCID ID: 0000-0001-7481-7978
2   Dr. Department of Plant and Animal Production, Sivas Technical Sciences Vocational School, Sivas Cumhuriyet University, Sivas, Turkey. ORCID ID: 0000-0002-2255-7016
3   Associate Professor, Department of Plant and Animal Production, Sivas Technical Sciences Vocational School, Sivas Cumhuriyet University, Sivas, Turkey. ORCID ID: 0000-0003-2523-7322

1. Edible Wild Plants and Their Importance in Nutrition

Wild plants have been used by people for different purposes for centuries depending on the way their life. The beneficial and harmful effects of these plants have been learned by experience and the information obtained has been passed down from generation to generation until today (Urhan et al., 2016; Dastan and Sarac, 2018; Mohammed et al., 2019a). Wild plants are mostly used for food and medical purposes due to their nutritional and functional properties all over the world (Konak et al., 2017; Saraç et al., 2018a; Mohammed et al., 2019b). Edible wild plants are plants that are collected and consumed in the season by local people in the regions where they grow naturally. These plants are recognized by the people in the regions where they grow and collected and evaluated for various purposes. When and how to evaluate which part of the plant is an important part of folk culture (Urhan et al., 2016; Mohammed et al., 2020a). There are many edible wild plants in the world that are collected from natural flora and consumed as fresh, cooked or dried in the form of salads, various regional dishes, spices and tea (Tunçtürk, 2013; Nohutçu et al., 2019; Mohammed et al., 2020b). It has been reported that there are over 10,000 wild plant species used as food worldwide (Baytop, 1999; Yücel et al., 2011; Urhan et al., 2016; Saraç et al., 2018a; Nohutçu et al., 2019). Edible parts of wild plants are very rich and inexpensive sources in terms of vitamin, mineral, fatty acids, fiber and protein content, which are important in daily diets (Turan et al., 2003; Yücel et al., 2012; Ceylan and Yücel, 2015; Pehlivan et al., 2018; Saraç et al., 2018b). In addition, studies have shown that various biochemical compounds found in the structure of wild plants have positive effects on health, and many of these compounds have strong biological activities such as antioxidants, antimicrobials and anticarcinogens (Mohammed et al., 2018; Saraç et al., 2018a; Saraç et al., 2018b; Nohutçu et al., 2019; Mohammed et al., 2021). In most epidemiological studies, it has been reported that there is a contrasting relationship between cancer and cardiovascular diseases and the consumption of wild plants, and this is due to antioxidant-properties compounds found in the structures of wild plants (Urhan et al., 2016; Nohutçu et al., 2019). Kadıoğlu (2014) stated that edible wild plants are not only alternatives to vegetables, but also important plants in terms of health and traditional medicine. She also noted that wild plants are rich in vitamins A and C and contain a significant amount of elements such as phosphorus, calcium and iron. Many other studies have found that wild plants are richer in mineral substance concentrations and nutritional value than traditional cultured vegetables (İyigün and Özer, 2001; Turan et al., 2003; Şekeroğlu et al., 2005; Ceylan and Yücel, 2015). Therefore, edible wild plants play an important role in human health due to their nutritional content and bioactive properties (Ceylan and Yücel,

2015; Konak et al., 2017). In recent years, due to both the nutritional value and the biochemical compounds they contain, the importance of wild plants that grow spontaneously in the natural flora in healthy nutrition has been understood more and more and their consumption is increasing accordingly (Tunçtürk, 2013). It has been reported by the Food and Agriculture Organization (FAO) that at least one million people around the world consume wild plants for food purposes (Ceylan and Yücel, 2015). Wild plants are considered as functional food in terms of both being a food and being good for health (Saraç et al., 2018b).

2. Functional Food Definition and Importance

It is believed that there is an important link between food and health. Especially in recent years, increasing foodborne health problems, increasing demand for natural products, and the tendency to live quality, long and healthy life increase the importance of the relationship between food and health (Dölekoğlu et al., 2014; Aslan and Ayaz, 2019). Many nutrients contain macro and micro nutrients required for metabolic activity, as well as components that have positive effects on our health (Coşkun, 2005).

The concept of functional food was first introduced in Japan in the 1980s (Vural, 2004; Dölekoğlu et al., 2014; Aslan and Ayaz, 2019). In addition to the adequacy, diversity and effectiveness of the nutrients it contains, nutrients that are good for one or more body functions, reduce the risk of disease, are not in the form of drugs, capsules or tablets, and whose effects are scientifically approved nutrients are defined as "functional food". In addition, functional food can be created by adding functional components to traditional foods through biotechnology, supporting health or preventing disease or helping treatment (Aslan and Ayaz, 2019). According to another definition, functional foods are foodstuffs or food components that, in addition to being nutritious, have a positive effect on the health, physical performance or mental state of the individual (Frewer et al., 2003; Vural, 2004; İşleroğlu et al., 2005; Dölekoğlu et al., 2014). Functional foods are classified as terpenoids, phenolic substances, fatty acids and structural fibers, carbohydrates and derivatives, amino acid-containing substances, probiotics (microorganisms), prebiotics (synbiotics) and minerals according to the chemical structures of their bioactive components (Aslan and Ayaz, 2019). Apart from this, functional foods are classified according to their content, properties, product groups, benefits and purposes, so the products that we know with different names can be included in the definition of functional food (Dölekoğlu et al., 2014). Functional foods can be a natural traditional foodstuff that has never been processed in daily diets, or they can also be nutrients that have been modified by genetic engineering or enriched with a functional nutrient (eggs containing omega-3, yoghurts

with probiotics, etc.) in order to achieve more positive effects (Coşkun, 2005; Aslan and Ayaz, 2019). For example, fruits and vegetables can be considered as the simplest form of functional foods (Dölekoğlu et al., 2014).

For any food to be defined as a functional food, it must have the following characteristics (Vural, 2004; Coşkun, 2005):

-   In addition to being nutritious, it should contribute to maintaining or improving health.

-   Its nutritional and health-positively impacting properties should have solid foundations in terms of nutritional science and medicine.

-   Daily consumption amounts must be determined.

-   Its consumption must be found to be reliable.

-   Physico-chemical properties should be well defined, these components should be determined qualitatively and quantitatively.

-   If it has acquired functional properties by processing, there should be no loss of nutritive properties.

-   It should be a food that is used frequently in daily nutrition, not consumed infrequently.

-   It should be in the form of natural consumption.

-   It should not be a substance used as a drug.

Functional foods are also called health foods, medicinal foods, regulatory foods, special nutritional foods and pharmacological foods (Coşkun, 2005; Dölekoğlu et al., 2014; Aslan and Ayaz, 2019). Functional food is a term that emphasizes that nutrients are associated with health (Coşkun, 2005). Therefore, functional foods have positive effects on health (Dölekoğlu et al., 2014). These effects are due to bioactive substances such as minerals, vitamins, polyunsaturated fatty acids, dietary fibers, antioxidants or prebiotics (Vural, 2004; Meral et al., 2012; Dölekoğlu et al., 2014; Aslan and Ayaz, 2019). Nutrition is thought to be responsible for 60% of total deaths and 70% of cancer cases in the world (Aslan and Ayaz, 2019). One of the most important effects of functional foods on health is the prevention and/or reduction of the risk of serious health problems such as cancer (Sarkar, 2007; Saraç et al., 2018b). In addition, functional food consumption is effective in preventing and treating cardiovascular diseases, maintaining the health of the gastrointestinal system, treating obesity, alleviating menopausal symptoms, preventing osteoporosis and maintaining eye health (Vural, 2004; Coşkun, 2005). Scientifically demonstrating the effectiveness of some nutrients in preventing and

treating diseases naturally has increased the importance of nutritional support in terms of health. Therefore, functional foods, nutraceuticals and natural health products have become more consumed (Coşkun, 2005).

The most commonly used functional food items in recent years are antioxidants (Meral et al., 2012; Aslan and Ayaz, 2019). Antioxidants are substances that prevent or delay oxidation at the beginning and/or developmental step. The presence of compounds with antioxidant activity in biological systems is an important and fundamental need for life (Nishina et al., 1991; Saraç et al., 2018b; Sevindik et al., 2018; Bal et al., 2019). Many epidemiological studies show that foods rich in antioxidants have a protective effect against diseases and their consumption reduces the risk of cancer, heart disease, hypertension and stroke (Konak et al., 2017). Studies have shown the antioxidant capacity of some wild plants is higher than synthetic antioxidants (Çoban and Patır, 2010; Saraç et al., 2018b). For this reason, it is recommended to meet the antioxidant intake from natural plants, vegetables or fruits instead of drugs. Antioxidants taken in a balanced way naturally do not reach toxic levels in the body. In addition, it helps to increase the functional effect with the synergistic effect of other functional components (Coşkun, 2005).

3. Consumption of Medicinal and Aromatic Plants as Functional Food

The idea that nutrients may have therapeutic properties is not new (Aslan and Ayaz, 2019). When we look at the findings obtained from the ancient times, people primarily benefited from plants in order to provide food and find solutions to health problems (Arslan et al., 2015; Nohutçu et al., 2019). Hippocrates, who was seen as the father of medicine about 2,500 years ago, said, "Our food should be our medicine and our medicine should be our food" (Coşkun, 2005; Aslan and Ayaz, 2019; Varlı et al., 2020). In addition, although functional foods have been newly defined as a concept, medicinal and aromatic plants, which are effective in preventing and treating diseases, have been used as functional food for centuries (Dölekoğlu et al., 2014).

Medicinal and aromatic plants, which do not have a standard classification among plants, have a very important place in human health and are used as both food and medicine today as in the past (Sarac, 2021; Saraç and Tüzün, 2021). The data obtained proves that medicinal and aromatic plants are the oldest and most widely used drugs (Arslan et al., 2015; Akgül et al., 2020; Varlı et al., 2020). It is estimated that there are between 20,000 and 72,000 medicinal and aromatic plants in the world (Baydar, 2009; Arslan et al., 2015; Saraç et al., 2018a; Nohutçu et al., 2019; Sarac, 2021). Approximately 80% of the world's population

uses medical herbal products in the first stage of preventive and post-disease treatment (Sevindik et al., 2017; Sevim, 2018; Varlı et al., 2020). Medicinal and aromatic plants are rich sources of bioactive secondary metabolites. The main secondary metabolites found in medicinal and aromatic plants; steroids, flavonoids, saponins, alkaloits, terpenes and phenolic compounds (Varlı et al., 2020). These secondary metabolites are responsible for a variety of bioactivities that can have an impact on animal metabolism or physiology (Saraç et al., 2018a; Sarac, 2021). Therefore, medicinal and aromatic plants have antimicrobial, antifungal, antiallergic, antidiabetic, cardiovascular system protective, antioxidant, anticancer, antithyroid, antihistaminic, antimalarial, antihelmintic, anti-inflammatory, antihypertensive, antispasmodic and analgesic properties (Sevindik et al., 2017; Varlı et al., 2020).

4. Macro and Micro Element Concentrations of Some Medicinal and Aromatic Plants

Living things need sufficient nutrient intake in order to perform various vital functions and lead a healthy life. Millions of people, especially in developing countries, are unable to meet their daily nutritional needs and also face one or more mineral elements deficiencies (Ceylan and Yücel, 2015; Dastan and Sarac, 2018). Mineral elements are of great importance in maintaining life on Earth. In order to continue their vital activities, living things need macro elements such as calcium (Ca), potassium (K), magnesium (Mg), sodium (Na) and phosphorus (P) in much more amounts than micro elements such as copper (Cu), iron (Fe), zinc (Zn), manganese (Mn) and molybdenum (Mo). Mineral elements have very important functions in human nutrition. For example, Ca, K and Mg are mineral elements necessary for repairing worn cells, developing a solid bone and tooth structure in humans, the formation of red blood cells and the ensuring a large number of body functions (Sevim, 2018). Fe, on the other hand, is a very important element that is necessary for the human body in different amounts periodically (Sevindik et al., 2020). It is especially found in hemoglobin, which carries oxygen in the blood, myoglobin in the muscles and respiratory enzymes, provides the absorption of some minerals such as Cu and Ca, and is necessary for the production of various enzymes (Sevim, 2018). Fe deficiency leads to various diseases, especially anemia (Sevindik et al., 2020). In addition, optimal intakes of elements such as Na, K, Mg, Ca, Mn, Cu, Zn and iodine (I) contribute to the reduction of risk factors in heart disease-related disorders and increase the intake of many non-nutritional beneficial substances such as carotenoids, vitamin C, tocopherol, α-linolenic acid, important other minerals, polyphenols and anthocyanins as a result of their consumption (Ceylan and Yücel, 2015).

Plants convert the water and nutrients they take from the soil into

compounds that will benefit the human body in their own metabolism (Nohutçu et al., 2019). Studies conducted so far shown that the macro and micro nutrient contents of medicinal and aromatic plants are important for an adequate and balanced diet (Özcan and Akbulut 2008; Sarma et al. 2011; Dastan and Sarac, 2018; Sevim, 2018).

Table 1. *Macro Element Concentrations of Some Medicinal and Aromatic Plants Consumed as Functional Foods (%)*

Plant	N	P	K	Ca	Mg	Reference
Rumex crispus L.	2.59	0.360	6.85	0.48	0.66	Dastan and Sarac, 2018
Orchis provincialis	1.97	0.23	3.38	1.13	0.47	Korkmaz and Türkiş, 2021
Polygonum cognatum Meissn.	3.50	0.259	3.9	0.51	0.44	Saraç et al., 2018a
Arum maculatum L.	4.05	0.35	2.82	0.68	0.12	Akpınar, 2021
Achillea millefolium L.	1.01	0.63	2.43	2.22	0.70	Saraç et al., 2021
Hypericum scabrum L.	0.24	0.30	2.01	0.22	0.19	Kadıoğlu, 2021
Helichrysum plicatum DC.	0.21	0.31	0.89	0.23	0.20	Kadıoğlu, 2021
Glaucium grandiflorum	3.25	0.110	2.13	0.44	0.10	Saraç et al., 2018b
Malva sylvestris L.	2.75	0.279	1.77	1.49	0.273	Kordalı et al., 2021
Alcea rosea L.	3.88	0.299	1.66	1.23	0.243	Kordalı et al., 2021
Gundellia tournefortii L.	3.64	0.11	3.78	0.22	0.57	Saraç et al., 2019
Prunus Mahaleb L.	3.42	0.37	1.67	1.68	0.52	Meraler, 2010
Rumex acetosella L.	-	-	2.86	2.18	2.60	Canbay and Santan, 2015
Rosmarinus officinalis L.	-	-	3.22	0.48	0.65	Canbay and Santan, 2015
Urtica dioica L.	-	-	2.57	0.92	0.57	Canbay and Santan, 2015
Prangosferul acea	-	-	0.086	0.032	0.010	Sevim, 2018
Ferula rigidula	-	-	0.104	0.036	0.008	Sevim, 2018
Eremurusspec tabilis	-	-	0.021	0.052	0.009	Sevim, 2018
Rheumribes	-	-	0.055	0.012	0.015	Sevim, 2018
Tilia sp.	2.65	0.24	1.21	2.48	0.51	Alpaslan et al., 1998
Aesculus hippocastanum L.	-	0.14	1.06	1.15	0.29	Alpaslan et al., 1998

Table 2. *Micro Element Concentrations of Some Medicinal and Aromatic Plants Consumed as Functional Foods (mg kg⁻¹)*

Plant	Fe	Zn	Mn	Cu	Reference
Rumex crispus L.	225.8	27.5	30.4	8.9	Dastan and Sarac, 2018
Orchis provincialis	428	38	30	17	Korkmaz and Türkiş, 2021
Polygonum cognatum Meissn.	144.7	40.3	30.1	7.5	Saraç et al., 2018a
Arum maculatum L.	50.2	62.3	16.1	0.0016	Akpınar, 2021
Achillea millefolium L.	360.4	47.6	85.5	28.3	Saraç et al., 2021
Hypericum scabrum L.	185	24.0	19.1	17.6	Kadıoğlu, 2021
Helichrysum plicatum DC.	1531.1	69.5	52.8	8.7	Kadıoğlu, 2021
Glaucium grandiflorum	205.9	21.1	22.7	6.1	Saraç et al., 2018b
Malva sylvestris L.	162.96	63.56	54.31	60.70	Kordalı et al., 2021
Alcea rosea L.	181.99	46.57	79.71	32.14	Kordalı et al., 2021
Gundellia tournefortii L.	268.45	16.75	19.46	8.26	Saraç et al., 2019
Prunus mahaleb L.	479	38	36	7.0	Meraler, 2010
Prunus mahaleb L.	19.63	32.81	6.23	5.54	Canbay and Santan, 2015
Rumex acetosella L.	70.52	17.48	2.47	4.58	Canbay and Santan, 2015
Urtica dioica L.	216.25	11.55	11.23	6.30	Canbay and Santan, 2015
Prangosferul acea	8.83	1.43	0.76	0.39	Sevim, 2018
Ferula rigidula	2.16	3.09	1.19	0.65	Sevim, 2018
Eremurusspec tabilis	9.88	2.9	1.87	0.31	Sevim, 2018
Rheumribes	13.13	1.01	1.06	0.26	Sevim, 2018
Tilia sp.	320	29	133	12	Alpaslan et al., 1998
Aesculus hippocastanum L.	443	12	226	6.5	Alpaslan et al., 1998

The macro element concentrations of some medicinal and aromatic plants consumed as functional foods are given in Table 1. The nitrogen, phosphorus and potassium concentrations of the plants varied between 0.21-4.05% N, between 0.11-0.63% P and between 0.021-6.85% K, respectively. Calcium concentration varies between 0.012-2.48% Ca and magnesium between 0.008-2.60% Mg. When the micro element concentrations of some medicinal and aromatic plants consumed as functional foods are evaluated, it is seen that the iron concentration varies between 2.16-1531.1 mg Fe kg⁻¹, and the zinc concentration varies between 1.01-69.5 mg Zn kg⁻¹ (Table 2). Manganese concentration varies between 0.76-226 mg Mn kg⁻¹,

and copper concentration varies between 0.0016-60.70 mg Cu kg^{-1}.

In recent years, the issue of determining the macro and micro nutrient content of medicinal and aromatic plants has started to attract attention (Kaya et al., 2004, Koç and Sari, 2009; Sevim,2018). Kadıoğlu et al. (2021), the leaves and flower parts of medicinal and aromatic plants are consumed as tea, Milani et al. (2019) stated that herbal tea substances are sources of minerals such as iron, magnesium, manganese, potassium and zinc, various vitamins and antioxidant compounds. In this study, when the macro and micro element concentrations of some medicinal and aromatic plants consumed as functional foods are evaluated as a whole, it is seen that both macro and micro element concentrations are above and below the limit values. When the values are examined, there are also very low concentration values. It is thought that this situation is caused by the nutrient content and growing conditions of the soils where medicinal and aromatic plants are grown and collected.

5. Conclusion

Due to the effects of nutrition on health and quality of life, conscious society individuals have begun to question the qualities of the foods they buy and their effects on health. In addition, the increase in mortality rates due to diseases such as chronic heart diseases and cancer has made it necessary for researchers to focus on the foods consumed, as well as risk factors such as smoking, alcohol and stress. Researchers state that the fastest growing sub-sector in the food sector is the functional food sector, followed by natural products. Today, foods come to the fore both with the macro and micro nutrients they contain and with their cumulative functional effects (Aslan and Ayaz, 2019). Functional foods, which have been used to prevent and treat diseases for many years, have attracted attention with their rapid growth trend in recent years (Dölekoğlu et al., 2014). Plants consumed as natural food sources and their medicinal effects cannot be completely separated from each other (Ceylan and Yücel, 2015). In recent years, studies have tried to reveal the nutritional values of medicinal and aromatic plants as well as their therapeutic effects. In order for medicinal and aromatic plants to be consumed consciously as functional foods and to be beneficial, the macro and micro nutrient content of these plants should be known. In this review, macro and micro element concentrations of some medicinal and aromatic plants consumed as functional foods are given. Accordingly, it is seen that most of the plants mentioned in the study are sufficient in terms of nutrient content. As a matter of fact, many scientific studies reveal that the macro and micro nutrient contents of medicinal and aromatic plants are important for adequate and balanced nutrition (Saraç et al., 2019; Saraç et al., 2020).

References

Akgül, H., Korkmaz, N., Dayangaç, A. & Sevindik, M. (2020). Antioxidant potential of endemic *Salvia absconditiflora*. *Turkish Journal of Agriculture-Food Science and Technology, 8*(10), 2222-2224.

Akpınar, Ç. (2021). Osmaniye ili ve çevresinden toplanan tirşik (*Arum maculatum* L.) bitkisinin besin elementi konsantrasyonlarının değerlendirilmesi. *OKU Fen Bilimleri Enstitüsü Dergisi, 4*(3), 211-216.

Alpaslan, M., Güneş, A. & İnal, A. (1998). Deneme Tekniği. *Ankara Üniversitesi, Ziraat Fakültesi Ders Kitabı,* 437 p.

Aslan, R., & Ayaz, K. (2019). Fonksiyonel Gıda: Besinler İlacımız Olabilir mi?. *Ayrıntı Dergisi, 7*(77), 45-49.

Arslan, N., Baydar, H., Kızıl, S., Karık, Ü., Şekeroğlu, N., & Gümüşçü, A. (2015). Tibbi aromatik bitkiler üretiminde değişimler ve yeni arayışlar. *Türkiye Ziraat Mühendisliği VIII. Teknik Kongresi*, 12-16.

Bal, C., Sevindik, M., Akgul, H., & Selamoglu, Z. (2019). Oxidative stress index and antioxidant capacity of *Lepista nuda* collected from Gaziantep/Turkey. *Sigma Journal of Engineering and Natural Sciences, 37*(1), 1-5.

Baydar, H. (2009). Tıbbi ve Aromatik Bitkiler Bilimi ve Teknolojisi (Genişletilmiş 3. Baskı). Süleyman Demirel Üniversitesi, Ziraat Fakültesi Yayın No: 51, Isparta.

Baytop, T. (1999). Türkiye'de Bitkilerle Tedavi [Therapy with medicinal plants in Turkey]. *İstanbul, Nobel Tıp Kitapevi*, 371.

Canbay, H. S., & Saltan, F. Z. (2015). Eskişehir'de halk arasında kullanılan bazı bitkilerdeki ağır metal ve besin elementlerinin belirlenmesi. *Süleyman Demirel Üniversitesi Fen Bilimleri Enstitüsü Dergisi*, *19*(1), 83-90.

Ceylan, F., & Yücel, E. (2015). Düzce ve çevresinde gıda olarak tüketilen yabani bitkilerin tüketim biçimleri ve besin öğesi değerleri. *Afyon Kocatepe Üniversitesi Fen ve Mühendislik Bilimleri Dergisi*, *15*(3), 1-17.

Coşkun, T. (2005). Fonksiyonel besinlerin sağlığımız üzerine etkileri. *Çocuk Sağlığı ve Hastalıkları Dergisi*, *48*(1), 61-84.

Çoban, Ö. E., & Patır, B. (2010). Antioksidan etkili bazı bitki ve baharatların gıdalarda kullanımı. *Gıda Teknolojileri Elektronik Dergisi*, *5*(2), 7-19.

Dastan, T., & Sarac, H. (2018). Determination of the nutritional element concentrations of Evelik plant (*Rumex crispus* L.). *Cumhuriyet Science Journal*, *39*(4), 1020-1024.

Dölekoğlu, C. Ö., Şahin, A., & Giray, F. (2015). Kadınlarda fonksiyonel gıda tüketimini etkileyen faktörler: Akdeniz illeri örneği. *Journal of Agricultural Sciences*, *21*(4), 572-584.

Frewer, L., Scholderer, J., & Lambert, N. (2003). Consumer acceptance of functional foods: issues for the future. *British food journal. 105*(10), 714-731.

İşleroğlu, H., Yıldırım, Z., & Yıldırım, M. (2005). Fonksiyonel bir gıda olarak keten tohumu. *GOÜ. Ziraat Fakültesi Dergisi, 22*(2), 23-30

İyigün, Ö., & Özer, Z. (2001). Muş ve yöresinde gıda olarak kullanılan yabancı otlar. *Türkiye Herboloji Derg., 4*(2), 66-73.

Kadıoğlu, B. (2021). *Hypericum scabrum* L. ve *Helichrysum plicatum* DC. bitkilerinin makro ve mikro bitki besin elementi içerikleri ile toprak özelliklerinin değerlendirilmesi. *Muş Alparslan Üniversitesi Tarımsal Üretim ve Teknolojileri Dergisi, 2*(1), 12-25.

Kadıoğlu, B., Kadıoğlu, S. & Tasğın, G. (2021). Erzurum ilindeki tıbbi ve aromatik bitki tüketicilerinin alışkanlıklarının belirlenmesi. *Bahçe, Yalova Atatürk Bahçe Kültürleri Merkez Araştırma Enstitüsü Dergisi, 50*(1), 7-17.

Kadıoğlu, Z. (2014). Erzincan İlinde Sebze Olarak Kullanılan Yabani Bitki Türleri. Anadolu Matbacılık Erzincan Bahçe Kültürleri Araştırma Enstitüsü Müdürlüğü Yayın No: 12.

Kaya, İ., İncekara, N., & Nemli, Y. (2004). Ege Bölgesi'nde sebze olarak tüketilen yabani kuşkonmaz, sirken, yabani hindiba, rezene, gelincik, çoban değneği ve ebegümecinin bazı kimyasal analizleri. *Yüzüncü Yıl Üniversitesi Tarım Bilimleri Dergisi, 14*(1), 1-6.

Konak, M., Merve, A., & Şahan, Y. (2017). Yenilebilir yabani bitki *Gundelia tournefortii*'nin antioksidan özelliklerinin belirlenmesi. *Uludağ Üniversitesi Ziraat Fakültesi Dergisi, 31*(2), 101-108.

Koc, H., & Sari, H. (2009). Trace metal contents of some medicinal, aromatic plants and soil samples in the Mediterranean region, Turkey. *Journal of Applied Chemical Research, 8*, 52-57

Kordalı, Ş., Bozhüyük, A. U., Beyzi, E., Güneş, A., & Turan, M. (2021). Tıbbi bitki olarak kullanılan *Malva sylvestris* L. ve *Alcea rosea* L. türlerinin antioksidant enzim, fenolik madde ve bitki besin element içerikleri. *Journal of the Institute of Science and Technology, 11*(1), 786-794.

Korkmaz, K., & Türkiş, S. Türkiye'deki bazı orkide türlerinin mineral besin elementi ve ağır metal konsantrasyonları. *Akademik Ziraat Dergisi, 10*(1), 137-144.

Meral, R., Doğan, İ. S., & Kanberoğlu, G. S. (2012). Fonksiyonel gıda bileşeni olarak antioksidanlar. *Journal of the Institute of Science and Technology, 2*(2), 45-50.

Meraler, S. A. (2010). "Mahlep (*Prunus mahaleb* L.)in Bitki Kısımlarında Mineral Bileşiminin Belirlenmesi", *Kilis 7 Aralık Üniversitesi Fen Bilimleri Enstitüsü*, Yüksek Lisans Tezi.

Milani, R. F., Silvestre, L. K., Morgano, M. A., & Cadore, S. (2019). Investigation of twelve trace elements in herbal tea commercialized in Brazil. *Journal of Trace Elements in Medicine and Biology*, *52*, 111-117.

Mohammed, F. S., Karakaş, M., Akgül, H., & Sevindik, M. (2019a). Medicinal properties of *Allium calocephalum* collected from Gara Mountain (Iraq). *Fresen Environ Bull, 28*(10), 7419-7426.

Mohammed, F. S., Günal, S., Şabik, A. E., Akgül, H., & Sevindik, M. (2020a). Antioxidant and Antimicrobial activity of *Scorzonera papposa* collected from Iraq and Turkey. *Kahramanmaraş Sütçü İmam Üniversitesi Tarım ve Doğa Dergisi, 23*(5), 1114-1118.

Mohammed, F. S., Günal, S., Pehlivan, M., Doğan, M., Sevindik, M., & Akgül, H. (2020b). Phenolic content, antioxidant and antimicrobial potential of endemic *Ferulago platycarpa. Gazi University Journal of Science, 33*(4), 670-677.

Mohammed, F. S., Sevindik, M., Bal, C., Akgül, H., & Selamoglu, Z. (2019b). Biological Activities of *Adiantum capillus-veneris* Collected from Duhok Province (Iraq). *Communications Faculty of Sciences University of Ankara Series C Biology, 28*(2), 128-142.

Mohammed, F. S., Pehlivan, M., Sevindik, E., Akgul, H., Sevindik, M., Bozgeyik, I., & Yumrutas, O. (2021). Pharmacological properties of edible *Asparagus acutifolius* and *Asparagus officinalis* collected from North Iraq and Turkey (Hatay). *Acta Alimentaria*, 50(1), 136-143.

Mohammed, F. S., Akgul, H., Sevindik, M., & Khaled, B. M. T. (2018). Phenolic content and biological activities of *Rhus coriaria* var. *zebaria. Fresenius Environmental Bulletin, 27*(8), 5694-5702.

Nishina, A., Kubota, K., Kameoka, H., & Osawa, T. (1991). Antioxidizing component, musizin, in *Rumex japonicus* Houtt. *Journal of the American Oil Chemists Society*, *68*(10), 735-739.

Nohutçu, L., Tunçtürk, M., & Tunçtürk, R. (2019). Yabani bitkiler ve sürdürülebilirlik. *Yüzüncü Yıl Üniversitesi Fen Bilimleri Enstitüsü Dergisi*, *24*(2), 142-151.

Özcan, M. M., & Akbulut, M. (2008). Estimation of minerals, nitrate and nitrite contents of medicinal and aromatic plants used as spices, condiments and herbal tea. *Food chemistry*, *106*(2), 852-858.

Pehlivan, M., Mohammed, F. S., Sevindik, M., & Akgul, H. (2018). Antioxidant and oxidant potential of *Rosa canina. Eurasian Journal of Forest Science, 6*(4), 22-25.

Sarac, H. (2021). Bioactive components and biological activities of the cardamom (*Elettaria cardamomum* L.) plant. *Research & Reviews In Science And Mathematics*, 91-108.

Saraç, H., Daştan, T., Demirbaş, A., Daştan, S. D., Karaköy, T., & Durukan, H. (2018a). Madımak (*Polygonum cognatum* Meissn.) bitki özütlerinin besin elementleri ve in vitro antikanserojen aktiviteleri yönünden değerlendirilmesi. *Ziraat Fakültesi Dergisi*, 340-347.

Saraç, H., Daştan, T., Durukan, H., Daştan, S. D., Demirbaş, A., & Karaköy, T. (2018b). Kırmızı Gelincik (Fam: Papaveraceae, *Glaucium grandiflorum* Boiss. &Huet var. *grandiflorum*) Bitkisinin farklı özütlerinin besin elementi içeriğinin ve in vitro antiproliferatif etkilerinin değerlendirilmesi. *Ziraat Fakültesi Dergisi*, 417-428.

Saraç, H., Demirbaş, A., Daştan, S. D., Ataş, M., Çevik, Ö., & Eruygur, N. (2019). Evaluation of nutrients and biological activities of kenger (*Gundellia tournefortii* L.) seeds cultivated in Sivas province. *Turkish Journal of Agriculture-Food Science and Technology*, *7*(sp2), 52-58.

Saraç, H., Durukan, H., & Demirbaş, A. (2021). Nutrient concentrations and antioxidant activity of *Achillea millefolium* L. (Yarrow), one of the important medicinal plants. *Turkish Journal of Agriculture-Food Science and Technology*, *9*(3), 590-594.

Saraç, H., & Tüzün, B. (2021). Activities of *Mentha pulegium* extract against breast cancer proteins. 1st International Conference on Applied Engineering and Natural Sciences, November 1-3, 2021, Turkey, 1018-1024.

Sarkar, S. (2007). Functional foods as self-care and complementary medicine. *Nutrition & Food Science, 37*(3), 160-167.

Sarma, H., Deka, S., Deka, H., & Saikia, R. R. (2012). Accumulation of heavy metals in selected medicinal plants. *Reviews of environmental contamination and toxicology*, 63-86.

Sevim, Ö. (2018). "Ağrıda Yetişen Çeşitli Tıbbi Bitkilerin Bazı Makro ve Mikro Element İçeriklerinin Belirlenmesi ve Metabolik Enzimlere Etkileri", *Ağrı İbrahim Çeçen Üniversitesi Fen Bilimleri Enstitüsü,* Yüksek Lisans Tezi.

Sevindik, M., Akgul, H., Dogan, M., Akata, I. & Selamoglu, Z. (2018). Determination of antioxidant, antimicrobial, DNA protective activity and heavy metals content of *Laetiporus sulphureus*. *Fresenius Environmental Bulletin, 27*(3), 1946-1952.

Sevindik, M., Akgul, H., Pehlivan, M. & Selamoglu, Z. (2017). Determination of therapeutic potential of *Mentha longifolia* ssp. *longifolia*. *Fresenius Environmental Bulletin, 26*(7), 4757-4763.

Sevindik, M., Akgul, H., Selamoglu, Z., & Braidy, N. (2020). Antioxidant and antigenotoxic potential of *Infundibulicybe geotropa* mushroom collected from Northwestern Turkey. *Oxidative medicine and cellular longevity*, *2020*.

Şekeroğlu, N., Özkutlu, F., Deveci, M., Dede, Ö., & Yılmaz, N. (2005). Ordu ve yöresinde sebze olarak tüketilen bazı yabani bitkilerin besin değeri yönünden incelenmesi. *Türkiye VI. Tarla Bitkileri Kongresi*, 5-9.

Tunçtürk, R. (2013). Fonksiyonel gıda olarak tüketilen semizotunun (*Portuleca oleracea* L.) tıbbi bitki olarak değerlendirilmesi. *Türk Bilimsel Derlemeler Dergisi*, *6*(1), 101-103.

Turan, M., Kordali, S., Zengin, H., Dursun, A., & Sezen, Y. (2003). Macro and micro mineral content of some wild edible leaves consumed in Eastern Anatolia. *Acta Agriculturae Scandinavica, Section B-Plant Soil Science*, *53*(3), 129-137.

Urhan, Y., Ege, M. A., Öztürk, B., & Elgin Cebe, G. (2016). Türkiye gıda bitkileri veritabanı. *Ankara Ecz. Fak. Derg., 40*(2), 43-57.

Varlı, M., Hancı, H., & Kalafat, G. (2020). Tıbbi ve aromatik bitkilerin üretim potansiyeli ve biyoyararlılığı. *Research Journal of Biomedical and Biotechnology*, *1*(1), 24-32.

Vural, A. (2004). Fonksiyonel gıdalar ve sağlık üzerine etkileri. *Gıda ve Yem Bilimi Teknolojisi*, *6*, 51-58.

Yücel, E., Tapırdamaz, A., Şengün, İ. Y., Yılmaz, G., & Ak, A. (2011). Kisecik Kasabası Karaman ve çevresinde bulunan bazı yabani bitkilerin kullanım biçimleri ve besin öğesi içeriklerinin belirlenmesi. *Biyolojik Çeşitlilik ve Koruma*, *4*(3), 71-82.

Chapter 4

SOME BIOSYSTEMATIC STUDIES ON THREE *THESIUM* L. TAXA SPREADING NATURALLY IN CENTRAL ANATOLIA

İlaha RAMAZANLI[1]

Onur KOYUNCU[2]

1 Eskişehir Osmangazi University Institute of Science and Technology, Eskişehir. https://orcid.org/0000-0002-6335-9622

2 Eskişehir Osmangazi University, Faculty of Arts and Sciences, Eskişehir. https://orcid.org/0000-0002-0364-6638

INTRODUCTION

Turkey is rich in plant diversity, highly endemism, variability in topographic structure and climate types, geographical location, having different soil groups, creating a bridge between Southern Europe and Southwest Asia, being the gene center of many species and genera, having different geological and geomorphological structures. It is one of the countries with the richest flora in the world (Düşen, 2004; Duman and Byfield, 2000; Davis and Hedge, 1975; Kabadere *et al*. 2021: Öztopçu Vatan *et. al*. 2011). At the same time, Turkey's location at the intersection of Iran-Turanian, Euro-Siberian and Mediterranean Phytogeographical Regions is one of the most important reasons for having this rich flora (Davis *et al.,* 1971).

Thesium genus is represented by approximately 350 species in the Santalaceae family (Forest and Manning, 2013; Nickrent and Garcia, 2015; The Angiosperm Phylogeny Group, 2016). As a result of molecular phylogenetic studies, six classes, including the Thesiaceae family, were revealed (Nickrent *et al.,* 2010; Nickrent & García, 2015). However, in the later classification (APG, 2016), the Thesiaceae family was not accepted and the *Thesium* genus was placed in the Santalaceae family (Gudzinskas *et al.* 2017). *Thesium* genus is distributed in South America, tropical and North Africa, South Africa, Asia and Europe (Germishuizen *et al.* 2006; Forest and Manning, 2013; Nickrent and Garcia, 2015). When we examine the literature, we see that most of the genus *Thesium* is concentrated in South Africa and some species are very valuable ethnobotanically for this country.

The genus *Thesium* was first described by Linnaeus in 1753. According to Linnaeus' description, there were four species of this genus. Later, De Candolle (1857) and Sonder (1857a) published studies on the genus *Thesium* simultaneously, but independently of each other. As a result of these publications, many inconsistencies and contradictions have emerged. To remove some of the conflicting information, Sonder (1857b) has published a new study. Later, a detailed taxonomic study was carried out by Hill (1915, 1925) on the species settled in South Africa. This study also includes the description of several new species (Moore *et al*., 2010). After Hill's study, 38 new species of *Thesium* were described in South Africa (for example, Brown, 1932; Brenan, 1979). However, there is no up-to-date identification key, as no

work has been done to consolidate and evaluate all available information on *Thesium* species grown in South Africa. As a result, it is thought that the genus *Thesium* is a plant group with high priority for South Africa and should be examined in detail from a taxonomic perspective (Victor *et al.*, 2015).

As a result of ethnobotanical studies on the genus *Thesium* (eg Watt and Breyer-Brandwijk, 1962; Archer, 1984; Neuwinger, 2000; Huang *et al.*, 2009), it is seen that this genus has a very important place in daily life for rural societies.

At the same time, ethnobotanical studies need to be done in more detail because the usage areas related to the genus are not well documented (Hendrych, 1972).

Although 18 species belonging to the genus *Thesium* were recorded in the seventh volume of the Flora of Turkey (Davis, 1982), according to the list of plants in Turkey, there are 16 species of the genus Thesium today. Fosur of these species are endemic (Kandemir, 2012).

When we examine the Turkish literature, there is no study except the flora records and various flora studies about the genus *Thesium*, except for the location information of the species belonging to this genus.

There is no previous study in the world or in Turkey on *Thesium* species (*T. billardieri, T. procumbens, T. scabriflorum*), which is the subject of this article. In this study, it is aimed to give current location information of *Thesium* species naturally distributed in Eskişehir, to identify them by performing anatomical and morphological studies on these species, and to contribute to possible future studies, especially on Eskişehir flora.

In the Flora of Turkey, 16 species of *Thesium* L. have been recorded so far. 4 of these species are endemic. These species are given in table 1 with their Turkish names.

Table 1. Naturally Distributed *Thesium* Taxa in Turkey. (For https://bizimbitkiler.org.tr/yeni/demos/technical/)

No	Taxa	Turkish Names	Phytogeographic Region	Endemism Status
1	*Thesium alpinum* L.	Yaylagüveleği	Euro-Siberian	Not
2	*Thesium arvense*	Tezgüvelek	Euro-Siberian	Not
3	*Thesium bergeri*	Korugüveleği	East	Not
4	*Thesium bertramii*	Özgüvelek	Iranian-Turanian	Endemic

5	*Thesium billardieri*	Meşegüveleği	Iranian-Turanian	Not
6	*Thesium*	Gavurgüveleği	East	Endemic
7	*Thesium*	Tuzgüveleği	Iranian-Turanian	Not
8	*Thesium*	Çatalgüvelek	Euro-Siberian	Not
9	*Thesium humile*	Bodurgüvelek	Mediterranean	Not
10	*Thesium*	Koçgüveleği	Iranian-Turanian	Not
11	*Thesium linophyllon*	Ulugüvelek	Euro-Siberian	Not
12	*Thesium*	Kocagüvelek	Iranian-Turanian	Not
13	*Thesium oreogetum*	Artosgüveleği	Iranian-Turanian	Endemic
14	*Thesium*	Yergüveleği	Iranian-Turanian	Not
15	*Thesium*	Kabagüvelek	Iranian-Turanian	Endemic
16	*Thesium tauricolum*	Güvelek	Iranian-Turanian	Not

MATERIAL

Plant materials

Thesium procumbens: Plant material was collected from the open areas behind the ARUM building, in Eskişehir Osmangazi University Meşelik Campus, N 39° 44′ 38,0″-E 030° 28′ 22,6″, 825m. OUFE:21520.

Thesium scabriflorum: Plant material was collected from natural areas around Alp Residences in Eskişehir Çankaya neighborhood, N 39° 45′ 01,2″-E 030° 31′ 44,9″, 918m., OUFE:21521.

Thesium billardieri: Plant material was collected from the rocky areas of the roadsides between Alpagut (Eskişehir) village to İnhisar (Bilecik). N 40° 01′ 43,4″-E 030° 29′ 27,7″, 200 m., OUFE:21519.
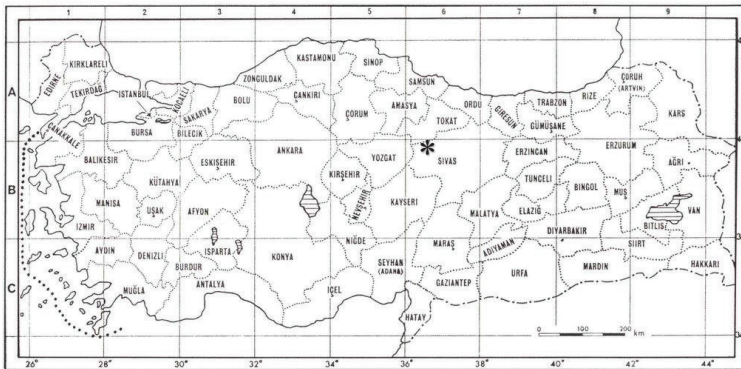

Figure 1. The locality where plant materials are collected.

METHODS

Morphological
The identification of the species was made with the aid of the assignment keys written by A. G. Miller, available in the seventh volume of "Flora of Turkey and the East Aegean Islands" edited by Davis (1982). Later, the measurements of the characters such as leaves, flowers, stems and fruits of the plant samples we collected were made with a ruler under the Leica EZ4 brand microscope.

Anatomical
For anatomical study, the morphological parts of the plant were kept in 70% ethanol until microscopic examinations were made. Then, leaf transverse and superficial, stem transverse and root transverse sections of the plant were taken with the help of a razor by hand and examined in the Zen 2.3 Program with the (Zeiss Axiobserver Z) branded light microscope in Eskişehir Osmangazi University Research and Application Center.

MORPHOLOGICAL FINDINGS

Thesium procumbens C. A. Mey.
Perennial herbaceous plants, stem simple or branched, green in color 4-24 cm, decumbent. Leaves linear, 20-40 × 1-3 mm. Inflorescence raceme; flowers are white; perianth bell, 1.8-3 mm; peduncle 2-2.8 mm. Brackets-1, edges scabrite, 7-12 × 0.5-1.1 mm; bracteoles-2, margins scabrite, 2.5-5.5 × 0.2-0.6 mm. Fruit glabrous, nut-ovoid, with reticulate veins, 2-4 mm.

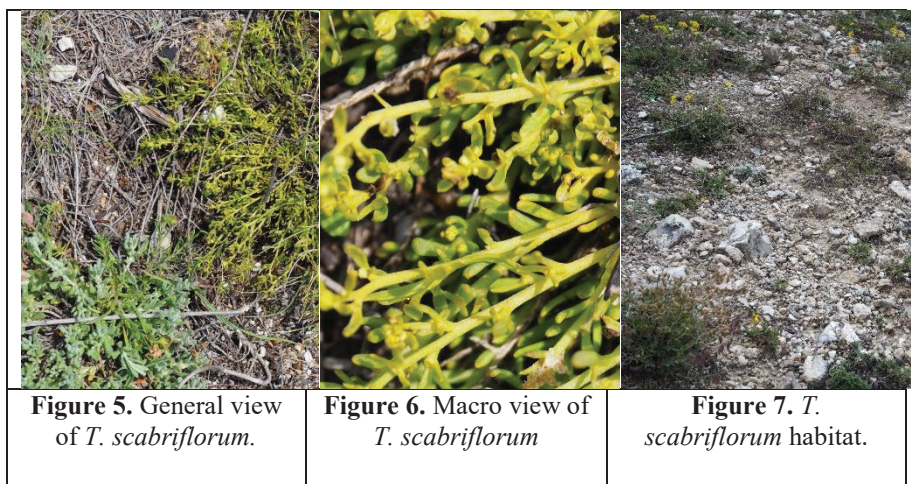| **Figure 2.** General view of *T. procumbens.* | **Figure 3.** A close view of *T. procumbens.* | **Figure 4.** *T. procumbens* habitat. |

Thesium scabriflorum P. H. Davis

Perennial herbaceous plant, all scabrite. Stem simple or branched, green, 2-9 cm, procumbent. Leaves linear, linear-elliptic, fleshy, 3-8 × 0.8-1 mm. Inflorescence raceme; flowers are white on the inside, pale green on the outside; perianth tube, 2-3 mm, peduncle 1-2 mm. Brackets-1, 4-6 × 0.5-1 mm; bracteoles-2, 1.8-3 × 0.2-0.5 mm. Fruit nut-ovoid, scabrid, with longitudinal veins, 3-4 mm.

Table 2. Comparison of the morphological characters of *T. procumbens* species and literature data.

Morphological	This study	A. G. Miller (1982)
Stem	Decumbent, glabrous, simple or branched 4-24cm	Decumbent 2-10(-15) cm
Leaf	Linear 20-40 × 1-3 mm	Linear, linear-eliptik (1-)2-10(-17) × 0,75-1,25 mm
Inflorences	Rasemose	Rasemose
Flower	White; perianth bell 1.8-3mm peduncle 2-2.8 mm	Beyaz; periant geniş çansı 1-1,5(-1,75) mm
Fruit	Nut-ovoid, glabrous, reticulated, 2-4 mm	Nut-ovoid, glabrous, reticulated, 2-2,5 × 1,25-1,75 mm
Bract	Scabrid edges, 7-12 × 0,5-1,1 mm	Leaf like, 2-3 times longer than fruit
Bracteol	Scabrid edges, 2,5-5,5 × 0,2-0,6 mm	-

| Figure 5. General view of *T. scabriflorum*. | Figure 6. Macro view of *T. scabriflorum* | Figure 7. *T. scabriflorum* habitat. |

Thesium billardieri Boiss.

Plant biennial, stem branched, 28-38 cm, erect. Leaves linear, linear-elliptic, 13-30 × 0.9-1.5 mm. Inflorescence raceme, sometimes branched; flowers are white; perianth bell, 2.3-3 mm, peduncle 1.5-6 mm. Brackets-1, 7-12 × 0.5-0.9 mm, bracteoles-2, 2- 3.5× 0.2-0.5 mm. Fruit nut ellipsoid, reticulate veined, glabrous, 3-4 mm.

| Figure 8. General view of *T. billardieri*. | Figure 9. Macro view of *T. billardieri* | Figure 10. *T. billardieri* habitat. |
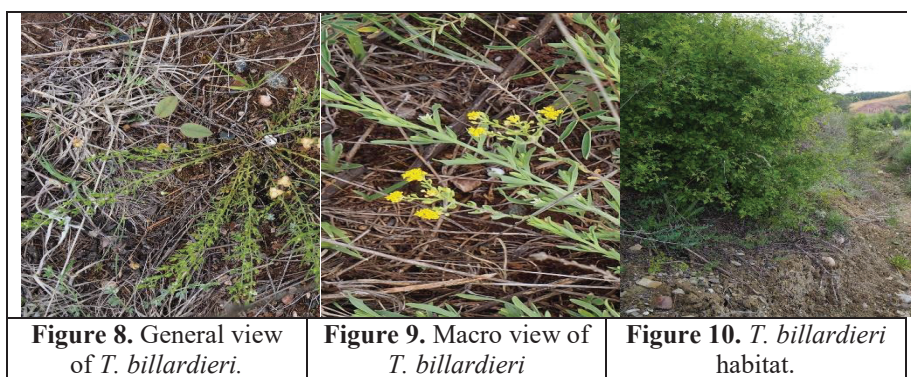
Table 3. Comparison of the morphological characters of *T. billardieri* with literature data.

Morphological Characters	This study	A. G. Miller (1982)
Stem	Erect branched 28-38cm	Procumbent to ascending Simple or slightly branched
Leaf	linear, linear-elliptical 13-30×0.9-1.5mm	Stem narrow, oblanceolate 3-30 × 1-1.5mm; thick at the base,
Inflorences	Racemose	Panicula 1-3(-5) flowering
Flower	White; perianth bell 2.3-3mm; peduncle 1.5-6 mm	White, with green veins; perianth bell (1.75-)2.75-3(-3.5)mm
Fruits	Nut-ellipsoid, glabrous, reticulated veins 3-4mm	Nut-obovate, glabrous, reticulated 4-5.5×2-2.75mm
Bract	7-12 × 0,5-0,9 mm	1-3(-4) times longer than the fruit
Bracteol	2- 3,5× 0,2-0,5 mm	-

Anatomical Findings
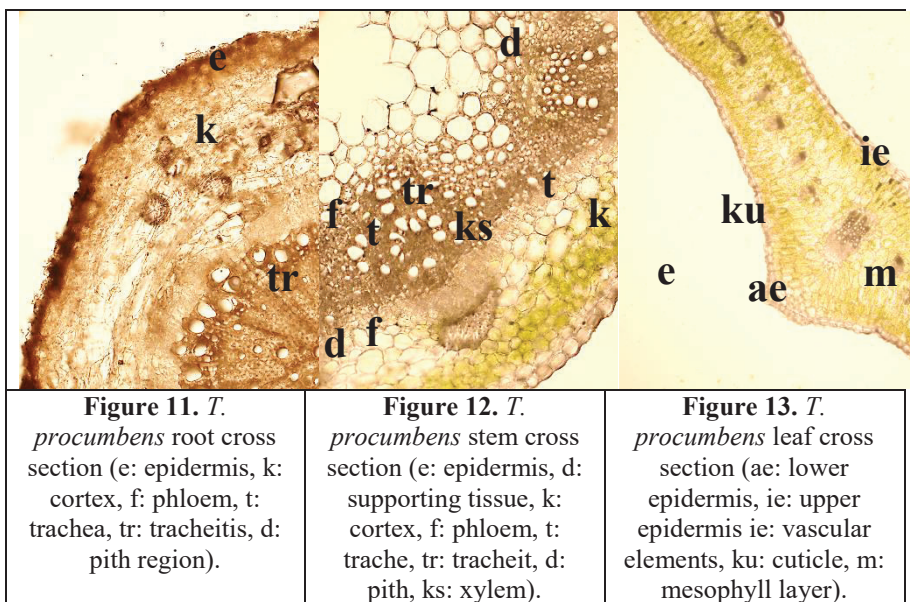
Thesium procumbens C. A. Mey.

Root
The outermost layer is a protective layer of epidermal cells. The presence of a thick cortex layer consisting of multi-row parenchymatic cells under the epidermis draws attention. The cortex layer consists of parenchymatic cells, and it can be mentioned that there are support tissue cells with sclerenchymatic

character and secretory tissue elements in it. Later, transmission elements consisting of several rows of phloem elements and xylem elements descending to the center are observed. The core region is parenchymatic.

Stem

The presence of a multi-row parenchymatic cortex layer is seen just below the protective layer consisting of 1-2 rows of epidermis cells. Within the cortex layer, there are support tissue elements consisting of sclerenchyma bundles. The structure consisting of several rows of phloem and multiple rows of xylem elements just below constitute the transmission elements. In the xylem, the trachea and tracheit cells can be easily separated from each other. In the center is the parenchymatic pith region.

| Figure 11. *T. procumbens* root cross section (e: epidermis, k: cortex, f: phloem, t: trachea, tr: tracheitis, d: pith region). | Figure 12. *T. procumbens* stem cross section (e: epidermis, d: supporting tissue, k: cortex, f: phloem, t: trache, tr: tracheit, d: pith, ks: xylem). | Figure 13. *T. procumbens* leaf cross section (ae: lower epidermis, ie: upper epidermis ie: vascular elements, ku: cuticle, m: mesophyll layer). |

Leaf

The lower and upper surfaces of the leaf can be easily distinguished by looking at the vein protrusion. The side where the vascular protrusion is located is the lower epidermis and the other side is the upper epidermis.

Just below the protective layer consisting of a single layer of epidermis, the mesophyll layer consisting of multiple layers of palisade parenchyma cells is seen. Chloroplasts are noted in the

palisade parenchyma. Phloem and xylem elements forming the main vein are in question in the center. In addition, lateral veins repeated 8-10 times on the right and left of the main vein are also seen.
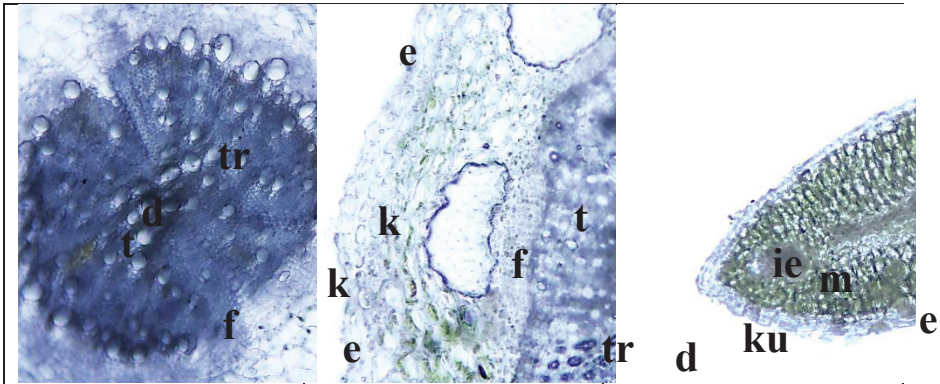
Epidermis cells are rectangular, with an average length of 3-4 times its width. Stomach cells are observed from place to place among the epidermis cells.

Epidermis cells are rectangular, with an average length of 3-4 times its width. Stomach cells are observed from place to place among the epidermis cells.

| **Figure 14.** *T. procumbens* leaf upper superficial section (e: epidermis). | **Figure 15.** *T. procumbens* leaf lower superficial section (e: epidermis). |

Thesium scabriflorum P. H. Davis

| **Figure 16.** *T. scabriflorum* root cross section (e: epidermis, k: cortex, f: phloem, t: trachea, tr: tracheitis, d: pith region). | **Figure 17.** *T. scabriflorum* stem cross section (e: epidermis, d: supporting tissue, k: cortex, f: phloem, t: trachea, tr: tracheitis, d: pith region). | **Figure 18.** *T. scabriflorum* leaf cross section (e: epidermis ie: vascular elements, ku: cuticle, m: mesophyll layer) |

Root

The outermost layer is the protective layer consisting of epidermal cells. Beneath the epidermis is a thick cortex layer composed of multiple rows of parenchymatic cells. The cortex layer consists of parenchymatic cells and there are support tissue cells with sclerenchymatic character in it. In addition, the presence of secretory tissue elements in the cortex layer can be mentioned. Then, transmission elements consisting of several rows of phloem elements and xylem elements descending to the center are observed. Tracheal and tracheit elements can be easily distinguished. The pith region consists of parenchymatic cells.

Stem

The 2-3-row epidermis forms the protective tissue. In the lower part, there is a cortex layer consisting of 8-10 rows of parenchymatic cells. The sclerenchyma bundles, which cover large areas in the cortex layer, form the supporting tissue. In addition, cortex elements with the character of storage parenchyma, where ergastic substances are stored, are also noteworthy. Conduction elements consist of 2-3 rows of phloem and xylem elements going up to the center. The core region consists of parenchyma cells.
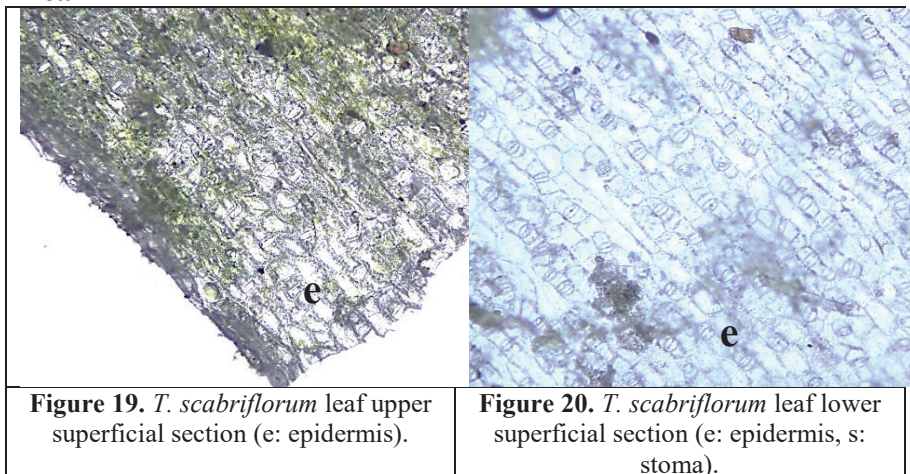
Leaf

Figure 19. *T. scabriflorum* leaf upper superficial section (e: epidermis).	**Figure 20.** *T. scabriflorum* leaf lower superficial section (e: epidermis, s: stoma).

Stomatal openings are observed from place to place between the protective layer consisting of 1-2 layers of epidermis

located just below the cuticle layer. In the mesophyll layer, which consists of 3-4 rows of palisade parenchyma, 3 vascular structures are seen, one in the burial center and one on both sides. Phloem and xylem elements forming the vascular structure and supporting tissue elements on their sides are seen.

It was determined that the epidermis cells showed a polygonal rectangular or square structure. The crystal structures of the cells attract attention. Among the epidermis cells, amarilis type stomatal cells are observed.

It was observed that the epidermis cells showed a rectangular structure. Among the epidermis cells, amarilis type stomatal cells are seen intensely.

Thesium billardieri Boiss.

Root
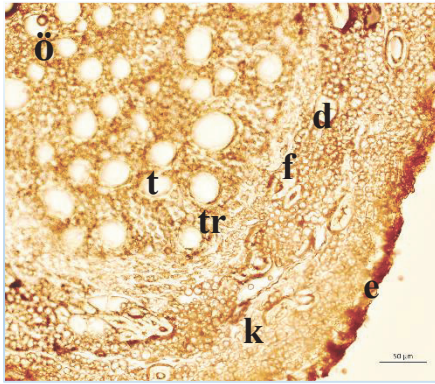
Figure 21. *T. billardieri* root cross section (e: epidermis, k: cortex, f: phloem, t: trachea, tr: tracheitis, d: supporting tissue, d: pith region).

The outermost layer is the protective layer consisting of epidermal cells. Beneath the epidermis is a thick cortex layer composed of multiple rows of parenchymatic cells. The cortex layer consists of parenchymatic cells and there are support tissue cells with sclerenchymatic character in it. In addition, the presence of secretory tissue elements in the cortex layer can be mentioned. Then, transmission elements consisting of several rows of phloem

elements and xylem elements descending to the center are observed. Tracheal and tracheit elements can be easily distinguished. The pith region consists of parenchymatic cells.

Stem
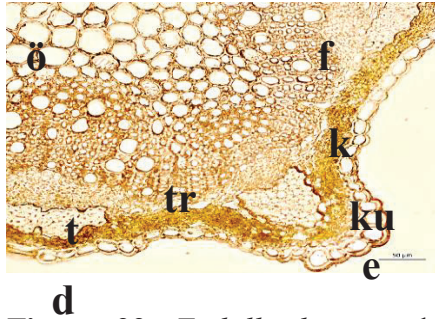
Figure 22. *T. billardieri* trunk cross section (e: epidermis, d: supporting tissue, k: cortex, ku: cuticle, f: phloem, t: trachea, tr: tracheit, d: pith region).

A single layer of epidermis forms the protective tissue. Under the protective tissue is the cortex layer, which consists of several rows of cells. The sclerenchyma bundles, which cover large areas in the cortex layer, form the supporting tissue. In addition, storage and secretory tissue elements are observed in the cortex layer. Conduction elements consist of 2-3 rows of phloem and xylem elements going up to the center. The core region consists of parenchyma cells.
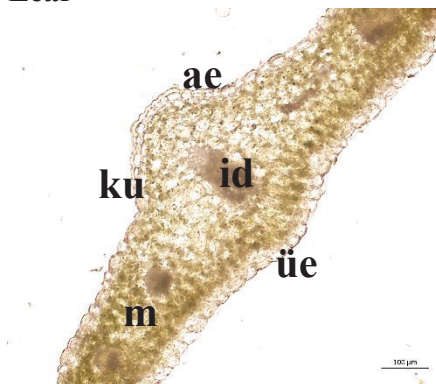
Leaf

Figure 23. *T. billardieri* leaf cross section (ae: lower epidermis, ue: upper epidermis, id: vascular bundle, ku: cuticle, m: mesophyll).

The lower and upper surfaces of the leaf can be easily distinguished by looking at the vein protrusion. The side where the vascular protrusion is located is the lower epidermis and the other side is the upper epidermis. The mesophyll layer consists of 10-12 rows of parenchymatic cells. Chloroplasts and ergastic substances are noteworthy in the parenchymatic mesophyll. Phloem and xylem elements forming the main vein are in question in the center. In addition, lateral veins repeated 3-4 times on the right and left of the main vein are also seen.
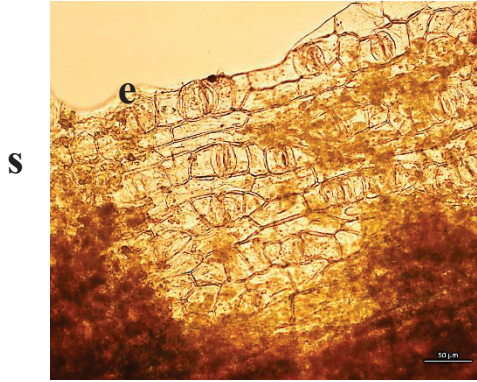
Figure 24. *T. billardieri* leaf lower superficial section (e: epidermis, s: stoma).

It was determined that the epidermis cells showed a polygonal rectangular or square structure. It is noteworthy that the cells have thick walls and no spaces. Among the epidermis cells, amarilis type stomatal cells are observed.
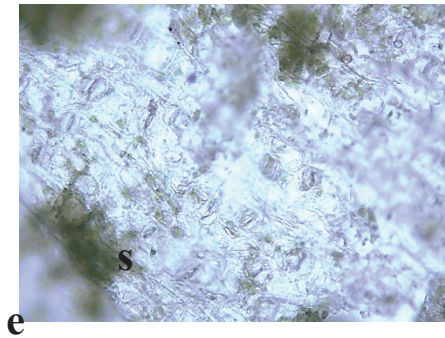
Figure 25. *T. billardieri* leaf upper superficial section (e: epidermis, s: stoma).

It was determined that the epidermis cells showed a polygonal rectangular or square structure. It is noteworthy that the cells have thick walls and no spaces. Among the epidermis cells, amarilis type stomatal cells are observed.

Herbarium samples

Herbarium samples of the herbal materials used in this research were prepared according to international rules and placed in Eskişehir Osmangazi University Herbarium Center (OUFE).

Figure 26. *T. procumbens* herbarium specimen (OUFE: 21520)	**Figure 27.** *T. scabriflorum* herbarium specimen (OUFE: 21521)	**Figure 28.** *T. billardieri herbarium* specimen (OUFE: 21519)

Acknowledgements: This article was prepared from İlaha Ramazanlı's master thesis.

2. CONCLUSION and DISCUSSION

In this study, 3 species of *Thesium* genus naturally distributed in Eskişehir were collected from different localities through field studies. Some of the collected samples were used for anatomical and morphological studies, while the other part was

turned into a herbarium sample and put in Eskişehir Osmangazi University Herbarium (OUFE).

In the morphological study conducted on the species that are the subject of the article, up-to-date data were obtained by determining the characteristics of the plants, these data were compared with the data in the 7th volume of the Flora of Turkey, the differences and similarities between them were revealed and some morphological measurements (flower stem, bract and bracteoles etc.) were made by us for the first time.

The descriptions of the species were reconstructed according to the morphological data obtained from the studies in this article.

Thesium procumbens: Perennial herbaceous plants, stem simple or branched, green in color 4-24 cm, decumbent. Leaves linear, 20-40 × 1-3 mm. Inflorescence raceme; flowers are white; perianth bell, 1.8-3 mm; peduncle 2-2.8 mm. Brackets-1, edges scabrite, 7-12 × 0.5-1.1 mm; bracteoles-2, margins scabrite, 2.5-5.5 × 0.2-0.6 mm. Fruit glabrous, nut-ovoid, with reticulate veins, 2-4 mm.

Thesium scabriflorum: Perennial herbaceous plant, all scabrite. Stem simple or branched, green, 2-9 cm, procumbent. Leaves linear, linear-elliptic, fleshy, 3-8 × 0.8-1 mm. Inflorescence raceme; flowers are white on the inside, pale green on the outside; perianth tube, 2-3 mm, peduncle 1-2 mm. Brackets-1, 4-6 × 0.5-1 mm; bracteoles-2, 1.8-3 × 0.2-0.5 mm. Fruit nut-ovoid, scabrid, with longitudinal veins, 3-4 mm.

Thesium billardieri: Plant biennial, stem woody branched at base, 28-38 cm, erect. Leaves linear, linear-elliptic, 13-30 × 0.9-1.5 mm. Inflorescence raceme, sometimes branched; flowers are white; perianth bell, 2.3-3 mm, peduncle 1.5-6 mm. Brackets-1, 7-12 × 0.5-0.9 mm, bracteoles-2, 2- 3.5× 0.2-0.5 mm. Fruit nut ellipsoid, reticulate veined, glabrous, 3-4 mm.

When the anatomical structures of the 3 Thesium species, which are the subject of this article, are examined, it is seen that the root structures are largely similar to each other. When we examine the root cross-sections of all 3 species, we see a protective layer consisting of 2-5 rows of epidermis cells on the outside, and a cortex layer consisting of 8-14 rows of parenchymatic cells below it. Conduction bundles consist of several rows of phloem and multiple rows of xylem elements extending to the center. The pith region with parenchymatic character is observed. In the transverse

sections of the trunk, the epidermis layer on the outside, the cortex layer consisting of parenchymatic cells under it, and the sclerenchyma bundles forming the support tissue, storage and secretory parenchyma cells are seen in it. Especially in *T. scabriflorum* species, cortical elements with storage parenchyma character where ergastic substances are stored, and in *T. billardieri* cortex elements with storage and secretory tissue character are observed. In all 3 species, vascular bundles are composed of phloem and xylem elements. Phloem elements; It consists of sieve tubes, companion cells, phloem parenchyma, and phloem sclerenchyma. If xylem; consists of trachea, tracheitis, xylem parenchyma and xylem sclerenchyma. The pith region is parenchymatic in all species.

When the leaf cross-sections of the species are examined, it is seen that the leaf structures of *T. procumbens* and *T. billardieri* are similar to each other. In both species, it is possible to easily distinguish the lower and upper sides of the leaf by looking at the vein protrusion. On the outside, the protective layer consisting of epidermis cells is seen, and underneath it, the mesophyll layer consisting of multi-rowed palisade parenchyma cells. In the center, the main vein consisting of phloem and xylem elements and 3-6 side veins are observed on its right and left. Chloroplasts are seen in the mesophyll layer of *T. procumbens* species, chloroplasts and ergastic substances are seen in *T. billardieri* species. The cuticle layer is observed in the cross section of the leaf of *T. scabriflorum* species, and the epidermis layer, which also contains stomatal openings, is observed under it. The mesophyll layer consists of 3-4 rows of palisade parenchyma and a total of 3 vascular structures are seen, one in the center and one on both sides. Epidermis cells in *T. scabriflorum* leaf lower superficial sections show a rectangular structure, *T. scabriflorum* leaf upper superficial sections and *T. billardieri* leaf lower and upper superficial sections show a rectangular or square structure. Among the epidermis cells, amarilis type stomatal cells are seen, densely in the lower superficial section of the *T. scabriflorum* leaf.

With this research, anatomical, morphological and chorological studies were carried out for the first time in 3 *Thesium* L. (Tezgüvelek) species naturally distributed in Eskişehir. The obtained data were compared with the data of previous studies on the subject and the differences were revealed. In addition, some anatomical, morphological and chorological features of the study

plants that were not recorded in the previous literature were determined for the first time in this article

When the data obtained from this study are evaluated, it is seen that there is a need for more detailed and more biosystematic studies on *Thesium* L. taxa in Turkey. As can be seen from this study we carried out locally, it is seen that anatomical and morphological characters vary widely in some taxa, especially in *Thesium billardieri* species, and the descriptions need to be expanded by revealing more clearly. After all these detailed studies, the genus identification key should be made again.

We believe that this thesis contributes to the determination, recognition and evaluation of the floristic richness of Eskişehir.

References

APG, 2016, An update of the Angiosperm Phylogeny Group classification for the orders and families of flowering plants, APG IV, Botanical Journal of the Linnaean Society, 181, 1-20.

Archer, W., 1984, Austral Toad-flax R. Brown (Santalaceae)-field notes and observations. The Victorian Naturalist 101, 81-85.

Brenan, J. P., 1979, Three new species of *Thesium* (Santalaceae) from South Africa. Kew Bulletin, 395-397.

Brown, N.E., 1932, *Thesium* L., in: Burtt-Davy, J. (Ed.), A manual of the flowering plants and ferns of the Transvaal with Swaziland, South Africa. Longmans, Green and Co., London, pp.455-462.

Burtt, B. L., 2001, Tournefort in Turkey (1701-1702), The Karaca Arboretum Magazine, 6, 2, 45-54.

Nova Guinea, New Series 6, 261-277.

Davis, P.H., Harper, P.C. and Hedge, I.C., 1971, Plant Life of South-West Asia, Botanical Society of Edinburgh.

Davis P.H., and Hedge I.C., 1975, "The Flora of Turkey: Past, Present and Future", Candollea 30, 331-351.

Davis, P. H., 1982, Flora of Turkey and The East Aegean Islands, Vol. 7, Edinburgh Univ. Press, Edinburgh.

De Candolle, A., 1857, Espéces nouvelles du genre *Thesium* présentées à la Société de physique et d'histoire naturelle de Genève dans sa séance du 25 Mai 1857. Ramboz et Schuchardt, Genève, pp. 1-8.

Der, J. P., 2005, Molecular phylogenetics and classification of Santalaceae. M.S. thesis. Carbondale, IL: Southern Illinois University.

Der, J. P., Nickrent, D. L., 2008, A molecular phylogeny of Santalaceae (Santalales). Systematic Botany, 33(1), 107-116.

Duman, H., Byfield, A., 2000, *Salvia albimaculata*, Curtir's Botanical Magazine, Blackwell Publishers, Vol. 17, Part 2, 47-48.

Düşen, O. D., 2004, Akdeniz Bölgesi'nde yayılış gösteren *Colchicum* L. (Liliaceae) cinsine ait türlerin taksonomik yönden araştırılması.

Fer A., Simier P, Arnaud MC, Rey L, Renaudin S., 1993, Carbon acquisition and metabolism in a root-hemiparasitic angiosperm, *Thesium humile* (Santalaceae), growing on wheat (*Triticum vulgare*), Australian Journal of Plant Physiology 20, 15-24.

Fer A., Russo, N., Simier, P., Arnaud, M. C., Thalouarn, P., 1994, Physiological changes in a root hemiparasitic angiosperm, *Thesium humile* (Santalaceae), before and after attachment to the host plant (*Triticum vulgare*). Journal of Plant Physiology, 143(6), 704-710.

Fernández, I., 1993, Apertural system and exine stratification in *Thesium divaricatum* (Santalaceae).Grana, 32(4-5), 308-310.

Botany 1, 731-734.

Bothalia 43, 214-216.

García, M. A., Nickrent, D. L., Mucina, L., 2018, Thesium nautimontanum, a new species of Thesiaceae (Santalales) from South Africa. PhytoKeys, 109, 41.

Germishuizen, G., Meyer, N., Steenkamp, Y., Keith, M., 2006, A checklist of South African plants. South African Botanical Diversity Network Report No.41. Sabonet, Pretoria.

Güner, A., Aslan, S., Ekim, T., Vural, M., Babaç, M.T., 2012, "Türkiye Bitkileri Listesi", ANG Vakfı, Nezahat Gökyiğit Botanik Bahçesi Yayınları, s.1290.

Güner, A., Özhatay, N., Ekim, T., Başer, K. H. C., 2000, "Flora of Turkey and the East Aegean Islands. Vol. 11", Edinburgh University Press, Edinburgh.

Hill, A.W., 1925, Order CXX. Santalaceae, in: Thiselton-Dyer, W.T. (Ed.), Flora Capensis Volume 5. L. Reeve & Co. LTD, London, p.135-212.

Hill, A.W., 1915, The genus *Thesium* in South Africa, with a key and descriptions of new species, Bulletin of Miscellaneous Information 1, 1-43.

Huang, T.-C., Huang, L.-H., Zhang, Y., Lin, Y., 2009, The illustration of common medicinal plants in Taiwan. Vol. 1. Committee on Chinese Medicine and Pharmacy, Dept. of Health, Executive Yuan.

Kabadere, S., Birgi, F., Oztopcu-Vatan, P., Filik İscen, C., İlhan, S., Some Biological Activities of the Moss Brachythecium populeum (Hedw.) Bruch, Schimp. & W.Gumbel (Bryophyta), Gazi University Journal of Science, 34 (2) 327-333.

Kandemir, A., 2012, *Thesium*. Şu sitede: Bizimbitkiler (2013). http://www.bizimbitkiler.org.tr , erişim tarihi: 01.05.2021.

Li, J., Boufford, D. E., Donoghue, M. J., 2001, Phylogenetics of *Buckleya* (Santalaceae) based on its sequences of nuclear ribosomal DNA. Rhodora 103, 137-150.

Moore, T. E., Verboom, G. A., Forest, F., 2010, Phylogenetics and biogeography of the   parasitic genus *Thesium* L. (Santalaceae), with an emphasis on the Cape of South Africa. Botanical Journal of the Linnean Society, 162(3), 435-452.

Moore, T.E., Verboom, G.A., Forest, F., 2010, Phylogenetics and biogeography of the parasitic genus *Thesium* L. (Santalaceae), with an emphasis on the Cape of South Africa. Botanical Journal of the Linnean Society 162, 435-452.

Neuwinger, H.D., 2000, African traditional medicine: a dictionary of plant use and applications. Medpharm Scientific Publishers, Stuttgart.

Nickrent D.L., Malécot V., Vidal-Russell R., Der J.P., 2010, A revised classification of Santalales. Taxon, 59(2), 538-558.

Nickrent, D. L., 1997, Parasitic plant connection.

Nickrent, D.L., García, M.A., 2015, *Lacomucinaea*, a new monotypic genus in Thesiaceae (Santalales). Phytotaxa 224, 173-184.

Öztopcu-Vatan, P., Savaroglu, F., Filik-Iscen, C., Kabadere, S., Ilhan, S., Uyar, R., Antimicrobial and antiproliferative activities of Homalothecium sericeum (Hedw.) Schimp. Extracts, Fresenius Environmental Bulletin, 20 (2), 461-466.

Renaudin, S., Cheguillaume, N., Gallant, D. J., 1981, Distribution and role of mineral compounds in the haustorium of a parasite of *Galium arenarium*, *Thesium humifusum*, before flowering. Canadian Journal of Botany 59, 1998-2002.

Victor, J.E., Smith, G.F., Van Wyk, A., 2015, Strategy for plant taxonomic research in South Africa 2015-2020. SANBI Biodiversity Series 26. South African National Biodiversity Institute, Pretoria.

Watt, J. M., Breyer-Brandwijk, M. G., 1962, The medicinal and poisonous plants of southern and eastern Africa, Second. ed. E. & S. Livingstone Ltd., London.

Chapter 5

ANALYSIS OF CAPTAN RESIDUE IN APPLES BY GC-MS AND GC-FID AFTER QUECHERS SAMPLE PREPARATION

Hacer Sibel Karapınar[1]

---

1 Scientific and Technological Research & Application Center, Karamanoglu Mehmetbey University, 70200, Karaman, Turkey

Scientific and Technological Research & Application Center, Karamanoglu Mehmetbey University, 70200, Karaman, Turkey

Orcid ID; 0000-0002-0123-3901, E-mail:sibelkarapinar@kmu.edu.tr

INTRODUCTION

Pesticides, chemical substances, or mixtures of substances are used to control undesirable organisms in agriculture by controlling, slowing down, or eliminating unwanted organisms. Pesticides include all chemicals that are classified as insecticides, herbicides, rodenticides, etc, (Singh et al., 2020). Pesticides are widely used in agriculture to protect the quantity and quality of food. Fruits and vegetables may contain residues from the use of pesticides. This situation can cause different toxic effects on human and environmental health (Carvalho, 2006). Today, large quantities of herbs and plants are used in the food and pharmaceutical industries around the world. Pesticides are often used to control or destroy any pests in agriculture during the plant growing process. Therefore, products used in the pharmaceutical and food industries may contain pesticide residues accumulated from agricultural practices and storage periods (Du et al., 2012).

N-[(trichloromethyl)thio]cyclohex-4-ene-1,2-dicarboximide is known as captan in ISO (IUPAC) (Authority et al., 2020). Captan is a plant disease management agent commonly used in agriculture. In most countries, using captan as a treatment for fungal illnesses is illegal (Shinde, Shiragave, Lakade, Thorat, & Banerjee, 2019).

Captan acts by inhibition of fungal metabolism and respiration process via a non-specific thiol reactant (Boran, Capkin, Altinok, & Terzi, 2012). During total diet investigations and market basket monitoring, captan is found in fruits and vegetables. Captan levels in fruit samples, have also been found to be exceedingly high and may exceed the maximum residue limit (MRL) values, according to compliance testing (D. Rawn et al., 2004). Adjuvants can increase capstan transport through the plant cuticle, although it is not a fungicide. Captan can be efficiently removed from vegetables and fruits with water (D. F. Rawn et al., 2008). Krol et al. reported that capstan residues in vegetables and fruits were greatly reduced when adequately rinsed under tap water (Krol, Arsenault, Pylypiw, & Incorvia Mattina, 2000). Similarly, in another study, it was determined that captan was successfully removed from tomatoes and carrots after washing with water, as many pesticides from tomatoes were not easily removed due to their characteristic absorbency and waxy surface (Burchat et al., 1998).

Gas chromatography (GC) and liquid chromatography (LC) are commonly used in different matrix types for pesticide residue analysis. Gas chromatography is frequently used for the analysis of semi-volatile and volatile pesticides, depending on different detectors. In addition, the mass spectrometer detector is commonly used because of its excellent sensitivity-selectivity, detecting compounds with different chemical properties (Ferrer

et al., 2005; Gómez-Ramos, Ferrer, Malato, Agüera, & Fernández-Alba, 2013; Kwon, Lehotay, & Geis-Asteggiante, 2012).

The most widely used approach for sample preparation in pesticide residue analysis is the QuEChERS method, which is "easy, fast, effective, inexpensive, safe and robust" [20]. The same final extracts prepared by the QuEChERS method can be injected into liquid and gas chromatography for detection, typically based on flame ionization (FID) and mass spectrometry (MS). Other versions of this method have been validated and applied by many legal laboratories applying multi-residue, multi-class methods to obtain high sample yields (Payá et al., 2007). Many companies today resell products used in the QuEChERS method that can be adapted to a variety of other applications beyond pesticide residue analysis (Lehotay et al., 2010). In recent years there has been a significant increase in the emphasis placed on pesticide residues and the increasing tension for better agricultural practices. Accordingly, many control centers in various countries have set tolerance values and maximum residue limits (MRLs) to protect the environment and the health of consumers. The MRL is a product boundary and not a security boundary. MRL is the maximum concentration (expressed in mg/kg) of pesticide residue legally permitted in animal feed and food products by the Codex Alimentarius Commission (Wanwimolruk, Kanchanamayoon, Phopin, & Prachayasittikul, 2015). In the Turkish Food Codex (TFC) Pesticide Maximum Residue Regulation, the captain's MRL value is 3 mg/kg (Bakırcı, Acay, Bakırcı, & Ötleş, 2014).

In this study, captan residue in 15 apple samples randomly taken from 4 different cold storages in Karaman in 3 different time periods was analyzed by GC-MS and GC-FID methods using the QuEChERS extraction method.

2. MATERIAL AND METHODS

2.1. Appliances and chemicals used

Pesticide analysis was performed on the Agilent Technologies 7890A GC-MS instrument. The FID detector (Agilent Technologies, 5188-5372 FID), the MS detector (Agilent Technologies, 5975C VL MSD with triple-axis detector), pure water device (Millipore ultrapure water, FONA 81849), homogenizer (IKA T 18 Basic Ultra-Turrax), analytical balance (Mettler Toledo, JB1603 C/FACT with 10^{-4} sensitivity), mixer (Waring Commercial, 8010ES), injector (Genject, 20002), centrifuge (Sigma, 2-16 KC and Zentaifugen), acetic acid (Merck, 100063), magnesium sulfate (Merck, 106067), primer-seconder amine (Thermo scientific, 60105-203), and acetonitrile (Merck, 1.00003). Pesticide standard was obtained from Sigma-Aldrich.

2.2. Material

According to the indiscriminate sampling method from the products harvested in 2014 in the province of Karaman, 15 apple samples were collected from 4 different cold storages in different time periods.

2.3. Standards Preparation

Certified Sigma-Aldrich brand standards with clear concentrations are used. Working standards at certain concentrations were prepared from 1000 mg/kg stock standards. Captan working standards at concentrations of 0.1, 0.5, 1.0, 1.5 mg/kg were finished to 100 mL with acetonitrile. The calibration curve and chemical structure of the captain standard are shown in Figures 1 and 2.
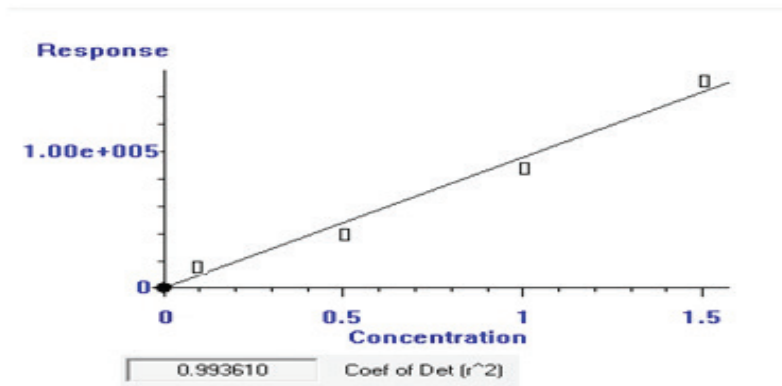
Figure 1. *Calibration curve of captan working standards*
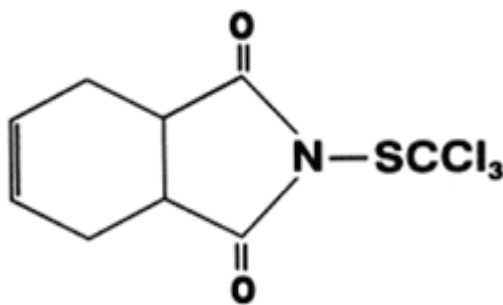
Figure 2. *Chemical structure of captan*

2.4. System conditions

An Agilent 7890A GC system with an Agilent G4513A series autosampler and a 5975C VL mass selective detector was used for the GC–MS study (MSD). An HP-5MS fused silica capillary column with a film

thickness of 30 m x 0.25 mm x 0.25 m was utilized to separate the analytes. The injector was set at 250°C, with a flow rate of 1.0 ml min^{-1} of helium as the carrier gas. The oven temperature was set to 70 °C for 2 minutes, then increased at a rate of 40 °C min^{-1} up to 150 °C, held for 4 minutes, then increased at a rate of 9 °C min^{-1} up to 200 °C, then increased at a rate of 24 °C min^{-1} up to 280 °C, and kept for 15 minutes. The temperatures of the ion source, quadrupole, and transfer line were set at 230, 150, and 280 °C, respectively. In electron impact (EI) mode, the mass spectrometer was operated at 70 eV. The injection volume was 1 ml and the solvent delay was 8 min.

An Agilent 6850 series gas chromatograph with a flame ionization detector (FID) was used for the GC-flame ionization detector (FID) analysis. Separations were carried out on an HP-5MS fused silica capillary column with a 30 m 0.25 mm 0.25 m film thickness. The temperatures of the detector and injector were 300 °C and 250 °C, respectively. The injection port was cut in half at a ratio of 1:15. The movie lasted 27.889 minutes in total. The nitrogen carrier gas flow rate was set to 5.0 ml min^{-1}.

2.5. Preparation of Examples for Analysis

Samples were got from cold storage in transparent and ziplock bags were stored in a refrigerator at +4 °C under laboratory conditions until analysis. Apple samples were completely ground and homogenized with mechanic grinders, and the extraction amounts were taken by weighing.

2.5.1. Extraction

QuEChERS method was used in the sample extract because it is an easy, fast, cheap, precise, reliable and effective method that is widely used in pesticide residue analysis (Lehotay, Kok, Hiemstra, & Bodegraven, 2005). 10 g of the grinded samples in 50 ml centrifuge tubes were taken and 10 ml of acetonitrile with 1% acetic acid, 1 g of sodium acetate and 4 g of $MgSO_4$ were attached and then shaken manually. The samples were then centrifuged in a centrifuge operating at 10000 rpm for 5 minutes. 2 ml samples were taken from the supernatants and transferenced to 30 mL glass tubes. 0.2 g PSA (primary secondary amine) and 0.6 g $MgSO_4$ were attached. Samples were centrifuged at 5000 rpm for 1 min. A sufficient amount of the supernatant of the centrifuged samples was taken and placed in vials to obtain a ready-to-analyze solution in GC-FID and GC-MS equipment (Anastassiades, Lehotay, Štajnbaher, & Schenck, 2003).

2.6. Method validation

The linearity, detection, quantification limits, and precision criteria were used to test the analytical method's validity. The approach has been validated in accordance with the directive EC SANCO/10684/2009. The

peak area vs the concentration of the appropriate calibration standards was plotted at the four calibration levels between 0.1 and 1.5 mg kg^{-1} to create calibration curves for compounds in the matrix. The slope of the calibration curve and the residual standard deviation of the regression line were used to calculate the limits of quantification (LOQ) and detection (LOD) (Shinde et al., 2019).

3. RESULTS AND DISCUSSION

Captan residue was evaluated by GC-MS and GC-FID methods using the QuEChERS extraction method in 15 apple samples randomly collected from four distinct cold storages in Karaman during three time periods. Pesticide residues were found in the majority of the 15 samples tested, according to the results. Figures 3, 4, and 5 show GC-FID, GC-MS chromatograms, and mass spectrums of the captan standard; Figure 6 shows GC-MS chromatograms of captan materials obtained from samples. Table 1 shows the chromatographic characteristics of captan materials. Table 2 shows the linearity data (correlation coefficient, equation, R2), LOD, and LOQ. Table 3 shows the average captan values of apple samples taken from cold storage.
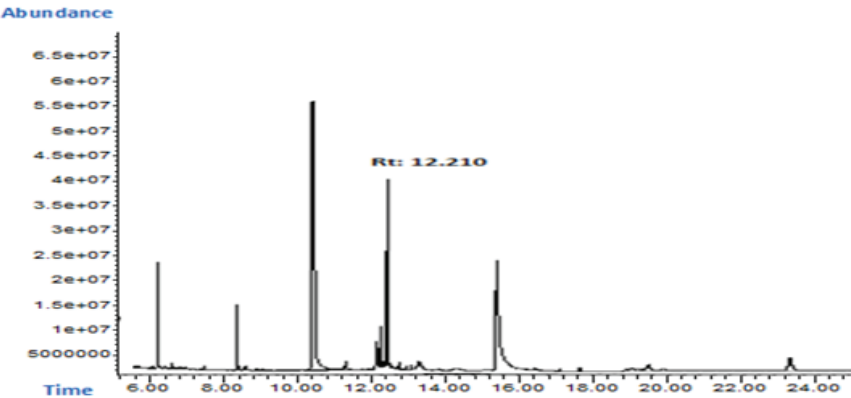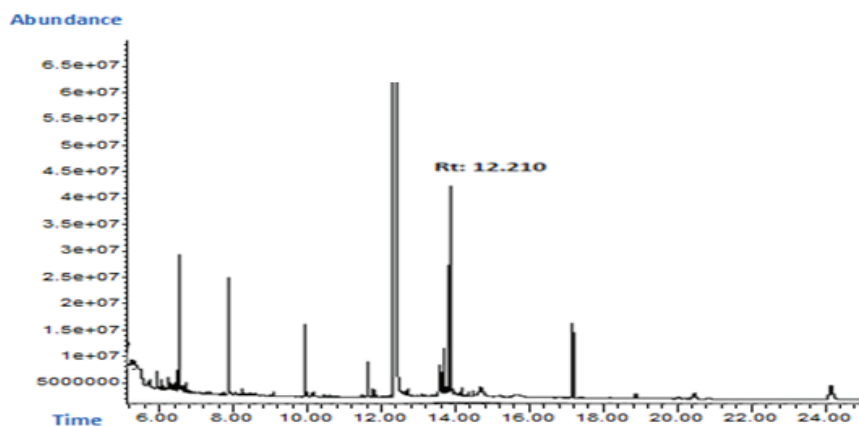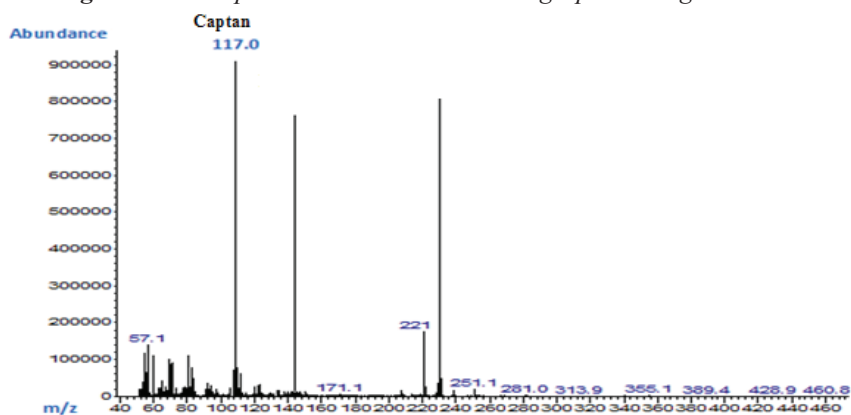

Figure 3. *The captan standard's GC-MS mass spectrum*

Figure 4. *The captan standard was chromatographed using GC-FID.*

Figure 5. *The captan standard's GC-MS chromatogram (total ion current)*

Table 1. *GC-MS analysis of chromatographic characteristics for the selected chemical*

Pesticide	Molecular Formula	MW (g/mol)	Target Ion (m/z)	Retention Time (min)
Captan	$C_9H_8Cl_3NO_2S$	300.578	117.0	12.210

*MW: Molecular weight

Table 2. *LOD, LOQ, and linearity data (equation, correlation coefficient, and R^2)*

Pesticide	Linearity range (mg/kg)	Regression Equation	R^2	LOD (mg/kg)	LOQ (mg/kg)
Captan	0.1 - 1.5	y = 10015x + 30539	0.994	0.05	0.15

* LOD stands for "limit of detection", while LOQ stands for "limit of quantification".
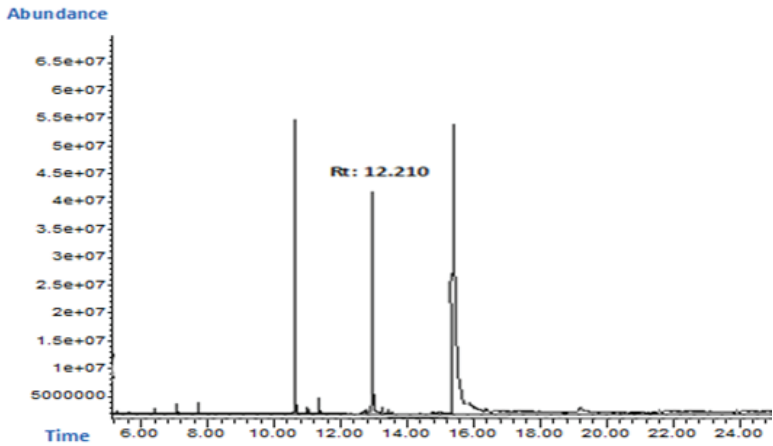
Figure 6. *The captan residue substance in the apple sample was chromatographed using GC-MS*

Table 3. *Captan average concentration in the samples (mg/kg)*

CAPTAN	1	2	3	4	5	6
1	6.52	8.46	9.48	7.60	8.48	10.92
2	6.32	8.84	9.14	*	8.98	10.32
3	*	8.36	9.76	7.20	8.52	10.88
4	6.60	8.94	9.46	7.08	8.75	10.30
5	6.78	*	9.54	7.92	8.46	*
6	6.84	8.04	9.32	*	8.94	*
7	*	8.32	9.23	*	*	10.82
8	6.50	*	9.14	7.56	*	10.24
9	6.58	8.70	9.96	7.69	8.44	ND
10	6.91	8.66	9.87	7.22	8.64	10.34
11	*	8.08	*	7.87	*	*
12	6.89	*	9.35	*	7.98	*
13	6.48	8.22	9.33	7.02	8.03	10.36
14	6.34	8.24	*	7.42	7.99	10.16
15	6.80	*	9.66	7.68	8.23	10.24
Average	6.63	8.44	9.48	7.48	8.45	10.46
± SD	± 0.21	± 0.30	± 0.27	± 0.31	± 0.35	± 0.29

*: None Detection

In our research, the use of captan pesticides on apples is prohibited according to EU standards. The maximum residue limit of the captain is 3 mg/kg according to the TFC directive. In this study, it was determined that the amount of captain in the samples had a higher amount of residue than the maximum allowable limit.

4. CONCLUSION

When considering studies done across the world, pesticides are extremely used in order to increase productivity. One of the most essential reasons to use pesticides is to combat agricultural insects in order to meet the growing population's nutritional needs. In addition, the pesticide is used in order to prolong the shelf life of products and increase productivity. Having all these in mind, manufacturers continue to use pesticides until the harvest period. For that reason, the waiting time of the used pesticide is more likely ignored. Today, agricultural production is carried out in many parts of the world, and reliability in the production and storage conditions of food has become very important. It is known that products, especially with GLOBALGAP certificates, have precedence in this competitive environment and that products without residual are preferred. It is required to fulfill necessary cultural measures as well as the conscious use of pesticides in order to increase both agricultural productivity and export in our country that is an agricultural country. It is ensured that manufacturers subject to GLOBALGAP applications fulfill these requirements. An increase in the rate of getting involved in GLOBALGAP certificates and application programs across the country would bring along quality and assurance. Apple export has an important part in the agriculture of Karaman. The majority of the apples harvested in Karaman are stored in the province's cold storage facilities. Apples are sold both domestically and internationally. Apples produced in Karaman are exported to the UE and Russia to Arabian countries in particular. In the study, pesticide residues were detected in the majority of the analyzed apples. Turkish Food Codex Directive on Maximum Residue of Pesticides was published in 2014. Captan substance that is not forbidden to use in Turkey was determined in the majority of 15 samples. Captan substance was determined in all samples at a higher level than the upper limits specified by the TFC directive. Pesticides should be used with greater awareness and control in order to ensure food security for our citizens while also protecting the environment and foreign trade. Pesticides that are low-risk or environmentally friendly are given priority in the EU and the US, with the ability to have the least negative impact on the environment and human health. In our country, priority has been given to environmentally friendly pesticides in support of both permission and consumption. It is known throughout the world to what extent EU countries make tiny distinctions in the foods they will consume and what kind of inspections they conduct. Considering that the number of batches of unapproved products sent to the EU by developed countries such as Germany and France is almost half of the products sent by Turkey, it should be known that residue analyzes in foods produced in our country are very important for human health. For this reason, it is

required to take precautions to prevent the return of the products exported to the European Union and Russia, to human health in particular. The products launched to the domestic market are required to be analyzed in pesticides, and it is required to raise awareness and advise manufacturers and merchants in this regard.

5. REFERENCES

Anastassiades, M., Lehotay, S. J., Štajnbaher, D., & Schenck, F. J. (2003). Fast and easy multiresidue method employing acetonitrile extraction/partitioning and "dispersive solid-phase extraction" for the determination of pesticide residues in produce. *Journal of AOAC International, 86*(2), 412-431.

Authority, E. F. S., Anastassiadou, M., Arena, M., Auteri, D., Brancato, A., Bura, L., . . . Crivellente, F. (2020). Peer review of the pesticide risk assessment of the active substance captan. *EFSA Journal, 18*(9), e06230.

Bakırcı, G. T., Acay, D. B. Y., Bakırcı, F., & Ötleş, S. (2014). Pesticide residues in fruits and vegetables from the Aegean region, Turkey. *Food Chemistry, 160*, 379-392.

Boran, H., Capkin, E., Altinok, I., & Terzi, E. (2012). Assessment of acute toxicity and histopathology of the fungicide captan in rainbow trout. *Experimental and Toxicologic Pathology, 64*(3), 175-179.

Burchat, C. S., Ripley, B. D., Leishman, P. D., Ritcey, G. M., Kakuda, Y., & Stephenson, G. R. (1998). The distribution of nine pesticides between the juice and pulp of carrots and tomatoes after home processing. *Food Additives & Contaminants, 15*(1), 61-71.

Carvalho, F. P. (2006). Agriculture, pesticides, food security and food safety. *Environmental science & policy, 9*(7-8), 685-692.

Du, G., Xiao, Y., Yang, H. R., Wang, L., Song, Y. l., & Wang, Y. T. (2012). Rapid determination of pesticide residues in herbs using selective pressurized liquid extraction and fast gas chromatography coupled with mass spectrometry. *Journal of separation science, 35*(15), 1922-1932.

Ferrer, C., Gómez, M. J., García-Reyes, J. F., Ferrer, I., Thurman, E. M., & Fernández-Alba, A. R. (2005). Determination of pesticide residues in olives and olive oil by matrix solid-phase dispersion followed by gas chromatography/mass spectrometry and liquid chromatography/tandem mass spectrometry. *Journal of Chromatography A, 1069*(2), 183-194.

Gómez-Ramos, M., Ferrer, C., Malato, O., Agüera, A., & Fernández-Alba, A. (2013). Liquid chromatography-high-resolution mass spectrometry for pesticide residue analysis in fruit and vegetables: screening and quantitative studies. *Journal of Chromatography A, 1287*, 24-37.

Krol, W. J., Arsenault, T. L., Pylypiw, H. M., & Incorvia Mattina, M. J. (2000). Reduction of pesticide residues on produce by rinsing. *Journal of agricultural and food chemistry, 48*(10), 4666-4670.

Kwon, H., Lehotay, S. J., & Geis-Asteggiante, L. (2012). Variability of matrix effects in liquid and gas chromatography–mass spectrometry analysis of

pesticide residues after QuEChERS sample preparation of different food crops. *Journal of Chromatography A, 1270*, 235-245.

Lehotay, S. J., Kok, A. d., Hiemstra, M., & Bodegraven, P. v. (2005). Validation of a fast and easy method for the determination of residues from 229 pesticides in fruits and vegetables using gas and liquid chromatography and mass spectrometric detection. *Journal of AOAC International, 88*(2), 595-614.

Lehotay, S. J., Son, K. A., Kwon, H., Koesukwiwat, U., Fu, W., Mastovska, K., . . . Leepipatpiboon, N. (2010). Comparison of QuEChERS sample preparation methods for the analysis of pesticide residues in fruits and vegetables. *Journal of Chromatography A, 1217*(16), 2548-2560.

Payá, P., Anastassiades, M., Mack, D., Sigalova, I., Tasdelen, B., Oliva, J., & Barba, A. (2007). Analysis of pesticide residues using the Quick Easy Cheap Effective Rugged and Safe (QuEChERS) pesticide multiresidue method in combination with gas and liquid chromatography and tandem mass spectrometric detection. *Analytical and bioanalytical chemistry, 389*(6), 1697-1714.

Rawn, D., Cao, X.-L., Doucet, J., Davies, D., Sun, W.-F., Dabeka, R., & Newsome, W. (2004). Canadian Total Diet Study in 1998: pesticide levels in foods from Whitehorse, Yukon, Canada, and corresponding dietary intake estimates. *Food additives and contaminants, 21*(3), 232-250.

Rawn, D. F., Quade, S. C., Sun, W.-F., Fouguet, A., Bélanger, A., & Smith, M. (2008). Captan residue reduction in apples as a result of rinsing and peeling. *Food Chemistry, 109*(4), 790-796.

Shinde, R., Shiragave, P., Lakade, A., Thorat, P., & Banerjee, K. (2019). Multi-residue analysis of captan, captafol, folpet, and iprodione in cereals using liquid chromatography with tandem mass spectrometry. *Food Additives & Contaminants: Part A, 36*(11), 1688-1695.

Singh, A., Dhiman, N., Kar, A. K., Singh, D., Purohit, M. P., Ghosh, D., & Patnaik, S. (2020). Advances in controlled release pesticide formulations: Prospects to safer integrated pest management and sustainable agriculture. *Journal of Hazardous Materials, 385*, 121525.

Wanwimolruk, S., Kanchanamayoon, O., Phopin, K., & Prachayasittikul, V. (2015). Food safety in Thailand 2: Pesticide residues found in Chinese kale (Brassica oleracea), a commonly consumed vegetable in Asian countries. *Science of the total environment, 532*, 447-455.

Chapter 6

ANTIOXIDANTS AND HEALTH

Önder AYBASTIER[1]

1 Associate Professor Dr., Bursa Uludag University, Faculty of Science and Arts, Department of Chemistry, Turkey, aybastier@uludag.edu.tr, ORCID: 0000-0002-0380-1992.

1. Free Radicals and Oxidative Stress

Free radicals are atoms or groups of atoms that contain unpaired electrons and are therefore reactive. Free radicals are chemical products that can be formed in the body during metabolism and by many external factors. Oxidative stress is defined as a state of imbalance between excessive free radicals and the insufficient scavenge of those radicals by antioxidant systems as a defense mechanism against oxidative damage. As a result, reactive oxygen species (ROS) or reactive nitrogen species (RNS) can accumulate inside the body and damage all biomolecules such as proteins and DNA. Furthermore, the defense systems should try to prevent uncontrolled ROS accumulation within the living organisms. These systems include both enzymatic molecules (for example superoxide dismutase, glutathione peroxidases and catalase) and non-enzymatic molecules, with glutathione and vitamin E with as the best known (Valko et al., 2007). Under normal conditions, living organisms control precisely regulated systems to maintain low ROS levels. Unfortunately, in case of an imbalance, excessive production of ROS occurs in biological systems (Fig. 1). This state is harmful to biological systems. Because ROS can readily react with biological molecules such as DNA and protein, leading to metabolic dysregulation, oxidation end products of lipids, proteins and DNA, and oxidative damage in cells, tissues, or even organs (Birben et al., 2012; Di Meo et al., 2016). Such damage can lead to the formation of various secondary reactive species and this can affect a number of cellular functions, including apoptosis, which often leads to disease development. Increase in ROS formation, decrease in antioxidant enzyme levels and/or errors in DNA repair mechanisms lead to increased oxidative DNA damage. Oxidative stress has been implicated in the formation mechanism of a number of degenerative disorders including cancer, arterial diseases, neurodegeneration, diabetes, rheumatoid arthritis and kidney disease (Andries et al., 2020; Pisoschi et al., 2021).

ADM: Antioxidant Defense Mechanism
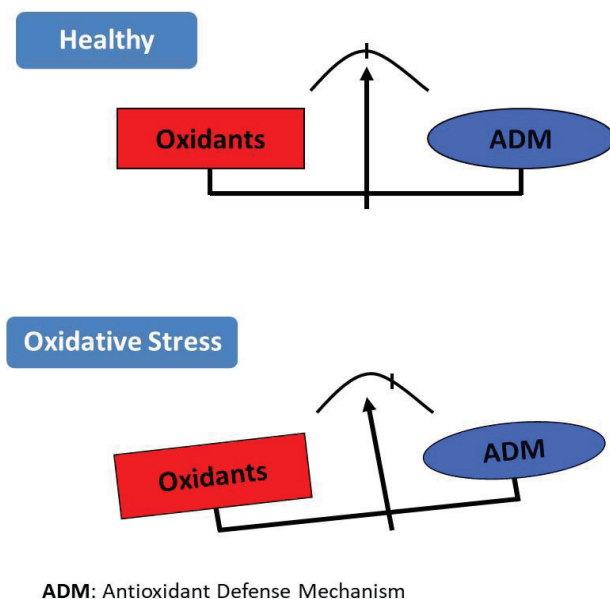
Figure 1. *Oxidant-antioxidant balance and occurrence of oxidative stress*

2. Antioxidants

Antioxidants are generally phenolic compounds that prevent the formation of free radicals or scavenge existing radicals from damaging their environment. Phenolic compounds are a broad group of chemicals that have two or more hydroxyl groups and one or more aromatic rings. Phenolic compounds are found free forms or conjugated with sugars, acids and other biomolecules in fruits, seeds, flowers, leaves, branches and stems of plants and take place as secondary metabolites in plants (Skrovankova et al., 2015). It is the most common group of substances found in plants, and the structure of thousands of plant phenolic compounds has been elucidated today. Newly discovered and identified phenolic substances are constantly being added to these phenolic compounds. Phenolic compounds are substances that play an important role in the growth and development of plants, protect plants against pests, and give the color and taste characteristics of fruits and vegetables. Furthermore, these compounds are involved in plant defense as signaling molecules to protect plants against ultraviolet radiation and different sources of stress, or animals to disperse seeds and attracting pollinators (Vuolo et al., 2019). These compounds, which can also be called polyphenols due to their structure, are found in significant amounts in the human diet as they are included in the content of

many plant foods (vegetables, fruits, nuts, etc.) and beverages (tea, wine, etc.). Due to the different consumption levels of people, the personal daily intake of herbal phenolic compounds varies between 50-800 mg (Pietta, 2000; Balasundram et al., 2006).

2.1. Classification of antioxidants

Antioxidants can be grouped under two groups as endogenous and exogenous (Fig. 2). Endogenous (synthesized by the organism) and exogenous (ingested with food) antioxidants protect the body from free radicals to maintain the oxidant/antioxidant balance and are used to neutralize free radicals. While endogenous antioxidants can be classified into two subgroups as enzymatic and non-enzymatic antioxidants, exogenous antioxidants are only non-enzymatic.
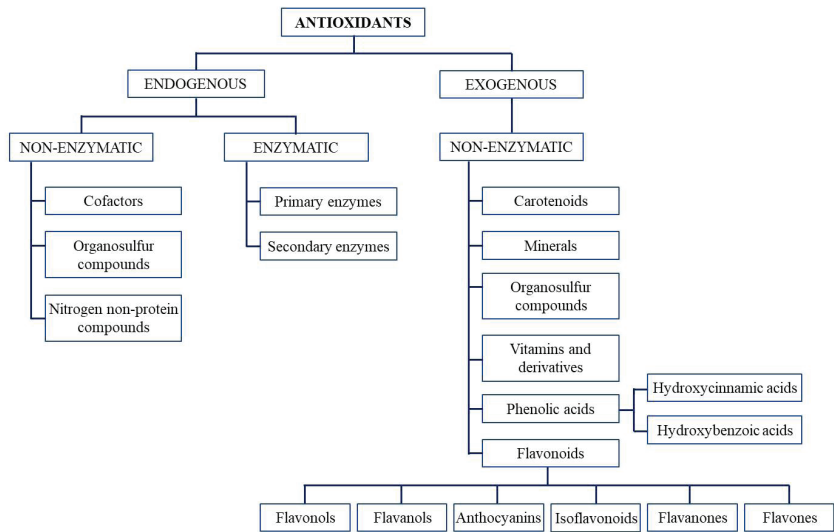

Figure 2. *Classification of antioxidants*

2.2. Endogenous antioxidants

2.2.1. Non-enzymatic

2.2.1.1. Cofactors:

Coenzyme Q10 or ubiquinone is an antioxidant that our body produces naturally (Fig. 3). The cells use coenzyme Q10 for maintenance and growth. It acts as a coenzyme in many key enzymatic steps of energy production in the cell. The potential usefulness of coenzyme Q10 in various diseases and mitochondrial disorders due to oxidative stress has been demonstrated in many studies. Coenzyme Q10 is one of the most

significant lipid antioxidants, which prevents the generation of free radicals and modifications of DNA, lipids and proteins (Saini, 2011).
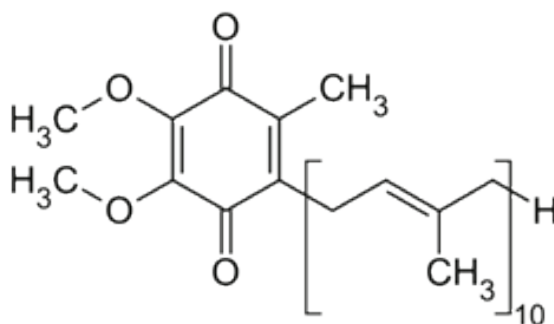
Figure 3. *Chemical structure of coenzyme Q10*

2.2.1.2. Organosulfur compounds:

Glutathione is a water-soluble tripeptide with a thiol structure, which is found in excess in the organism (Fig. 4). It is formed by the combination of glutamate, cysteine and glycine amino acids. Glutathione, which prevents the formation of oxidative stress in the cell, is found in the cytosol, chloroplast and endoplasmic reticulum from the cell parts. It is essential for the normal functioning of the immune system and strengthens the immune system by activating lymphocytes (Li et al., 2007).
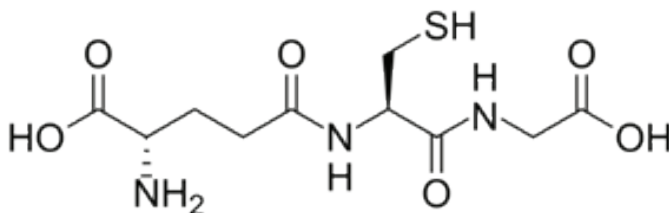

Figure 4. *Chemical structure of glutathione*

2.2.1.3. Nitrogen non-protein compounds:

Uric acid is the end product of purine metabolism in humans and is the most abundant endogenous antioxidant that scavenges free radicals in the body (Fig. 5). Uric acid is thought to be responsible for about half of the total antioxidant capacity of the blood. Inactivates uric acid, hydroxyl, singlet oxygen, superoxide, peroxynitrite anion, peroxynitric acid. It acts as a preservative by preventing lipid peroxidation. In addition to being a

powerful free radical scavenger, uric acid also acts as a chelator of metal ions such as Fe and Cu (Kumar et al., 2015).
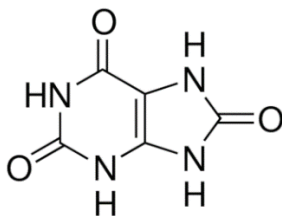

Figure 5. *Chemical structure of uric acid*

2.2.2. Enzymatic

Free radicals formed by various mechanisms in the cell are removed by some enzymes. Many enzymes contribute directly or indirectly to the free radical scavenging mechanism. The working mechanisms of the most important of them are as follows:

2.2.2.1. Primary enzymes

Superoxide dismutase (SOD) : It catalyzes the single-electron dismutation of superoxide to hydrogen peroxide and oxygen.

$$2\ O_2^{\bullet-} + 2\ H^+ \longrightarrow H_2O_2 + O_2$$
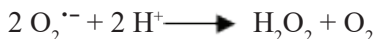
There are two isoenzymes of SOD in human cells, especially Cu-Zn-SOD containing copper and zinc ions in the cytosol, and mitochondrial Mn-SOD containing manganese ions (Chaudiere and Iliou, 1999).

Catalase (CAT): It is found in every aerobic cell. It neutralizes hydrogen peroxide by converting it to water and oxygen.

$$2\ H_2O_2 \longrightarrow 2\ H_2O + O_2$$

Liver, kidney, myocardium, striated muscles and erythrocytes are the sites where catalase is most active. Although H_2O_2 formed as a result of superoxide dismutase activity is not a radical, it can cause oxidative damage as it is the precursor of the most reactive species, the $OH^{\bullet}$ radical. Therefore, catalase tries to reduce the concentration of hydrogen peroxide.

Glutathione peroxidase (GPx) : It is responsible for the reduction of hydroperoxides in the presence of H_2O_2. In this reaction, hydrogen peroxide is reduced to water and organic hydroperoxides to alcohol, while glutathione (GSH) is oxidized to oxidized glutathione (GSSG). (Chaudiere and Iliou, 1999).

$$H_2O_2 + 2\ GSH \longrightarrow GSSG + 2\ H_2O$$

$$ROOH + 2\ GSH \longrightarrow ROH + H_2O + GSSG$$
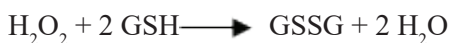
2.2.2.2. Secondary enzymes

Glutathione reductase (GR) : It is an enzyme that catalyzes the conversion of oxidized glutathione (GSSG), which is formed as a result of the reduction of hydroperoxides by glutathione peroxidase, to reduced glutathione (GSH).

$$GSSG + NADPH + H^+ \longrightarrow 2\ GSH + NADP^+$$
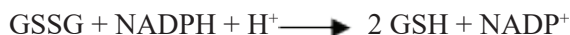
Glucose-6-phosphate dehydrogenase (G6PD): This enzyme is the first and rate-limiting enzyme of the pentose phosphate pathway. The main purpose of the pentose phosphate metabolic pathway is to provide nicotinamide adenine dinucleotide phosphate (NADPH) to the organism as a reducing power and to synthesize ribose phosphates. NADPH plays an important role in protecting proteins and other molecules from oxidative damage. In addition, it is thought that the G6PD enzyme protects the cell against H_2O_2 by stimulating the synthesis of antioxidant enzymes such as catalase and glutathione peroxidase (Thomas et al., 1991).

2.3. Exogenous antioxidants

2.3.1. Non-enzymatic

2.3.1.1. Carotenoids

Carotenoids are orange, yellow and red pigments commonly found in vegetables and fruits. They are insoluble in water, soluble in vegetable oils. The number of carotenoid substances known today is about 600. Carotenoids are unsaturated, aliphatic chains with attached methyl groups and conjugated double bonds. Carotenoids are transported by lipoprotein particles. It is known that carotenoids scavenge singlet molecular oxygen and peroxyl radicals, and show their antioxidant effect by protecting cell membranes and lipoproteins from reactive oxygen species (Nimse and Pal, 2015). It has been reported that eating a diet rich in carotenoids reduces the risk of some degenerative diseases such as cancer, cardiovascular and eye diseases. These effects are associated with antioxidant properties that protect tissues and cells from oxidative damage (Stahl and Sies, 2003). The most important carotenoids thought to have high antioxidant capacities are (Fig. 6):

(a)

(b)

(c)

(d)
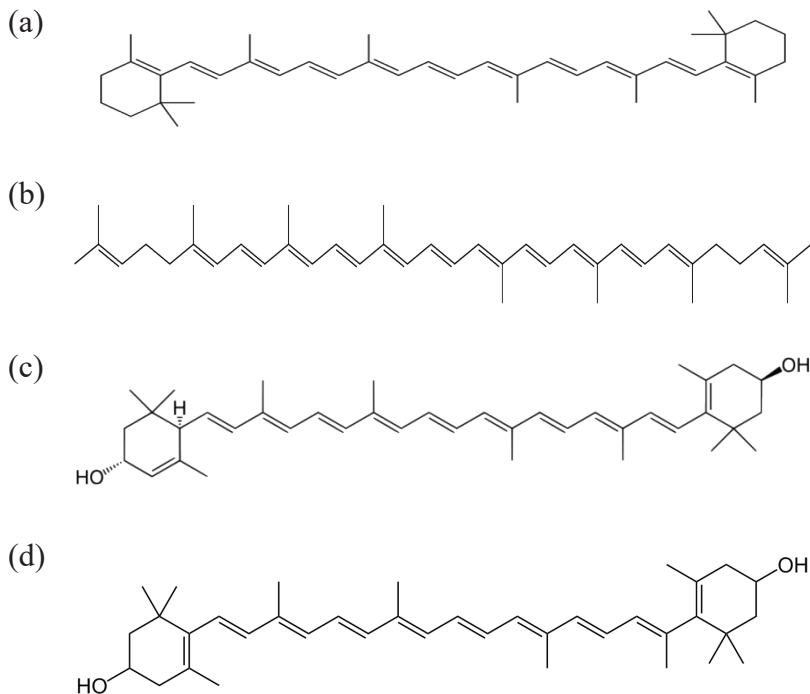
Figure 6. Chemical structures of carotenoids: (a) β-carotene, (b) lycopene, (c) lutein, (d) zeaxanthin

Lycopene: Lycopene is an aliphatic hydrocarbon. It is the most important carotenoid found in tomatoes, watermelon, pink grapefruit, rosehip and papaya and gives them their color (Gupta et al., 2003). Like all carotenoids, it is heat stable. Lycopene is the most abundant carotenoid in plasma. Since humans cannot synthesize carotenoids, they have to take them from outside as food. Tomatoes are the most consumed lycopene-rich foods in the diet. The antioxidant property of lycopene comes from its single oxygen scavenger and scavenging function, and thus protecting cells against oxidative stress. It has been suggested that lycopene reduces the risk of various diseases due to its ability to prevent oxidative stress (Männisto et al., 2007).

β-Carotene: β-Carotene, which is in the class of hydrocarbon carotenoids such as lycopene, gives plants their yellow, red and orange colors. It is especially abundant in orange-colored fruits and vegetables such as carrots. It is used as a color additive and antioxidant in the food industry. β-carotene is the provitamin of vitamin A and is converted to vitamin A when the body is deprived of vitamin A. Many studies have been

done on β-carotene, and its antioxidant activity has been found to be lower than tocopherels. However, β-carotene can protect liposomes against lipid peroxidation (Woodall et al., 1997).

Lutein: Lutein is a carotenoid that is only synthesized by plants and is abundant in green vegetables such as spinach and cabbage. Animals obtain lutein directly or indirectly from plants. Lutein is found in egg yolks and animal fats. Lutein and zeaxanthin accumulate in the human retina. Thanks to its antioxidant activity, lutein partially protects the eye against lipopolysaccharides, which cause inflammation in some parts of the eye in uveitis (Rong-Rong et al., 2011). The incidence of macular degeneration and cataracts decreases in people who consume plenty of lutein-sourced vegetables. Lutein is the main pigment in the retina and provides visual sensitivity. Lutein is a natural eye defender that protects the retina from too much light. As age progresses, the amount of lutein in the retina decreases. In addition to protecting the macula, lutein protects the lens against sunlight and reduces the development of cataracts. Lutein is also protective against atherosclerosis (Dwyer et al., 2001).

Zeaxanthin: Zeaxanthin is one of two carotenoids found in the retina. The macular center has the most zeaxanthin, while the peripheral retina has more lutein. The chemical formulas of lutein and zeaxanthin are the same and they are isomers but not stereoisomers. The difference between the two is the position of a double bond in one of the three rings. Because of this difference, lutein has three chiral centers and zeaxanthin has two. It is used as a food additive for coloring purposes. Some studies have shown that lutein and or zeaxanthin supplementation is protective against macular degeneration (Murillo et al., 2019). Zeaxanthin is one of the most common carotenoids in nature. It is the pigment that gives corn, saffron and many other plants their unique color. When zeaxanthin is broken down, picrocrocin and safranal are formed, which are responsible for the taste and aroma of saffron (Di Marco et al., 2019).

2.3.1.2. Minerals

Zinc is an essential element for the continuation and reproduction of vitality and the maintenance of the activities of the immune system. Control of systemic and cellular zinc balance is vital for all biological systems. Zinc, which is redox stable, replaces redox reactive metals such as iron and copper in critical cellular and extracellular regions. Thus, it acts as an inhibitor of free radical formation and a protector from oxidative stress. It is also involved in the structure of superoxide dismutase, an enzyme with antioxidant effect, and metallothioneins, which protect tissues from the harmful effects of free radicals (Baltaci and Mogulkoc, 2012).

Selenium is considered to be a very important micronutrient in human nutrition. This is because it is a component of glutathione peroxidase, an antioxidant enzyme that prevents oxidative damage in the body. In this way, it reduces the peroxidation of fatty acids of lipid membranes. Selenium has been shown to reduce tumorigenesis in various experimental models. There are many potential mechanisms proposed to explain the anticarcinogenic effect of selenium, such as its antioxidant effect, enhancement of immune functions, and alteration of carcinogen metabolism and suppression of testosterone production. It also helps to retain Vitamin E in plasma lipoproteins (Lobanov et al., 2008).

2.3.1.3. Organosulfur compounds

Allylic sulfides are found in vegetables such as garlic, onions, and leeks. The allylic sulfides in these plants are dispersed when the plants are cut or crushed. When oxygen reaches plant cells, various biotransformation products are released. It is thought that all of these have different characteristics. It is claimed that allylic sulfides have antimutagenic and anticarcinogenic properties as well as protecting the immune and cardiac system. It is thought that allylic sulfides inhibit the growth of tumors, fungi, parasites and platelet/leukocyte binding factors. They also activate liver detoxification enzymes (Kalayarasan et al., 2009; Iciek et al., 2012)

Indole complexes bind chemical carcinogens in the gastrointestinal tract and activate detoxification enzymes. Biotransformation products of indoles from flavonoids occur under the action of stomach acid. Indole-containing vegetables also contain significant amounts of vitamin C. For example, a substance containing indole-ascorbic acid was found in cabbage juice. This compound, which is called ascorbigen, has been shown to be heat resistant and decomposes into indole and ascorbic acid when subjected to acidic hydrolysis (Mor et al., 2004).

2.3.1.4. Vitamins and derivatives

Vitamin A is found in animals as long-chain fatty acid esters of retinol, and in plants as β-carotenes, a provitamin. β-carotene is an antioxidant, it plays a role in the capture of free peroxide radicals in tissues. Oral retinol esters are hydrolyzed in the small intestine and retinol is absorbed directly from the small intestine. Oral β-carotenes are enzymatically decomposed by the use of molecular oxygen in the presence of bile salts and 2 molecules of retinal are formed. Retinal is enzymatically reduced to retinol in the intestinal mucosa by a specific reductase using NADPH, with a small amount being oxidized to retinoic acid. After absorption, retinoic acid is metabolized to more polar compounds and excreted in urine and bile, and is not stored in the liver and other tissues.

After absorption, retinol is re-esterified with long-chain saturated fatty acids and enters the bloodstream. Retinyl esters are taken up by the liver from the bloodstream and hydrolyzed in hepatocytes. They are re-esterified as retinyl palmitate for storage in liver lipid droplets. Retinol stored in the liver is liberated by the hydrolysis of its esters and transported to target tissues. Most target cells of vitamin A metabolize retinol to retinale and retinoic acid. Retinol, retinal and retinoic acid have specific biological functions. Retinol likely functions as a hormone. Retinal is the necessary precursor of the visual pigment rhodopsin: Retinoic acid and its metabolites act on epithelial differentiation and function as oligosaccharide transporters in the synthesis of glycoproteins (Palace et al., 1999; Zhang et al., 2019).

Vitamin C is a water-soluble vitamin that is required for biological functions and cannot be stored in the body (Fig. 7). It is abundant in citrus fruits, green peppers, tomatoes, liver and kidneys. Vitamin C biosynthesis in animals occurs via the glucuronic acid metabolic pathway. Vitamin C cannot be synthesized in humans, monkeys, guinea pigs, and some birds and fish because they lack the enzyme L-glonolactone oxidase (lactonase). It is necessary for growth and development. It is an essential cofactor for many enzymes. It is also an antioxidant that protects against infections and helps iron absorption. Vitamin C transforms into ascorbate radical by donating an electron to the lipid radical to terminate the lipid peroxidation chain reaction. Ascorbate radical pairs react rapidly to produce an ascorbate molecule and a dehydroascorbate molecule. Vitamin C protects biomembranes against lipid peroxidation damage by eliminating radicals before initiating peroxidation. When the radicals formed are not eliminated, they attach to lipids, enzymes, proteins and DNA, forming pathological disorders and cancer. In addition, vitamin C is effective in the regeneration of vitamin E. As an antioxidant, it reduces the tocopheroxyl radical to α-tocopherol. Vitamin C is also known as a prooxidant due to its strong reducing properties. Hydrogen peroxide can be formed directly by the oxidation of ascorbic acid and by the Fenton and Haber – Weiss reaction; may cause the formation of hydroxyl radical from hydrogen peroxide (Nimse and Pal, 2015).
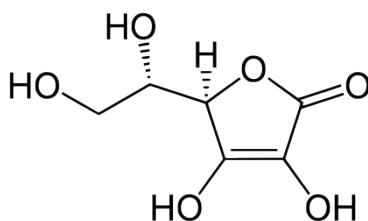
Figure 7. *Chemical structure of Vitamin C*

Vitamin E is a plant-derived vitamin that is soluble in fat and organic solvents, and is essential for the functions of the immune, circulatory, nervous and reproductive systems in all living things (Fig. 8). They are heat resistant but not resistant to oxidation and UV rays. Vitamin E has tocopherol (α, β, γ, δ) and tocotrienol (α, β, γ, δ) forms. Its most bioactive form is α-tocopherol. It is abundant in young green plants, vegetable oils, milk, eggs and liver (Altıner et al., 2017).

Vitamin E has an anticarcinogenic effect. There are studies that prevent the growth of prostate, colon, lung and breast cancers. It has protective properties against cardiovascular diseases, arthritis and various neurological disorders. In particular, it inhibits biological activity due to DNA damage induced by carcinogens. On the immune system; It acts by increasing the number and activity of helper T cells. It also accelerates the synthesis of immunoglobulin by stimulating B lymphocytes. Vitamin E is in the structure of cytochrome b and c in the electron transport chain. However, it is known that the vitamin is also effective in the synthesis of long-chain unsaturated fatty acids and nucleic acid metabolism (Altıner et al., 2017). The main task of Vitamin E is to protect the unsaturated fatty acids in the phospholipids of the cell membranes from peroxidation as a chain breaker. As an antioxidant; It functions to stop lipid peroxyl radicals and terminate lipid peroxidation chain reactions (Nimse and Pal, 2015).
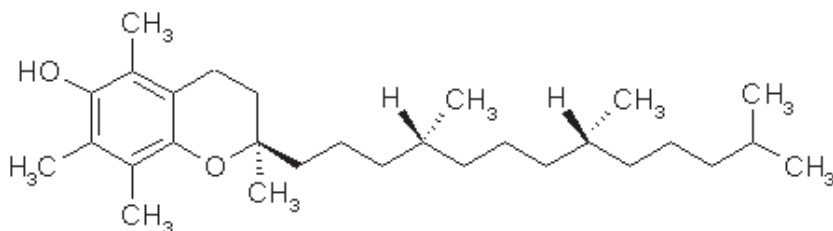
Figure 8. *Chemical structure of α-tocopherol*

Vitamin K is a fat-soluble vitamin. It is heat resistant, resistant to oxidation, alkalis, acids and light. Although it is a fat-soluble vitamin, it does not accumulate in the body and does not cause toxicity problems. Vitamin K is an effective substance in blood coagulation, converting blood plasma fibrinogen to fibrin. It prevents excessive bleeding. It exists in two forms, K_1 and K_2. K_1 (phylloquinone) is found in many foods, especially dark green leafy vegetables. K_2 (menaquinone) is synthesized by bacteria naturally found in the intestines. Vitamin K also has antioxidant properties. It protects cell membranes from damage by free radicals (Vervoort et al., 1997).

2.3.1.5. Phenolic acids:

Phenolic acids are aromatic carboxylic acids containing one or more hydroxyl groups. They are collected in two groups as hydroxybenzoic and hydroxycinnamic acids (Fig. 9). Hydroxybenzoic acids, which are in the structure of C6-C1 phenylmethane, are generally found in small amounts in plants. The most common hydroxybenzoic acids are gallic acid, salicylic acid, hydroxybenzoic acid, vanillic acid and syringic acids. Hydroxycinnamic acids, which are in the C6-C3 phenylpropane structure, differ according to the localization and structure of the hydroxyl group attached to the phenylpropane ring. Hydroxycinnamic acids are precursors of flavonoids. The most abundant hydroxycinnamic acids are; caffeic acid, ferulic acid, sinapic acid, p-coumaric acid and o-coumaric acid. Hydroxycinnamic acids; they are abundant in fruits and plants such as plums, apples, pears and grapes. Most of them in plants are esterified with sugars and organic acids. Phenolic acids; They are very important compounds that have been widely used in recent years, especially with the detection of their protective effects against many diseases such as cancer and cardiovascular diseases. They show strong antioxidant effects against free radicals and other reactive oxygen species. Studies have shown that phenolic acids have strong inhibitory activity against oxidation induced by peroxyl radicals. In addition, phenolic acids have a significant anti-aging effect on the body due to their anti-inflammatory, immune-enhancing and blood circulation-improving properties (Neo et al., 2010; Ravichandran et al., 2012).
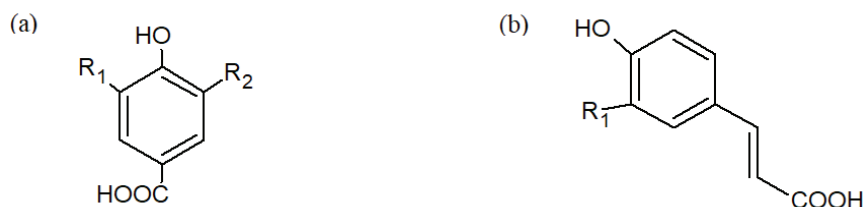
Figure 9. *Chemical structures of (a) hydroxycinnamic acids, (b) hydroxybenzoic acids*

2.3.1.6. Flavonoids:

The carbon skeleton of flavonoids consists of two phenyl rings joined by the propane chain and contains 15 carbon atoms. They are found in plants and cannot be synthesized in the human body. The hydroxyl groups in the structure of flavonoids are easily glycosylated due to their reactive properties. Flavonoids; are the most abundant polyphenols in foods. Today, over 6000 different types of flavonoids have been defined (Saldamlı,

2007). Changes in the heterocyclic ring in the structure of flavanoids cause the formation of main compound groups such as flavonols, flavones, flavanones, flavanols (catechins), isoflavones and anthocyanins.

Anthocyanins: Anthocyanins exist as glycosides with sugars. Anthocyanins are water-soluble pigments that give vegetables and fruits various colors in pink, red and blue hues. Its aglycones are anthocyanidins. Anthocyanins have important roles in defense, pollination and reproduction functions as well as antioxidant and protection from UV-light in plants. The colors of the flowers are due to anthocyanins. Anthocyanins, which protect plants from free radicals that cause DNA damage and cell death, have been shown to reduce the risk of chronic heart diseases in humans, improve visual activity and antiviral activity. These natural pigments are of great interest in the food industry and alternative medicine due to their health-beneficial properties such as antioxidant, anticancer, antidiabetic and anti-inflammatory, as well as attractive colors (Castañeda-Ovando et al., 2009; Garzón and Wrolstad, 2009).

Flavones and Flavonols: The most common class of flavonoids are flavonols. In the middle ring, hydrogen is attached to the third carbon atom in flavones, and hydroxyl group is attached to flavonols. Like anthocyanidins, they exist as glycosides with sugars. The most important flavonols; quercetin, rutin, camferol, myricetin, isoramnetin. It has been found to have antioxidant and anti-inflammatory effects (Heim et al., 2002).

Flavonones: Unlike flavones, flavonones do not have double bonds in their middle ring. These glycosides, which are common in citrus fruits, are responsible for the bitter taste in plants. The most important flavonones are naringin, hesperidin and naringenin. Hesperidin is abundant in oranges and lemons, and naringin is abundant in grapefruit. (Saldamli, 2007).

Flavanols (Catechins): Catechins, which form the most common flavonoid group found in foods, are colorless compounds found in almost every fruit. They take place as intermediates in flavonoid biosynthesis. Catechins are systematically referred to as flavan-3-ol. They easily react with oxygen in the air to form proanthocyanidins. Proanthocyanidins transform into anthocyanidins when heated in an acidic environment, taking on a typical red-violet color. Catechin is the most important flavonoid found in green tea. It has been the focus of attention due to its antioxidant, anticarcinogenic and anti-obesity properties. Due to the short plasma half-life of catechin, it must be consumed frequently to reap its nutritional benefits. It has been reported that tea catechins isolated from green tea have antiviral, antibacterial and anti-odour effects (Lee et al., 2002).

Isoflavones: Isoflavones, which are isomers of flavones, are commonly

found in soybeans and soy products and have a phytoestrogenic effect. Phytoestrogenic isoflavones; glycitein, daidzein and genistein. In our body, genistein interacts with the beta estrogen receptor and has an effect of one-third of the strength of estrogen. genistein; It creates an estrogen-like effect on the ovary, breast, prostate, endometrium, vascular and bone tissues. Isoflavones are also found in various legumes, but the main source is soybean (Cornwell et al., 2004).

3. Effects of Antioxidants on Health

The beneficial effects of antioxidants on human health depend on factors such as bioavailability and quantity after ingestion. Clinical studies are necessary to determine safe limits for the consumption of these compounds, as they may show toxic effects when consumed in high doses. Phenolic compounds have been applied in pharmacy, food chemistry, materials engineering, special machines and textile, demonstrating that these compounds are innovation focus in a wide range of technological fields (Araujo et al., 2021). The beneficial effects on health of phenolic compounds are mainly attributed to their metabolites. (Iglesias-Carres et al., 2019). The health benefit of these compounds includes antiallergenic, anti-inflammatory, anti-microbial, antioxidant, antithrombotic, vasodilatory and cardio protective effects (Araujo et al., 2021; Kumar et al., 2021).

Antioxidants can react by decreasing local concentration of molecular oxygen, scavenging chain initiating radicals like hydroxyl HO•, alkoxyl RO• or peroxyl ROO• and breaking the chain of radical sequence (Martysiak and Wenta, 2012). The hydroxyl radical is the most reactive radical and has very short half-lives. Antioxidants can scavenge free radicals due to their hydrogen donating ability. Because of these properties, antioxidants help reduce oxidative stress. The antioxidant activities of phenolic compounds differ according to their chemical structures. For example, polymeric polyphenols have better antioxidant properties than monomeric polyphenols. Similarly, the antioxidant effect differs depending on the position and number of the hydroxyl and methoxy groups in the benzene ring. The presence and positions of sugar groups in flavonols also affect the antioxidant activity of the compounds (Ruiz-Cabello et al., 2015; Aybastıer and Demir, 2017).

Improving the bioavailability of antioxidants is essential to increase their therapeutic potential in the prevention of diseases caused by oxidative stress. Some alternatives such as chemical and physical modification, use of polymers and nanotechnology are used to increase the bioavailability of these compounds, and change parameters such as absorption, metabolism, and solubility (Chen et al., 2019). Despite their beneficial effects on health, many studies have pointed out that antioxidant compounds ingested in

high concentrations can act as pro-oxidants and thus cause harmful effects. However, their pro-oxidative properties cannot be simply defined as harmful, and the benefits and risks depend on the concentration and situation used (Murakami, 2014). The potential of phenolic compounds to act as pro-oxidants depends on the type of compound and the concentration used. Therefore, their use should be carried out with caution in order to avoid possible harmful effects on health. Furthermore, it should be emphasized that more clinical studies must be carried out in order to establish safe concentration margins for the consumption of these compounds (Araujo et al., 2021).

The association between nutrition and health has received great attention in recent years. Many studies have shown that formation of oxidation in the biomolecules were decreased by different antioxidants, with different antioxidant powers, hence, other antioxidant could also prove efficacy in decreasing the production of biomolecule damage (Dawbaa et al., 2017; Aybastıer et al., 2018). However, more studies should be done on the effects of different antioxidants on preventing biomolecular damage through oxidation and on healthy living.

The use of antioxidant compounds, which can prevent or delay oxidative damage by inactivating reactive oxygen species, has attracted great interest in recent years. For this purpose, natural products and medicinal plants containing many antioxidant compounds are offered for sale. In the prevention of various diseases, the unconscious use of herbal products and plant-derived active substances is increasing with the thought that they are not harmful because they are natural. The structure and activities of most of the antioxidant compounds in plants have not been fully elucidated, and many active substances have both oxidant and antioxidant properties. There is not enough information about the toxicities of many herbal products and their possible effects on human health. Although it has been stated in in vitro cell culture studies that some herbal products can increase oxidative damage, be mutagenic, and induce DNA damage at high concentrations, there are also studies stating the opposite.

References

Altıner, A., Atalay, H., Bilal, T. 2017. Bir Antioksidan Olarak E Vitamini. Balıkesir Sağlık Bilimleri Dergisi, 6(3): 149-157.

Andries, A., Rozenski, J., Vermeersch, P., Mekahli, D., Schepdael, A.V. 2020. Recent progress in the LC–MS/MS analysis of oxidative stress biomarkers. Electrophoresis, 42(4): 402-428.

Araujo, F.F., Farias, D.P., Neri-Numa, I.A., Pastore, G.M. 2021. Polyphenols and their applications: An approach in food chemistry and innovation potential. Food Chemistry, 338: 127535.

Aybastıer, O., Demir, C. 2017. Antioxidant Activity Assay of Phenolic Compounds Isolated from Origanum Onites L. Aromatic Water by High Performance Liquid Chromatography. Annals of Nutritional Disorders &Therapy, 4(3): 1048.

Aybastıer, O., Dawbaa, S., Demir, C. 2018. Quantification of DNA damage products by gas chromatography tandem mass spectrometry in lung cell lines and prevention effect of thyme antioxidants on oxidative induced DNA damage. Mutation Research Fundamental Molecular Mutagenesis, 808: 1-9.

Balasundram, N., Sundram, K., Samman S. 2006. Phenolic compounds in plants and agri-industrial by-products: antioxidant activity, occurrence, and potential uses. Food Chemistry, 99(1): 191-203.

Baltaci, A.K., Mogulkoc, R. 2012. Leptin and zinc relation: In regulation of food intake and immunity. Indian Journal of Endocrinology and Metabolism, 16: 3.

Birben, E., Sahiner, U.M., Sackesen, C., Erzurum, S., Kalayci, O. 2012. Oxidative Stress and Antioxidant Defense. WAO Journal, 5(1): 9-19.

Castañeda-Ovando, A., Pacheco-Hernández, MmL., Páez-Hernández, M.A., Rodríguez, J.A., Galán-Vidal, C.A. 2009. Chemical studies of anthocyanins: A review. Food Chemistry, 113: 859–871

Chaudiere, J. and Ferrari-Iliou, R. 1999. Intracellular Antioxidants: From Chemical to Biochemical Mechanisms. Food and Chemical Toxicology, 37: 949-962.

Chen, L., Gnanaraj, C., Arulselvan, P., El-Seedi, H., Teng, H. 2019. A review on advanced microencapsulation technology to enhance bioavailability of phenolic compounds: Based on its activity in the treatment of Type 2 Diabetes. Trends in Food Science & Technology, 85: 149-162.

Cornwell, T., Cohick, W., Raskin, I. 2004. Dietary Phytoestrogens and Health. Phytochemistry, 65: 995–1016.

Dawbaa, S., Aybastıer, O., Demir, C. 2017. Ultrasensitive determination of DNA oxidation products by gaschromatography-tandem mass spectrometry and

the role of antioxidants in the prevention of oxidative damage. Journal of Chromatography B, 1051: 84-91.

Di Marco, S., Carnicelli, V., Franceschini, N., Di Paolo, M., Piccardi, M., Bisti, S., Falsini, B. 2019. Saffron: A Multitask Neuroprotective Agent for Retinal Degenerative Diseases, Antioxidants, 8: 224.

Di Meo, S., Reed, T.T., Venditti, P., Victor, V.M. 2016. Harmful and Beneficial Role of ROS. Oxidative Medicine and Cellular Longevity, 7909186.

Dwyer, J.H., Navab, M., Dwyer, K.M., Hassan, K., Sun, P., Shircore, A., Hama-Levy, S., Hough, G., Wang, X.P., Drake, T., Merz, C.N.B., Fogelman, A.M. 2001. Oxygenated carotenoid lutein and progression of early atherosclerosis. The Los Angeles Atherosclerosis Study, 103(24): 2922–7.

Garzón, G.A., Wrolstad, R.E. 2009. Major anthocyanins and antioxidant activity of Nasturtium flowers (Tropaeolum majus). Food Chemistry, 114: 44–49.

Gupta, S.K., Trivedi, D., Srivastava, S., Joshi, S., Halder, N., Verma, S.D. 2003. Lycopene Attenuates Oxidative Stress InducedExperimental Cataract Development: An In Vitro and In Vivo Study. Nutrition, 19: 794–799.

He, R.R., Tsoi, B., Lan, F., Yao, N., Yao, X.S., Kurihara, H. 2011. Antioxidant properties of lutein contribute to the protection against lipopolysaccharide-induced uveitis in mice. Chinese Medicine, 6:38.

Heim, K.E., Tagliaferro, A.R., Bobilya, D.J. 2002. Flavonoid antioxidants: chemistry, metabolism and structure-activity relationships. Journal of Nutritional Biochemistry, 13: 572–584.

Iciek, M.B., Pachel, D.K., Kwiecien, I., Dudek, M.B. 2012. Effects of Different Garlic-derived Allyl Sulfideson Peroxidative Processes and Anaerobic SulfurMetabolism in Mouse Liver. Phytotherapy Research, 26: 425-431.

Iglesias-Carres, L., Mas-Capdevila, A., Bravo, F.I., Aragonès, G., Arola-Arnal, A., et al. 2019. A comparative study on the bioavailability of phenolic compounds from organic and nonorganic red grapes. Food Chemistry, 299: 125092.

Kalayarasan, S., Prabhu, P.N., Sriram, N., Manikandan, R., Arumugam, M., Sudhandiran, G. 2009. Diallyl sulfide enhances antioxidants and inhibits inflammation through the activation of Nrf2 against gentamicin-induced nephrotoxicity in Wistar rats. European Journal of Pharmacology, 606: 162-171.

Kumar, A.N., Aruna, P., Naidu, J.N., Kumar, R. 2015. Review of Concepts and Controversies of Uric Acid as Antioxidant and Pro-Oxidant. Archives Medical Review Journal, 24(1): 19-40

Kumar, K., Srivastav, S., Sharanagat, V.S. 2021. Ultrasound assisted extraction (UAE) of bioactive compounds from fruit and vegetable processing by-products: A review. Ultrasonics-Sonochemistry, 70: 105325.

Lee, M.J., Maliakal, P., Chen, L., Meng, X., Bondoc, F.Y. et al. 2002. Pharma-cokinetics of Tea Catechins after Ingestion of Green Tea and (-)-Epigal-locatechin-3-gallate by Humans: Formation of Different Metabolites and Individual Variability. Cancer Epidemiology, Biomarkers & Prevention, 11: 1025–1032.

Li, P., Yin, Y.L., Li, D., Kim, S.W., Wu, G. 2007. Amino acids and immune fun-ction. British Journal of Nutrition, 98: 237–252.

Llana-Ruiz-Cabello, M., Gutierrez-Praena, D., Puerto, M., Pichardo, S., Jos, A., et al. 2015. In vitro pro-oxidant/antioxidant role of carvacrol, thymol and their mixture in the intestinal Caco-2 cell line. Toxicology in Vitro, 29(4): 647-656.

Lobanov, A.V., Hatfield, D.L., Gladyshev, V.N. 2008. Reduced reliance on the trace element selenium during evolution of mammals. Genome Biology, 9(3): R62.

Männisto, S., Yaun, S., Hunter, D., Spiegelman, D., Adami H. et al. 2007. Dietary carotenoids and risk of colorectal cancer in a pooled analysis of 11 cohort studies. American Journal of Epidemiology, 165(3): 246–55.

Martysiak, D.M., Wenta, W. 2012. A comparison of ABTS and DPPH methods for assessing the total antioxidant capacity of human milk. Acta Scientia-rum Polonorum, 11(1): 83-89.

Mor, M, Silva, C., Vacondio, F., Plazzi, P.V., Bertoni, S. Et al. 2004. Indole-ba-sed analogs of melatonin: in vitro antioxidant andcytoprotective activities. Journal of Pineal Research, 36: 95-102.

Murakami, A. 2014. Dose-dependent functionality and toxicity of green tea pol-yphenols in experimental rodents. Archives of Biochemistry and Biophy-sics, 557: 3-10.

Murillo, A.G., Hu, S., Fernandez, M.L. 2019. Zeaxanthin: Metabolism, Proper-ties, and Antioxidant Protection of Eyes, Heart, Liver, and Skin. Antioxi-dants, 8: 390.

Neo, Y.P., Ariffin, A., Tan, C.P., Tan, Y.A. 2010. Phenolic acid analysis and anti-oxidant activity assessment of oil palm (E. guineensis) fruit extracts. Food Chemistry, 122: 353–359.

Nimse, S.B. and Pal, D. 2015. Free radicals, natural antioxidants, and their reac-tion mechanisms. RSC Advances, 5, 27986–28006.

Palace, V.P., Khaper, N., Quin, Q., Singal, P. 1999. Antioxidant Potentials of Vitamın A and Carotenoids and Their Relevance to Heart Disease. Free Radical Biology & Medicine, 26, 746-761.

Pietta, P.G. 2000. Flavonoids as antioxidants. Journal of Natural Products, 63(7): 1035-42.

Pisoschi, A.M., Pop, A., Iordache, F., Stanca, L., Predoi, G. et al. 2021. Oxida-tive stress mitigation by antioxidants – An overview on their chemistry

and influences on health status. European Journal of Medicinal Chemistry, 209:112891

Ravichandran, K., Ahmed, A.R., Knorr, D., Smetanska, I. 2012. The effect of different processing methods on phenolic acid content and antioxidant activity of red beet. Food Research International, 48: 16–20.

Saini, R. 2011. Coenzyme Q10: The essential nutrient. Journal of Pharmacy & Bioallied Sciences, 3(3): 466–467.

Saldamlı, İ. 2007. Gıda Kimyası, Hacettepe Üniversitesi Yayınları, Ankara.

Skrovankova S., Sumczynski D., Mlcek J., Jurikova T., Sochor J. 2015. Bioactive compounds and antioxidant activity in different types of berries. International Journal of Molecular Sciences, 16(10): 24673-24706.

Stahl, W. and Sies, H. 2003. Antioxidant activity of carotenoids. Molecular Aspects of Medicine, 24: 345–351.

Thomas, D., Cherest, H., Surdin-Kerjan, Y. 1991. Identification of the structural gene for glucose-6-phosphate dehydrogenase in yeast. Inactivation leads to a nutritional requirement for organic sulfur. The EMBO Journal, 10(3): 547–53.

Valko, M., Leibfritz, D., Moncol, J., Cronin, M.T.D., Mazur, M., et al. 2007. Free radicals and antioxidants in normal physiological functions and human disease. The International Journal of Biochemistry & Cell Biology, 39(1): 44-84.

Vervoort, L.M.T., Ronden, J.E., Thijsen, H.H.W. 1997. The Potent Antioxidant Activity of the Vitamin K Cycle in Microsomal Lipid Peroxidation. Biochemical Pharmacology, 54: 871-876.

Vuolo, M.M., Lima, V.S., Marostica, M.R. 2019. Phenolic compounds: Structure, classification, and antioxidant power. In Bioactive Compounds: Health Benefits and Potencial Applications. Woodhead Publishing, pp: 33-50.

Woodall, A.A., Lee, S.W.M., Weesie, R.J., Jackson, M.J., Britton, G. 1997. Oxidation of carotenoids by free radicals: relationship between structureand reactivity. Biochimica et Biophysica Acta, 1336: 33–42.

Zhang, T., Wang, Z., Wang, X., Sun, W., Cui, X. Et al. 2019. Effects of vitamin A on antioxidant functions, immune functions and production performance in male sika deer (Cervus nippon) during the first antler growth period. Italian Journal of Animal Science, 18(1): 98-104.

Chapter 7

FINITE ELEMENT SIMULATION OF THE WEAKLY COUPLED SYSTEM OF NONLINEAR DAMPED WAVE EQUATIONS WITH DISTINCT SCALE-INVARIANT TERMS

Harun SELVİTOPİ[1]

1 Harun Selvitopi, Dr. Öğr, Üyesi, Department of Mathematics, Faculty of Sciences, Erzurum Technical University, 25050, Erzurum, Turkey, ORCID ID: 0000-0001-5958-7625

In this study, we focus on the weakly coupled system of nonlinear wave equations
with scale-invariant damping term and mass in the linear part,

$$u_{tt} - \Delta u + \frac{\mu_1}{1+t} u_t + \frac{\vartheta_1^2}{(1+t)^2} u = |v|^p \quad x \in \mathbb{R}, \quad t > 0$$

$$v_{tt} - \Delta v + \frac{\mu_1}{1+t} v + \frac{\vartheta_1^2}{(1+t)^2} v = |u|^p \quad x \in \mathbb{R}, \quad t > 0$$

$$(u, u_t, v, v_t)(0, x) = (u_0, u_1, v_0, v_1)(x), \quad x \in \mathbb{R}$$

(1)

where $\mu_1, \mu_2, \vartheta_1, \vartheta_2$ are nonnegative constant and $p, q > 1$.

It is already well known that the scale-invariant wave equation with damping term is an important phenomena in physics and engineering. Therefore, the weakly coupled system of semilinear wave equations with scale-invariant damping term, mass and power nonlinearity has been studied to prove the existence of the solution wide range in recent years. The global in time solution of the nonlinear hyperbolic system with damping has been proved for the small initial data when the space dimension is 1 or 3 in [1]. The global existence of solution of the system of nonlinear damped wave equations with respect to the critical exponent has been proved using $Lp - Lq$ estimates in [2]. In [3], asymptotic behavior of system of nonlinear damped wave equations has been shown. The global solution of the semilinear wave equation with space-time dependent damping has been shown unique in [4]. The asymptotic behavior of solutions for a system of weakly coupled heat equations and corresponding system of damped wave equations has been shown in [5]. The global existence of the solution of weakly coupled nonlinear damped wave system has been proved limiting the critical exponents in [6]. In [7], the critical exponents of semilinear space and time damped wave system were determined. But in this paper the critical exponents has been determined merely space dependent damping and merely time dependent damping. In [8], the critical exponents of nonlinear system (1) has been determined and the global existence results(in time) of nonlinear system (1) has been proven.

As we know FEM is one of the most effective numerical method to solve the "wave-like" partial differential equations. Therefore FEM

has been widely used to acquire the numerical solution of the "wave-like" problems. For instance, a continuous Galerkin method has been applied to obtain the numerical results of the wave equation in [9]. In [10], domain decomposition finite element/finite difference method has been performed for the hyperbolic equation. The system in (1) is not only "wave-like" but also "Klein-Gordon-like" system of equations. Finite element/finite difference hybrid scheme which FDM and FEM was considered in time and space direction respectively has been proposed to acquire the numerical solution of the Klein-Gordon equation in de Sitter space-time in [11]. In [12], wavelet Galerkin method has been considered for the nonlinear wave problems. The nonlinear Klein-Gordon and sine-Gordon equations were solved using wavelet Galerkin method with Runge-Kutta method in [12]. It is quite inconvenient to obtain the exact solution of power nonlinear scale-invariant damped wave systems. Therefore the numerical results are obtained for the problems which has power nonlinearity. To our knowledge, the exact and the numerical solution of the nonlinear system (1) has not been acquired yet. The lack of the exact and numerical solution of the system (1) motivate us to obtain the numerical solution of the system (1). The paper is organized as follows: In Section 2, system of equations in (1) is discretized using two different hybrid numerical schemes. The acquired numerical results different numerical schemes are displayed by graphics and discussion is given in Section 3. Finally, we give the main conclusions of this study in Section 4.

NUMERICAL METHODS

In this section we will apply the FDM and FEM to acquire the numerical solution of the system (1). In the solution procedure we will use the FDM for discritization of the temporal variable and we will also use the FEM to disctritize the spatial variable. The nonlinear system of equations obtain by applying the FDM/FEM scheme to the system (1) will be linearized using the Newton method which is most preferred linearization method.

Preliminary Preparation for Numerical Solution: The system (1) is $1 + 1$ power nonlinear weakly coupled scale-invariant wave equations system with damping and mass terms. The relationship

between damping terms $\frac{\mu_1}{1+t}u_t, \frac{\mu_2}{1+t}v_t$ and mass terms $\frac{\vartheta_1^2}{(1+t)^2}u, \frac{\vartheta_2^2}{(1+t)^2}v$ is defined with the quantity $\delta_i = (\mu_i - 1)^2 - 4v_i^2$, $i = 1,2$. In this work, the relation between μ_1, μ_2 and ϑ_1, ϑ_2 is considered $\delta_i = 1$, $i = 1,2$.

Through the transformations $u(t,x) = (1+t)^{\frac{-\mu_1}{2}}\emptyset(t,x)$ and $v(t,x) = (1+t)^{\frac{-\mu_2}{2}}\psi(t,x)$ in the system (1) we get the initial boundary value problem as follow:

$$
\begin{aligned}
&\emptyset_{tt} - \Delta\emptyset = (1+t)^{\frac{-\mu_1}{2}(p-1)}|\psi|^p \quad x \in \mathbb{R}, \quad t > 0 \\
&\psi_{tt} - \Delta\psi = (1+t)^{\frac{-\mu_2}{2}(q-1)}|\emptyset|^q \quad x \in \mathbb{R}, \quad t > 0 \\
&(\emptyset, \emptyset_t, \psi, \psi_t)(0,x) = (\emptyset_0, \emptyset_1, \psi_0, \psi_1)(x), \quad x \in \mathbb{R}
\end{aligned}
\tag{2}
$$

where $\mu_1, \mu_2 > 0$.

Finite Element Method:

We propose the FDM/FEM hybrid numerical scheme to acquire the numerical solution of the system (2). In the solution procedure we will apply the central difference approximation for the time variable and the Galerkin finite element method is also applied for the space variable with zero boundary condition.

We apply the standard FEM in [13] to nonlinear system (2) and we obtain the weak formulation of the system (2) is given by employing linear function space $L = H_0^1(\Omega): u, v \in L$ as:

$$
\begin{aligned}
&(\emptyset_{tt}, w_1) + (\nabla\emptyset, \nabla w_1) - (1+t)^{\frac{-\mu_1}{2}(p-1)}(|\psi|^p, w_1) \\
&\qquad = 0 \\
&(\psi_{tt}, w_2) + (\nabla\psi, \nabla w_2) - (1+t)^{\frac{-\mu_2}{2}(q-1)}(|\emptyset|^q, w_2) \\
&\qquad = 0 \\
&\qquad\qquad w_1, w_2 \in H_0^1(\Omega)
\end{aligned}
\tag{3}
$$

where $(.,.)$ represents the L^2 inner product.

Then, we apply the central difference approximation for the temporal variable and Crank-Nicolson(C-N) and backward differences approximation for the spatial variable according to time level in (3), we obtain;

$$\left(\frac{\emptyset^{n+1} - 2\emptyset^n + \emptyset^{n-1}}{\Delta t^2}, w_1\right) + [\theta(\nabla\emptyset^{n+1}, \nabla w_1)$$
$$+ (1-\theta)(\nabla\emptyset^n, \nabla w_1)]$$
$$- [\theta(1 + t^{n+1})^{\frac{-\mu_1}{2}(p-1)}(|\psi^{n+1}|^p, w_1)$$
$$+ (1-\theta)(1$$
$$+ t^n)^{\frac{-\mu_1}{2}(p-1)}(|\psi^n|^p, w_1)] = 0$$
$$\left(\frac{\psi^{n+1} - 2\psi^n + \psi^{n-1}}{\Delta t^2}, w_2\right) + [\theta(\nabla\psi^{n+1}, \nabla w_2)$$
$$+ (1-\theta)(\nabla\psi^n, \nabla w_2)]$$
$$- [\theta(1 + t^{n+1})^{\frac{-\mu_2}{2}(q-1)}(|\emptyset^{n+1}|^q, w_2)$$
$$+ (1-\theta)(1$$
$$+ t^n)^{\frac{-\mu_2}{2}(q-1)}(|\emptyset^n|^q, w_2)] = 0$$

(4)

where $\theta \in \{1/2, 1\}$. Specifying the FEM discretization, system (4) becomes [13]: Find
$\emptyset_h, \psi_h \in L_h$ such that

$$\left(\frac{\emptyset_h^{n+1} - 2\emptyset_h^n + \emptyset_h^{n-1}}{\Delta t^2}, w_{1_h}\right) + [\theta(\nabla\emptyset_h^{n+1}, \nabla w_{1_h})$$
$$+ (1-\theta)(\nabla\emptyset_h^n, \nabla w_{1_h})]$$
$$- [\theta(1 + t^{n+1})^{\frac{-\mu_1}{2}(p-1)}(|\psi_h^{n+1}|^p, w_{1_h})$$
$$+ (1-\theta)(1$$
$$+ t^n)^{\frac{-\mu_1}{2}(p-1)}(|\psi_h^n|^p, w_{1_h})] = 0$$
$$\left(\frac{\psi_h^{n+1} - 2\psi_h^n + \psi_h^{n-1}}{\Delta t^2}, w_{2_h}\right) + [\theta(\nabla\psi_h^{n+1}, \nabla w_{2_h})$$
$$+ (1-\theta)(\nabla\psi_h^n, \nabla w_{2_h})]$$
$$- [\theta(1 + t^{n+1})^{\frac{-\mu_2}{2}(q-1)}(|\emptyset_h^{n+1}|^q, w_{2_h})$$
$$+ (1-\theta)(1 + t^n)^{\frac{-\mu_2}{2}(q-1)}(|\emptyset_h^n|^q, w_{2_h})]$$
$$= 0$$

(5)

$$\forall w_{1_h}, w_{2_h} \in L_h$$

Then we obtain the weak formulation with respect to time step using linear element on
interval $[x_i, x_{i+1}]$ as:

$$
\begin{aligned}
&\left(\emptyset_h^{n+1}, w_{1_h}\right) + \theta\Delta t^2\left(\nabla\emptyset_h^{n+1}, \nabla w_{1_h}\right) \\
&\quad - \left[\theta(1 + t^{n+1})^{\frac{-\mu_1}{2}(p-1)}\left(\left|\psi_h^{n+1}\right|^p, w_{1_h}\right)\right. \\
&\quad - 2(\emptyset_h^n, w_{1_h}) \\
&\quad + (1 - \theta)\Delta t^2\left(\nabla\emptyset_h^n, \nabla w_{1_h}\right) \\
&\quad + (1 - \theta)(1 \\
&\quad + t^n)^{\frac{-\mu_1}{2}(p-1)}\left(|\psi_h^n|^p, w_{1_h}\right)] \\
&\quad + \left(\emptyset_h^{n-1}, w_{1_h}\right) = 0 \\
&\left(\psi_h^{n+1}, w_{1_h}\right) + \theta\Delta t^2\left(\nabla\psi_h^{n+1}, \nabla w_{1_h}\right) \\
&\quad - \left[\theta(1 + t^{n+1})^{\frac{-\mu_2}{2}(p-1)}\left(\left|\emptyset_h^{n+1}\right|^q, w_{1_h}\right)\right. \\
&\quad - 2(\psi_h^n, w_{1_h}) \\
&\quad + (1 - \theta)\Delta t^2\left(\nabla\psi_h^n, \nabla w_{1_h}\right) \\
&\quad + (1 - \theta)(1 \\
&\quad + t^n)^{\frac{-\mu_2}{2}(p-1)}\left(|\emptyset_h^n|^q, w_{1_h}\right)] \\
&\quad + \left(\psi_h^{n-1}, w_{1_h}\right) = 0
\end{aligned}
$$

(6)

The system (6) can be written in the matrix-vector form:

$$
\begin{aligned}
&\begin{bmatrix} H & 0 \\ 0 & H \end{bmatrix}\begin{bmatrix} \emptyset^{n+1} \\ \psi^{n+1} \end{bmatrix} + \theta\begin{bmatrix} G_1 & 0 \\ 0 & G_2 \end{bmatrix}\begin{bmatrix} \emptyset^{n+1} \\ \psi^{n+1} \end{bmatrix}^p \\
&\quad + \begin{bmatrix} K & 0 \\ 0 & K \end{bmatrix}\begin{bmatrix} \emptyset^n \\ \psi^n \end{bmatrix} \\
&\quad + (1 - \theta)\begin{bmatrix} G_1 & 0 \\ 0 & G_2 \end{bmatrix}\begin{bmatrix} \emptyset^n \\ \psi^n \end{bmatrix}^q = \begin{bmatrix} 0 \\ 0 \end{bmatrix}
\end{aligned}
$$

(7)

where the H, K, C, G_1 and G_2 matrices with the entry;

$$
H_{ij} = \int_{x_i}^{x_{i+1}}\left(N_i N_j + \theta\Delta t^2\frac{\partial N_i}{\partial x}\frac{\partial N_j}{\partial x}\right)dx
$$

$$
K_{ij} = \int_{x_i}^{x_{i+1}}\left(-2N_i N_j + (1 - \theta)\Delta t^2\frac{\partial N_i}{\partial x}\frac{\partial N_j}{\partial x}\right)dx
$$

$$
G_{1ij} = \int_{x_i}^{x_{i+1}}\left(\Delta t^2|N_i|^p N_j\right)dx
$$

$$
G_{2ij} = \int_{x_i}^{x_{i+1}}\left(\Delta t^2|N_i|^q N_j\right)dx
$$

We apply the central difference approximation to the initial condition;

$$\emptyset_t(0,x) = 0 \tag{8}$$
$$\psi_t(0,x) = 0$$

for the initial time step, we obtain;

$$\frac{\emptyset^{n+1} - \emptyset^n}{2\Delta t} = 0$$
$$\frac{\psi^{n+1} - \psi^n}{2\Delta t} = 0 \tag{9}$$

Then we apply the (9) to the nonlinear system of equations (7), we obtain the nonlinear
system of equations for the first unknown time step as:

$$\begin{bmatrix} S & 0 \\ 0 & S \end{bmatrix}\begin{bmatrix} \emptyset^{n+1} \\ \psi^{n+1} \end{bmatrix} + \theta\begin{bmatrix} G_1 & 0 \\ 0 & G_2 \end{bmatrix}\begin{bmatrix} \emptyset^{n+1} \\ \psi^{n+1} \end{bmatrix}^p \tag{10}$$
$$+ (1-\theta)\begin{bmatrix} G_1 & 0 \\ 0 & G_2 \end{bmatrix}\begin{bmatrix} \emptyset^n \\ \psi^n \end{bmatrix}^q = \begin{bmatrix} 0 \\ 0 \end{bmatrix}$$

where the S matrix with the entry,

$$S_{ij} = \int_{x_i}^{x_{i+1}} \left(-N_i N_j + \Delta t^2 \frac{\partial N_i}{\partial x}\frac{\partial N_j}{\partial x}\right) dx$$

Finite Difference Method: In the previous subsection, we apply the FEM to the system (2) with implicit and C-N schemes. For the accuracy and the reliability of the obtained numerical results using FEM we propose FDM/FDM hybrid numerical method with implicit and C-N schemes to acquire the numerical solution of the system (2).

We use the central difference approximation both the temporal and spatial variable for equations in system (2). For this purpose, we denote the $t_k = k\Delta t$, for $k = 0, 1, \ldots, s$ with the time step size $\Delta t = \frac{1}{s}$ and $x_m = m\Delta x$, for $m = 0, 1, \ldots, h$ with the space step size $\Delta x = \frac{1}{h}$.

If we apply the central difference approximation for the system (2), we obtain;

$$\frac{\emptyset_i^{n+1} - 2\emptyset_i^n + \emptyset_i^{n-1}}{\Delta t^2} - \theta\left(\frac{\emptyset_{i+1}^{n+1} - 2\emptyset_i^{n+1} + \emptyset_{i-1}^{n+1}}{\Delta x^2}\right)$$
$$- (1-\theta)\left(\frac{\emptyset_{i+1}^n - 2\emptyset_i^n + \emptyset_{i-1}^n}{\Delta x^2}\right)$$
$$- \theta(1+t^{n+1})^{\frac{-\mu_1}{2}(p-1)}|\psi_i^{n+1}|^p - (1$$
$$- \theta)(1+t^n)^{\frac{-\mu_1}{2}(p-1)}|\psi_i^n|^p = 0$$
$$\frac{\psi_i^{n+1} - 2\psi_i^n + \psi_i^{n-1}}{\Delta t^2} - \theta\left(\frac{\psi_{i+1}^{n+1} - 2\psi_i^{n+1} + \psi_{i-1}^{n+1}}{\Delta x^2}\right)$$
$$- (1-\theta)\left(\frac{\psi_{i+1}^n - 2\psi_i^n + \psi_{i-1}^n}{\Delta x^2}\right)$$
$$- \theta(1+t^{n+1})^{\frac{-\mu_2}{2}(q-1)}|\emptyset_i^{n+1}|^q - (1$$
$$- \theta)(1+t^n)^{\frac{-\mu_2}{2}(q-1)}|\emptyset_i^n|^q = 0$$

(11)

where $\emptyset_i^n = \emptyset(x_i, t_n), \psi_i^n = \psi(x_i, t_n)$ and $\theta \in \{^1/_2, 1\}$. Denoting the mesh rate $r = \frac{\Delta t^2}{\Delta x^2}$, the system (11) is rewritten according to time step as:

$$-r\theta\emptyset_{i+1}^{n+1} + (1+2r\theta)\emptyset_i^{n+1} - r\theta\emptyset_{i-1}^{n+1}$$
$$- r(1-\theta)\emptyset_{i+1}^n + \big(1 + 2(1-\theta)\big)\emptyset_i^n$$
$$- r(1-\theta)\emptyset_{i-1}^n$$
$$- \theta\Delta t^2(1+t^{n+1})^{\frac{-\mu_1}{2}(p-1)}|\psi_i^{n+1}|^p$$
$$- (1-\theta)\Delta t^2(1+t^n)^{\frac{-\mu_1}{2}(p-1)}|\psi_i^n|^p$$
$$+ \emptyset_i^{n-1} = 0$$
$$-r\theta\psi_{i+1}^{n+1} + (1+2r\theta)\psi_i^{n+1} - r\theta\psi_{i-1}^{n+1}$$
$$- r(1-\theta)\psi_{i+1}^n + \big(1 + 2(1-\theta)\big)\psi_i^n$$
$$- r(1-\theta)\psi_{i-1}^n$$
$$- \theta\Delta t^2(1+t^{n+1})^{\frac{-\mu_2}{2}(q-1)}|\emptyset_i^{n+1}|^q$$
$$- (1-\theta)\Delta t^2(1+t^n)^{\frac{-\mu_2}{2}(q-1)}|\emptyset_i^n|^q$$
$$+ \psi_i^{n-1} = 0$$

(12)

If we set $\overrightarrow{\Phi^n} = [\emptyset_1^n, \emptyset_2^n, \dots, \emptyset_m^n]^T$, and $\overrightarrow{\Psi^n} = [\psi_1^n, \psi_2^n, \dots, \psi_m^n]^T$, we rewrite the system (12)
with matrix form

$$(I + r\theta A)\overrightarrow{\Phi^{n+1}} + (I + r(1 - \theta)A)\overrightarrow{\Phi^n}$$
$$- \theta\Delta t^2 (1 + t^{n+1})^{\frac{-\mu_1}{2}(p-1)} \left|\overrightarrow{\Psi^{n+1}}\right|^p$$
$$- (1 - \theta)\Delta t^2 (1 + t^n)^{\frac{-\mu_1}{2}(p-1)} \left|\overrightarrow{\Psi^n}\right|^p \qquad (13)$$
$$+ \overrightarrow{\Phi^n} = 0$$
$$(I + r\theta A)\overrightarrow{\Psi^{n+1}} + (I + r(1 - \theta)A)\overrightarrow{\Psi^n}$$
$$- \theta\Delta t^2 (1 + t^{n+1})^{\frac{-\mu_2}{2}(q-1)} \left|\overrightarrow{\Phi^{n+1}}\right|^q$$
$$- (1 - \theta)\Delta t^2 (1 + t^n)^{\frac{-\mu_2}{2}(q-1)} \left|\overrightarrow{\Phi^n}\right|^q$$
$$+ \overrightarrow{\Psi^n} = 0$$

where I is unit matrix and

$$A = \begin{bmatrix} 2 & -1 & 0 & \cdots & & 0 \\ -1 & 2 & -1 & & & \\ & \vdots & & \ddots & & \vdots \\ & & & -1 & 2 & -1 \\ 0 & & \cdots & 0 & -1 & 2 \end{bmatrix}$$

Newton Method: Applying the FEM and FDM for the nonlinear system (2), we obtain the nonlinear systems of equations (7) and (13). To linearize the nonlinear systems (7) and (13) we apply the Newton method. We consider the X_0 is the first approximation of the solution of nonlinear system $F(X) = 0$. Then, to obtain the numerical solution of the (7) and (13) take account of the iterative method:

$$X_{l+1} = X_l - J^{-1}(X_0)F(X_l), \qquad for \qquad l = 1, 2, \dots \qquad (14)$$

where $J(X_0)$ is the Jacobian matrix of F in the vector X_0. We rewrite the iterative system of (7) with respect to $(n + 1)^{th}$ time step as:

$$\begin{bmatrix} H & 0 \\ 0 & H \end{bmatrix} X + \beta = \begin{bmatrix} 0 \\ 0 \end{bmatrix} \qquad (15)$$

where

$$\beta = \theta \begin{bmatrix} G_1 & 0 \\ 0 & G_2 \end{bmatrix} \begin{bmatrix} \emptyset^{n+1} \\ \psi^{n+1} \end{bmatrix}^p + \begin{bmatrix} K & 0 \\ 0 & K \end{bmatrix} \begin{bmatrix} \emptyset^n \\ \psi^n \end{bmatrix}$$
$$+ (1-\theta) \begin{bmatrix} G_1 & 0 \\ 0 & G_2 \end{bmatrix} \begin{bmatrix} \emptyset^n \\ \psi^n \end{bmatrix}^q$$

and $X = \begin{bmatrix} \emptyset^{n+1} \\ \psi^{n+1} \end{bmatrix}$.

Representing,

$$F(X) = \begin{bmatrix} H & 0 \\ 0 & H \end{bmatrix} \begin{bmatrix} \emptyset^{n+1} \\ \psi^{n+1} \end{bmatrix} + \theta \begin{bmatrix} G_1 & 0 \\ 0 & G_2 \end{bmatrix} \begin{bmatrix} \emptyset^{n+1} \\ \psi^{n+1} \end{bmatrix}^p$$
$$+ \begin{bmatrix} K & 0 \\ 0 & K \end{bmatrix} \begin{bmatrix} \emptyset^n \\ \psi^n \end{bmatrix} \qquad (16)$$
$$+ (1-\theta) \begin{bmatrix} G_1 & 0 \\ 0 & G_2 \end{bmatrix} \begin{bmatrix} \emptyset^n \\ \psi^n \end{bmatrix}^q$$

After these implementation to obtain the numerical solution of nonlinear system (7) we applied the Newton method to find the root of nonlinear system (16). In the process of the application of the Newton method we need the jacobian matrix of $F(X)$, but we can not determine jacobian matrix analytically due to the unknown of the partial derivatives of $F(X)$. Therefore we calculated the jacobian matrix of $F(X)$ approximately as:
For $\Delta x > 0$, the approximation of derivative of the jacobian matrix,

$$\frac{\partial F_i}{\partial X_j}(X_0) = \frac{F_i(X_0 + \overrightarrow{\Delta X}) - F_i(X_0)}{\Delta X} \quad for \quad i,j$$
$$= 1,2,\dots,m \qquad (17)$$

Where $\overrightarrow{\Delta X} = \Delta x \cdot e_j$, with e_j being the jth canonical vector of $\mathbb{R}^n$. All elements of the $J(X_0)$ can be calculated using the approach (17). After this process, because of $F(X_0)$ is known, replacing $F(X_0)$ in the system (14) and solving the linear system, acquire the X_1. This procedure will be recapitulation continuously to satisfy the condition,

$$\|X_{l+1} - X_l\|_{L\infty(\Omega)} < \epsilon \quad \text{for any } \epsilon > 0.$$

In the process of obtaining numerical results we consider the $\epsilon > 10^{-8}$.
Applying aforementioned numerical methods for the nonlinear system (2) we have acquired the numerical solution of $\emptyset(t,x)$ and

$\psi(t, x)$. To obtain the numerical solution of $u(t, x)$ and $v(t, x)$ we use the transformations $u(t, x) = (1 + t)^{-\frac{\mu_1}{2}} \emptyset(t, x)$ and $v(t, x) = (1 + t)^{-\frac{\mu_2}{2}} \psi(t, x)$.

NUMERICAL RESULTS and DISCUSSION

The numerical results of the nonlinear system (1) will be given in this section considering different values of μ_1 and μ_2. The solution domain considered for the space interval $\Omega = [0,1]$ with $t \geq 0$. In the solution procedure the spatial step size was considered $\Delta x = 10^{-3}$ and the temporal step size was also considered $\Delta t = 10^{-3}$. We use the bump function

$$B(x; C, R) = \begin{cases} \exp\left(\dfrac{1}{R^2} - \dfrac{1}{R^2 - |x - C|^2}\right) & if \quad |x - C| < R \\ 0, & if \quad |x - C| \geq R \end{cases}$$

where $C \in \Omega$ is the center and R is the radius satisfying $0 < R < 1$ for the initial conditions. The boundary of the solution domain was taken zero for the all numerical examples.

Two Bubbles Case: In this case we consider the initial condition with two bubbles in the form;

$$\begin{bmatrix} u_0(x) \\ v_0(x) \end{bmatrix} = \begin{bmatrix} B(x, 0.2, 0.4) + B(x, 0.2, 0.6) \\ B(x, 0.2, 0.4) + B(x, 0.2, 0.6) \end{bmatrix} \quad \forall x \in \Omega$$
$$\begin{bmatrix} u_1(x) \\ v_1(x) \end{bmatrix} = \begin{bmatrix} 0 \\ 0 \end{bmatrix} \tag{18}$$

like in Figure 1. In Figure 2. and Figure 3. we show the behavior of the u and v in time for $\mu_1 = \mu_2 = 1$ and $\mu_1 = \mu_2 = 3$ using FEM and FDM. In Figure 2. and Figure 3. we have been observed the numerical results obtaining by FEM and FDM with Crank-Nicolson and implicit schemes for u and v respectively for $\mu_1 = \mu_2 = 10$. The numerical results shows us from Figure 2. to Figure 3. when the μ_1 and μ_2 increase the wavelength of u and v becomes shorter.
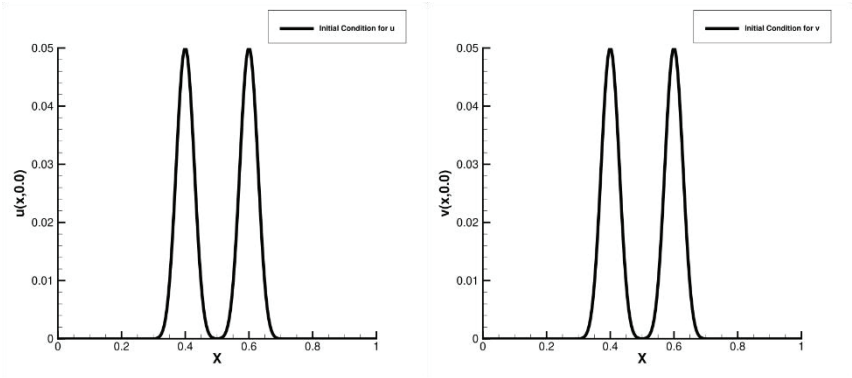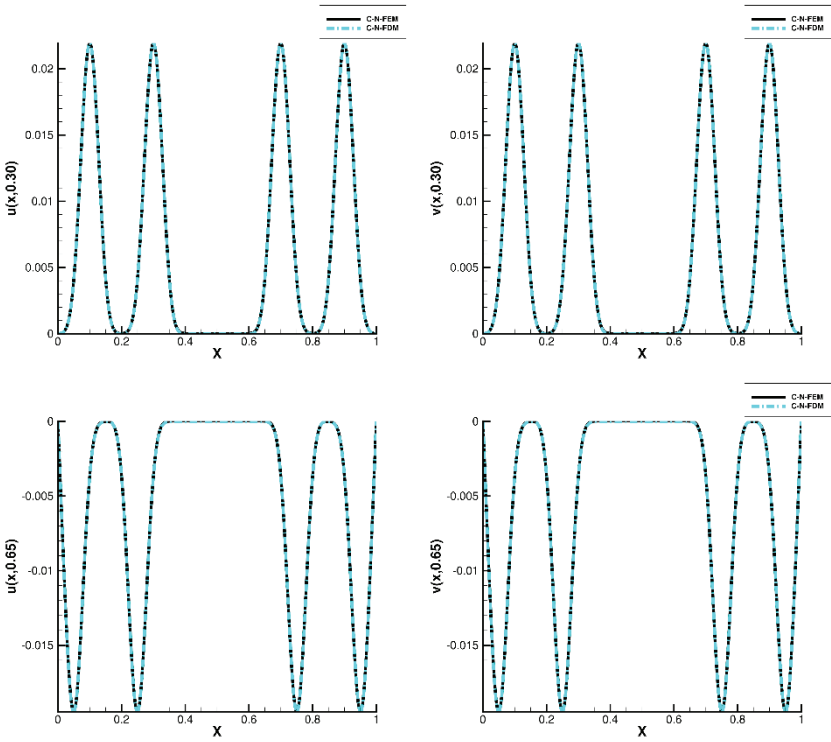
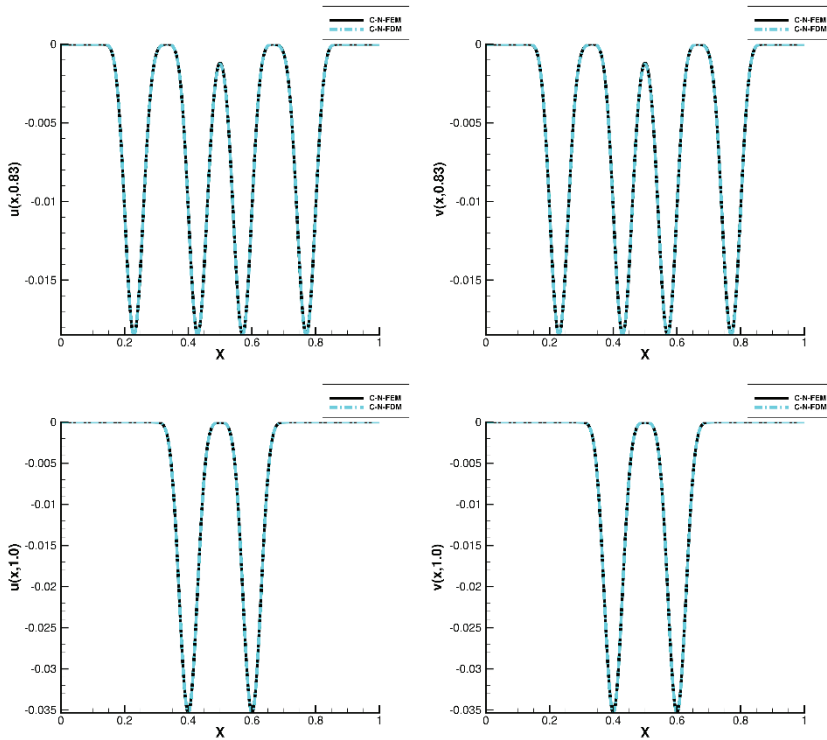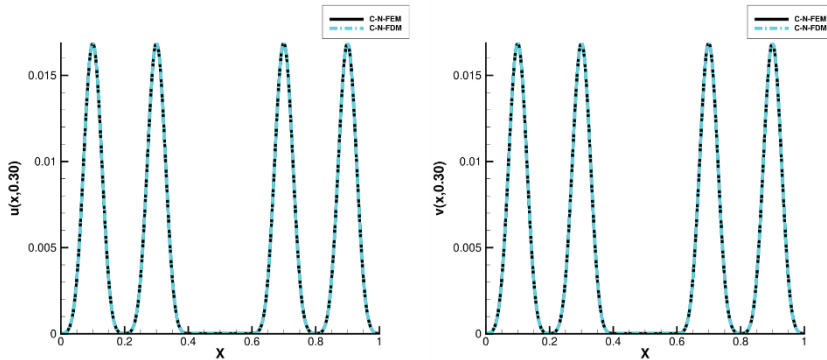Figure 1. Plot of initial function for u and v respectively.

Figure 2. First and second column shows plot of numerical solution of u and v by FEM and
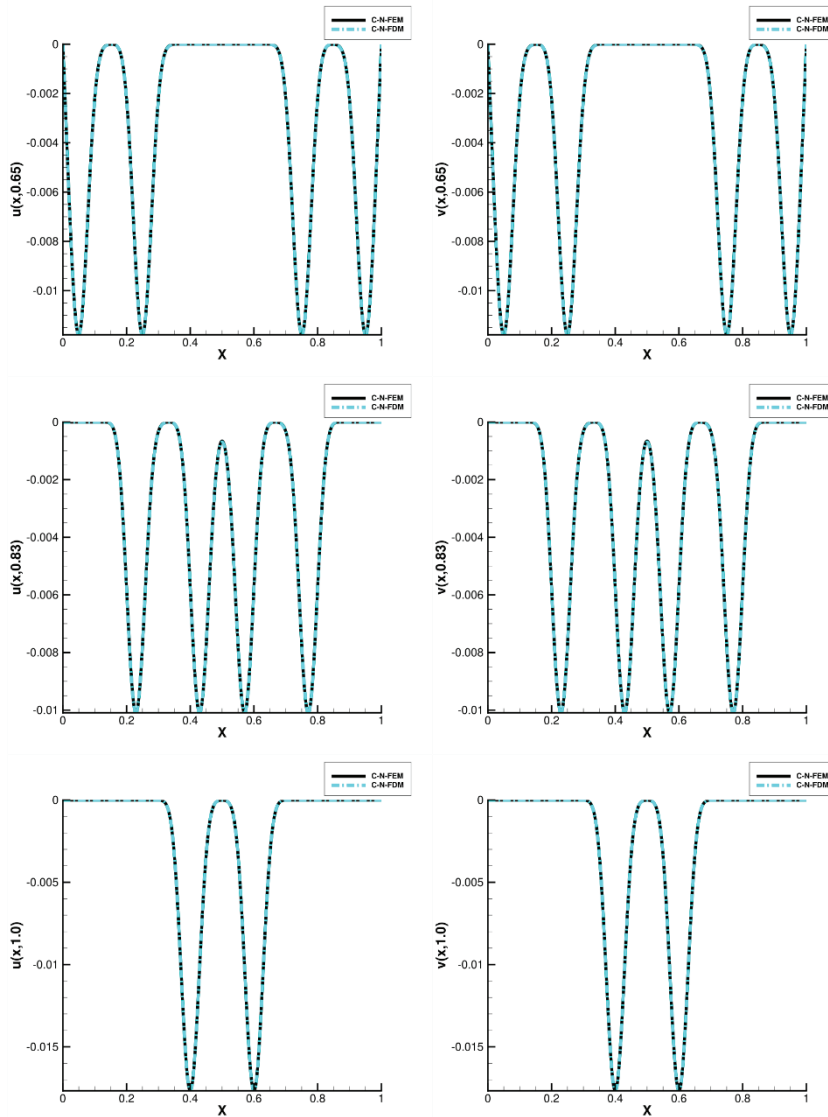FDM with Cranck-Nicolson $\left(\theta = {}^1/_2\right)$ schemes at time= $0.30, 0.65, 0.83, 1.0$ for $\mu_1 = \mu_2 = 1$.

Figure 3. First and second column shows plot of numerical solution of u and v by FEM and FDM with Cranck-Nicolson $\left(\theta = {}^1/_2\right)$ schemes at time= $0.30, 0.65, 0.83, 1.0$ for $\mu_1 = \mu_2 = 3$.

Three Bubbles Case: In this case we consider the initial condition with three bubbles in the form;

$$\begin{bmatrix} u_0(x) \\ v_0(x) \end{bmatrix}$$
$$= \begin{bmatrix} B(x, 0.2, 0.3) + B(x, 0.2, 0.5) + B(x, 0.2, 0.7) \\ B(x, 0.2, 0.3) + B(x, 0.2, 0.5) + B(x, 0.2, 0.7) \end{bmatrix} \quad \forall x \quad (19)$$
$$\in \Omega$$

$$\begin{bmatrix} u_1(x) \\ v_1(x) \end{bmatrix} = \begin{bmatrix} 0 \\ 0 \end{bmatrix}$$

We show the plot of initial function in (19) with Figure 4. and the Figure 5. shows the long time behavior of nonlinear system in (1) for $\mu_1 = \mu_2 = 10$.
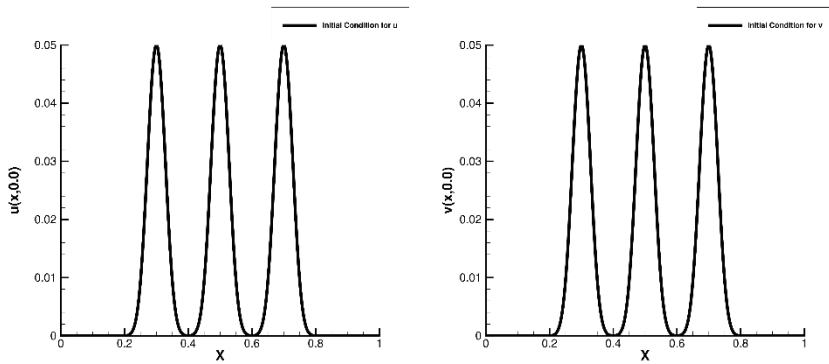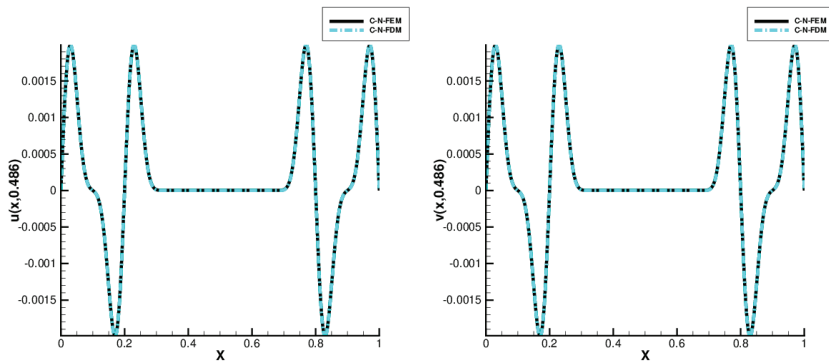

Figure 4. Plot of initial function for u and v respectively.
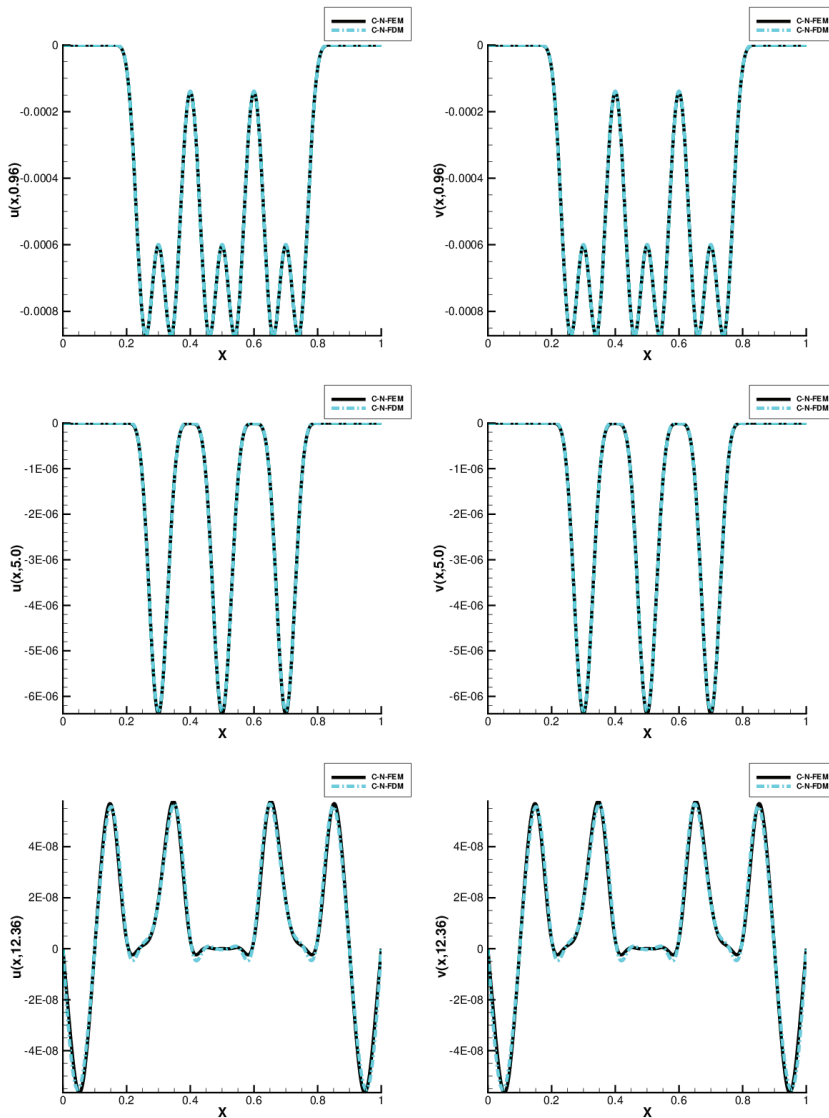
Figure 5. First and second column shows plot of numerical solution of u and v by FEM and FDM with Cranck-Nicolson $\left(\theta = \frac{1}{2}\right)$ schemes at time$= 0.486, 0.96, 5.0, 12.36$ for $\mu_1 = \mu_2 = 10$.

Convergent test and Comparison: Finite Difference Method is an efficient numerical method for the time dependent partial differentials equations. For this purpose we compare the numerical solutions obtained using FDM/FEM and FDM/FDM numerical schemes for $\theta = 1$ and $\mu_1 = \mu_2 = 1$ using different space step

size at different time step. We can observe from the Figure 7. finite element solutions for different grid sizes at time= 1 and time= 2 is very close to each other because the differences between the numerical solutions for different grid sizes are less then $5E - 05$. The exact solution of aforementioned system is not known. Therefore, we use the FDM solution as a reference solution to check the convergence of the numerical method. Difference between the numerical solutions obtained using FEM and FDM for the spatial variable is shown in Figure 9. It shows the $|\text{FEM}_{\text{solution}} - \text{FDM}_{\text{solution}}| < 1E - 07$. Therefore we can say the proposed numerical scheme are very efficient and relevant for the power nonlinear system of damped wave equations.
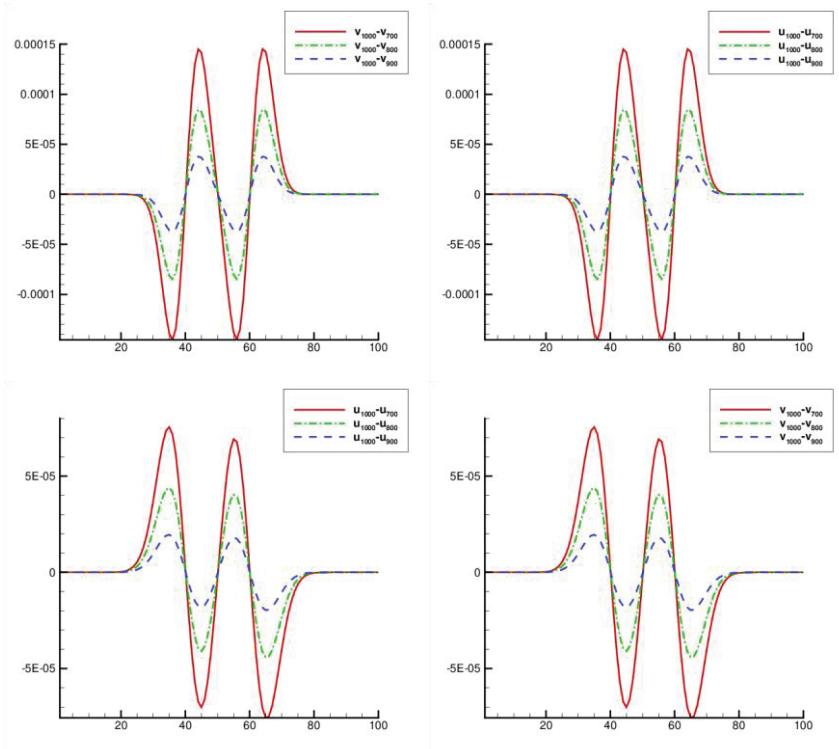

Figure 6. First(time= 1) and second(time= 2) row shows the differences between FEM solution for different grid size ($h = 1000, h = 900, h = 800, h = 700$) for u and v at time= 1 and time= 2 for $\theta = 1$ and $\mu_1 = \mu_2 = 1$.
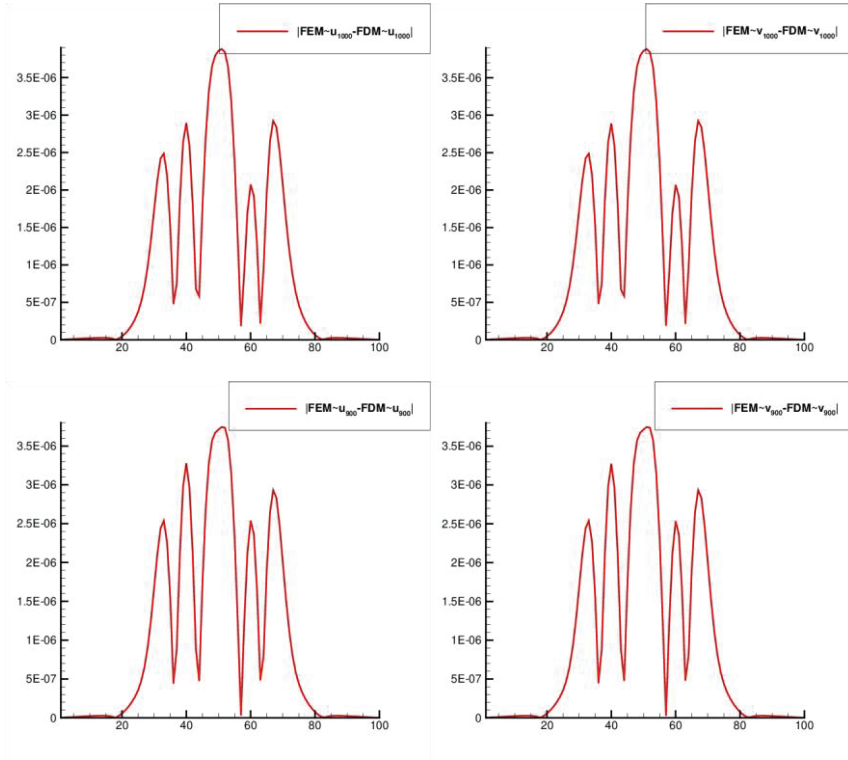
Figure 7. First(time= 1) and second(time= 2) row shows the differences between FEM and FDM solutions for $h = 1000$ and $h = 900$ grid size for u and v at time= 1 and time= 2 for $\theta = 1$ and $\mu_1 = \mu_2 = 1$.

Conclusions

The numerical solution of the weakly coupled system of nonlinear wave equations with distinct scale-invariant damping and mass terms is acquired using finite difference/finite element hybrid numerical scheme. The mathematical model of the aforementioned problem is power nonlinear damped system of wave equations. Therefore in the linearization process we have used the Newton linearization method. We also propose the finite difference/finite difference numerical scheme for the reliability and accuracy of the obtained numerical results using FDM/FEM numerical scheme. We observed that the obtained numerical results using implicit and Crank-Nicolson FDM/FEM and FDM/FDM numerical schemes are very close to each other. The proposed numerical schemes provide us to solve the matrix-vector system without decoupled the

equations consider in (1). Additionally, the proposed FDM/FEM numerical scheme will be a very popular example to acquire the numerical solution of the power nonlinear system of coupled wave equations with damping term.

References

[1] F. Sun, M. Wang, Existence and nonexistence of global solutions for a nonlinear hyperbolic system with damping, Nonlinear Analysis., 66 (2007), 2889–2910.

[2] H. Takeda, Global existence and nonexistince of solutions for a system of nonlinear damped wave equaitons, J. Math. Anal. Appl., 360(2) (2009), 631–650.

[3] T. Ogawa, H. Tekeda, Large time behavior of solutions for a system of nonlinear damped wave equaitons, J. Diff. Equ., 251(11) (2011), 3090–3113.

[4] Y. Wakasugi, Small data global existence for the semilinear wave equaiton with space-time dependent damping, J. Math. Anal. Appl., 393(1) (2012), 66–79.

[5] K. Nishihara, Asymptotic behavior solutions for a system of semilinear heat equaitons and the corresponding damped wave system, Osaka J. Math., 49 (2012), 331–348.

[6] K. Nishihara, Y. Wakasugi, Critical exponent for the Cauchy problem on the weakly coupled damped wave system, Nonlinear Analysis., 108 (2014), 249–259.

[7] K. Nishihara, Y. Wakasugi, Critical exponents for the Cauchy problem to the system of wave equaitons with time or space dependent damping, Bull. Inst. Math. Acad. Sin.(N.S.), 10(3) (2015), 283–309.

[8] W. Chen, Palmieri, Weakly Coupled system of semilinear wave equaitons with distinct scale-invariant terms in linear part, Z. Angew. Math. Phys, 70(2) (2019), https://doi.org/10.1007/s00033-019-1112-4

[9] M. Anderson, J.H. Kimn, A numerical approach to space-time finite elements for the wave equation, J. Comp. Phys., 226 (2007), 466–476.

[10] L. Beilina, Domain decomposition finite element/finite difference method for the conductivity reconstruction in a hyperbolic equation, Commun. Nonlinear Sci. Numer. Simulat., 37 (2016), 222–237.

[11] H. Selvıtopı , M. Yazıcı, Numerical Results For The Klein-Gordon Equation in de Sitter Spacetime, Math. Meth. Appl. Scien., 42 (2019), 5446–5454.

[12] X. Liu, J. Wang, Y. Zhou, A space-time fully decoupled wavelet Galerkin method for solving a class of nonlinear wave problems, Nonlinear Dyn., 90 (2017), 599–616.

[13] J. N. Reddy, ”An introduction to finite element method”, McGraw-Hill, Newyork, 1993.

Chapter 8

COVID-19 ANTIVIRAL THERAPY

Hülya ÇELİK[1]

1 Ağrı Ibrahim Cecen University, Faculty of Pharmacy Department of Pharmaceutical Techno-
logy Departmen 03200 Ağrı/TÜRKİYE

The whole world is faced with a viral epidemic that threatens the lives of millions of people, caused by a new respiratory infection at the end of 2019. Although the COVID-19 epidemic, which emerged in China, was tried to be prevented by the measures of the World Health Organization, it turned into a pandemic and spread all over the world. SARS-CoV-2, the virus that causes COVID-19 disease since January 2020, has caused more than 273 million confirmed cases and 5 million deaths, as of the data announced by Johns Hopkins University on 17 December 2021. (https://www.trthaber.com/koronavirus-data). As a result of the researches, it was determined that the new coronavirus SARS-CoV-2 caused the disease. (Sürmelioğlu and Demirkan, 2020, Fraser et al. 2020).

Coronavirus (Latin: corona = Crown) While coronaviruses are classified by their subtypes, they are called alpha, beta, gamma, and delta. When the genome of the current pandemic-causing SARS-CoV-2 was analyzed, it was 96% similar to the alpha and beta subspecies derived from bats. (Velavan and Meyer 2020).

While scientists were trying to take the necessary precautions in the face of this new threat, the lack of an antiviral drug that could be effective against the pathogen SARS CoV2 was the biggest obstacle in terms of treatment.

In the treatment of COVID-19 used today, drugs whose efficacy has not been fully proven and which are thought to be beneficial with their therapeutic effects in in vitro studies with therapeutic results in different indications are used (Sanders et al.2020).

What is the Source of the Disease and the Ways of Transmission?

Although studies on the source of the disease continue, studies so far suggest that wild animals sold illegally in the Huanan Seafood Wholesale Market cause this virus. Pets such as cats and dogs were also examined, but no evidence was found that these animals were carriers. As a result, the

source of the disease has not yet been determined in this regard. (Til, 2020, Asokan et al. 2020).

As for the transmission routes, researches have proven that the disease is mainly transmitted by droplets. These droplets are known to be effective within two meters. Droplets are scattered around by coughing and sneezing of sick individuals and remain suspended in the air for up to three hours. In addition, it has also been seen in blood and urine samples of virus-positive individuals. Exactly how many days after the diseased individual becomes contagious is still an issue under investigation. Studies on parameters such as this that vary from person to person are ongoing. (Türken and Köse2020).

It is known that the incubation period of the disease is between 1 and 14 days. When the reported cases were examined, it was seen that the youngest patient was 1.5 months old. The disease can be seen as symptomatic or asymptomatic. Symptoms vary between patients. Some of these symptoms are as follows; runny nose, sore throat, dry cough, nausea, vomiting, diarrhea. It has been stated that the most common of these symptoms is dry cough with a rate of 50%. PCR tests are performed in symptomatic patients. In doubtful cases, chest radiography should be examined. The frosted glass structures seen in the graph are proof that the fault is covid-19. (Ciotti et al. 2020).

Coronavırus

Human coronaviruses (HCoVs) represent an important group of coronaviruses (CoV) associated with many respiratory diseases of varying severity, including the common cold, pneumonia and bronchitis. Today, HCoVs are considered one of the fastest growing viruses due to their high rate of genomic nucleotide availability and recombination. In recent years, the evolutionary process of HCoVs has also been accelerated due to reasons such as urbanization and poultry farming. These factors have allowed the frequent intermingling of species and facilitated the crossing of the species barrier and the genomic recombination of these viruses. So far, six known HCoVs have been identified, namely HCoV-229E, HCoV-NL63, HCoV-OC43, HCoV-HKU1, severe acute respiratory syndrome coronavirus (SARS-CoV) and Middle East respiratory syndrome coronavirus (MERS-CoV); Of these, four HCoV (HCoV-229E, HCoV-NL63, HCoV-OC43 and HCoV-HKU1) circulate in human populations worldwide and cause human cold infections. In severe cases, these four HCoV can cause life-threatening pneumonia and bronchiolitis, especially in the elderly, children, and immunocompromised patients. Apart from respiratory tract diseases, they can also cause enteric and neurological disorders (Lim et al 2016).

For years, HCoVs have been known as mild respiratory pathogens

affecting the human population. However, it was the emergence of SARS-CoV that pushed these human viruses into the field of research. Therefore, most of the HCoV research today is associated with SARS-CoV. The recent MERS-CoV outbreak is mostly confined to the Middle East region. However, there is a chance that more emerging or re-emerging HCoVs will emerge threatening global public health, as evidenced by the high death rates in the last two outbreaks: SARS-CoV (10%) and MERS-CoV (35%)) are likely to be found. Therefore, more information is needed to study the pathogenesis of all HCoVs and to develop antiviral therapeutics and vaccines (Lim et al 2016b). Coronaviruses (CoV) are known as a large family of viruses that cause various ailments, from the common cold to more serious diseases such as severe respiratory failure, MERS-CoV, SARS. To date, many subtypes of Coronaviruses mostly cause colds in humans. On December 31, 2019, a new type of coronavirus was detected in Wuhan city of China's Hubei province, and the name of the disease was accepted as COVID-19. There is not enough information about the newly detected COVID-19 virus. Therefore, there were difficulties in its treatment, and the disease spread rapidly. Due to the spread of the disease between continents and reaching serious dimensions in many countries, the World Health Organization has described this epidemic as a "pandemic". Pandemic is a term used for epidemic diseases that affect more than one continent and many countries in the world. While efforts continue to treat existing patients and prevent the spread of the virus, new information is gained, scientific studies are conducted, and approaches are frequently renewed (Til 2020).

Antiviral Drugs Used in the Treatment of COVID-19

Antiviral treatments used around the world; preventing the virus from entering the cell, reducing or inhibiting virus replication, suppressing the increased and uncontrollable inflammatory response caused by the disease, It is used with the aim of neutralizing the virus with immune plasma treatments containing antibodies against the virus obtained from patients who survived the disease (Uğuz and Eşkut 2020).

Klorokin(CQ)
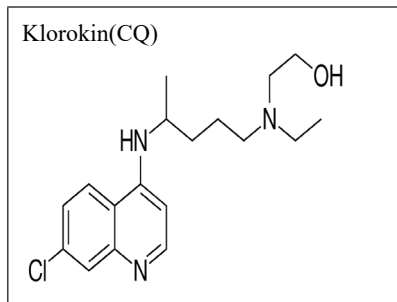
Chloroquine has not been approved by the FDA to treat the corona virus. On the other hand, the FDA has not yet approved any therapeutic agent or drug for the treatment of COVID-19. However, for chloroquine, which is used in the treatment of other diseases, physicians are allowed to prescribe it for off-label use when they find it necessary, but its effectiveness and safety in terms of coronavirus have not been fully proven. In the statements made by the FDA; It has been stated that chloroquine can help reduce the spread of the disease, reduce the proliferation of the virus in mild and moderate patients, as well as shorten the duration of symptoms. (Mutlu et al.2020)


Hidroksiklorokin (HCQ)
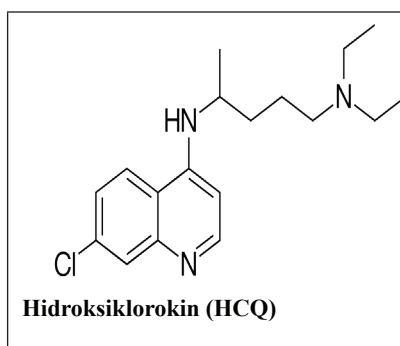
Hydroxychloroquine (HCQ) is a chloroquine derivative drug. Its mechanism of action is polymerase enzyme inhibition. It increases the pH of the phagolysosome and interferes with the glycosylation of virus and cell receptors. Hydroxychloroquine inhibits the replication of SARS-CoV-2 in vitro. Hydroxychloroquine is known to be a cheap and safe drug for short-term use, with low drug-drug interaction. Although it is not known exactly whether it is effective in the treatment of COVID 19, this risk seems to be taken. Its side effects are moderate nausea and diarrhea, QTc prolongation, and the possibility of retinopathy after more than 5 years of use. Its dosage is 2 x 400 mg on the first day, and 2 x 200 mg for 4 days on the following days. It is recommended to check the ECG in those taking other QTc prolonging drugs together. It should not be used if the QTc complex is 500msec. When HCQ is taken at a dose of 600 mg/day with azithromycin for 10 days; A significant reduction in viral load was noted. In the COVID-19 treatment guideline of the TR Ministry of Health, Hydroxychloroquine is recommended for both outpatients and hospitalized patients (Li et al. 2020, Brufsky et al.2020)
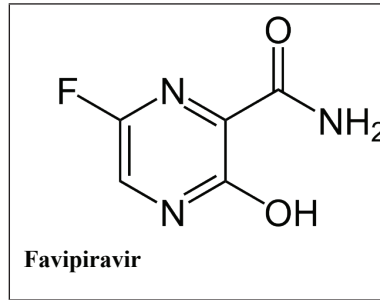
Favipiravir

Favipiravir is known as an antiviral drug that selectively and potently inhibits RNA-dependent RNA polymerase of RNA viruses. It has been shown to affect influenza and, to some extent, Ebola virus disease. It has also been shown as a result of studies that 2019-nCoV is a single-stranded RNA beta coronavirus with the RdRp gene similar to SARS-CoV and MERS-CoV. Therefore, favipiravir is one of the potential drug candidates for COVID-19. In an in vitro study, SARS-CoV-2 was inhibited by favipiravir in Vero E6 cells with an EC50 of 61.88 µMol. However, in another study, it was observed that favipiravir did not show a significant antiviral effect against SARS-CoV-2 virus at concentrations below 100 µML in vitro. In an open-label, controlled study of 80 laboratory-approved patients, a comparison was made between 35 patients who received oral favipiravir plus aerosol inhalation with interferon (IFN)-α and 45 patients who received lopinavir/ritonavir plus aerosol inhalation with interferon (IFN)-α. It was determined that the viral excretion time was shorter in the group receiving favipiravir compared to the control group. The most common side effects are known as abnormal liver function tests, psychiatric symptom reactions, digestive system problems and high uric acid levels. This study has not yet been published in a scientific journal because there were several concerns about outcomes as there were no concomitant treatments, key differences between groups, no blinding or placebo control. The available information is currently insufficient to recommend favipiravir for the treatment of COVID-19, therefore additional studies are needed. There are still many ongoing randomized controlled trials in China. Favipiravir, in the Ministry of Health's COVID-19 treatment guide; It is recommended in probable/definite cases with severe pneumonia, alone or in combination with Hydrochloroquine. In addition, it is recommended as a 5-day treatment, as 2x1600 mg/day on the first day and 2x600 mg/day on the next 4 days, in cases whose clinic aggravates or whose pneumonia symptoms increase while receiving HCQ treatment (Du et al. 2020).
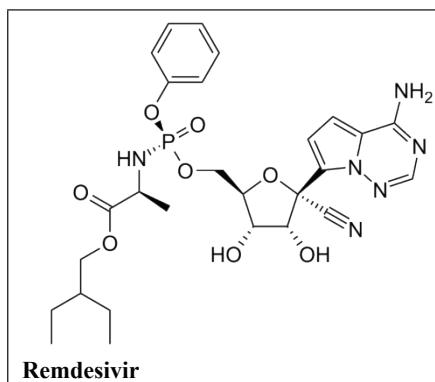
Remdesivir

Remdesivir is known as a new antiviral drug developed by Gilead Sciences, originally used in the treatment of Ebola virus disease and Marburg virus infections. Remdesivir is a prodrug form of a nucleotide analog that inhibits viral RNA polymerase, which is metabolized to an intracellular adenosine triphosphate analog. Remdesivir shows a broad spectrum of action against many families of viruses, including filoviruses (e.g. Ebola) and coronaviruses [e.g. SARS-CoV and Middle East respiratory failure syndrome coronavirus (MERSCoV)], and has demonstrated prophylactic and therapeutic efficacy against these coronaviruses. Remdesivir showed a significant improvement in the first case of COVID-19 in the United States, and several clinical trials were subsequently initiated to evaluate the efficacy and safety of remdesivir in patients hospitalized for 2019-nCoV infection. Clinical improvement occurred in 36 (68%) of 53 patients when remdesivir was used in hospitalized patients with severe COVID-19. However, since there was no placebo or active comparator in this study, it does not seem possible to obtain a clear result, and the results of the ongoing randomized-controlled clinical trials should be awaited in order to evaluate the clinical efficacy of remdesivir (Uğuz et al. 2020).

Lopinavir/ritonavir(LPV/r)


LOPINAVIR
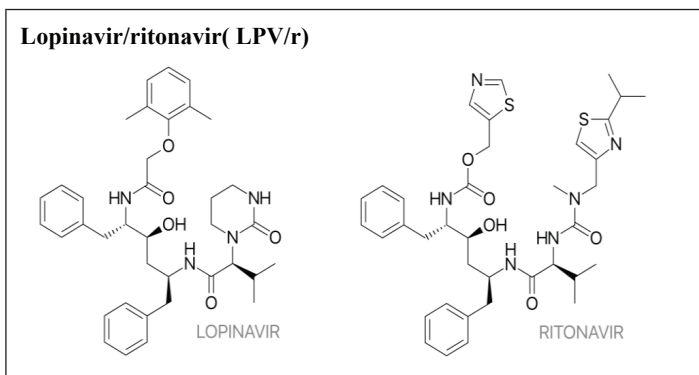
RITONAVIR

Lopinavir/ritonavir (LPV/r) is a protease inhibitor used for the treatment of human immunodeficiency virus (HIV) and was previously found to inhibit SARS-CoV1 in vitro. The protease enzyme is a key enzyme for the polyprotein formation of the coronavirus. Although conflicting results have been obtained in the treatment of severe acute respiratory syndrome (SARS), it is one of the antiviral drugs that hope in the treatment of COVID-19 due to its strong effect in vitro and in vivo for Middle East respiratory syndrome coronavirus (MERS CoV), especially with interferon (IFN) beta. has been. (Ozyılmaz 2020)(Sürmelioğlu and Demirkan, 2020)

Lopinavir is known as a protease inhibitor fortified with ritonavir and used to treat HIV infection. Protease is an enzyme and has an important place in coronavirus polyprotein processing. Lopinavir and/or ritonavir have anti-coronavirus activity in vitro. Most in vitro studies have revealed that SARS-CoV is inhibited by lopinavir and the EC50 of lopinavir is also acceptable. Lopinavir acts antiviral against SARS-CoV-2 virus in Vero E6 cells. Prophylaxis after administration of LPV/r was found to reduce the risk of MERS infection by 40%, although some concerns arose in the design part of the study.

Disease progression could not be prevented in 2 patients within 1-3 days from the start of treatment with LPV/r. According to the results shown by the threshold cycle value of nasopharyngeal swabs, a similarity was found in the reduction in viral load between LPV/r treated and untreated patients. In the COVID-19 treatment guide of the TR Ministry of Health; lop/r (2 x 400/100, 10-14 days) is included in the treatment as an alternative agent to Hydrochloroquine in pregnant women with a definite diagnosis. (The guide recommended untreated follow-up for uncomplicated COVID-19 patients in pregnant women, and recommended treatment for pregnant women diagnosed with COVID-19 if there is a risk factor or severe). Existing data suggest that for now, the role of LPV/r in the treatment of COVID-19 is limited. In addition, in cases where it is used; It should be noted that LPV/r has serious drug interactions (CYP3A4, CYP2D6, CYP1A2, CYP2B6, CYP2C8, CYP2C9, CYP2C19, P-gp, UGT1A1). The most common side effects are gastrointestinal, hepatotoxic side effects and it causes hyperlipidemia (Mutlu et al. 2020).

Nitazoksanid
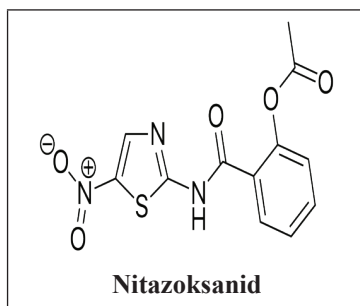
Nitazoxanide and its active metabolite tizoxanide have potent in vitro activity against SARS CoV-2 and MERS CoV, with EC50 values of 2.12 μM and 0.92 μM, respectively, in Vero E6 cells. Apart from coronavirus, it is also a broad-spectrum antiviral drug and shows activity against influenza, parainfluenza, respiratory syncytial virus, rotavirus and norovirus. This broad-spectrum antiviral activity is related to pathways regulated by the host during viral replication rather than virus-specific pathways. Nitazoxanide affects hereditary antiviral mechanisms via cytoplasmic RNA and type 1 interferon pathways. It has broad spectrum antiviral activity. Accordingly, the efficacy of nitazoxanide in influenza and other acute respiratory infections has been investigated in various randomized clinical trials, but the results have not been found yet. However, although the in vitro activity of nitazoxanidine against SARS-CoV-2 is promising, more information is needed for its effectiveness against COVID-19 (Rossignol et al. 2016).

İvermektin
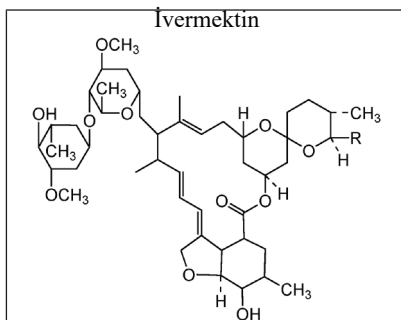
Ivermectin is a broad spectrum antiparasitic drug approved by the FDA. It has antiviral activity against many viruses in vitro. Ivermectin integrase produces protein nuclear import and inhibition of HIV-1 replication. Ivermectin also inhibits host nuclear import and viral proteins. It limits some RNA virus infections, including influenza and West Nile viruses. Ivermectin antiviral drug also acts against some DNA viruses both in vitro and in vivo. In an in vitro study, ivermectin exhibited an inhibitory

effect against SARS-CoV-2, which was thought to be due to ivermectin's inhibition of IMPα/β1-associated nuclear import of viral proteins (as shown in other RNA viruses), and this inhibition was also associated with the immune response of the virus. It is another thought that is claimed to disrupt the escape mechanisms. In order to use ivermectin in the treatment of COVID-19, in vitro, in vivo and clinical studies should be performed (Caly et al. 2020).
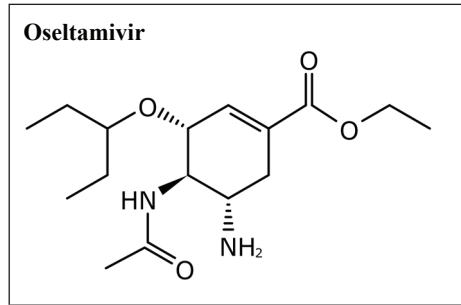
Oseltamivir is a neurominidase inhibitor used in the treatment of influenza. Oseltamivir was used in the treatment of concomitant influenza infections during the MERS epidemic. Although it has no place in the treatment of COVID-19, it is recommended to add oseltamivir to the treatment in rare cases where COVID-19 and influenza occur together. However, since favipravir is also effective against influenza, it is not necessary to add oseltamivir to the treatment in patients receiving favipiravir (https://covid19bilgi.saglik.gov.tr/depo/rehberler/covid-19).
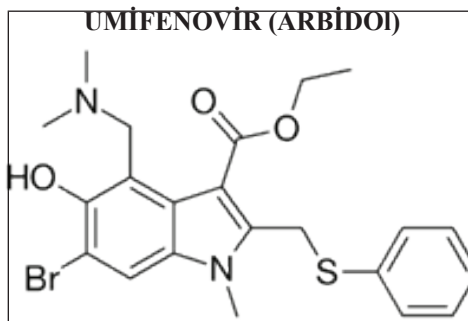
Umifenovir (UMF) is a broad-spectrum oral antiviral drug of Russian origin licensed for the prevention and treatment of influenza and other respiratory infections. It was approved in Russia in 1996 and in China in 2006 for the treatment and prevention of influenza A and B. Umifenovir

it is a small molecule indole derivative. Poorly soluble in hydrophilic media, bioavailability varied, respectively, by route of administration and pharmacokinetics. UMF, hepatitis C virus (HCV), hepatitis B virus (HBV), Chikungunya virus (CHIKV), Coxsackie virus B5, Hanta in vitro It has also been effective on viruses such as viruses and reoviruses.(Inkaya etal.2020). SARS-CoV replication of UMF proved to be inhibited. Since SARS-CoV is effective due to its effect on a wide metabolic pathway and spectrum It has also been tried in the treatment of COVID disease. (LPV/r) monotherapy with UMF monotherapy was compared in treatment and it was observed that viral replication was suppressed in all UMF recipients. Therefore, it has been suggested that UMF monotherapy is superior to LPV/r. (lian et al.2019)

Tosilizumab

Tosilizumab, membrana bağlı reseptörleri veya çözünür interlökin-6 oreseptörlerini (rIL-6) inhibe edebilen monoklonal bir antikordur. Esas olarak romatoid artrit hastalıklarının tedavisinde kullanılmak üzere onay alan bir ilaçtır. Ancak son zamanlarda CART (chimeric antigen receptor T-cell) tedavisi alan kanser hastalarında meydana gelen sitokin salınım sendromunun tedavisi için de ayrıca kullanılmaktadır. Tosilizumab tek doz veya en fazla 2 doz uygulanır. Bu nedenle, romatizmal hastalıklarda uzun süreli kullanımda meydana gelen; bakteriyel, fungal infeksiyon eğilimi, çene osteonekrozu gibi çeşitli yan etkilerin görülmesi pek beklenilmeyen etkilerdir. Önerilen kullanım dozu ise; 4-8 mg/kg veya 400 mg standart intravenöz doz kabul edilir (Mutlu vd. 2020) Tocilizumab, CYP3A4 substratlarının serum konsantrasyonunu azaltır, bu nedenle eşzamanlı kullanım sırasında tedavinin izlenmesi gerekir. Anakinra ile immünosupresif ajanların eşzamanlı kullanımından kaçınılmalıdır. Tosilizumab, CYP3A4 substratlarının serum konsantrasyonunu azaltır, bu nedenle, eşzamanlı kullanımda tedavi izlemi gerekmektedir. Anakinra ile eş zamanlı immunsupresan ilaçların kullanımından kaçınmak gerekmektedir. (Cao,2020, Surmelioglu and Demirkan 2020)

As a result;

Currently, there is no specific treatment for COVID-19 with proven safety and efficacy. In order to find an effective treatment for COVID-19 disease, more than 100 randomized controlled studies are currently being conducted with a large number of drugs and studies are continuing. Treatment options should be made within the framework of randomized controlled studies and their use should be provided based on the information obtained by other scientific researches, and it is thought to be more rational in this way. However, due to the urgency of the current situation and the

limited scientific data, treatment options and possibilities for which there is limited data that they may be effective are widely used for COVID-19 patients all over the world. As with viral infections in general, information from SARS and influenza suggested that early initiation of antiviral therapy is more beneficial, and it is recommended to start antiviral drugs as early as possible. The combined use of possible treatment options in patients with COVID-19 should be considered individually and by evaluating the whole of the relevant literature, and necessary precautions should be taken regarding the interactions and undesirable side effects of the drugs used (Mutlu et al. 2020).

Every day, new scientific activities, new drugs, new forms of treatment are emerging. This means that it is promising for the treatment of viral infectious diseases. In order to control virus infections, it is necessary to know the mechanism by which they act. Once this issue is adopted, drugs can be administered or developed.

REFERENCES

Sürmelıoğlu, N., Demırkan, K. Covıd-19 Tedavisinde Kullanılan İlaçlar ve Akılcı İlaç Kullanımı, Archives Medical Review Journal, volume 29, ıssue özel sayı, 44 – 53, 2020

Fraser, N., Brierley, L., Dey, G., Polka, J. K., Pálfy, M., & Coates, J. A. (2020). Preprinting a pandemic: The role of preprints in the COVID-19 pandemic. *BioRxiv*, 2020.05.22.111294. https://doi.org/10.1101/2020.05.22.111294

Velavan, T. P. & Meyer, C. G. The COVID-19 epidemic. *Trop. Med. Int. Health* **25**, 278–280 (2020).

Sanders JM, Monogue ML, Jodlowski TZ, Cutrell JB. Pharmacologic treatments for coronavirus disease 2019 (COVID-19): A review. JAMA. 2020;323:1824-1836.

Asokan I, Rabadia SV, Yang EH. The COVID-19 Pandemic and its Impact on the Cardio-Oncology Population. Curr Oncol Rep. 2020;22(6):60. doi: 10.1007/s11912-020- 00957-0

Türken, M., & Köse, Ş. 2020). Türken, M., ve Köse, Ş. (2020). Covid-19 bulaş yolları ve önleme. Tepecik Eğitim ve Araştırma Hastanesi Dergisi, 30, 36-42.

Ciotti M, Ciccozzi M, Terrinoni A, Jiang WC, Wang CB, Bernardini S. The COVID-19 pandemic. Crit Rev Clin Lab Sci. 2020;1-24. doi: 10.1080/10408363.2020.1783198

Lim, Y., Ng, Y., Tam, J. ve Liu, D. (2016). İnsan Koronavirüsleri: Virüs-Konak Etkileşimlerinin İncelenmesi. *Hastalıklar* , *4* (4), 26. doi: 10.3390 / hastalıklar4030026

Til, A. (2020). Yeni Koronavirüs Hastalığı Hakkında Bilinmesi Gerekenler. Ayrıntı Dergisi, 8 (85), 53-57.

Uğuz M, Eşkut B. Covid 19 enfeksiyon tedavisi. Med Res Rep. 2020;3(Suppl.1):17-31

MUTLU, O., UYGUN, İ., & ERDEN, F. (2020). Koronavirüs Hastalığı (COVID-19) Tedavisinde Kullanılan İlaçlar. Kocaeli Üniversitesi Sağlık Bilimleri Dergisi, 6(3), 167-173.

Li X, Wang Y, Agostinis P, Rabson A, Melino G, Carafoli E et al. Is hydroxychloroquine beneficial for COVID-19 patients?. Cell Death & Disease. 2020;11(7):1-6.

Brufsky A. Hyperglycemia, hydroxychloroquine, and the COVID-19 pandemic. J Med Virol. 2020:6. doi: 10.1002/jmv.25887

Du YX, Chen XP. Favipiravir: pharmacokinetics and concern about clinical trials for 2019-nCoV infection. Clin Pharmacol Ther. 2020;108(2):242-247.

Ozyılmaz E. Antiviral agents. J Crit Intensive Care. 2020;11(Suppl. 1):27−29

Rossignol JF. Nitazoxanide, a new drug candidate forthe treatment of Middle East respiratorysyndrome coronavirus. J. Infect. Public Health 2016;9:227-230. doi: 10.1016/j.jiph.2016.04.001

Caly L, Druce JD, Catton MG, Jans DA, Wagstaff KM. The FDA approved drug ivermectin inhibits the replication of SARS-CoV-2 in vitro. Antiviral Res. 2020. doi: 10.1016/j. antiviral.2020.104787

T.C. Sağlık Bakanlığı COVID-19 Bilgilendirme Sayfası. Available from: https:// covid19bilgi.saglik.gov.tr/depo/rehberler/covid-19-rehberi/COVID19_ REHBERI_ERISKIN_HASTA_TEDAVISI.pdf. Erişim tarihi: 12 Ekim 2020.

Inkaya, A.Ç.; Ta¸s, Z.; Akova, M. COVID-19'un Güncel Tedavisi. Yalçın ¸S Özet A, editörler. Kanser ve COVID-19 Pandemisi. 2020, 1, 27–37.

lian N, Xie H, lin s, Huang J, Zhao J, lin Q. Umifenovir treatment is not associated with improved outcomes in patients with coronavirus disease 2019: a retrospective study. Clin Microbiol Infect. 2020:s1198-743X(20) 30234-2.

Cao X. COVID-19: immunopathology and its implications for therapy. Nat Rev Immunol. 2020;20(5):269-270.

Chapter 9

HONEY FROM PAST TO PRESENT

İsmühan Potoğlu Erkara[1]

Okan Sezer[2]

1 Eskişehir Osmangazi University, Faculty of Science and Letters, Department of Biology, 26040, Eskişehir, Turkey, 0000-0001-5780-4999

2 Eskişehir Osmangazi University, Faculty of Science and Letters, Department of Biology, 26040, Eskişehir, Turkey, 0000-0001-7304-1346

There are many blessings and riches that nature offers to people. Honey is one of the most valuable nutrients that nature offers to humans. Honey is not only a satisfying substance in the stomach, but also a sweet and magical food that brings health and vitality to people. The bees that make up the honey are the most social, hardworking, productive and mysterious creatures among living beings. Beekeeping has a very important place in human life and national economy. Since historical times, people have benefited from the honey produced by bees in various ways (Aydoğan et al., 1990).

Archaeological excavations in many parts of the world and pictures found in Mesolithic rocks in Europe and Asia show that human beings have been dealing with beekeeping since 8000 years ago. Many historical artifacts have been found proving that the Hittites were beekeeping in Anatolia around 1300 BC, and articles related to beekeeping were found in the lithographic laws. While beekeeping was carried out in frameless hives and without technical intervention until the 1850s after Christ, modern beekeeping has been started with the first framed hive developed by the American beekeeper Langstroth (İnci, 1985).

Today, more than 391000 plant species grow naturally. About 500 of these plants are nectar plants (Atkins, 1946; Cherghton, 1974; Crane, 1978; 1984; Antonelli et al., 2020). According to the information obtained from the ten-volume work of Davis (Davis, 1965-1988) named "Flora of Turkey and the East Aegean Islands", approximately 9222 plant species naturally grow in Turkey, 3000 of which are endemic. About 450 of these plants are important for beekeeping. Turkey is one of the most suitable countries for beekeeping, as it has a flora rich in nectar plants (Sorkun, 2002).

Honey is one of the oldest products known to be used in traditional medicine. Its uses include the treatment of diseases of the respiratory tract, gastrointestinal tract, and various other diseases. It is also known that honey is used as a pain reliever and healer in the treatment of wounds (including surgical wounds), burns and skin ulcers (Mulu et al., 2004).

Nectar, the most important ingredient of honey, is produced by plants. The most precise and easiest method for identifying nectar-bearing plants is pollen analysis in honey. Early research in different parts of the world has shown that the botanical and geographical origins of honey can be established by all pollen content (Lieux, 1972; Agwu et al., 1986; Battesti and Goeury, 1992). The first comprehensive melithopalynological study in Turkey was conducted by Sorkun and İnceoğlu (1984). 162 pollen types were determined from 94 honey samples collected from the Central Anatolian Region of Turkey. Nectar-containing flowering plants were obtained from pollen analyzes of honey samples from different regions of

Turkey 26 (Sorkun et al., 1989), 20 and 53 from different regions of Turkey (Sorkun and Doğan, 1995a; 1999) from Rize Anzer. It was identified and determined from 28 honey samples (Sorkun and Doğan, 1995b), 24 from Konya (Kaplan and İnceoğlu, 2002), 41 honey samples from Eskişehir (Potoğlu Erkara et al., 2009).

Turkey is among the most important countries in the world with its 4.4 million hives and 71 thousand tons of honey production (Kandemir, 2005). Although it is the second country in the world in terms of the presence of hive, the average honey production per hive in our country is around 16 kg and is below the world average of 20 kg. However, Turkey's lagging position in the world honey trade does not harmonize with the existing hive and honey production. Considering both our share in world honey trade and honey production per colony, it is clear that our country has not sufficiently benefited from its beekeeping potential. On the other hand, the production of bee products other than honey and the use of honey bees to ensure adequate pollination in plant production are not common in our country. As it is known, bees cause great increases in the amount and quality of the product by providing the pollination needed by the plants to produce seeds and fruits in plant production. For this reason alone, those engaged in agriculture should also attach importance to beekeeping. Considering that the contribution of beekeeping to the economy through pollination is at least 10-15 times the contribution made by honey and beeswax, beekeeping has the potential to contribute greatly to the country's economy in this way (Kandemir, 2005).

When the flowers start to open with the spring, pollination begins between the flowers. Pollination is known as the transport of pollen to the female organ of the flower. While the pollen of 20% of flowering plants is pollinated by the wind (Anemogam), the pollen of the others is pollinated by insects (Entomogam), birds (Ornithogam) or water. While honey bees collect pollen, also known as bee bread, in order to meet the nutritional needs of themselves and their larvae, they also contribute effectively to pollination (Sönmez and Altan, 1992).

Insect-pollinated plants produce nectar, which is food for insects, in order to increase the chances of pollination. Generally, flowers secrete abundant nectar in the early morning hours. When the sun rises and the temperature rises, nectar secretion also decreases, and then nectar production begins to increase again in the cool of the evening (Sönmez and Altan, 1992).

The bee collects nectar (nectar) from nectariums (nectar glands). Nectariums are of two types according to their location on plants: floral (nectarium in flower) and extra-floral (nectarium out of flower). Known

as the raw material of honey, nectar is a liquid containing dissolved sugar, and it has been determined that nectar contains various amounts of protein, amino acids, enzymes, fats, organic acids, vitamins, alkaloids and antioxidants. As the sugar concentration of nectar increases, the rate of preference by bees also increases. The presence of substances different from the compounds found in nectar in honey shows that the honey bee adds different compounds to honey during maturation in its stomach (Krell, 1996).

The sugar concentration in the nectar of plants belonging to the Lamiaceae, Fabaceae, Boraginaceae, Asteraceae, Rosaceae family varies between 16-55%, and bees collect nectar mostly from the members of these families in the world and in Turkey (Sorkun and İnceoğlu, 1984; Herrera, 1985).

Rhododendron L. plant is the source of honey, which is usually produced in the Black Sea region and is often called bitter honey, crazy honey or poisonous honey. It is known that nectar collected from the flowers of the rhododendron plant contains andromedotoxin, an alkaloid, and that people who eat rhododendron honey, which grows on the coastline from Hopa to Adapazarı in the Black Sea Region, cause vomiting, dizziness, blackouts and buzzing in the ears, and this is due to a decrease in blood pressure (Tutkun, 2000).

Bees collect only nectar from some plants, pollen from some plants, and both nectar and pollen from others (Ötleş, 1995). Bees do not collect pollen to make honey. They use the pollen they collect for feeding themselves, the larvae and the queen bee. After meeting their nutritional needs, they frequently store the remaining pollen in the honeycomb cells. They put honey on it in a very thin layer so that its contact with the air is cut off. Bees consume this food, which we call bee bread, when they cannot find pollen in nature (Ötleş, 1995).

Pollen has a curative and protective effect against many diseases due to its high vitamin, mineral and protein content. The effects of pollen on human health can be summarized as follows; It gives energy and strength, improves the immune system. It has also been found to have a positive effect on respiratory tract, digestive system, circulatory system and excretory system disorders. It has been found that it has positive effects in the rehabilitation of cancer, in the regulation of sexual functions, and in infections with the effect of antibiotics (Sorkun, 1987).

Bee products; It consists of honey, beeswax, pollen, royal jelly, propolis and bee venom. Honey, pollen and propolis is the product collected from plants by the honey bee (*Apis mellifera*) and stored in the cells of the comb by adding some chemical components to its structure. Beeswax, royal jelly

and bee venom are the products secreted from the body of the bee (Sorkun, 1987).

Bee products are highly nutritious for living things due to the rich source of nutrients they contain, and they have a very complex structure in terms of chemical structures. Therefore, bee products cannot be produced artificially (Sorkun, 1987).

Honey, which is the most known and consumed among bee products, has been used as a food source by human beings for centuries. Honey; It is a sweet product that occurs as a result of the nectar (honey essence) in the flowers of plants or the sweet substances secreted by some iso-winged insects by making use of the living parts of the plants, after being collected by the honey bees, changing their composition in their bodies and maturing in the honeycomb eyes (Ötleş, 1995).

It has been reported that various honeys have the potential to be used in the treatment of infections caused by various microorganisms (Taormina et al., 2001; Mundo et al., 2004; Lusby et al., 2005). Literature information shows that the antimicrobial activity of honey is mainly provided by 4 different mechanisms. These mechanisms are summarized as osmotic effect, acidity, H_2O_2 formation and plant-derived chemical content of honey (White, 1979; Taormina et al., 2001; French et al., 2005). It is thought that the differences between the antimicrobial properties of honeys depend on the floral source (Taormina et al., 2001). It has been reported that the antimicrobial properties of honey are also the reason why they have a protective effect in food samples (Mundo et al., 2004).

More than 180 compounds have been identified in honey, consisting of various carbohydrates, amino acids, water, vitamins, minerals, flavonoids, organic acids, acetylcholine, pollen, pigments, wax and enzymes. Some of these are bee-based, some are plant-based compounds (Sato and Miyata, 2000).

Each country has established their own country's honey standards as a result of the analysis of honey with different physical and chemical structures obtained from their own nectar plants. Turkish Food Codex Honey Communiqué is essential for honey standards in Turkey. The item 6th of the Turkish Food Codex Honey Communiqué is given in Table 1.

Table 1. Item 6th of the Turkish Food Codex Honey Communiqué Covering the Properties of Honey

hygiene	*Honey cannot contain any foreign matter, parasite, bee, bee parts and baby bees, except for the organic and inorganic substances found in its natural structure. * No pathogenic microorganisms that threaten human health can be found in honey. * There is no naphthalene in honey.
Amount of invert sugar	It cannot be less than 65% in flower honey and 60% in secretory honey.
moisture content	Cannot be more than 20%
amount of sucrose	It cannot be more than 5% in flower honey and 10% in secretory honey.
Mineral matter-ash content	It cannot exceed 0.6% in flower honey and 1.2% in secretion honey.
Acidity amount	Cannot be more than 40 meq/kg
Diastase number	Cannot be less than 8
amount of HMF	Cannot be more than 40 mg/kg
commercial glucose	not found
Starch	not found
organaleptic properties	Honey should have its own natural smell and taste.

Factors such as the color, clarity, consistency, odour, flavor, and crystallization rate of honey constitute the physical properties of honey (Sorkun et al., 1989). First of all, nectar, which is the raw material, is effective in the physical properties of honey. While the bees collect the nectar, which is the raw material of honey, from flowering plants, they also carry the pollen they collect from different plants to the hive to use in their nutrition and store them in the honeycomb cells (Sorkun et al., 1989).

Melitopalynology helps to find the floristic origin of honey. For this, pollen analyzes are made in honey. By identifying the pollens in honey, the plant taxa of these pollens in the research area are determined. This plays an important role in the determination of nectar sources, the geographical origin of honey, the determination of honey quality and the classification of honey. At the same time, it can be explained what plants give honey a nice smell, taste, flavor and late crystallization, and it can also be determined which plants impair honey quality such as bad smell, bitterness and rapid crystallization. By making use of these data, a special flora can be created that will yield superior honey. Bees can travel up to 5 km from the hive. In this area, it is possible to remove the plants that give honey bad properties, to place important honey plants around the hive, or to transport the hives to the regions where the plants that give honey superior properties are located (Kaplan and İnceoğlu, 2002).

It is also possible to pre-diagnose poor quality or poisonous honeys that are harmful to human health with melitopalynological studies. With these studies, the inspection and evaluation of honey produced in different regions can be carried out in a healthier way (Dalgıç, 1994). In addition, low quality sugar honey produced by feeding bees with large amounts of sugar syrup can also be detected by pollen analysis (Pınar, 2003).

Each country prepares a list of nectar plants for its various regions by conducting melissopalynological studies (Moar, 1985; Feller-Demalsy et al., 1987a; 1987b; 1989; Villanueva, 1994; Ramanujam and Kalpana, 1995; Coffey and Breen, 1997). This method has been used for many years to determine the quality of honey in various countries (Maurizio and Hodges, 1951).

Pollen analysis in honey was first performed by Pfister in 1845. Pollen analysis in Turkish honey was first studied by Quistani in 1976 (Sorkun et al., 1989). Sorkun and İnceoğlu (1984), one of the Turkish researchers, performed pollen analysis in honey for the first time between 1979-1981.

In recent years, the rapid increase in the population and the emergence of random new settlements without scientific investigations, the gases coming out of the factory chimneys, the waste materials polluting the surrounding water, soil and atmosphere also negatively affect the flora. In addition, pesticides thrown into agricultural areas cause the disappearance of endemic and non-endemic plants.

With honey analysis studies, the quality of honey is positively affected and its value in the marketing of honey increases. The increase in pollen analyzes and biochemical analysis studies on honey will not only help our consumers and beekeepers to be informed in a healthy way, but also will enable the honey produced in our country to be promoted abroad more effectively.

HONEY AND ITS IMPORTANCE

According to the honey communique, secretory honey is the substance that honey bees (*Apis mellifera*) collects nectar outside of flowers or the secretions of plants or some living things living on plants, mixes them with their own specific substances, changes them and stores them in the cells of the comb. Flower honey is honey produced by bees from nectar in flowers (Anonymous, 2004).

It is possible to collect the factors that significantly affect the quality of honey under six headings: nectar-bearing plant type and variety, bee type, environment, education of the beekeeper, time and form of honey harvest, and storage conditions of the harvested honey (Yurtsever and Sorkun, 2003).

The quality of honey is determined by explaining its chemical composition, physical properties and pollen content (Ünlü, 1994).

Chemical analyzes revealed that honey is not only a sweet food, but also contains antioxidant substances that can neutralize oxidizing breakdown products. In a study conducted by Doğan (Doğan, 2003), it was reported that Anzer honey plays an active role in stomach damage in chronic alcoholics and prevents stomach damage when taken before alcohol. Nagai et al. (Nagai et al., 2001) revealed that the antioxidant activity of honey is closely related to its botanical source.

In some studies, it has been stated that honey gives very important results in healing infected burns and wounds. This bacteriostatic property of honey is due to its high sugar concentration and acid reaction. It is reported that these two factors inhibit bacterial growth (Tetik, 1968; Petrov and Önder, 1976). Since honey inhibits the growth of *Helicobacter pylori* bacteria, which causes stomach and intestinal ulcers, both in vivo and in vitro, it is also applied clinically (Sato and Miyata, 2000).

While honey is an excellent source of energy (Sato and Miyata, 2000), it also has immune-boosting, antibacterial, antifungal and antiviral properties (Taormina ve ark., 2001; Sato ve Miyata, 2000).

Honey is also used as an additive in food and cosmetics, as it has the ability to absorb moisture (hygroscopic) (Krell, 1996).

Honey can also be used to detect heavy metal ions. It has been observed that the lead and cadmium concentrations are high in honey obtained from the hives located close to the city centers where traffic is heavy in our country (Demirsoy, 1985; Önder ve Tezcan, 1988). In the research conducted after the Chernobyl nuclear explosion in 1986 in the Asian continent, it was stated that the honey bees in the region were exposed to radioactive fallout, and radioactive pollution was also observed in nectar sources and honey in Europe (Krell, 1996).

The main factor that determines the quality of honey is its geographical and botanical characteristics. To determine the botanical origin of a honey, melissopalynological analyzes can be applied (Persano Oddo ve ark., 1988). The pollen particles in honey provide information about the plants that are the main nectar source and their botanical origin (Jato ve ark., 1991). Pollen sources can be determined by pollen analysis and plants that provide nectar and pollen for bees during different seasons can be determined (Ramanujam ve ark., 1992).

Honey can be classified according to their origin by pollen analysis in honey (Sorkun, 1985). Which plant has the most pollen in honey, honey is called by the name of that plant. Thus, it is accepted that honey is taken

from pollen-producing plants in proportion to the pollen ratio (Sorkun, 1985).

The fact that the proportion of pollen belonging to the same taxon in honey is more than 45% indicates that honey is unifloral (originated from a single flower). The flavor, color and taste of these honeys are characteristic (Deodikar, 1965). The bee tends to collect nectar or pollen from flowers of one species at a time. However, if a single species is not dominant in the region in terms of density, bees collect nectar and pollen from the flowers of various taxa. This is reflected in the pollen content of honey. Honey formed in this way is called multifloral (multi-floral origin) (Deodikar, 1965). In recent years, itinerant beekeepers have been making great efforts especially for the production of unifloral honey (*Eucalyptus*, *Acacia*, *Citrus* balı etc.). These honeys are both easier to market and consumers can reach the type of honey they want more easily (Persano Oddo et al., 1988).

It is stated that the total pollen count (TPS-10 g) value of honey can be a criterion for distinguishing fake and pure honey. In studies conducted for this purpose, Lieux (1972), Moar (1985) and Feller-Demalsy et al. (1987a-b) determined the TPS value in 10 grams of honey using *Lycopodium* spores.

In recent years, melissapalynological studies have intensified and gained importance in many countries of the world. In our country, in parallel with these developments, studies on pollen analysis in honey are increasing day by day.

Lieux (1972) determined the nectar-bearing plants that are the source of honey by analyzing 54 honey samples collected from the Louisiana region of the U.S.A.

Moar (1985) identified unifloral honeys in 119 honey samples from 42 different regions of New Zealand. It has been determined that these honeys have dominantly *Trifolium repens* and *Lotus* from Fabaceae family, *Thymus* and *Wiedemannia* from Lamiaceae family, *Echium vulgare* from Boraginaceae family, *Leptospermum* and *Metrosideros* from Myrtaceae family, *Discaria* pollen from Rhamnaceae family.

Agwu et al. (1989) determined the dominant pollen in the local honeys by analyzing 8 honey samples collected from Nsukka region of Nigeria.

Ramos et al. (1999) detected the dominant pollen in 25 honey samples collected from 12 different regions of the Canary Islands. In addition, they determined nectar-bearing plants that are the source of the honeys of the region.

Valencia et al. (2000) conducted pollen analysis on 39 honey samples from the Leon region of Spain, and determined that the pollen from

Ericaceae family *Erica*, Fagaceae family *Castanea sativa*, Asteraceae family *Helianthus annuus*, Fabaceae family *Lotus corniculatus*, Rosaceae family *Rubus ulmifolius* pollen were dominant in the honeys of the region.

Andrada et al. (1998) examined 34 honey samples from Argentina-Buanos Aires. According to the results obtained from the study, the pollens of *Eucalyptus* from the Myrtaceae family, *Helianthus annuus* from the Asteraceae family, *Diplotaxis tenuifolia* from the Brassicaceae family were determined as dominant in the honeys of the region. Besides, the most pollen belonging to Fabaceae, Asteraceae, Brassicaceae families were found.

Feller-Demalsy et al. (1987a) performed pollen analysis on 42 honey samples collected from Sackathewan, Canada. As a result of the study, they determined that the pollen of *Brassica* from the Brassicaceae family, *Melilotus*, *Trifolium hybridum*, *T. repens* and *Medicago sativa* from the Fabaceae family were dominant in honey samples.

Ramanujam et al. (1992) determined that the biggest nectar source plants for bees in India were *Syzygium cumini* from the Myrtaceae family and *Borassus flabellifer* from the Arecaceae family during the summer period. Plants that are a source of pollen for bees during the winter were determined as *Eucalytus globulus* from the Myrtaceae family and *Sapindus emarginatus* from the Sapindaceae family.

Many studies have been carried out in our country on this subject. İnceoğlu and Sorkun (1984) determined the nectar source plants of the Central Anatolia Region honeys by making pollen analyzes on 94 honey samples collected from 10 provinces of the Central Anatolia Region and the districts, villages and highlands of these provinces. The taxa that the researchers found dominantly pollen were *Achillea*, *Xeranthemum*, *Lapsana communis*, *Centaurea triumfetti* from the Asteraceae family, *Brassica oleracea* from the Brassicaceae family, *Lamium amplexicaule* and *Teucrium orientale* from the Lamiaceae family, *Peganum harmala* from the Zygophyllaceae family, *Vicia cracca*, *Lotus*, *Hedysarum* and *Astragalus* from Fabaceae family, *Rubus* from Rosaceae family, *Heliotropium suaveolens* from Boraginaceae family, *Consalida raveyi* from Ranunculaceae family were determined.

Pollen analysis was carried out on 10 honey samples collected from Rize-İkizdere region in 1983 by Sorkun and Yuluğ (1985) and nectar-bearing plants were determined. In addition, the antibacterial and antifungal properties of honey were also examined. *Trifolium pratense*, *T. repens*, and *Lotus corniculatus* pollen from Fabaceae, *Helianthemum nummularium* from the Cistaceae, *Cynoglossum glochidiatum* from the Boraginaceae and *Castanea sativa* from the Fagaceae families were

determined in dominant amounts in Rize-İkizdere honeys.

Sorkun et al. (1989) conducted pollen analysis on 26 honey samples collected from various districts and villages of Rize between 1984-1986. As a result, it was determined that *Castanea sativa* from the Fagaceae family is the nectar source in most of the honeys in this region.

Sorkun et al. (1999) studied a total of 227 controlled-produced honey samples, including 127 natural flowers, 33 natural secretions, 44 added flowers and 23 added secretion honeys, which they collected from various provinces of Turkey between 1994-1996. In this study, they determined the physical, chemical and palynological criteria that will be the basis for distinguishing natural and artificial honeys. In the palynological analyzes, nectar-bearing plants and the total number of pollen in 10 g honey were determined. In natural flower honeys, the most common pollen taxa are as follows: *Centaurea*, *Helianthus annuus*, *Xanthium* from Asteraceae, *Astragalus*, *Hedysarum*, *Lotus*, *Onobrychis*, *Sophora*, *Trifolium*, *Vicia* from Fabaceae, *Castanea sativa* from Fagaceae, *Eryngium*, *Pimpinella anisum* from Apiaceae, *Eucatyptus camaldulensis* from Myrtaceae, *Gossypium* from Malvaceae, *Isatis* from Brassicaceae, *Lamium*, *Marrubium*, *Salvia*, *Teucrium* from Lamiaceae, *Linaria* from Scrophulariaceae, *Olea* from Oleaceae, *Salix* from Salicaceae and *Triticum* from Poaceae families. The obvious distinguishing factor of potassium, proline, sucrose and TPS in distinguishing natural flower honeys from additive flower honeys; fructose and glucose amounts were found to be helpful criteria in this distinction. The most important criteria distinguishing natural secretory honeys from additive secretory honeys are sodium, potassium, K/Na ratio and proline amount; It has been stated that sucrose and TPS may be helpful criteria in this distinction.

Çakır (1990) conducted pollen analysis on 20 honey samples collected from Balıkesir region. In the study, it was determined that the dominant nectar plants of the region were *Helianthus annuus* from the Asteraceae, *Castanea sativa* from the Fagaceae, *Trifolium* from the Fabaceae, *Cistus creticus* from the Cistaceae and *Paliurus* from the Rhamnaceae families.

As a result of the pollen analysis carried out by Gemici (1991) on 17 honey samples from the İzmir region, Chenopodiaceae, Ericaceae, Brassicaceae, Poaceae families together with *Castanea sativa* from Fagaceae, *Papaver* from Papaveraceae, *Vitex agnus-castus* from Verbenaceae and *Cistus* from Cistaceae were determined as dominant.

Göçmen and Gökçeoğlu (1992) performed pollen analysis on 6 honey samples collected from Bursa. It has been determined that the plants that contain the most nectar and are used in honey production in the Bursa region are *Castanea sativa*, *Helianthus annuus*, *Daucus carota*, *Rosa*,

Trifolium and *Tilia argentea*.

Kaplan (2002) determined that the pollens of Fabaceae, Brassicaceae, Rubiaceae, Euphorbiaceae, *Salix* from Salicaceae, *Ranunculus* from Ranunculaceae and *Centaurea triumfetti* from Asteraceae were dominant as a result of microscopic analysis of 24 honey samples collected from Konya region in 1992.

Dalgıç (1994) examined 50 honey samples collected from different provinces of the Aegean Region between the years 1991-1993, biochemically and palynologically. She determined that the taxa with the most pollen in the honey samples of this region are Fabaceae, Lamiaceae, Apiaceae, Brassicaceae families and so *Helianthus annuus* from Asteraceae, *Cistus* from Cistaceae and *Castanea sativa* from the Fagaceae families.

Pollen analysis was performed on 25 honey samples collected from Antalya province by Silici (1995). In this study, it was determined that pollen from Apiaceae family and *Raphanus raphanistrum* from Brassicaceae, *Eucalyptus* from Myrtaceae, *Cirsium* from Asteraceae, *Plantago* from Plantaginaceae and so *Ulmus* from Ulmaceae families were dominant in local honeys.

Başoğlu et al. (1996) in their study of 25 honey samples collected from various regions of Turkey in 1993, reported that the criteria to distinguish fake honey from pure honey could be potassium/sodium ratio, proline and total pollen count (TPS-10 g) values.

Yılmaz (1969) determined 25 different pollen types belonging to 16 families in 17 honey samples collected from İzmit region in 1994. It was determined that pollen of *Castanea sativ*a (Fagaceae), *Helianthemum* (Cistaceae), *Rhododendron* (Ericaceae) and *Symphytum* (Boraginaceae) were found in dominant amounts in this region honey.

Microscopic, organoleptic and chemical analyzes were performed on 29 honey samples obtained from Kemaliye-Erzincan region between 2002-2003 by Yurtsever and Sorkun (2005). In the honeys of the region, it has been determined that the taxa with dominant amount of pollen are *Astragalus* and *Trifolium* from Fabaceae family, *Sanguisorba* from Rosaceae family, *Paliurus* from Rhamnaceae family and *Salix* from Salicaceae family.

Bağcı and Tunç (2006) performed pollen analysis on 21 honey samples collected from Konya-Karaman region in 2002. As a result of these analyzes, they determined that the important honey plants of the region were Apiaceae and Rosaceae families and so *Astragalus*, *Trifolium*, *Lotus*, *Onobrychis* from Fabaceae, *Carduus*, *Centaurea*, *Achillea*, *Tragopogon* from Asteraceae, *Brassica* from Brassicaceae, *Mentha* and *Salvia* from

Lamiaceae, *Plantago* from Plantaginaceae, *Linaria* from Scrophulariaceae.

Erdogan et al. (2006) determined that pollen from the family Fabaceae, Brassicaceae, Labiatae, Salix from the Salicaceae family, Centaurea from the Asteraceae family were dominant as a result of the pollen analysis he conducted on 65 honey samples collected from the Adapazarı region in 2005.

Potoglu Erkara et al. (Potoğlu Erkara et al., 2009) determined that Apiaceae, Asteraceae, Boraginaceae, Brassicaceae, Fabaceae, Fagaceae, Lamiaceae, Rosaceae, Plantaginaceae, Poaceae, and Cistaceae families constitute important honey plants as a result of pollen analysis performed on 41 honey samples collected in 2007-2008.

ANTIMICROBIAL EFFECT MECHANISM OF HONEY SAMPLES

Literature information shows that the antimicrobial activity of a honey in general is provided by four different mechanisms. These mechanisms are summarized as osmotic effect, acidity, H2O2 formation and plant-derived chemical content of honey (White, 1979; Taormina et al., 2001).

Osmotic Effect: Honey is a saturated substance containing 84% glucose and fructose. The amount of water in its content is only 15-21% of its weight. Therefore, the average moisture content of honey is low and water activity is low. Low water activity is one of the most important factors suppressing the growth of mainly bacteria and some yeasts. Some yeasts may develop and degrade in honey with increased water activity. However, microbial growth and fermentation do not occur in environments with a water content of less than 17.1%. It is known that the water activity of honey is between 0.562 and 0.62 (average 0.6). In the range of 0.94-0.99, the growth of some bacterial species is completely suppressed. Although the effect of the water potential of the environment on microorganisms is different for each microorganism, they can withstand environments with a maximum water activity of 0.99 (Ünlütürk and Turantaş, 1998).

Effect of H_2O_2: Hydrogen peroxide (H_2O_2) is a strong oxidant substance. Natural honey contains small amounts of hydrogen peroxide. During the conversion of nectar into honey, bees secrete glucose oxidase enzyme from the glands under the pharynx. This enzyme reacts with glucose in the presence of water and oxygen to form gluconic acid and H_2O_2. H_2O_2 is an important factor in the antimicrobial activity of honey. It is produced as a sterilization tool during the maturation of honey. It provides some protection of honey. However, it does not have a very strong effect, because there is a trace amount of enzyme in honey, but the enzyme is passive since the formation of gluconic acid together with H_2O_2

reduces the pH of the environment. When honey is diluted with water, the enzyme is activated and H_2O_2 decomposes into water and oxygen (Çakır and Tümen, 1990).

Acidity: The pH of honey generally varies between 3.2-4.5 and this low pH shows a suppressive feature for the growth of many pathogens. While the pH they need for their development varies between 7.2-7.4, *E. coli* can tolerate pH 4.3 and *P. aeroginosa* up to 4.4. Acidity is an important antimicrobial effect in undiluted honey. Since the pH of honey diluted with water or buffer solution increases, its antimicrobial effect on many pathogens decreases (Ünlütürk and Turantaş, 1998).

Honey is a very dense substance due to its physical and chemical structure. It has a very high sugar content and low water activity. Due to these properties, honey adversely affects the growth of microorganisms in the environment. However, in general, microfungi are resistant to environments with low water activity. For this reason, they can develop even in an environment with low water activity such as honey (Ünlütürk and Turantaş, 1998). In a study by Çakır and Tümen (1990), honey from Balıkesir region showed antibacterial activity against *S.aureus*, *B.subtilis, E.coli, Pseudomonas multophica* and *Klebsiella pneumonia*, while *Candida albicans* M lV 270, *Aspergillus niger* KUEN 1147 and *Aspergillus fumigatus* KUEN 1145. It has been reported that it has no antimicrobial effect against 1145 (Çakır and Tümen, 1990). According to Patten, none of these honeys used in the study of Brady et al. with "Manuka Honey" and "Non Manuka Honey" showed antifungal effects on the clinical isolate microfungi tested. Researchers similarly attribute these results to the resistance of microfungi to environments with low water activity (Molan, 1997). According to the findings obtained in the in vitro antimicrobial effect study conducted by Aksoy and Dığrak (2006) with the agar-well method, it was determined that honey samples taken from Bingöl Center and four different regions have antimicrobial effects against various bacteria and yeasts. Honey sample taken from Karlıova Region was determined as the most effective honey on *E. coli* with a 35 mm Inhibition zone. In the analyzes made with honey samples collected from Eskişehir and its surroundings, it was determined that honeys are the most effective honeys on *E.coli* with a 38 mm inhibition zone. It has been shown that the honeys of Bingöl and its region have 19-45 mm inhibition zones on B. subtilis, 16-51 mm inhibition zones on S. aureus, 14-21 mm on *P. aeroginosa*, 25-51 mm inhibition zones on *M. luteus* (Aksoy and Dığrak, 2006). A desired feature in the investigation of antimicrobial agents is the specific effect of the research material on some microorganisms.

When it is scanned in the literature, it is understood that some honeys have similar specific activities against the test microorganisms whose

activities were investigated. The antimicrobial activity of two different natural honeys obtained from Southwest Nigeria by Adebolu (2005) at different concentrations on *Escherichia coli, Campylobacter jejuni, Salmonella enterocolifis* and *Shigella dysenteriae* test microorganisms was investigated by agar well method. According to the findings obtained with the zone measurements, it was determined that both honeys were most effective on E. coli with an inhibition zone of 15 and 17 mm. Honeys with this type of selective activity should be considered as important sources for the treatment of infections caused by microorganisms that have antimicrobial effects. Sources of antimicrobial effects of honey; Osmotic effect due to low water activity, hydrogen peroxide content, low acid pH, low protein content, high sugar concentration, low redox potential density of honey, and its phytochemical structure is different (Allen and Molan, 1997).

According to Allen and Molan (1997), using the test microorganisms *Actinomyces pyogenes, Kebsiella pneumoniae, Nocardia asteroides, Staphylococcus aureus* (coagulase positive), *Streptococcus agalactiae, Streptococcus dysgalactiae* and *Streptococcus uberi*, "Manuka Honey" and "Artwarewa Honeyific" in three different honeys, including; In a study conducted at concentrations of 0.1%, 5% and 10%, the growth of all test microorganisms was inhibited at a minimum concentration of 1%, while no growth was observed in "Manuka Honey" and "Rewarewa Honey" at 10% concentration. Weston et al. (2000), Wilix et al. (1992), Lozano-Chiu et al. (1999), disc and well diffusion methods were also used in the studies to determine the degree of antimicrobial activity. It has been reported that varying levels of effect were obtained at different concentrations. However, spectrophotometric methods in determining the MIC value provide more sensitive data in a short time and require lower costs compared to other methods (Patton et al., 2006).

Natural honey contains trace amounts of Hydrogen peroxide. Hydrogen peroxide is a toxic compound for the cell due to its strong oxidant properties. According to the literature information obtained, White (1979) in 1963 determined that the antimicrobial activity of honey was also due to the hydrogen peroxide contained in its composition. In a study conducted with "Manuka Honey" honey, the antimicrobial activities of honey samples with added catalase enzyme and honey samples without catalase enzyme were investigated by Agar Diffusion method. Intense antimicrobial activity was observed in honey samples without the addition of catalase enzyme. Lower antimicrobial activity was observed in honeys whose H_2O_2 content was removed by adding catalase enzyme (Cooper et al., 2002). According to the literature, while intense antimicrobial activity was observed on test bacteria *Salmonella typhimurium, E.coli,*

Shigella sonnei, Listeia monocytogenes in honey samples without added catalase, honey samples lost their antimicrobial activity to a large extent after treatment with catalase (Taormina et al., 2001). In addition to all these factors, the chemical content of honey may also be the cause of antimicrobial activity. Literature information indicates the inhibitory effect of phenolic compounds in honey on microorganisms. Particular attention is paid to the pollen content of honey by the countries importing honey in Europe. Because the high percentage of pollen containing various mineral substances, vitamins and enzymes in honey increases the quality of honey even more (Dalgıç, 1994). Pollen, which is known to be more valuable than the honey that is bought and sold in tons every year in Europe, is of great value as it is a protein, vitamin, lipid and mineral source for honey bees. The strength of the colony is directly proportional to the excess amount of pollen. Therefore, experienced beekeepers collect the pollen in a trap in the season when the pollen is abundant and give it to the bee in the season when the pollen is low (Dalgıç, 1994). This information should be conveyed to other beekeepers in Turkey by the Ministry of Agriculture and Rural Affairs. Our country shows great differences in terms of both its geographical structure and climatic characteristics. Parallel to this, it is a fact that the pollen content of our honey will also differ (Dalgıç, 1994).

Today, 9224 plant species, of which 3000 are endemic, naturally spread in our country. It is still not known for certain from which of these species the bees collect nectar or pollen. It is seen that most of the honey samples produced in our country are of multifloral origin. In order to know the quality and source of honey, it is in their own interest for our beekeepers to harvest the honey they obtain from each region and from each plant separately (Erdoğan et al., 2006).

Honey, whose source and quality is known, can be marketed more easily. Marketing problems are encountered in honey of unknown origin. Since there is no legal regulation on this issue in our country, the manufacturer does not attach much importance to this issue. For this reason, it is necessary to take measures that encourage the producer to milk after each nectar flow (Erdoğan et al., 2006). In addition, in order to raise awareness of the consumer, the pollen and percentage ratios in honey should be written on the labels on the commercial honey jars. Some pollen can cause allergies in some people. Therefore, it is very important for consumer health to know the pollen content of the honeys of each region and to detect the allergic pollen, if any. Knowing the taxa to which the pollen in honey belongs can contribute to both increasing honey production and removing the plants that give honey bad properties from the environment. It may be recommended to move the hives to areas with dense nectar plants or to grow plants that give honey superior properties around the hives. The

joint guidance of beekeepers and cultivated plant producers is also closely related to the field of agriculture and forestry. Yield and quality can be increased in cultivated fruit and vegetable cultivation, which is cultivated and planted by human hands, by means of bees that provide very good pollination.

LITERATURES

Adebolu, T. T. (2005). Effect of natural honey on local isolates of diarrhea-causing bacteria in southwestern Nigeria. *African Journal of Biotechnology*, *4*(10), 1172-1174.

Agwu, C. C., & Akanbi, T. O. (1986). A palynological study of honey from four vegetation zones of Nigeria. *Pollen et spores*, *27*(3-4), 335-348.

Agwu, C. O. C., Obuekwe, A. I., & Iwu, M. M. (1989). Pollen Analytical and Thin-Layer Chromotographic Examination of Nsukku (Nigeria) Honey. Pollen et Spores, 31 (1-2), 29-43.

Aksoy, Z., & Dığrak, M. (2006). Bingöl yöresinde toplanan bal ve propolisin antimikrobiyal etkisi üzerinde in vitro araştırmalar. *Fırat Üniversitesi Fen ve Mühendislik Bilimleri Dergisi*, *18*(4), 471-478.

Allen, K. L., & Molan, P. C. (1997). The sensitivity of mastitis-causing bacteria to the antibacterial activity of honey. *New Zealand Journal of Agricultural Research*, *40*(4), 537-540.

Andrada, A., Valle, A., Aramayo, E., Lamberto, S., & Cantamutto, M. (1998). Pollen analysis of honeys from the Austral Mountainous Area, Buenos Aires Province, Argentine. *Investigacion Agraria. Produccion y Proteccion Vegetales (Espana)*. Argentina, 13(3), 265-275.

Anonim (2004). Türk Gıda Kodeksi Bal Tebliği. Tarım ve Köy İşleri Bakanlığı, 2001/110 EC sayılı AB Bal Tebliğine Uyum Değişiklikleri, Ankara, 1-5.

Antonelli, A., Smith, R. J., Fry, C., Simmonds, M. S., Kersey, P. J., Pritchard, H. W., ... & Qi, Y. D. (2020). *State of the World's Plants and Fungi* (Doctoral dissertation, Royal Botanic Gardens (Kew); Sfumato Foundation).

Atkins, E. L. (1946). The Hive and Honey Bee. lllinois, Journal Printing Company.

Aydoğan, A., Özalp, E., & Bozkurt, M. (1990). Yerli ballarımızın kimyasal yapıları üzerine araştırmalar. Türk Hij Den Biyol Derg, 48, 55-84.

Bağcı, Y., & Tunç, B. (2006). Hadim-Taşkent (Konya), Sarıveliler (Karaman) Yöresi Ballarında Polen Analizi. *Selçuk Üniversitesi Fen Fakültesi Fen Dergisi*, *2*(28), 73-82.

Basoglu, F. N., Sorkun, K., Loker, M., Dogan, C., & Wetherilt, H. (1996). Saf ve sahte ballarin ayirt edilmesinde fiziksel, kimyasal ve palinolojik kriterlerin saptanmasi. *Gida*, *21*(2), 67-73.

Battesti, M. J., & Goeury, C. (1992). Efficacité de l'analyse mélitopalynologique quantitative pour la certification des origines géographique et botanique des miels: le modèle des miels corses. *Review of Palaeobotany and palynology*, *75*(1-2), 77-102.

Cherghton, H. C. (1974). Bees and People. Moscow, MIR Publishers.

Coffey, M. F., & Breen, J. (1997). Seasonal variation in pollen and nectar sources of honey bees in Ireland. *Journal of Apicultural Research*, *36*(2), 63-76.

Cooper, R. A., Halas, E., & Molan, P. C. (2002). The efficacy of honey in inhibiting strains of Pseudomonas aeruginosa from infected burns. *The Journal of burn care & rehabilitation*, *23*(6), 366-370.

Crane, E. (1978). Honey, lnternational Bee Research Association. Morrison and Gibb Ltd. Edinburg, London.

Crane, E. (1984). Bees, honey and pollen as indicators of metals in the environment. *Bee world*, *65*(1), 47-49.

Çakır, H. (1990). *Balıkesir yöresi ballarında dominant ve sekonder polenler* (Master's thesis, Uludağ Üniversitesi).

Çakır, H., & Tümen, G. (1990). Balıkesir Yöresi Ballarının Antimikrobiyal ve Antifungal Etkileri. *X. Ulusal Biyoloji Kongresi, Erzurum*, *210*.

Dalgıç, R. (1994). Türkiye Ege Bölgesi Ballarının Biyokimyasal ve Palinolojik Yönden lncelenmesi. Doktora Tezi, Ege Üniversitesi Fen Bilimleri Enstitüsü, İzmir, 3-4.

Davis, P. H. (1965-1988). Flora of Turkey and the East Aegean Islands. Vol. 1-9. Edinburg University Press, Edinburg.

Demirsoy, M. (1985). Araç Egzoz Gazlarının Hava Kirliliğine Olan Etkileri. Çevre '85 Sempozyumu, İzmir.

Deodikar, G. B. (1965). Melittopalynotogy. lnd. Bee J., 27: 59-72.

Doğan, A. (2003). Sıçanların Mide Mukozalarında Etanolün İndüklediği Lezyonlar Üzerine Anzer Balının Etkisinin İncelenmesi. Yüksek Lisans Tezi, Hacettepe Üniversitesi Fen Bilimleri Enstitüsü, Ankara, 50-55.

Erdoğan, N., Pehlivan, S., & Doğan, C. (2006). Pollen Analysis of Honeys from Hendek-Akyazı and Kocaali Districts of Adapazarı Province (Turkey). *Mellifera*, *6*.

Feller-Demalsy, M. J., Parent, J., & Strachan, A. A. (1987). Microscopic analysis of honeys from Alberta, Canada. *Journal of Apicultural Research*, *26*(2), 123-132.

Feller-Demalsy, M. J., Parent, J., & Strachan, A. A. (1987). Microscopic analysis of honeys from Saskatchewan, Canada. *Journal of Apicultural Research*, *26*(4), 247-254.

Feller-Demalsy, M. J., Parent, J., & Strachan, A. A. (1989). Microscopic analysis of honeys from Manitoba, Canada. *Journal of Apicultural Research*, *28*(1), 41-49.

French, V. M., Cooper, R. A., & Molan, P. C. (2005). The antibacterial activity of honey against coagulase-negative staphylococci. *Journal of Antimicrobial Chemotherapy*, *56*(1), 228-231.

Gemici, Y. (1991). İzmir yöresi ballarında polen analizi. *Doğa Turk-Journal of Botany*, *15*, 291-296.

Göçmen, M., & Gökçeoğlu, M. (1992). Bursa yöresi ballarında polen analizi. *Doğa Türk-Journal of Botany*, *16*, 373-381.

Herrera, J. (1985). Nectar secretion patterns in southern Spanish Mediterranean scrublands. *Israel Journal of Plant Sciences*, *34*(1), 47-58.

İnci, A. (1985). Dünyada Arıcılık. Teknik Arıcılık, 2, 2-6.

Jato, M. V., Sala-Llinares, A., Iglesias, M. I., & Suarez-Cervera, M. (1991). Pollens of honeys from north-western Spain. *Journal of Apicultural Research*, *30*(2), 69-73.

Kandemir, l. (2005). Modern Arıcılık El Kitabı. Temel Petek Yayınları, lstanbul.

Kaplan, A., & İnceoğlu, Ö. (2002). Pollen analysis of Konya region honeys. *OT Sistematik Botanik Dergisi*, *9*(1), 101-109.

Kaplan, A., & İnceoğlu, Ö. (2002). Pollen analysis of Konya region honeys. *OT Sistematik Botanik Dergisi*, *9*(1), 101-109.

Krell, R. (1996). *Value-added products from beekeeping* (No. 124). Food & Agriculture Org..

La-Serna Ramos, I. E., Pérez, B. M., & Ferreras, C. G. (1999). Pollen characterization of multifloral honeys from La Palma (Canary Islands). *Grana*, *38*(6), 356-363.

Lieux, M. H. (1972). A melissopalynological study of 54 Louisiana (USA) honeys. *Review of Palaeobotany and Palynology*, *13*(2), 95-124.

Lozano-Chiu, M., Nelson, P. W., Paetznick, V. L., & Rex, J. H. (1999). Disk diffusion method for determining susceptibilities of Candida spp. to MK-0991. *Journal of clinical microbiology*, *37*(5), 1625-1627.

Lusby, P. E., Coombes, A. L., & Wilkinson, J. M. (2005). Bactericidal activity of different honeys against pathogenic bacteria. *Archives of medical research*, *36*(5), 464-467.

Maurizio, A., & Hodges, F. E. D. (1951). Pollen analysis of honey. *Bee world*, *32*(1), 1-5.

Moar, N. T. (1985). Pollen analysis of New Zealand honey. *New Zealand journal of agricultural research*, *28*(1), 39-70.

Molan, P. C. (1997). Finding New Zealand honeys with outstanding antibacterial and antifungal activity. *New Zealand Beekeeper*, *10*, 20-6.

Mulu, A., Tessema, B., & Derbie, F. (2004). In vitro assessment of the antimicrobial potential of honey on common human pathogens. *The Ethiopian Journal of Health Development*, *18*(2), 107-111.

Mundo, M. A., Padilla-Zakour, O. I., & Worobo, R. W. (2004). Growth inhibition of foodborne pathogens and food spoilage organisms by select raw honeys. *International journal of food microbiology*, *97*(1), 1-8.

Nagai, T., Sakai, M., Inoue, R., Inoue, H., & Suzuki, N. (2001). Antioxidative activities of some commercially honeys, royal jelly, and propolis. *Food chemistry*, *75*(2), 237-240.

Önder, F., & Tezcan, S. (1988). Egzoz Gazlarının Bal Arılarına Etkileri. Teknik Arıcılık, 18: 16-17.

Ötleş, S. (1995). Bal ve Bal Teknolojisi (Kimyası ve Analizleri) Alaşehir Meslek Yüksekokulu Yayınları.

Patton, T., Barrett, J., Brennan, J., & Moran, N. (2006). Use of a spectrophotometric bioassay for determination of microbial sensitivity to manuka honey. *Journal of Microbiological methods*, *64*(1), 84-95.

Persano Oddo, L., Piazza, M. G., Accorti, M., & Stefanini, R. (1988). Diagnosis of unifloral honeys. 3: Application of statistical approach to honey classification. *Apicoltura (Italy)*.

Petrov, V., & Öder, E. (1976). Balın Biyolojik Orijini 1. *Atatürk Üniversitesi Ziraat Fakültesi Dergisi*, *7*(3), 167-168.

Pınar, N. M. (2003). Palinoloji Laboratuvar Kılavuzu. Ankara Üniversitesi Fen Fakültesi Döner Sermaye İşletmesi Yayınları, Ankara, 6-32.

Potoğlu Erkara ve ark. (2009). Palynochemical analyses and antimicrobial activity of Honey Samples in and around Eskişehir, Turkey. ESOGÜ Project Number: 200619030.

Ramanujam, C. G. K., & Kalpana, T. P. (1995). Microscopic analysis of honeys from a coastal district of Andhra Pradesh, India. *Review of Palaeobotany and Palynology*, *89*(3-4), 469-480.

Ramanujam, C. G. K., Reddy, P. R., & Kalpana, T. P. (1992). Pollen analysis of apiary honeys from East Godavari district, AP. *Journal of the Indian Institute of Science*, *72*(4), 289.

Sato, T., & Miyata, G. (2000). The nutraceutical benefit, part iii: honey. *Nutrition (Burbank, Los Angeles County, Calif.)*, *16*(6), 468-469.

Silici, S. (1995). *Antalya yöresi ballarında polen analizi* (Master's thesis, Akdeniz Üniversitesi).

Sorkun, K. (1985). Balda Polen Analizi. Teknik Arıcılık Dergisi, 1:28-30.

Sorkun, K. (1987). Arı Ürünleri. Bilim Teknik Dergisi, 20, 20-21.

Sorkun, K. (2002). Honey Origin and Types from Turkey. The First German Congress for Bee Products and Apitherapy, Passau, Deutschland.

Sorkun, K., & Dogan, C. (1995). Pollen Analysis of Rize-Anzer (Turkish) Honey. *Apiacta*, *3*, 75-81.

Sorkun, K., & Doğan, C. (1995). Pollen Analysis in Honey collected from Different Regions of Turkey. Hacettepe Bulletin of Natural Sciences and Engineering, Vol 24, Series A and C.

Sorkun, K., & Doğan, C. (1999). Pollen Analysis of Honeys From Central, Eastem And southeastern Anatolia in Turkey. Hacettepe Bulletin of Natural Sciences and Engineering, Vol 28, Series A, 35-50.

Sorkun, K., & İnceoğlu, Ö. (1984). İç Anadolu Bölgesi ballarında polen analizi. *Doğa bilim dergisi*, *8*(2), 222-228.

Sorkun, K., & İnceoğlu, Ö. (1984). İç Anadolu Bölgesi ballarında bulunan dominant polenler. *Doğa Bilim Dergisi*, *8*(3), 377-381.

Sorkun, K., & Yuluğ, N. (1985). Rize-İkizdere yöresi ballarında polen analizi ve antimikrobik özellikleri. Doğa Bilim Dergisi, A29(1), 118-123.

Sorkun, K., Doğan, C., Gümüş, Y., Başoğlu, N., Bulakeri, N. & Ergün, K. (1999). Türkiye'de üretilen doğal ve yapay kaynaklı balların ayırt edilmesine esas olacak fiziksel, kimyasal ve palinolojik kriterlerin belirlenmesine yönelik araştırmalar; Tübitak Tarım, Orman ve Gıda Teknolojileri Araştırma Grubu, Proje no:TOGTAG-1270, Bursa.

Sorkun, K., Güner, A., & Vural, M. (1989). Pollen analysis of honey from Rize. *Doga Turk Botanik Dergisi*, *13*, 547-554.

Sönmez, R. & Altan, Ö. (1992). Teknik Arıcılık. Ege Üniversitesi Ziraat Fakültesi Yayınları, No:499, Bornova, İzmir, 246.

Taormina, P. J., Niemira, B. A., & Beuchat, L. R. (2001). Inhibitory activity of honey against foodborne pathogens as influenced by the presence of hydrogen peroxide and level of antioxidant power. *International journal of food microbiology*, *69*(3), 217-225.

Tetik, l. (1968). Yerli, Tabii, Süzme Ballarımızın Besleyici Değeri Ve Tüzüğü Yönünden Kimyasal Bileşimlerinin Araştırılması. Doktora Tezi, Ankara Üniversitesi Veteriner Fakültesi, Ankara.

Tutkun, E. (2000). Teknik arıcılık el kitabı. *Türkiye Kalkınma Vakfı Yayın*, (6), 235.

Ünlü, E. (1994). Bursa'da Pazarlanan Ballar Üzerine Kimyasal ve Palinolojik Araştırmalar. Doktora Tezi, Uludağ Üniversitesi Fen Bilimleri Enstitüsü, Bursa, 2-6.

Ünlütürk, A., & Turantaş, F. (1998). Gıda mikrobiyolojisi. *Mengi Tan Basımevi, İzmir*, *605*.

Valencia-Barrera, R. M., Herrero, B., & Molnar, T. (2000). Pollen and organoleptic analysis of honeys in Leon province (Spain). *Grana*, *39*(2-3), 133-140.

Villanueva-G, R. (1994). Nectar sources of European and Africanized honey bees (Apis mellifera L.) in the Yucatán peninsula, Mexico. *Journal of Apicultural Research*, *33*(1), 44-58.

Weston, R. J., Brocklebank, L. K., & Lu, Y. (2000). Identification and quantitative levels of antibacterial components of some New Zealand honeys. *Food Chemistry*, *70*(4), 427-435.

White, J. W. (1979). Composition of honey. ln: Crane, E. (Ed.) Honey: A compherensive survey. Heinemann, London, 157-158.

Willix, D. J., Molan, P. C., & Harfoot, C. G. (1992). A comparison of the sensitivity of wound-infecting species of bacteria to the antibacterial activity of manuka honey and other honey. *Journal of applied bacteriology*, *73*(5), 388-394.

Yılmaz, N. (1969). İzmit yöresinden toplanan bal ve polen örneklerinde element analizi ile bal örneklerinde polen analizi, Bilim uzmanlık tezi. Hacettepe Üniv.

Yurtsever, N. & Sorkun, K. (2003). Doğal Bir Arı Ürünü Olan Balın Hijyen ve Kalitesini Etkileyen Faktörler. II. Marmara Arıcılık Kongresi Bildirileri, Yalova, 221-222.

Yurtsever, N., & Sorkun, K. (2005). Kemaliye-Erzincan yöresinde üretilen balların mikroskobik ve organoleptik analizleri ile yöre ballarının botanik kökeninin saptanması. *Mellifera*, *5*(9), 12-23.

Chapter 10

MAGNETIC LEVITATION PROPERTIES OF MGB$_2$ BULK SUPERCONDUCTORS PRODUCED BY HOT-PRESS WITH *IN-SITU* SINTERING

Burcu SAVAŞKAN[1]
Sait Barış GÜNER[2]

1 Energy Systems Engineering, Faculty of Technology, Karadeniz Technical University, 61830 Of, Trabzon, Turkey.
2 Department of Physics, Faculty of Arts and Sciences, Recep Tayyip Erdogan University, 53100 Rize, Turkey, E-mail: bsavaskan@ktu.edu.tr

1. Introduction

Magnesium diboride (MgB_2) is an intermetallic superconducting material with a 39 K transition temperature discovered in 2001 [1]. MgB_2 ceramics have been a lot of attention within the scientific community for the last 20 years. The main reason of this interest is an excellent superconducting material for practical applications and also it's unique two−band structure offers insights into the mechanism of superconductivity. MgB_2 is an intermetallic compound and it forms with alternate layers of Mg in B honeycomb lattice, as shown in Figure 1.
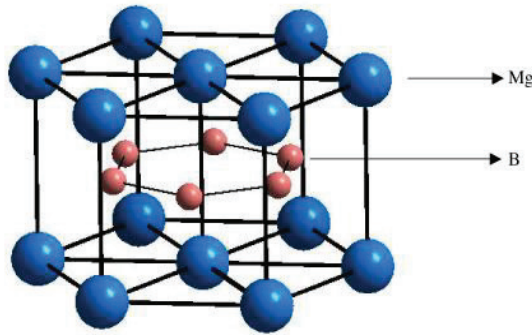
Figure 1. *Schematic of hegzagonal structure of MgB$_2$ [2].*

MgB_2 bulks present some advantages; medium critical temperature (T_c = 39 K), low material cost, relative easy fabrication and short processing time [3, 4]. MgB_2 bulks can be fabricated by spark plasma sintering (SPS) method in less than two hours and less expensive than the technique used for the growth of high temperature superconducting like (RE)BCO (where RE= rare earth mostly Y, Gd) bulks [5]. MgB_2 has the lowest theoretical density (ρ=2.625 g/cm^3) in all the superconducting material. This advantage is greatly useful for practical applications especially in the aerospace industry and portable applications [6]. Furthermore, MgB_2 can work liquid H_2 (~20 K) or liquid Ne (~27 K), which are cheaper alternative coolants to liquid He. The conventional low temperature superconductors (LTS) like Nb_3Sn, Nb-Ti used in most practical applications need to be operated at or below liquid He (~ 4.2 K). In bulk MgB_2 the grain boundaries don't form a strong barrier to current flow and it support the supercurrents, which are contrast with high temperature superconductors (HTS). Ceramic nature of HTS cuprates causes brittleness and lower mechanical strength. On the contrary, MgB_2 bulks can be made easy preparation of large dimensions and different shape manufacture; such as tape, cylinder, bulk, ring or disk,

shown in Figure 2 [7]. The coherence lengths of MgB_2 ($\xi_{ab}(0) = 37{,}120$ Å and $\xi_c(0) = 16$–36 Å) are quite high compared to other HTS materials, so big size defects can act as pinning centres [8]. These unique properties make MgB_2 bulks an exciting candidate for superconducting (trapped field magnets, TFM) magnets applications such as NMR, MRI, magnetic drug delivery, electric motors, wind powder generations and transmission cables etc. [9,10]. All these applications require large size and good quality superconducting bulks with high trapped field (B_T) value, high critical current density (J_c) value and good levitation force capability [11,12].
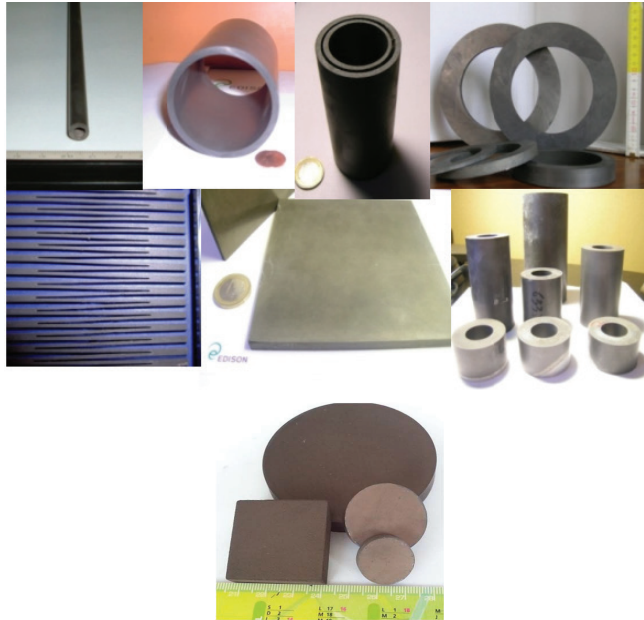
Figure 2. *EDISON SpA, R&D Division, Foro Buonaparte 31, Milano, Italy [7].*

Practical applications of bulk superconductor materials can be classified two main categories [12]:

(*i*) Superconducting "permanent magnet" magnet called as trapped field magnets (TFMs)

(*ii*) Magnetic levitation devices

A bulk superconductor magnetized by applied magnetic field concentric supercurrents induced throughout the sample volume. When

the applied magnetic field decreased to the zero, supercurrents continue and the resulting magnetic field called as "Trapped magnetic field " and its magnitude significantly higher than conventional permanent magnets, such as NeFeB or SmCo. The trapped field value directly proportional superconducting sample radius and critical current density (J_c). Although (RE)BCO bulks can have high critical current density (J_c) values that allow record trapped field value, such as 17.6 T at 26 K in GdBaCuO disk, they can suffer from inhomogeneous J_c distribution. On the contrary, MgB_2 bulks present a homogeneous trapped field and critical current density distribution within the sample. As shown in Table 1, several group have reported the trapped magnetic field of MgB_2 bulks. This table displays the trapped magnetic field value of MgB_2 bulks around 3 T at 20 K, this value appears like average compared to (RE)BCO bulks. Today, MgB_2 bulks have been used to produce trapped fields of greater than 5 T, such as a record trapped field is 5.4 T at 12 K on a surface of a MgB_2. Therefore, it is considered that in the future MgB_2 bulks can be used high-temperature superconducting maglev and wind turbine generator systems.

Magnetic fields offer the ability to levitate mass and can allow an object to rotate around an axis with contactless motion. Superconducting materials are perfect conductors and display perfect diamagnetic behaviour [13]. Bulk superconductors can provide passive magnetic levitation and the stability is greatly enhanced by flux pinning ability and hence a permanent magnet (PM) can stably levitate above a bulk superconductor, figure 3 (a). A remarkable demonstration of bulk superconducting levitation is levitation of large masses, as shown in Figure 3 (b), the levitation of a sumo wrestler of around 200 kg in Tokyo, Japan. Today, using the interaction between the permanent magnet and superconducting material over 1000 kg masses have been levitated.
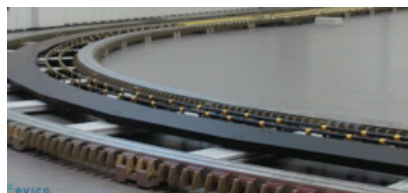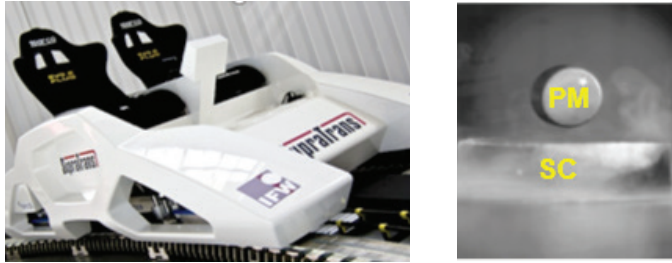
Figure 3. *(a) Permanent magnet (PM) stably levitated over a bulk HTS [14], (b) The levitation of a sumo, (c) SupraTrans project, a prototype train, is an innovation transportation concept based on superconducting levitation, Dresden University, Germany [13].*

Magnetically levitated transportation system (superconducting maglev) allows vehicle to move with minimal friction, zero magnetic drag, environment-friendless and low energy consumption. High-temperature superconducting maglev is regarded as one of the main technology modes for the future rail transit [15]. To date, investigations of Maglev have always planned to use multi-seeded YBCO as superconducting material [16]. However, MgB_2 bulks enters more and more applications, they have not been seriously considered for Maglev projects.

The fabrication method is an important way to improve superconducting properties of MgB_2 bulks such as flux trapping, critical current density, J_c, trapped magnetic field, B_T, and magnetic levitation capability. The most popular fabrication route adopted for MgB_2 bulks is conventional *in-situ* sintering, where Mg and B powders are reacted to produce MgB_2. However, in this route the resulting sample is generally around 50 % dense because of large pores inside sintered sample arising from the volatility of Mg and 25 % volume contraction in MgB_2 phase formation [3, 17]. Different techniques and synthesis method have been developed to obtain dense compacts MgB_2 samples such as high pressure sintering [18], spark plasma sintering [5] and techniques based on infiltration and growth [19]. Several research groups have been trying to optimization of sintering parameters such as pressure, sintering temperature, dwell time, heating/cooling rate and multi-step heating on the structural and superconducting properties of MgB_2 bulks [8, 11, 20]. In our previous research we have optimised the sintering process such 10-15 % excess Mg content in the precursor powder for the best superconducting properties and magnetic levitation performance [21].

As compared to (RE)BCO bulks, the studies on magnetic levitation performance of MgB_2 bulks are very few, therefore the competition

between MgB_2 and RE(BCO) in the magnetic levitation applications is so far not determine. In this work, we have investigated the effects of hot-press method MgB_2 bulk superconductors, synthesized by a pellet/ closed tube method at 775 °C under Ar atmosphere after hot pressing, on the vertical levitation force and lateral (guidance) force properties in zero-field cooling (ZFC) and field-cooling regimes (FC).

2. Experimental details

2. 1. Sample preparation

Amorphous nano B (<250 nm, >98.5 %, Pavezyum) powder and high purity of Mg (-325 mesh, 99.8% Alfa Aesar) powder were mixed using a mortar. We used 10 wt % excess Mg powder (in the starting composition of Mg and B powders) to reduce the MgO content and hence improve the connectivity [21, 22]. Three precursor pellets of diameter 20 mm and thickness 4 mm, each weighing 1.5 g, were pressed under a load of 12 ton. The mould including the pellet was heated to 250 °C and 300 °C, respectively. Then the mould including the pellet was surrounded around by a heating resistor. The mould was heated from room temperature to 250 °C for ten minutes by using a dc power supply under 12 ton pressure, and then the applied current was turned off. Thus, the hot-press process was completed. Following this process, manufactured compact pellet samples were wrapped in Titanium foil and put into in a tube furnace at 775 °C and held there for 120 minutes in Ar atmosphere.
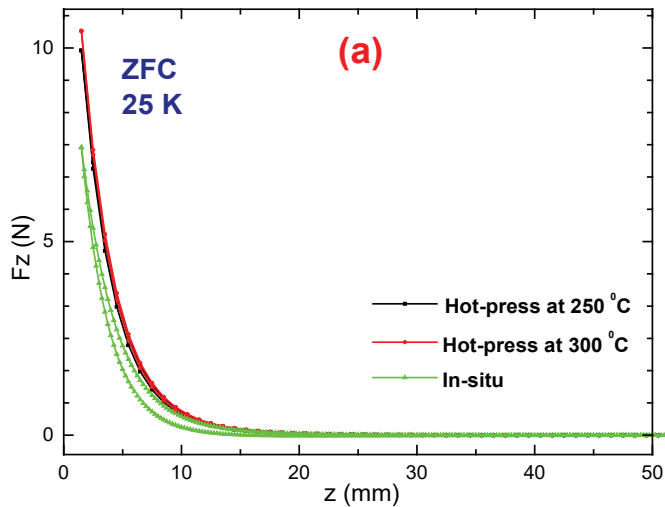
2. 2. Levitation Force Measurements

Vertical levitation force (F_z) versus vertical distance (z) and lateral levitation forces (F_x) versus lateral distance (x) measurements between the bulk MgB_2 sample and the cylindrical NdFeB permanent magnet were performed. This measurement system made by Şükrü Çelik and financially promoted by The Scientific and Technological Research Council of Turkey, with project no 110T622. The detailed information of this system can be found in Ref. [23].

3. Results and Discussions

The vertical levitation force (F_z) measurements in ZFC and FC regimes were performed at 20 K and 25 K temperatures. In FZC regime; firstly, the sample was fixed approximately on the central axis of the PM. Then the system was vacuumed. The cooling distance between sample and PM was chosen as z=50 mm. As soon as the sample was cooled at z= 50 mm above the PM (where PM's magnetic field is negligible) the $F_z(z)$ measurements were carried out during the vertical traverse of the PM from z= 50 mm to a minimum distance of z= 1.5 mm, followed by a vertical traverse of z= 1.5 mm.

The vertical levitation force (F_z) as a function of the vertical distance for in-situ and hot-pressed MgB$_2$ samples under ZFC regime at 20 and 25 K is shown in Figure 1. As shown in Fig. 1 (a) and (b), the F_z curves display repulsive character, levitation force increase exponentially with the decrease of the levitation gap finally reached at a maximum value (F_{zmax}) at the closest distance between sample and PM. The variation of levitation force shows a hysteretic behaviour that is known as the most common feature of the magnetic levitation [25]. At 25 K, The F_{zmax} values are 10.44 N for 300 °C hot-pressed MgB$_2$ sample, 9.93 N for 250 °C hot-pressed MgB$_2$ sample and 7.44 N for conventional *in-situ* MgB$_2$ sample, as shown Fig. 1 (a). The sample with the highest F_z at all measured temperature is the 300 °C hot-press MgB$_2$ sample, followed by sample hot-press at 250 °C. The $F_{z\,max}$ values at 20 K showed a similar tendency as those at 20 K.
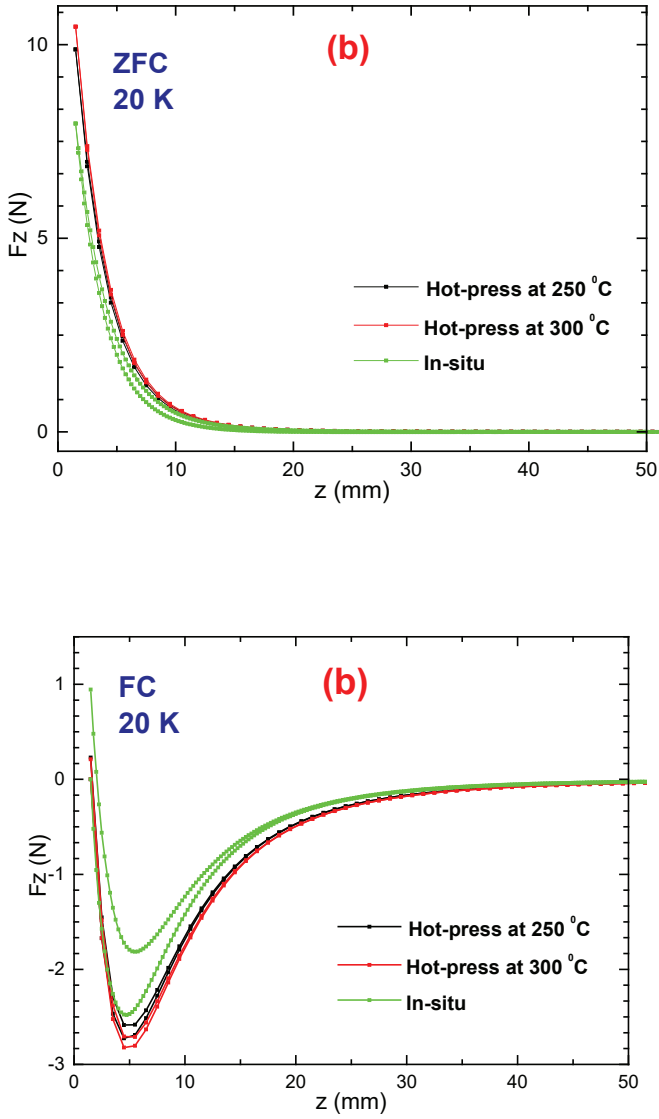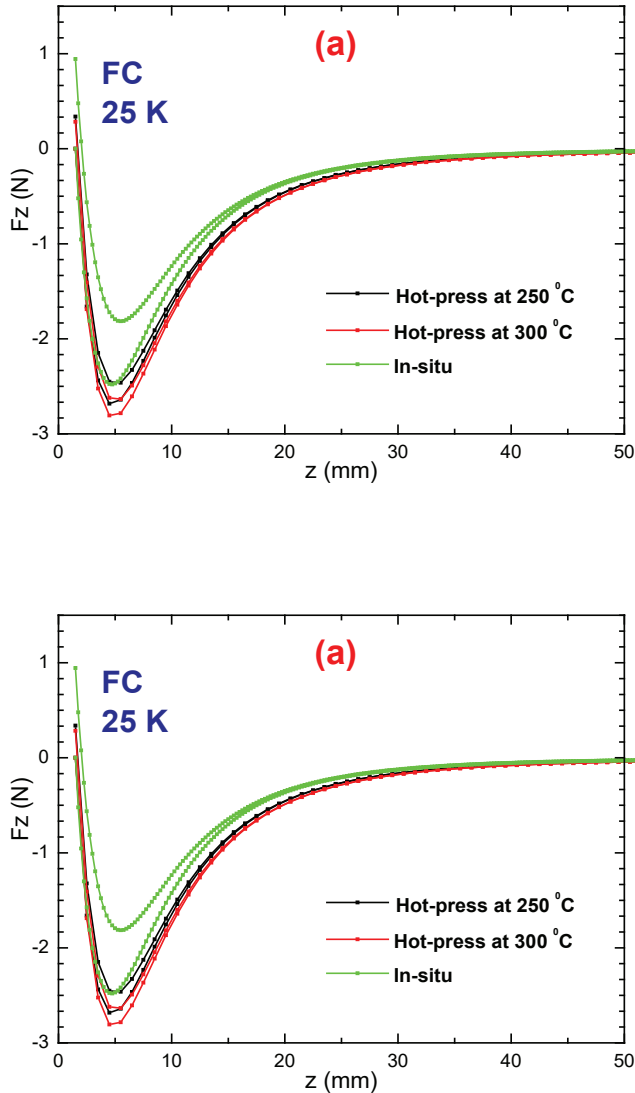
Figure 1. *The vertical levitation forces (F_z) versus the vertical distance (z) for in-situ and hot press MgB_2 bulk samples under ZFC regime at (a) 25 K and (b) 20 K.*

In FC regime; the F_z measurements were carried out by cooling the sample at $z= 1.5$ mm above the PM. Then, the measurements were carried out during the PM was vertically moving from $z= 1.5$ mm to a maximum vertical distance of $z= 50$ mm, followed by a traverse to $z= 1.5$ mm. The

vertical levitation force (F_z) as a function of the vertical distance for in-situ and hot-pressed MgB_2 samples at the temperatures of 20 K and 25 K under FC regime, is shown in Figure 2.

**Figure 2**. *The vertical levitation forces (F_z) versus the vertical distance (z) for in-situ and hot press MgB_2 bulk samples under FC regime at (a) 25 K and (b) 20 K.*

In Fig. 1, F_z curves consist of only repulsive (positive) part, while in Fig. 2 curves consist of both attractive (negative) and repulsive parts of magnetic levitation force. The hysteresis loops broaden under FC regime

due to the trapped magnetic flux and induced currents circulating inside the sample. In addition, the hysteresis behaviour is related to dynamic of current penetration inside the MgB_2 sample. As known, the ZFC regime can get a bigger levitation force but a poor stability, while in FC regime the bulk MgB_2 can get a good stability due to the trapped flux inside the sample but a reduced levitation force [24, 25]. That is, the attractive force in FC case is stronger, while the repulsive force is stronger in ZFC case. As shown in Fig. 2, the maximum attractive force values at 25 and 20 K are seen for 300 °C hot-press sample as -2.81 N and -2.82 N, respectively. Comparing to hot press MgB_2 samples with *in-situ* MgB_2 sample show low attractive force, implying that the magnetic flux can move easily in the sample, due to the decrease in superconducting properties of MgB_2.

The lateral levitation force (F_x) versus lateral distance (x) measurements were carried out by first cooling the sample at z= 1.5 mm distance above the PM, after the centres of the sample and the PM were overlapped at x= 0 mm. Then, the measurements were carried out the PM was horizontally moving from the centre of the sample (x=0) to x= 10 mm (right), then to x= -10 mm (left), and finally to x= 10 mm (right), while the fixed measurement height was chosen as 1.5 mm in vertical direction.
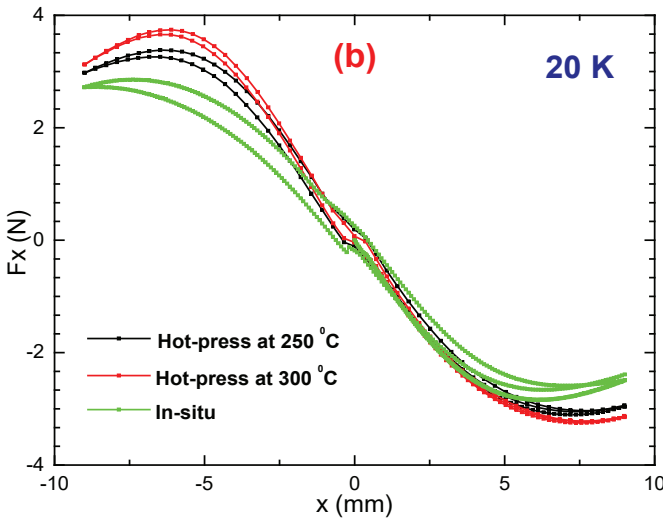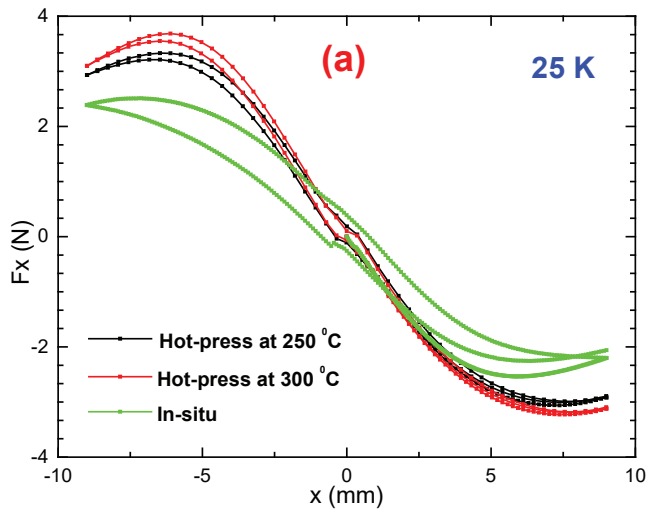
Figure 3. *Relationship between guidance force and lateral displacement for in-situ and hot-press MgB$_2$ samples at (a) 25 K, (b) 20 K. The gap between MgB$_2$ bulk and PM was kept 1.5 mm during the test.*

The lateral levitation force (F_x) known as guidance force for levitation applications such as Maglev or magnetic bearings and influence the lateral stability. Figure 3 shows the guidance forces (F_x) versus lateral distance (x) for *in-situ* and hot-pressed MgB$_2$ samples at the temperatures of 20 K and 25 K. In guidance force measurements, the vertical distance is kept constant at 1.5 mm from the PM is moved laterally. While the PM moves laterally from the centre of the sample to the right direction, the lateral force increases and displaying attractive character. It means that some magnetic flux was trapped while the cooling process in the presence of external magnetic field. Also, while the PM moves laterally to the left direction, the lateral force increases, displaying a repulsive force. As can be seen in Figure 3, 300 °C hot-press MgB$_2$ sample show higher repulsive and attractive lateral forces at 25 and 20 K, comparing the other samples.

4. Conclusions

Magnesium diboride (MgB$_2$) bulk superconductors, due to their impressive transition temperature of 39 K for superconductivity, have been widely investigated. In this study, hot-press technique was applied to improve magnetic levitation performance of sintered bulk MgB$_2$. Vertical Levitation force and guidance force in bulk MgB$_2$ is strongly connected

with high dense bulk MgB_2 sample. The hot-press at 300 °C MgB_2 sample gives the best performance for the vertical and lateral levitation forces. Finally, this study has demonstrated clearly that the hot press method has significant potential for fabrication high quality MgB_2 samples for magnetic levitation applications such as Maglev and contactless bearing systems.

Acknowledgements

References

[1] J. Nagamatsu, N. Nakagawa, T. Muranaka, Y. Zenitani and J. Akimitsu, Nature 410(2001) 63.

[2] K. Vinod, R. G. Abhilash Kumar and U. Syamaprasad, "Prospects for MgB_2 superconductors for magnet application", Supercond. Sci. Technol**.,** 20 (2007) R1.

[3] A. G. Bhagurkar, A. Yamamoto, L. Anguilano, A. R. Dennis, J. H. Durrell, N. Hari Babu and D. A. Cardwell, "A trapped magnetic field of 3 T in homogeneous, bulk MgB_2 superconductors fabricated by a modified precursor infiltration and growth process", Supercond. Sci. Technol. 29 (2016) 035008 (8pp).

[4] B. Savaskan, M. Abdioglu, K. Ozturk, "Determination of magnetic levitation force properties of bulk MgB_2 for different permanent magnetic guideways in different cooling heights", Journal of Alloys and Compounds 834 (2020) 155167.

[5] J. G. Noudem, P. Bernstein, L. Dupont, F. G. R. Martin, G. G. Sotelo, D. H. N. Dias, R. Andrade Jr, M. Muralidhar and M. Murakami, "Spark plasma sintering of bulk MgB_2 and levitation force measurements", Supercond. Sci. Technol. 33 (2020) 024001 (6pp).

[6] L. Yang, H. Suo, L. Ma, M. Liu, Y. Dai, J. Cheng, Z. Zhang and Q. Wang, "A novel sintering protocol to enhance the connectivity of exsitu MgB_2 bulks in an open system by using Mg vapor", Supercond. Sci. Technol. 33 (2020) 045006 (7pp).

[7] G. Giunchi, G. Ripamonti, T. Cavallin, E. Bassani, "The reactive liquid Mg infiltration process to produce large superconducting bulk MgB_2 manufacts", Cryogenics 46 (2006) 237–242.

[8] M. Prakasam, F Balima, J Noudem and A Largeteau, Dense MgB_2 Ceramics by Ultrahigh Pressure Field-Assisted Sintering, Ceramics (2020).

[9] P. Badica, G.Aldica, M.A.Grigoroscuta, M. Burdusel, I. Pasuk, D. Batalu, K. Berger, A. Koblischka-Veneva, M. R. Koblischka, "Reproducibility of small $Ge_2C_6H_{10}O_7$-added MgB_2 bulks fabricated by ex situ Spark Plasma Sintering used in compound bulk magnets with a trapped magnetic feld above 5 T", Nature (2020).

[10] M. Miryala, S. S. Arvapalli, N. Sakai, M. Murakami, H. Mochizuki, T. Naito, H. Fujshiro, M. Jirsa, A. Murakami, J. Noudem, "Complex pulse magnetization process and mechanical properties of spark plasma sintered bulk MgB_2", Materials science and engineering, 273 (2021) 115390.

[11] M. Muralidhar, K. Inoue, M. R. Koblischka, M. Tomita, M. Murakami, "Optimization of processing conditions towards high trapped fields in MgB_2 bulks", Journal of Alloys and Compounds, 608 (2014) 102-109.

[12] B. Savaskan, S. B. Guner, A. Yamamoto and K. Ozturk, "Trapped magnetic field and levitation force properties of multi-seeded YBCO superconductors with different seed distance", Journal of Alloys and Compounds, 829 (2020) 154400 (8pp).

[13] O. de Haas, L. Schultz, P. Verges, C. Beyer, S. Röhlig, H. Olsen, L. Kühn, D. Berger, U. Noteboom, "Superconductively levitated transport system – the SupraTrans project", IEEE Transactions on Applied Superconductivity, (2005).

[14] J. R. Hull, M. Murakami, "Applications of Bulk High-Temperature Superconductors",

[15] L. Kou, Z. Deng, H. Li, Z. Ke, "A two-dimension force model between high-temperature superconducting bulk YBCO and Halbach- Type Permanent Magnetic Guideway", IEE Appl. Supercond., (2021)

[16] K. Ozturk, M. Kabaer, M. Abdioglu, "Effect of onboard PM position on the magnetic force and stiffness performance of multi-seeded YBCO", Journal of Alloys and Compounds 644 (2015) 267-273.

[17] A. G. Bhagurkar, A. Yamamoto, L. Wang, M. Xia, A. R. Dennis, J. H. Durrell, T. A. Aljohani, N. H. Babu & D.A. Cardwell, High Trapped Fields in C-doped MgB_2 Bulk Superconductors Fabricated by Infltration and Growth Process, Nature (2018) 8:13320.

[18] C. E. J. Dancer et al. "A study of the sintering behaviour of magnesium diboride." J. Europ. Cer. Soc., 29 (2009)1817–1824.

[19] G. Giunchi, G. Ripamonti, T.Cavallin, & E. Bassani, "Reactive liquid Mg infltration process to produce large superconducting bulk MgB_2 manufacts", Cryogenics, 46 (2006)237–242.

[20] M. Muralidhar, K. Nozaki, H. Kobayashi, X. L. Zeng, A. Koblischka-Veneva, M. Koblischka, K.. Inoue and M Murakami, "Optimization of sintering conditions in bulk MgB_2 material for improvement of critical current density", J. Alloys Compd., 649 (2015) 833–42.

[21] S. B. Güner, B. Savaşkan, K. Öztürk, Ş. Çelik, C. Aksoy, F. Karaboğa, E. T. Koparan, E. Yanmaz, Investigation on superconducting and magnetic levitation force behaviour of excess Mg doped-bulk MgB_2 superconductors, Cryogenics, (101) 2019 131-136.

[22] R.. Zeng, L Lu, J. L. Wang, J. Horvat, W. X. Li, D. Q. Shi, S. X.. Dou, M Tomsic and M. Rindfleisch, Significant improvement in the critical current density of in situ MgB_2 by excess Mg addition, Supercond. Sci. Technol. 2007, 43-47.

[23] S. Çelik, "Design of magnetic levitation force measurement system at any low temperatures from 20 K to room temperature", J Alloys Compd., 662 (2015) 546-556.

[24] M. Murakami, T. Oyama, H. Fujimoto, S. Gotoh, K.Yamaguchi, Y.Shioha-ra, N. Koshizuoka, S. Tanaka, "Melt Processing Of Bulk High T_c Super-conductors and Their Application", IEEE Transactions on Magnetics 27 (1991) 1479-1486,

[25] B. Savaskan, E. Taylan Koparan, S. Celik, K. Öztürk, E. Yanmaz, "Inves-tigation on the levitation force behaviour of malic acid added bulk MgB_2 superconductors", Physica C 502 (2014) 63-69.

[26] K. Ozturk, M. Kabaer, M. Abdioğlu, "Effect of onboard PM position on the magnetic force and stiffness performance of multi-seed", Journal of Alloys and Compounds, 410 (2015) 267-273.

[27] B. Savaskan, E. T. Koparan, S. B. Güner, S Celik, E Yanmaz, "The size effect on the magnetic levitation force of MgB_2 bulk superconductors", Cryoge-nics 80 (2016) 108-114.

Chapter 11

AN APPLICATION OF GENERALIZED LINEAR MODEL APPROACH ON ECONOMETRIC STUDIES

Neslihan İYİT[1]

Harun YONAR[2]

Aynur YONAR[3]

---

1 Assoc.Prof.Dr., Statistics Department, Faculty of Science, Selcuk University, Konya, Turkey

*Corresponding Author: Email: niyit@selcuk.edu.tr

ORCID ID: 0000-0002-5727-6441

2 Assist.Prof.Dr., Biostatistics Department, Veterinary Faculty, Selcuk University, Konya, Turkey

ORCID ID: 0000-0003-1574-3993

3 Assist.Prof.Dr., Statistics Department, Faculty of Science, Selcuk University, Konya, Turkey

ORCID ID: 0000-0003-1681-9398

1.Introduction

Traditional linear model having the restrictive assumptions of "normality" and "homogeneity of variances" establishes a linear relationship between a normally distributed dependent variable and explanatory variables as follows;

$$Y = X\beta + \varepsilon \tag{1}$$

where Y is the $n \times 1$ dimensional dependent variable vector, X is the $n \times (p+1)$ dimensional design matrix of explanatory variables, β is the $(p+1) \times 1$ dimensional unknown parameter vector, and ε is the $n \times 1$ dimensional random error terms vector (Wackerly et al., 2014). Explicit form of the traditional linear model given in Eq.(1) in vector-matrix notation is also as follows (Sengupta and Jammalamadaka, 2003);

$$
\underbrace{\begin{pmatrix} Y_1 \\ Y_2 \\ . \\ . \\ . \\ Y_n \end{pmatrix}}_{Y_{n \times 1}} = \underbrace{\begin{pmatrix} 1 & X_{11} & . & . & . & X_{1p} \\ 1 & X_{21} & & & & X_{2p} \\ . & & . & & & \\ . & & & . & & \\ . & & & & . & \\ 1 & X_{n1} & . & . & . & X_{np} \end{pmatrix}}_{X_{n \times (p+1)}} \underbrace{\begin{pmatrix} \beta_0 \\ \beta_1 \\ . \\ . \\ . \\ \beta_p \end{pmatrix}}_{\beta_{(p+1) \times 1}} + \underbrace{\begin{pmatrix} \varepsilon_1 \\ \varepsilon_2 \\ . \\ . \\ . \\ \varepsilon_n \end{pmatrix}}_{\varepsilon_{n \times 1}} \tag{2}
$$

The basic assumptions on the random error terms vector in traditional linear model can be given as follows (Scott Long, 1997);

- Random error terms vector (ε) has zero mean vector, and $\sigma^2 I$ variance-covariance matrix $(\varepsilon \sim (0, \sigma^2 I))$. So variances of the random error terms are constant called as "homogeneity of variances" $(\mathrm{Var}(\varepsilon_i) = \sigma^2 \ ; \ i = 1, 2, ..., n)$.

- Random error terms are uncorrelated $\left(Cov(\varepsilon_i, \varepsilon_j) = 0;\ i \neq j\right)$.

- Random error terms vector $\left(\boldsymbol{\varepsilon}\right)$ is assumed to be normally distributed $\left(\varepsilon \sim N\left(0, \sigma^2 I\right)\right)$ for the hypothesis tests and confidence intervals.

In traditional linear models, when one or more of the above assumptions are not satisfied, "data transformation" techniques such as variance balancing transformation, or weighted least squares method are used. In linear models, "linearity" is defined by the fact that the dependent variable is a linear function of the model parameters (Scott Long, 1997). In cases where "linearity" assumption is not satisfied, some transformation techniques such as logarithmic transformation and inverse transformation are used to linearize the model, and instead of working with the original variables, the transformed variables are used. (Montgomery et al., 2012). In the relationship between a dependent variable and explanatory variables, generalized linear model (GLM) approach, which is a generalization of traditional linear model, can be used in cases where the above-given basic assumptions on the random error terms and "linearity" are not satisfied (Montgomery et al., 2012).

2.Material and Methods

2.1. Generalized Linear Models

Generalized linear model (GLM) was first introduced by Nelder and Wedderburn (1972). GLM is used to model the relationship between a dependent variable belonging to the exponential distribution family and explanatory variables. (Montgomery et al., 2012). GLM is a general class of statistical models that includes linear and nonlinear regression models especially logistic regression, Poisson regression, Negative Binomial regression, geometric regression, log-linear models, and etc. shown in Figure 1 (Olsson, 2002; Montgomery et al., 2012).
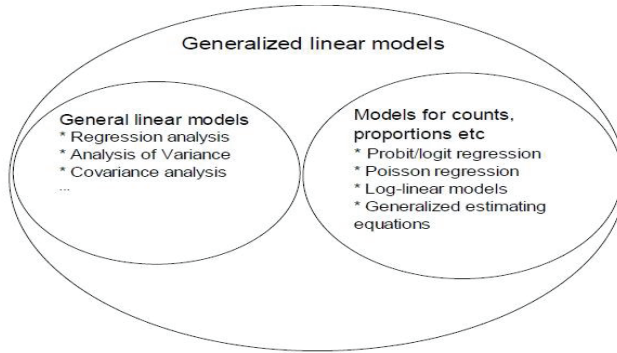
Figure 1. Development Chart of Generalized Linear Models (Olsson, 2002)

The restrictions created by the assumptions of "normality" and "homogeneity of variances" in traditional linear model is removed by the usage of the GLM, and it is widely used where the distribution of the dependent variable belongs to the exponential distribution family. The fact that the distributions of dependent variables used in economic, financial and actuarial risk assessments are mostly suitable for the exponential distribution family has made the usage of GLM very popular in these areas.

2.2. Components of Generalized Linear Models

GLM has 3 components. The first one is the "random component" structure, the second one is the "systematic part" of the model, and the third one is the "link function" structure (McCullagh and Nelder, 1989)

- **Random Component Structure**

Random component structure in GLM states that the distribution of the dependent variable is a member of the exponential distribution family (Agresti and Kateri, 2011).

The general form of the distribution of the dependent variable used in the GLM, belonging to the family of exponential distributions is as follows;

$$f(y;\theta,\phi) = \exp\left\{\frac{y\theta - b(\theta)}{a(\phi)} + c(y,\phi)\right\} \qquad (3)$$

where $a(\cdot)$, $b(\cdot)$, and $c(\cdot)$ are known functions determined according to the distribution of the dependent variable (Olsson, 2002).

The expected value and variance of the dependent variable belonging to the exponential family in GLM are as follows;

$$E(Y) = b'(\theta) \qquad (4)$$
$$Var(Y) = b''(\theta) a(\phi) \qquad (5)$$

where θ; called as the canonical parameter is the position parameter of the distribution. ϕ is the dispersion or scale parameter (Fox, 2015).

Normal, Binomial, Poisson, Gamma and Inverse Normal distributions are members of the exponential distributions family (Montgomery et al., 2012). The structures of $a(\cdot)$, $b(\cdot)$, and $c(\cdot)$ functions, expected values and variances for these distributions are given in Table 1.

Table 1. The structures of $a(\cdot)$, $b(\cdot)$, and $c(\cdot)$ functions, expected values and variances for some discrete and continuous distributions that are members of the exponential distributions family (McCullagh and Nelder, 1989; Olsson, 2002; Dobson and Barnett, 2008; Fox, 2015)

Distribution	$a(\phi)$	$b(\theta)$	$c(y,\phi)$	$E(Y) = b'(\theta)$	$V(\mu) = b''(\theta)$
Normal	σ^2	$\theta^2/2$	$-1/2\left[y^2/\phi + \log(2\pi\phi)\right]$	$\theta = \mu$	1
Binomial	1	$n\log(1+e^{\theta})$	$\log\binom{n}{y}$	$n\left[\dfrac{e^{\theta}}{1+e^{\theta}}\right] = np$	$np(1-p)$

Poisson	1	e^{θ}	$-\log y!$	$e^{\theta}=\mu$	μ
Gamma	$1/v$	$-\log(-\theta)$	$\phi^{-1}\log(y/\phi)-\log\left(y\Gamma(\phi^{-1})\right)$	$\dfrac{1}{\theta}=\mu$	μ^{2}
Inverse Gaussian	$\dfrac{1}{\gamma}$	$-\sqrt{-2\theta}$	$-1/2\left[\log(2\pi y^{3}\phi)+1/(\phi y)\right]$	$\dfrac{1}{\sqrt{-2\theta}}=\dfrac{1}{\mu^{2}}$	μ^{3}

- **Systematic Component Structure**

The systematic component of GLM is the part of the linear estimator. In GLM, linear estimator (η); is the structure that relates the expected value (mean) of the dependent variable to the linear form of the explanatory variables via a link function as follows (Olsson, 2002; Agresti, 2015);

$$\boldsymbol{\eta} = \boldsymbol{X\beta} \tag{6}$$

- **Link Function Structure**

The link function relates the random component structure to the systematic component structure in GLM as follows (De Jong and Heller, 2008; Ozaltın and İyit, 2018);

$$\boldsymbol{\eta} = g\left[E(Y)\right] = g(\boldsymbol{\mu}) = \boldsymbol{X\beta} \tag{7}$$

In GLM, the main purpose is to convert the expected value of the dependent variable to a linear form by means of a suitable link function (Montgomery et al., 2012). Therefore, the link function is the function that establishes the relationship between the expected value of the dependent variable and the linear estimator (Agresti, 2015).

The selection of the suitable link function for the distribution of the dependent variable in GLM is very important, and the most suitable link function is selected depending on the distribution of the dependent variable. Otherwise, the problems that may occur in case of not performing an appropriate transformation

in linear models also arise if the appropriate link function cannot be selected in the GLM (Myers et al., 2012; Yonar and İyit, 2018).

2.3. Parameter Estimation Methods in Generalized Linear Models

In statistics, the two most commonly used approaches in parameter estimation are maximum likelihood (ML) and least squares (LS) methods. In GLMs, the ML method based on the likelihood principle is used in the parameter estimation (Agresti, 2015). The ML estimators are the values that maximize the general form of the log-likelihood function given as follows;

$$l(\theta, \phi; y) = \log L(\theta, \phi; y) = \sum_{i=1}^{n} \frac{y_i \theta_i - b(\theta_i)}{a(\phi)} + \sum_{i=1}^{n} c(y_i, \phi) \qquad (8)$$

Since the derivatives of the log-likelihood function given in Eq.(8) with respect to the parameter vector (β) cannot be obtained in open form in GLMs, iterative methods such as Newton-Raphson (NR), Fisher-Scoring (FS) and the hybrid method using these two methods are generally needed in the phase of maximizing the log-likelihood function (McCullagh and Nelder, 1989; Olsson, 2002; Dobson and Barnett, 2008; İyit et al., 2016).

2.4. Goodness-of-fit Test Statistics for Generalized Linear Models

Goodness-of-fit test statistics for GLMs are used in the selection of the best link function among the link functions used to model the relationship between the expected value of the dependent variable and the systematic component of the model. In this study, we will consider the approach of using information criteria (IC) to test goodness-of-fit in GLMs. The smallest values of the information criteria determine the structure of the best link function with the highest goodness-of-fit (Olsson, 2002; Agresti, 2015)

Information criteria used to compare appropriate link functions to find the most suitable one in GLM are given in Table

2. In Table 2, l is the value of the log-likelihood function, k is the number of parameters in the model, and N represents the number of observations (Olsson, 2002; İyit, 2018).

Table 2. Information criteria used as a measure of goodness-of-fit in GLMs

Information criteria	Formula
Akaike Information Criteria (AIC)	$-2l + 2k$
Corrected Akaike Information Criteria (AICc)	$-2l + \dfrac{2kN}{N-k-1}$
Schwarz Bayesian Information Criteria (BIC)	$-2l + k\ln(N)$
Consistent Akaike Information Criteria (CAIC)	$-2l + k\left(\ln(N)+1\right)$

2.5. Statistical Inferences for Generalized Linear Models

The hypotheses used in testing the significance of the model coefficients in the GLM are as follows;

$$H_0 : \beta_i = 0$$
$$H_1 : \beta_i \neq 0 \qquad\qquad i = 1, 2, ..., k$$

(9)

In this study, Wald test is used to test the significance of the model coefficients of the explanatory variables in the GLM and Wald test statistics is given as follows (Agresti and Kateri, 2011);

$$W = \left(\frac{\hat{\beta}_i}{s.e.(\hat{\beta}_i)}\right)^2 \quad i = 1, 2, ..., k \qquad\qquad (10)$$

where $s.e.(\hat{\beta}_i)$ is the standard error of $\hat{\beta}_i$. Wald test statistics has

χ_1^2 distribution. (Cynthia and Rivera, 2017; Yonar and İyit, 2021).

3. An Application of Generalized Linear Models to Examine the Economic Growth of High Risk Group Countries

In this study, for investigating the economic growth of the countries in 2008 Global Economic Crisis, "gross national product (GNP) per capita" as the dollar value of a country's final output of goods and services in a year, divided by its population is taken as the main indicator. High risk group countries as Cameroon, Ivory Coast, Kenya, Nepal, Sri Lanka, and Sudan are determined as the countries having less than 1,005 $ according to World Data Bank (2018). So "GNP" is taken as the dependent variable as an important indicator of one country's economic growth. Statistically significant explanatory variables are taken as "imports" (US Dollar) as total purchase amount of goods manufactured abroad by buyers in the country, and "CO_2 emission" (metric tons per person) as carbon dioxide emissions amount of emissions from the combustion of fossil fuels and cement production for the high risk group countries from World Bank (2018). IBM SPSS Statistics 23, Stata and Excel software are used for the statistical evaluations and the level of significance is determined as $\alpha = 0.05$ in all statistical hypothesis tests (Yonar, 2020).

In this study, gross national product (GNP) per capita as the dependent variable is assumed to have gamma distribution coming from the exponential distributions family. In the first step of constructing GLM with gamma distribution, the most appropriate link function will be determined for modeling economic growth data of high risk group countries in 2008 global economic crisis taking into account the explanatory variables of imports and CO2 emissions. Information criteria values as the goodness-of-fit test statistics for different link functions are given in Table 3.

Table 3. Goodness-of-fit test statistics for different link functions in the GLM with gamma distribution for the economic growth data of high risk group countries

Link Function	AIC	AICc	BIC	CAIC
Log	297,342*	337,342*	296,509*	300,509*
Inverse	298,121	338,121	297,288	301,288
Inverse Square	298,539	338,539	297,707	301,707

According to the values of the goodness-of-fit test statistics given in Table 3, the best link function is determined as the "log-link function" with the smallest values of the information criteria. Model results for the statistically significant explanatory variables in the GLM with gamma distribution for the economic growth data of high risk group countries are given in Table 4 at the level of significance $\alpha = 0.05$.

Table 4. Generalized linear model with gamma distribution results for the economic growth data of high risk group countries

Explanatory Variables	$\hat{\beta}$	$s.e(\hat{\beta})$	95% Confidence Interval for β		Hypothesis Test		
			Lower Bound	Upper Bound	Wald Chi-Square test statistics value	d.f	p-value
Constant	24.698	0.5230	23.673	25.723	2230.382	1	0.000
Imports	-0.040	0.0151	-0.070	-0.010	7.017	1	0.008
CO_2 emissions	2.313	0.7648	0.814	3.812	9.149	1	0.002

Estimated log-link function of the GLM with gamma distribution for the economic growth data of high risk group countries in 2008 global economic crisis is as follows;

$$\log(\hat{\mu}_i) = 24.698 - 0.040(\text{Im ports})_i + 2.313(CO2\,emissions)_i$$
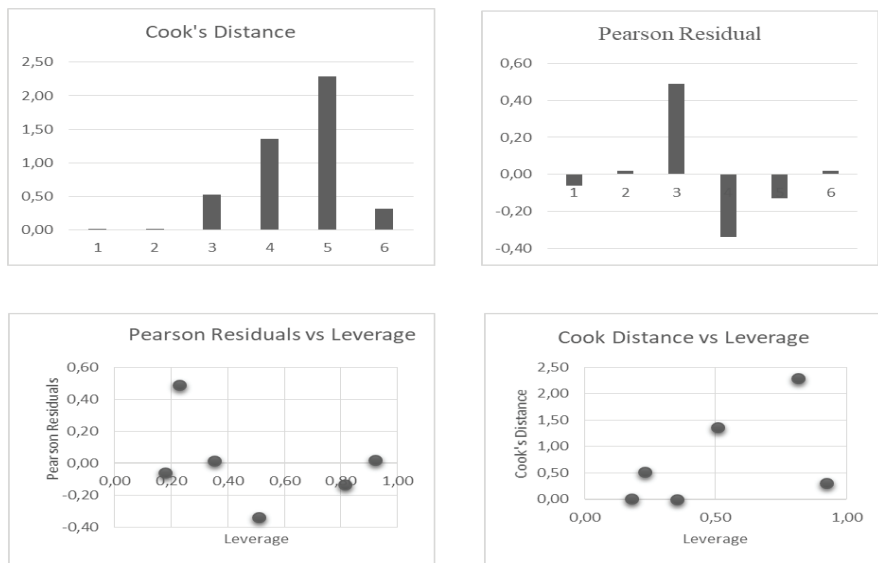$$i = Cameroon,\ Ivory\,Coast,\ Kenya,\ Nepal, \quad (11)$$
$$Sri\,Lanka,\ Sudan$$

Estimated expexted value (mean) of the GLM with gamma distribution for the economic growth data of high risk group countries in 2008 global economic crisis is as follows;

$$\hat{\mu}_i = \exp\big(24.698 - 0.040(\mathrm{Im}\,ports)_i + 2.313(CO2\,emissions)_i\big)$$
$$i = Cameroon,\ Ivory\,Coast,\ Kenya,\ Nepal, \tag{12}$$
$$Sri\,Lanka,\ Sudan$$

Thus, after model building stage, it is necessary to examine the residuals and model diagnostics in order to determine the adequacy of the GLM with gamma distribution for the economic growth data of high risk group countries.

In the model diagnostics and residual analysis part for GLM with gamma distribution for the economic growth data of high risk group countries in 2008 global economic crisis, Cook's distance to investigate the effect of outlier observations, leverage point as an indication of the effect of an observation on the GLM, and Pearson residuals are dealt with to detect outlier and influential observation are given in Figure 2.

Figure 2. GLM diagnostics for the economic growth data of high risk group countries

As seen in Figure 2, there is no outlier observation since the Cook's distance values of the observations are less than 1. Leverage values close to 1 are distant observations, but can be ignored because they are not influential. In addition to these model diagnostics, the residuals are randomly distributed in the residual analysis part indicating that the GLM with gamma distribution for the economic growth data of high risk group countries is adequate.

4. Conclusion

As the main conclusion from the estimated expected value (mean) of the GLM with gamma distribution for the economic growth data of high risk group countries in 2008 global economic crisis given in Eq.(12), 1 US Dollar increase in "imports" $exp(-0.040) = 0.9608$ times decreases estimated value of "GNP per capita". On the other hand 1 metric tons per person increase in "CO2 emissions" $exp(2.313) = 10.1047$ times increases the estimated value of "GNP per capita".

In the light of this study, in the next study GLMs with gamma distribution for the economic growth data of all risk group countries will be established to provide a broad perspective to the world economy in the aspect of the GNP per capita, imports and CO_2 emissions.

References

Agresti, A. and Kateri, M. (2011). Categorical Data Analysis, In: International encyclopedia of statistical science, Eds: Springer

Agresti, A. (2015). Foundations of Linear and Generalized Linear Models, John Wiley & Sons.

Cynthia, M. and Rivera, R. (2017). Applications of Regression Models in Epidemiology, John Wiley & Sons.

De Jong, P. and Heller, G. Z. (2008). Generalized Linear Models for Insurance Data, *Cambridge Books*.

Dobson, A. J. and Barnett, A. (2008). An Introduction to Generalized Linear Models, CRC Press.

Fox, J. (2015). Applied Regression Analysis and Generalized Linear Models, Sage Publications.

İyit, N., Yonar, H., and Genç, A. (2016). Generalized linear models for European Union countries energy data. Acta Physica Polonica, A, 130(1), 397-400.

İyit, N. (2018). Modelling world energy security data from multinomial distribution by generalized linear model under different cumulative link functions. Open Chemistry, 16(1), 377-385.

McCullagh, P. and Nelder, J. A. (1989). Generalized Linear Models, CRC Press.

Myers, R. H., Montgomery, D. C., Vining, G. G. and Robinson, T. J. (2012). Generalized Linear Models: with Applications in Engineering and the Sciences, John Wiley & Sons.

Montgomery, D. C., Peck, E. A. and Vining, G. G. (2012). Introduction to Linear Regression Analysis, John Wiley & Sons.

Nelder, J. A. and Wedderburn, R. W. (1972). Generalized linear models, *Journal of the Royal Statistical Society: Series A (General)*, 135 (3), 370-384.

Olsson, U. (2002). Generalized linear models, *An applied approach. Studentlitteratur, Lund*, 18.

Ozaltın, O., and İyit, N. (2018). Modelling the US diabetes mortality rates via generalized linear model with the Tweedie distribution. Int. J. Sci. Res, 7(2), 1326-1334.

Scott Long, J. (1997). Regression models for categorical and limited dependent variables, Advanced Quantitative Techniques in the Social Sciences, 7.

Sengupta, D. and Jammalamadaka, S. R. (2003). Linear Models: an Integrated Approach, World Scientific.

Yonar, H., and İyit, N. (2018). Modeling the causality relationships between Gdp/Gni and electricity consumption according to income levels of countries by Generalized Estimating Equations. Selçuk Üniversitesi Sosyal Bilimler Enstitüsü Dergisi, (39), 191- 200.

Yonar, H. (2020). Investigation of Economic Growth and Risk Assessments of Countries with Generalized Linear Models. Statistics Department, Graduate School of Natural Sciences, Selcuk University.

Yonar, H., and İyit, N. (2021). Some generalized estimating equations models based on causality tests for investigation of the economic growth of the country groups. Foundations of Computing and Decision Sciences, 46(3), 297-315.

Wackerly, D., Mendenhall, W. and Scheaffer, R. L. (2014). Mathematical Statistics with   Applications, Cengage Learning.

WorldBank   (2018).   World   Development   Indicators   [online], https://www.worldbank.org/: [7   August 2020].

World   Data   Bank   (2018).   Income   Groups   of   Countries   [online], https://datahelpdesk.worldbank.org/knowledgebase/articles/906519-

world-bank-country-   and-lending-groups: [5 November 2020].

Chapter 12

THE CHARACTERIZATION OF THE SPHERICAL PROJECTIONS OF DUAL BEZIER CURVES

Muhsin İNCESU [1]

1 Asst.Prof. Dr. Muhsin Incesu, Mus Alparslan University, Math. Edu. Dept. ORCID: https://orcid.org/0000-0003-2515-9627 e-mail: m.incesu@alparslan.edu.tr

1. Introduction:

Dual spherical curves corresponding to a ruled surface were studied before by Tas and Ilarslan (2019), Guven, Nurkan and Karacan (2014), Ayyildiz, Coken and Yucesan (2007), Yayli and Saracoglu (2011a; 2011b), Okullu, Kocayigit and Aydin (2019). After the introducing of dual numbers by Clifford (1873), there were good developments in the theory of mechanisms and especially in robot technology. After Study (1891), many scientists have worked in this field by reducing the study of ruled surfaces to the study of dual spherical curves. Especially Müller (1962), Hacısalihoğlu (1972; 1983), Mc Carthy and Roth (1981), Ting and Soni (1983), Tiler and Hanson (1984), Hoschek (1985), Gürsoy [1990a; 1990b, 1992], Potmann (1995), Zha (1997), Gursoy and Kucuk (1999; 2004), Nesovic et al. (2016), Hathout, Bekar and Yayli (2017), Guler and Kasap (2018), Taş (2016), Taş and Gürsoy (2018), Küçük (2004), Kazaz,Özdemir and Guroğlu (2008), Mevroidis and Roth (1997), Incesu and Gürsoy (2004; 2018), Incesu (2021) were studied the ruled surfaces and kinematics.

In this paper the dual spherical projection curves of a given Bézier curve in space $\mathbb{D}^3$ have been investigated. The Frenet frame of this projection curves at a point is given in terms of the dual and real part of a given Bézier curves.

2. Main Results:

Let a dual Bézier curve with control points $\hat{P}_i = P_i + \varepsilon P_i^* \in D^3$ (where $P_i, P_i^* \in R^3$ for $i = 0,1,\dots,n$.) be defined as

$$\hat{B}(t) = \sum_{i=0}^{n} B_i^n(t)\hat{P}_i$$

for $t \in [0,1]$ Since each control point $\hat{P}_i = P_i + \varepsilon P_i^*$ then for $t \in [0,1]$ the dual Bézier curve can be written as

$$\hat{B}(t) = \sum_{i=0}^{n} B_i^n(t)P_i + \varepsilon \sum_{i=0}^{n} B_i^n(t)P_i^* \qquad = B(t) + \varepsilon B^*(t)$$

where $B(t)$ and $B^*(t)$ are real Bézier curves of degree n with control points $P_0, P_1, \dots, P_n$ and $P_0^*, P_1^*, \dots, P_n^*$ respectively.

The projection of the dual Bézier curve $\hat{B}(t)$ to unit dual sphere D-module is a curve in Fig. 2 denoted by $\tilde{B}(t)$ and defined by

$$\tilde{B}(t) = \frac{B(t)}{\|B(t)\|} + \varepsilon \left(\frac{B^*(t)}{\|B(t)\|} - \frac{\langle B(t), B^*(t) \rangle}{\|B(t)\|^3} B(t) \right) \qquad (3)$$

So this following theorem can be stated.

Theorem 2.1: Let $\hat{B}(t) = B(t) + \varepsilon B^*(t)$ be a dual Bézier curve with control points $\hat{P}_0, \hat{P}_1, \ldots, \hat{P}_n \in D^3$ where $\hat{P}_i = P_i + \varepsilon P_i^*$, $P_i, P_i^* \in R^3$ for $i = 0,1,\ldots,n$. Then the projection curve $\tilde{B}(t)$ of the dual Bézier curve $\hat{B}(t)$ to unit dual sphere is

$$\tilde{B}(t) = \frac{B(t)}{\|B(t)\|} + \varepsilon \left(\frac{B^*(t)}{\|B(t)\|} - \frac{\langle B(t), B^*(t) \rangle}{\|B(t)\|^3} B(t) \right)$$

For shortness this spherical curve can be stated as

$$\tilde{B} = \frac{B}{\|B\|} + \varepsilon \left(\frac{B^*}{\|B\|} - \frac{\langle B, B^* \rangle}{\|B\|^3} B \right)$$

According to E.Study's theorem any dual unit vector corresponds to a oriented line in R^3. Since for every $t \in [0,1]$ the projection curve $\tilde{B}(t)$ of the dual Bézier curve $\hat{B}(t)$ to unit dual sphere is a dual unit vector, for any $t_0 \in [0,1]$, the projection curve $\tilde{B}(t_0)$ also corresponds to a oriented line in R^3. So the projection curve $\tilde{B}(t)$ corresponds to a ruled surface in R^3. The oriented line corresponding to $\tilde{B}(t_0)$ is a line with direction of the vector $\bar{B}(t_0)$ and its distance from origine is $\|\bar{B}^*(t_0)\|$.

the magnitude $\|\bar{B}^*\|$ of the dual part of the projection curve $\tilde{B}(t)$ of the dual Bézier curve $\hat{B}(t)$ is obtained as follows:

$$\|\bar{B}^*\| = \frac{1}{\|B\|^2} \sqrt{\langle B \times B^*, B \times B^* \rangle} = \frac{\|B \times B^*\|}{\|B\|^2} = \frac{\|B^*\| \sin\theta}{\|B\|}$$
$$(5)$$

where θ is an angle between the vectors B and B^*.

Proposition 2.1: Let $\hat{B}(t) = B(t) + \varepsilon B^*(t)$ be a dual Bézier curve with control points $\hat{P}_0, \hat{P}_1, \ldots, \hat{P}_n \in D^3$ where $\hat{P}_i = P_i + \varepsilon P_i^*$, $P_i, P_i^* \in R^3$ for $i = 0,1,\ldots,n$. Then

$$\|B(t)\|' = \frac{\langle B(t), B'(t) \rangle}{\|B(t)\|}$$

satisfies.

Proof: $\|B(t)\|' = \sqrt{\langle B(t), B(t) \rangle}' = \frac{\langle B(t), B(t) \rangle'}{2\sqrt{\langle B(t), B(t) \rangle}} = \frac{\langle B(t), B'(t) \rangle}{\|B(t)\|}$ is

obtained.

In this case, the first derivative of the curve $\tilde{B}$ is obtained as follows after necessary operations.

Theorem 2.2: Let the dual spherical projection curve $\tilde{B}(t)$ of the given the dual Bézier curve $\hat{B}(t)$ to dual unit sphere for every $t \in [0,1]$ be given. For shortness, if the curves $B(t)$ and $B^*(t)$ are denoted by B and B^* respectively then the first derivative of the curve $\tilde{B}$ and magnitude is

$$\tilde{B}' = \frac{B'\|B\|^2 - \langle B, B' \rangle B}{\|B\|^3}$$

$$+ \varepsilon \left[\frac{B^{*'}}{\|B\|} - \frac{B^*\langle B, B' \rangle}{\|B\|^3} - \left(\frac{\langle B^*, B' \rangle + \langle B^{*'}, B \rangle}{\|B\|^3} - \frac{3\langle B^*, B \rangle \langle B, B' \rangle}{\|B\|^5} \right) B \right.$$
$$\left. - \frac{\langle B^*, B \rangle}{\|B\|^3} B' \right]$$

and

$$\|\tilde{B}'\|$$
$$= \frac{\|(B'\|B\|^2 - \langle B, B' \rangle B)\|}{\|B\|^3}$$
$$+ \varepsilon \left[\frac{\|B\|^4 \langle B^{*'}, B' \rangle - \langle B^*, B \rangle \|B\|^2 \|B'\|^2 - (\langle B^{*'}, B \rangle + \langle B^*, B' \rangle) \|B\|^2 \langle B, B' \rangle + 2\langle B^*, B \rangle \langle B, B' \rangle^2}{\|B\|^3 \|(B'\|B\|^2 - \langle B, B' \rangle B)\|} \right]$$

In order to obtain the second derivative of the curve $\tilde{B}$, when the derivative is taken according to the t parameter in the first derivative expression, after the necessary operations, the second derivative is obtained as follows.

Theorem 2.3: Let the dual spherical projection curve $\tilde{B}(t)$ of the given the dual Bézier curve $\hat{B}(t)$ to dual unit sphere for every $t \in [0,1]$ be given. Then the second derivative of the curve $\tilde{B}$ is

$$
\tilde{B}'' = \frac{B''}{\|B\|} - \frac{2\langle B, B'\rangle B'}{\|B\|^3} - \left(\frac{\|B'\|^2 + \langle B'', B\rangle}{\|B\|^3} - \frac{3\langle B, B'\rangle^2}{\|B\|^5}\right)B +
$$

$$
+\varepsilon \left[\begin{array}{c} \dfrac{B^{*''}}{\|B\|} - \dfrac{2\langle B, B'\rangle B^{*'}}{\|B\|^3} - \left(\dfrac{\|B'\|^2 + \langle B'', B\rangle}{\|B\|^3} - \dfrac{3\langle B, B'\rangle^2}{\|B\|^5}\right)B^* - \dfrac{\langle B^*, B\rangle}{\|B\|^3}B'' \\[2mm] + \left(\dfrac{6\langle B, B'\rangle(\langle B^*, B'\rangle + \langle B^{*'}, B\rangle)}{\|B\|^5} - \dfrac{\langle B^*, B''\rangle + 2\langle B^{*'}, B'\rangle + \langle B, B^{*''}\rangle}{\|B\|^3}\right)B \\[2mm] + \left(\dfrac{3\langle B^*, B\rangle(\|B'\|^2 + \langle B'', B\rangle)}{\|B\|^5} - \dfrac{15\langle B^*, B\rangle\langle B, B'\rangle^2}{\|B\|^7}\right)B - \left(2\dfrac{\langle B^*, B'\rangle + \langle B^{*'}, B\rangle}{\|B\|^3} - 6\dfrac{\langle B^*, B\rangle\langle B, B'\rangle}{\|B\|^5}\right)B' \end{array}\right]
$$

Although the calculations are somewhat lengthy and complex, the vectoral or cross product of the first and second derivatives of the curve $\tilde{B}(t)$ is obtained as follows.

Theorem 2.4: Let $\hat{B}(t) = B(t) + \varepsilon B^*(t)$ be a dual Bézier curve with control points $\hat{P}_0, \hat{P}_1, \dots, \hat{P}_n \in D^3$ where $\hat{P}_i = P_i + \varepsilon P_i^*$, $P_i, P_i^* \in R^3$ for $i = 0,1,\dots,n$. Then The cross product of the vectors $\tilde{B}' \times \tilde{B}''$ of the projection curve $\tilde{B}(t)$ of the dual Bézier curve $\hat{B}(t)$ to unit dual sphere is

$$
\tilde{B}' \times \tilde{B}'' = \frac{1}{\|B\|^2}B' \times B'' + \left(\frac{\|B'\|^2 + \langle B'', B\rangle}{\|B\|^4} - \frac{\langle B, B'\rangle^2}{\|B\|^6}\right)B \times B' - \frac{\langle B, B'\rangle}{\|B\|^4}B \times B''
$$

$$
+\varepsilon \left[\begin{array}{c} \left(\dfrac{\langle B^*, B''\rangle + 2\langle B^{*'}, B'\rangle + \langle B, B^{*''}\rangle}{\|B\|^4} - \dfrac{2\langle B, B'\rangle(\langle B^*, B'\rangle + \langle B^{*'}, B\rangle)}{\|B\|^6} + \dfrac{6\langle B^*, B\rangle\langle B, B'\rangle^2}{\|B\|^8} - \dfrac{4\langle B^*, B\rangle(\|B'\|^2 + \langle B'', B\rangle)}{\|B\|^6}\right)B \times B' \\[2mm] + \dfrac{1}{\|B\|^2}B' \times B^{*''} + \left(\dfrac{\langle B, B'\rangle^2}{\|B\|^6} - \dfrac{(\|B'\|^2 + \langle B'', B\rangle)}{\|B\|^4}\right)B' \times B^* - \dfrac{\langle B, B'\rangle}{\|B\|^4}B \times B^{*''} \\[2mm] + \left(\dfrac{\|B'\|^2 + \langle B'', B\rangle}{\|B\|^4} - \dfrac{\langle B, B'\rangle^2}{\|B\|^6}\right)B \times B^{*'} + \left(\dfrac{4\langle B, B'\rangle\langle B^*, B\rangle}{\|B\|^6} - \dfrac{\langle B^*, B'\rangle + \langle B^{*'}, B\rangle}{\|B\|^4}\right)B \times B'' \\[2mm] - \dfrac{2\langle B^*, B\rangle}{\|B\|^4}B' \times B'' - \dfrac{\langle B, B'\rangle}{\|B\|^4}B^* \times B'' + \dfrac{1}{\|B\|^2}B^{*'} \times B'' \end{array}\right]
$$

Theorem 2.5: Let the dual spherical projection curve $\tilde{B}(t)$ of the given the dual Bézier curve $\hat{B}(t)$ to dual unit sphere for every $t \in [0,1]$ be given. Then the third order derivative of $\tilde{B}$ is

$$\tilde{B}''' = \frac{B'''}{\|B\|} - \frac{3\langle B,B'\rangle B''}{\|B\|^3} + \left(9\frac{\langle B,B'\rangle^2}{\|B\|^5} - 3\frac{\|B'\|^2 + \langle B'',B\rangle}{\|B\|^3}\right)B'$$

$$+ \left(9\frac{\langle B,B'\rangle(\|B'\|^2 + \langle B'',B\rangle)}{\|B\|^5} - 15\frac{\langle B,B'\rangle^3}{\|B\|^7} - \frac{3\langle B'',B'\rangle + \langle B''',B\rangle}{\|B\|^3}\right)B$$

$$+\varepsilon\left[\begin{array}{c} \dfrac{B^{*'''}}{\|B\|} + \left(\dfrac{9\langle B,B'\rangle^2}{\|B\|^5} - \dfrac{3\langle B,B'\rangle(\|B'\|^2 + \langle B'',B\rangle)}{\|B\|^3}\right)B^{*'} - \dfrac{3\langle B,B'\rangle}{\|B\|^3}B^{*''} \\[3mm] + \left(\dfrac{9\langle B,B'\rangle(\|B'\|^2 + \langle B'',B\rangle)}{\|B\|^5} - \dfrac{15\langle B,B'\rangle^3}{\|B\|^7} - \dfrac{3\langle B'',B'\rangle + \langle B''',B\rangle}{\|B\|^3}\right)B^{*} - \dfrac{\langle B^{*},B\rangle}{\|B\|^3}B''' \\[3mm] \left[\begin{array}{c}\dfrac{9(\|B'\|^2 + \langle B'',B\rangle)(\langle B^{*'},B\rangle + \langle B^{*},B'\rangle)}{\|B\|^5} + \dfrac{9\langle B,B'\rangle[\langle B^{*},B''\rangle + 2\langle B^{*'},B'\rangle + \langle B,B^{*''}\rangle]}{\|B\|^5} \\[3mm] - \dfrac{\langle B^{*},B'''\rangle + 3\langle B^{*'},B''\rangle + 3\langle B',B^{*''}\rangle + \langle B^{*'''},B\rangle}{\|B\|^3} - 45\dfrac{\langle B,B'\rangle^2}{\|B\|^7}(\langle B^{*},B'\rangle + \langle B^{*'},B\rangle) \\[3mm] +3\dfrac{\langle B^{*},B\rangle[2\langle B'',B'\rangle + \langle B''',B\rangle]}{\|B\|^5} + 105\dfrac{\langle B^{*},B\rangle\langle B,B'\rangle^3}{\|B\|^9} - 45\langle B,B'\rangle\langle B^{*},B\rangle\dfrac{(\|B'\|^2 + \langle B'',B\rangle)}{\|B\|^7}\end{array}\right]B \\[3mm] + \left(\dfrac{9\langle B^{*},B\rangle\langle B,B'\rangle}{\|B\|^5} - 3\dfrac{\langle B^{*'},B\rangle + \langle B^{*},B'\rangle}{\|B\|^3}\right)B'' \\[3mm] + \left[\begin{array}{c}\dfrac{9\langle B^{*},B\rangle(\|B'\|^2 + \langle B'',B\rangle)}{\|B\|^5} - 3\dfrac{\langle B^{*},B''\rangle + 2\langle B^{*'},B'\rangle + \langle B,B^{*''}\rangle}{\|B\|^3} \\[3mm] \dfrac{18\langle B,B'\rangle[\langle B^{*},B'\rangle + \langle B^{*'},B\rangle]}{\|B\|^5} - \dfrac{45\langle B^{*},B\rangle\langle B,B'\rangle^2}{\|B\|^7}\end{array}\right]B' \end{array}\right]$$

According to these results the determinat value $det(\tilde{B}', \tilde{B}'', \tilde{B}''')$ of the functions $\tilde{B}', \tilde{B}'', \tilde{B}'''$ can be calculated as follows.

Theorem 2.6: Let the dual spherical projection curve $\tilde{B}(t)$ of the given the dual Bézier curve $\hat{B}(t)$ to dual unit sphere for every $t \in [0,1]$ be given. Then the determinant value $det(\tilde{B}', \tilde{B}'', \tilde{B}''')$ is as follow:

$$det(\tilde{B}', \tilde{B}'', \tilde{B}''') = \frac{det(B', B'', B''')}{\|B\|^3} + \left(\frac{\|B'\|^2 + \langle B'', B\rangle}{\|B\|^5} - \frac{\langle B, B'\rangle^2}{\|B\|^7}\right) det(B, B', B''') - \frac{\langle B, B'\rangle}{\|B\|^5} det(B, B'', B''')$$
$$+ \left(\left(2 - \frac{1}{\|B\|}\right)\left(\frac{3\langle B, B'\rangle(\|B'\|^2 + \langle B'', B\rangle)}{\|B\|^7} + 3\frac{\langle B, B'\rangle^3}{\|B\|^9}\right) - \frac{3\langle B'', B'\rangle + \langle B''', B\rangle}{\|B\|^5}\right) det(B, B', B'')$$

$$+\varepsilon \begin{bmatrix} \dfrac{det(B', B'', B^{*'''})}{\|B\|^3} - \dfrac{3\langle B, B'\rangle}{\|B\|^5} det(B', B'', B^{*''}) - 3\dfrac{\langle B^{*}, B\rangle}{\|B\|^5} det(B', B'', B''') \\[2mm] + \left(\dfrac{3\langle B, B'\rangle(\|B'\|^2 + \langle B'', B\rangle)}{\|B\|^7} - \dfrac{3\langle B, B'\rangle^3}{\|B\|^9} - \dfrac{3\langle B'', B'\rangle + \langle B''', B\rangle}{\|B\|^5}\right) det(B', B'', B^{*}) \\[2mm] + \begin{bmatrix} \dfrac{3(\|B'\|^2 + \langle B'', B\rangle)(\langle B^{*'}, B\rangle + \langle B^{*}, B'\rangle)}{\|B\|^5}\left(3 - \dfrac{2}{\|B\|^2}\right) - \dfrac{\langle B^{*}, B'''\rangle + 3\langle B^{*'}, B''\rangle + 3\langle B^{*''}, B'\rangle + \langle B^{*'''}, B\rangle}{\|B\|^3} \\[2mm] + 3\dfrac{\langle B, B'\rangle^2}{\|B\|^7}(\langle B^{*'}, B'\rangle + \langle B^{*}, B'\rangle)\left(-15 + \dfrac{10}{\|B\|^2}\right) \\[2mm] + \dfrac{3\langle B, B'\rangle[\langle B^{*}, B''\rangle + 2\langle B^{*'}, B'\rangle + \langle B, B^{*''}\rangle]}{\|B\|^5}\left(3 - \dfrac{1}{\|B\|^2}\right) + 3\langle B, B'\rangle\langle B^{*}, B\rangle\dfrac{(\|B'\|^2 + \langle B'', B\rangle)}{\|B\|^7}\left(-15 + \dfrac{4}{\|B\|^2}\right) \\[2mm] + 3\dfrac{\langle B^{*}, B\rangle\langle B, B'\rangle^3}{\|B\|^9}\left(35 - \dfrac{19}{\|B\|^2}\right) + \dfrac{\langle B^{*}, B\rangle[3\langle B'', B'\rangle + \langle B''', B\rangle]}{\|B\|^5}\left(3 + \dfrac{2}{\|B\|^2}\right) \end{bmatrix} det(B', B'', B) \\[2mm] + \left(\dfrac{\|B'\|^2 + \langle B'', B\rangle}{\|B\|^5} - \dfrac{\langle B, B'\rangle^2}{\|B\|^7}\right) det(B, B', B^{*'''}) + \dfrac{1}{\|B\|^3} det(B', B^{*''}, B''') - \dfrac{3\langle B, B'\rangle B''}{\|B\|^5} det(B, B^{*'}, B'') \\[2mm] + \left(3\dfrac{\langle B, B'\rangle(\|B'\|^2 + \langle B'', B\rangle)}{\|B\|^7} - 3\dfrac{\langle B, B'\rangle^3}{\|B\|^9} - \dfrac{3\langle B'', B'\rangle + \langle B''', B\rangle}{\|B\|^5}\right) det(B, B', B^{*''}) \\[2mm] + \left((-1 + \langle B, B'\rangle)\dfrac{3\langle B, B'\rangle^2}{\|B\|^9}(\|B'\|^2 + \langle B'', B\rangle) + (1 - \langle B, B'\rangle)\dfrac{3(\|B'\|^2 + \langle B'', B\rangle)^2}{\|B\|^7}\right) det(B, B', B^{*'}) \\[2mm] + \left(\dfrac{\langle B^{*}, B''\rangle + 2\langle B^{*'}, B'\rangle + \langle B, B^{*''}\rangle}{\|B\|^5} - \dfrac{2\langle B, B'\rangle(\langle B^{*}, B'\rangle + \langle B^{*'}, B\rangle)}{\|B\|^7} + \dfrac{7\langle B^{*}, B\rangle\langle B, B'\rangle^2}{\|B\|^9} - \dfrac{5\langle B^{*}, B\rangle(\|B'\|^2 + \langle B'', B\rangle)}{\|B\|^7}\right) det(B, B', B''') \\[2mm] + \left(\dfrac{3\langle B, B'\rangle^3}{\|B\|^9} + \dfrac{6\langle B, B'\rangle^2(\|B'\|^2 + \langle B'', B\rangle)}{\|B\|^7} - \dfrac{9\langle B, B'\rangle(\|B'\|^2 + \langle B'', B\rangle)}{\|B\|^7} + \dfrac{3(\|B'\|^2 + \langle B'', B\rangle)^2}{\|B\|^5}\right) det(B, B'', B^{*'}) \\[2mm] + \left(5\dfrac{\langle B, B'\rangle\langle B^{*}, B\rangle}{\|B\|^7} - \dfrac{(\langle B^{*}, B'\rangle + \langle B^{*'}, B\rangle)}{\|B\|^7}\right) det(B, B'', B''') - \dfrac{\langle B, B'\rangle}{\|B\|^5} det(B, B^{*'}, B''') \\[2mm] + \left(\dfrac{\langle B, B'\rangle^2}{\|B\|^7} - \dfrac{(\|B'\|^2 + \langle B'', B\rangle)}{\|B\|^5}\right) det(B', B^{*}, B''') - \dfrac{\langle B, B'\rangle}{\|B\|^5} det(B, B^{*''}, B''') + \dfrac{det(B^{*'}, B'', B''')}{\|B\|^3} \\[2mm] - \dfrac{\langle B, B'\rangle}{\|B\|^5} det(B, B'', B^{*''''}) + \left(\dfrac{\|B'\|^2 + \langle B'', B\rangle}{\|B\|^5} - \dfrac{\langle B, B'\rangle^2}{\|B\|^7}\right) det(B, B^{*''}, B''') \end{bmatrix}$$

Theorem 2.7: Let the dual spherical projection curve $\tilde{B}(t)$ of the given the dual Bézier curve $\hat{B}(t)$ to dual unit sphere for every $t \in [0,1]$ be given. Then the magnitude of the cross product of the vectors $\tilde{B}', \tilde{B}''$ is

$$\|\tilde{B}' \times \tilde{B}''\| = \left\|\frac{1}{\|B\|^2}B' \times B'' + \left(\frac{\|B'\|^2 + \langle B'', B\rangle}{\|B\|^4} - \frac{\langle B, B'\rangle^2}{\|B\|^6}\right)B \times B' - \frac{\langle B, B'\rangle}{\|B\|^4}B \times B''\right\| +$$

$$+ \frac{\left\langle \begin{bmatrix} \left[\left(\dfrac{\langle B^{*}, B''\rangle + 2\langle B^{*'}, B'\rangle + \langle B, B^{*''}\rangle}{\|B\|^4} - \dfrac{2\langle B, B'\rangle(\langle B^{*}, B'\rangle + \langle B^{*'}, B\rangle)}{\|B\|^6}\right) \\[1mm] + \dfrac{6\langle B^{*}, B\rangle\langle B, B'\rangle^2}{\|B\|^8} - \dfrac{4\langle B^{*}, B\rangle(\|B'\|^2 + \langle B'', B\rangle)}{\|B\|^6}\right] B \times B' \\[1mm] + \dfrac{1}{\|B\|^2}B' \times B^{*''} + \left(\dfrac{\langle B, B'\rangle^2}{\|B\|^6} - \dfrac{(\|B'\|^2 + \langle B'', B\rangle)}{\|B\|^4}\right)B' \times B^{*} - \dfrac{\langle B, B'\rangle}{\|B\|^4}B \times B^{*''} \\[1mm] + \left(\dfrac{\|B'\|^2 + \langle B'', B\rangle}{\|B\|^4} - \dfrac{\langle B, B'\rangle^2}{\|B\|^6}\right)B \times B^{*'} \\[1mm] + \left(\dfrac{4\langle B, B'\rangle\langle B^{*}, B\rangle}{\|B\|^6} - \dfrac{\langle B^{*}, B'\rangle + \langle B^{*'}, B\rangle}{\|B\|^4}\right)B \times B'' \\[1mm] - \dfrac{2\langle B^{*}, B\rangle}{\|B\|^4}B' \times B'' - \dfrac{\langle B, B'\rangle}{\|B\|^4}B^{*} \times B'' + \dfrac{1}{\|B\|^2}B^{*''} \times B'' \end{bmatrix}, \begin{bmatrix} \dfrac{1}{\|B\|^2}B' \times B'' - \dfrac{\langle B, B'\rangle}{\|B\|^4}B \times B'' + \\[1mm] + \left(\dfrac{\|B'\|^2 + \langle B'', B\rangle}{\|B\|^4} - \dfrac{\langle B, B'\rangle^2}{\|B\|^6}\right)B \times B' \end{bmatrix}\right\rangle}{\left\|\dfrac{1}{\|B\|^2}B' \times B'' + \left(\dfrac{\|B'\|^2 + \langle B'', B\rangle}{\|B\|^4} - \dfrac{\langle B, B'\rangle^2}{\|B\|^6}\right)B \times B' - \dfrac{\langle B, B'\rangle}{\|B\|^4}B \times B''\right\|}$$

obtained. So this following theorem can be given here.

Theorem 2.8: Let the dual spherical projection curve $\tilde{B}(t)$ of the given the dual Bézier curve $\hat{B}(t)$ to dual unit sphere for every

$t \in [0,1]$ be given. Then the Frenet frame on the $\tilde{B}(t)$ at the point t is given as:

$$T = \frac{B'\|B\|^2 - \langle B, B'\rangle B}{\|B'\|B\|^2 - \langle B, B'\rangle B\|} +$$

$$+\varepsilon \frac{\left[\begin{array}{l}\frac{B^{*\prime}}{\|B\|} - \frac{B^*\langle B, B'\rangle}{\|B\|^3} - \frac{\langle B^*, B\rangle}{\|B\|^3}B' \\ -\left(\frac{\langle B^*, B'\rangle + \langle B^{*\prime}, B\rangle}{\|B\|^3} - \frac{3\langle B^*, B\rangle\langle B, B'\rangle}{\|B\|^5}\right)B\end{array}\right]}{\frac{\|B'\|B\|^2 - \langle B, B'\rangle B\|}{\|B\|^3}}$$

$$+\frac{\left\langle\left[\begin{array}{l}\frac{B^{*\prime}}{\|B\|} - \frac{B^*\langle B, B'\rangle}{\|B\|^3} - \frac{\langle B^*, B\rangle}{\|B\|^3}B' \\ -\left(\frac{\langle B^*, B'\rangle + \langle B^{*\prime}, B\rangle}{\|B\|^3} - \frac{3\langle B^*, B\rangle\langle B, B'\rangle}{\|B\|^5}\right)B\end{array}\right], \frac{B'\|B\|^2 - \langle B, B'\rangle B}{\|B\|^3}\right\rangle}{\frac{\|B'\|B\|^2 - \langle B, B'\rangle B\|^3}{\|B\|^9}}\left(\frac{B'\|B\|^2 - \langle B, B'\rangle B}{\|B\|^3}\right)$$

$$B = \frac{\frac{1}{\|B\|^2}B' \times B'' + \left(\frac{\|B'\|^2 + \langle B'', B\rangle}{\|B\|^4} - \frac{\langle B, B'\rangle^2}{\|B\|^6}\right)B \times B' - \frac{\langle B, B'\rangle}{\|B\|^4}B \times B''}{\left\|\frac{1}{\|B\|^2}B' \times B'' + \left(\frac{\|B'\|^2 + \langle B'', B\rangle}{\|B\|^4} - \frac{\langle B, B'\rangle^2}{\|B\|^6}\right)B \times B' - \frac{\langle B, B'\rangle}{\|B\|^4}B \times B''\right\|} +$$

$$+\varepsilon\left[\begin{array}{l}\frac{\left[\begin{array}{l}\left(\frac{\langle B^*, B''\rangle + 2\langle B^{*\prime}, B'\rangle + \langle B, B^{*\prime\prime}\rangle}{\|B\|^4} - \frac{2\langle B, B'\rangle(\langle B^*, B'\rangle + \langle B^{*\prime}, B\rangle)}{\|B\|^6}\right) \\ +\frac{6\langle B^*, B\rangle\langle B, B'\rangle^2}{\|B\|^8} - \frac{4\langle B^*, B\rangle(\|B'\|^2 + \langle B'', B\rangle)}{\|B\|^6}\end{array}\right)B \times B' \\ +\frac{1}{\|B\|^2}B' \times B^{*\prime\prime} + \left(\frac{\langle B, B'\rangle^2}{\|B\|^6} - \frac{(\|B'\|^2 + \langle B'', B\rangle)}{\|B\|^4}\right)B' \times B^* - \frac{\langle B, B'\rangle}{\|B\|^4}B \times B^{*\prime\prime} \\ +\left(\frac{\|B'\|^2 + \langle B'', B\rangle}{\|B\|^4} - \frac{\langle B, B'\rangle^2}{\|B\|^6}\right)B \times B^{*\prime} + \\ +\left(\frac{4\langle B, B'\rangle\langle B^*, B\rangle}{\|B\|^6} - \frac{\langle B^*, B'\rangle + \langle B^{*\prime}, B\rangle}{\|B\|^4}\right)B \times B'' \\ -\frac{2\langle B^*, B\rangle}{\|B\|^4}B' \times B'' - \frac{\langle B, B'\rangle}{\|B\|^4}B^* \times B'' + \frac{1}{\|B\|^2}B^{*\prime} \times B''\end{array}\right]}{\left\|\frac{1}{\|B\|^2}B' \times B'' + \left(\frac{\|B'\|^2 + \langle B'', B\rangle}{\|B\|^4} - \frac{\langle B, B'\rangle^2}{\|B\|^6}\right)B \times B' - \frac{\langle B, B'\rangle}{\|B\|^4}B \times B''\right\|} + \\ +\frac{\left\langle\left[\begin{array}{l}\left(\frac{\langle B^*, B''\rangle + 2\langle B^{*\prime}, B'\rangle + \langle B, B^{*\prime\prime}\rangle}{\|B\|^4} - \frac{2\langle B, B'\rangle(\langle B^*, B'\rangle + \langle B^{*\prime}, B\rangle)}{\|B\|^6}\right) \\ +\frac{6\langle B^*, B\rangle\langle B, B'\rangle^2}{\|B\|^8} - \frac{4\langle B^*, B\rangle(\|B'\|^2 + \langle B'', B\rangle)}{\|B\|^6}\end{array}\right)B \times B' \\ +\frac{1}{\|B\|^2}B' \times B^{*\prime\prime} + \left(\frac{\langle B, B'\rangle^2}{\|B\|^6} - \frac{(\|B'\|^2 + \langle B'', B\rangle)}{\|B\|^4}\right)B' \times B^* - \frac{\langle B, B'\rangle}{\|B\|^4}B \times B^{*\prime\prime} \\ +\left(\frac{\|B'\|^2 + \langle B'', B\rangle}{\|B\|^4} - \frac{\langle B, B'\rangle^2}{\|B\|^6}\right)B \times B^{*\prime} + \\ +\left(\frac{4\langle B, B'\rangle\langle B^*, B\rangle}{\|B\|^6} - \frac{\langle B^*, B'\rangle + \langle B^{*\prime}, B\rangle}{\|B\|^4}\right)B \times B'' \\ -\frac{2\langle B^*, B\rangle}{\|B\|^4}B' \times B'' - \frac{\langle B, B'\rangle}{\|B\|^4}B^* \times B'' + \frac{1}{\|B\|^2}B^{*\prime} \times B''\end{array}\right], \left[\begin{array}{l}\left(\frac{\|B'\|^2 + \langle B'', B\rangle}{\|B\|^4} - \frac{\langle B, B'\rangle^2}{\|B\|^6}\right)B \times B' + \\ +\frac{1}{\|B\|^2}B' \times B'' - \frac{\langle B, B'\rangle}{\|B\|^4}B \times B''\end{array}\right]\right\rangle}{\left\|\frac{1}{\|B\|^2}B' \times B'' + \left(\frac{\|B'\|^2 + \langle B'', B\rangle}{\|B\|^4} - \frac{\langle B, B'\rangle^2}{\|B\|^6}\right)B \times B' - \frac{\langle B, B'\rangle}{\|B\|^4}B \times B''\right\|^3}\left[\begin{array}{l}\left(\frac{\|B'\|^2 + \langle B'', B\rangle}{\|B\|^4} - \frac{\langle B, B'\rangle^2}{\|B\|^6}\right)B \times B' + \\ +\frac{1}{\|B\|^2}B' \times B'' - \frac{\langle B, B'\rangle}{\|B\|^4}B \times B''\end{array}\right]\end{array}\right]$$

$$N = B \times T$$

Theorem 2.9: Let the dual spherical projection curve $\tilde{B}(t)$ of the given the dual Bézier curve $\hat{B}(t)$ to dual unit sphere for every $t \in [0,1]$ be given. Then the dual curvatures of the $\tilde{B}(t)$ at the point t are given as:

$$\kappa = \frac{\left\| \frac{1}{\|B\|^2} B' \times B'' + \left(\frac{\|B'\|^2 + \langle B'', B \rangle}{\|B\|^4} - \frac{\langle B, B' \rangle^2}{\|B\|^6} \right) B \times B' - \frac{\langle B, B' \rangle}{\|B\|^4} B \times B'' \right\|}{\frac{\|(B'\|B\|^2 - \langle B, B' \rangle B)\|^3}{\|B\|^9}} +$$

$$+ \varepsilon \left[\frac{\left\langle \begin{bmatrix} \left[\left(\frac{\langle B^*, B'' \rangle + 2\langle B^{*\prime}, B' \rangle + \langle B, B^{*\prime\prime} \rangle}{\|B\|^4} - \frac{2\langle B, B' \rangle(\langle B^*, B' \rangle + \langle B^{*\prime}, B \rangle)}{\|B\|^6} \right) \\ + \frac{6\langle B^*, B \rangle\langle B, B' \rangle^2}{\|B\|^8} - \frac{4\langle B^*, B \rangle(\|B'\|^2 + \langle B'', B \rangle)}{\|B\|^6} \right] B \times B' \\ + \frac{1}{\|B\|^2} B' \times B^{*\prime\prime} + \left(\frac{\langle B, B' \rangle^2}{\|B\|^6} - \frac{(\|B'\|^2 + \langle B'', B \rangle)}{\|B\|^4} \right) B' \times B^* - \frac{\langle B, B' \rangle}{\|B\|^4} B \times B^{*\prime\prime} \\ + \left(\frac{\|B'\|^2 + \langle B'', B \rangle}{\|B\|^4} - \frac{\langle B, B' \rangle^2}{\|B\|^6} \right) B \times B^{*\prime} \\ + \left(\frac{4\langle B, B' \rangle\langle B^*, B \rangle}{\|B\|^6} - \frac{\langle B^*, B' \rangle + \langle B^{*\prime}, B \rangle}{\|B\|^4} \right) B \times B'' \\ - \frac{2\langle B^*, B \rangle}{\|B\|^4} B' \times B'' - \frac{\langle B, B' \rangle}{\|B\|^4} B^* \times B'' + \frac{1}{\|B\|^2} B^{*\prime} \times B'' \end{bmatrix} , \begin{bmatrix} \frac{1}{\|B\|^2} B' \times B'' - \frac{\langle B, B' \rangle}{\|B\|^4} B \times B'' + \\ + \left(\frac{\|B'\|^2 + \langle B'', B \rangle}{\|B\|^4} - \frac{\langle B, B' \rangle^2}{\|B\|^6} \right) B \times B' \end{bmatrix} \right\rangle}{\frac{\|(B'\|B\|^2 - \langle B, B' \rangle B)\|^3}{\|B\|^9}} + \right.$$

$$\left. -3 \frac{\left\| \frac{1}{\|B\|^2} B' \times B'' + \left(\frac{\|B'\|^2 + \langle B'', B \rangle}{\|B\|^4} - \frac{\langle B, B' \rangle^2}{\|B\|^6} \right) B \times B' - \frac{\langle B, B' \rangle}{\|B\|^4} B \times B'' \right\| \begin{bmatrix} \|B\|^4 \langle B^{*\prime}, B' \rangle - \langle B^*, B \rangle \|B\|^2 \|B'\|^2 + 2\langle B^*, B \rangle\langle B, B' \rangle^2 \\ - (\langle B^{*\prime}, B \rangle + \langle B^*, B' \rangle) \|B\|^2 \langle B, B' \rangle \end{bmatrix}}{\frac{\|(B'\|B\|^2 - \langle B, B' \rangle B)\|^5}{\|B\|^9}} \right]$$

and the torsion

$$\tau = \frac{\begin{pmatrix} \frac{det(B',B'',B''')}{\|B\|^3} + \left(\frac{\|B'\|^2 + \langle B'',B\rangle}{\|B\|^5} - \frac{\langle B,B'\rangle^2}{\|B\|^7}\right)det(B,B',B''') - \frac{\langle B,B'\rangle}{\|B\|^5}det(B,B'',B''') \\ + \left(\left(2 - \frac{1}{\|B\|}\right)\left(\frac{3\langle B,B'\rangle(\|B'\|^2 + \langle B'',B\rangle)}{\|B\|^7} + 3\frac{\langle B,B'\rangle^3}{\|B\|^9}\right) - \frac{3\langle B'',B'\rangle + \langle B''',B\rangle}{\|B\|^5}\right)det(B,B',B'') \end{pmatrix}}{\left\|\frac{1}{\|B\|^2}B' \times B'' + \left(\frac{\|B'\|^2 + \langle B'',B\rangle}{\|B\|^4} - \frac{\langle B,B'\rangle^2}{\|B\|^6}\right)B \times B' - \frac{\langle B,B'\rangle}{\|B\|^4}B \times B''\right\|^2} +$$

$$+\varepsilon \left[\frac{\begin{bmatrix} \frac{det(B',B'',B^{*'''})}{\|B\|^3} - \frac{3\langle B,B'\rangle}{\|B\|^5}det(B',B'',B^{*''}) - 3\frac{\langle B^*,B\rangle}{\|B\|^5}det(B',B'',B''') \\ + \left(\frac{3\langle B,B'\rangle(\|B'\|^2 + \langle B'',B\rangle)}{\|B\|^7} - \frac{3\langle B,B'\rangle^3}{\|B\|^9} - \frac{3\langle B'',B'\rangle + \langle B''',B\rangle}{\|B\|^5}\right)det(B',B'',B^*) \\ + \begin{bmatrix} \frac{3(\|B'\|^2 + \langle B'',B\rangle)(\langle B^{*'},B\rangle + \langle B^*,B'\rangle)}{\|B\|^5}\left(3 - \frac{2}{\|B\|^2}\right) - \frac{\langle B^*,B'''\rangle + 3\langle B^{*'},B''\rangle + 3\langle B^{*''},B'\rangle + \langle B^{*'''},B\rangle}{\|B\|^3} \\ + 3\frac{\langle B,B'\rangle^2}{\|B\|^7}(\langle B^*,B'\rangle + \langle B^{*'},B\rangle)\left(-15 + \frac{10}{\|B\|^2}\right) \\ + \frac{3\langle B,B'\rangle[\langle B^*,B''\rangle + 2\langle B^{*'},B'\rangle + \langle B,B^{*''}\rangle]}{\|B\|^5}\left(3 - \frac{1}{\|B\|^2}\right) + 3\langle B,B'\rangle\langle B^*,B\rangle\frac{(\|B'\|^2 + \langle B'',B\rangle)}{\|B\|^7}\left(-15 + \frac{4}{\|B\|^2}\right) \\ + 3\frac{\langle B^*,B\rangle\langle B,B'\rangle^3}{\|B\|^9}\left(35 - \frac{19}{\|B\|^2}\right) + \frac{\langle B^*,B\rangle[3\langle B'',B'\rangle + \langle B''',B\rangle]}{\|B\|^5}\left(3 + \frac{2}{\|B\|^2}\right) \end{bmatrix}det(B',B'',B) \\ + \left(\frac{\|B'\|^2 + \langle B'',B\rangle}{\|B\|^5} - \frac{\langle B,B'\rangle^2}{\|B\|^7}\right)det(B,B',B''') + \frac{1}{\|B\|^3}det(B^{*'},B'',B''') - \frac{3\langle B,B'\rangle B''}{\|B\|^5}det(B',B^{*''},B'') \\ + \left(3\frac{\langle B,B'\rangle(\|B'\|^2 + \langle B'',B\rangle)}{\|B\|^7} - 3\frac{\langle B,B'\rangle^3}{\|B\|^9} - \frac{3\langle B'',B'\rangle + \langle B''',B\rangle}{\|B\|^5}\right)det(B,B',B^{*''}) \\ + \left((-1 + \langle B,B'\rangle)\frac{3\langle B,B'\rangle^2}{\|B\|^9}(\|B'\|^2 + \langle B'',B\rangle) + (1 - \langle B,B'\rangle)\frac{3(\|B'\|^2 + \langle B'',B\rangle)^2}{\|B\|^7}\right)det(B,B',B^{*'}) \\ + \left(\frac{\langle B^*,B''\rangle + 2\langle B^{*'},B'\rangle + \langle B,B^{*''}\rangle}{\|B\|^5} - \frac{2\langle B,B'\rangle(\langle B^*,B'\rangle + \langle B^{*'},B\rangle)}{\|B\|^7} + \frac{7\langle B^*,B\rangle\langle B,B'\rangle^2}{\|B\|^9} - \frac{5\langle B^*,B\rangle(\|B'\|^2 + \langle B'',B\rangle)}{\|B\|^7}\right)det(B,B',B''') \\ + \left(\frac{3\langle B,B'\rangle^3}{\|B\|^9} + \frac{6\langle B,B'\rangle^2(\|B'\|^2 + \langle B'',B\rangle)}{\|B\|^7} - \frac{9\langle B,B'\rangle(\|B'\|^2 + \langle B'',B\rangle)}{\|B\|^7} + \frac{3(\|B'\|^2 + \langle B'',B\rangle)^2}{\|B\|^5}\right)det(B,B'',B^{*'}) \\ + \left(5\frac{\langle B,B'\rangle\langle B^*,B\rangle}{\|B\|^7} - \frac{(\langle B^*,B'\rangle + \langle B^{*'},B\rangle)}{\|B\|^7}\right)det(B,B',B''') - \frac{\langle B,B'\rangle}{\|B\|^5}det(B^*,B'',B''') \\ + \left(\frac{\langle B,B'\rangle^2}{\|B\|^7} - \frac{(\|B'\|^2 + \langle B'',B\rangle)}{\|B\|^5}\right)det(B',B^*,B''') - \frac{\langle B,B'\rangle}{\|B\|^5}det(B,B^{*'},B''') + \frac{det(B^{*'},B'',B''')}{\|B\|^3} \\ - \frac{\langle B,B'\rangle}{\|B\|^5}det(B,B'',B^{*'''}) + \left(\frac{\|B'\|^2 + \langle B'',B\rangle}{\|B\|^5} - \frac{\langle B,B'\rangle^2}{\|B\|^7}\right)det(B,B^{*'},B''') \end{bmatrix}}{\left\|\frac{1}{\|B\|^2}B' \times B'' + \left(\frac{\|B'\|^2 + \langle B'',B\rangle}{\|B\|^4} - \frac{\langle B,B'\rangle^2}{\|B\|^6}\right)B \times B' - \frac{\langle B,B'\rangle}{\|B\|^4}B \times B''\right\|^2} +$$

$$-2\frac{\left\langle \begin{pmatrix} \frac{det(B',B'',B''')}{\|B\|^3} - \frac{\langle B,B'\rangle}{\|B\|^5}det(B,B'',B''') \\ + \left(\left(2 - \frac{1}{\|B\|}\right)\left(\frac{3\langle B,B'\rangle\|B'\|^2}{\|B\|^7}\right)\right)det(B,B',B'') \\ + \left(2 - \frac{1}{\|B\|}\right)\left(\frac{3\langle B,B'\rangle\langle B'',B\rangle}{\|B\|^7}\right)det(B,B',B'') \\ - \frac{3\langle B'',B'\rangle + \langle B''',B\rangle}{\|B\|^5}det(B,B',B'') \\ + \left(2 - \frac{1}{\|B\|}\right)3\frac{\langle B,B'\rangle^3}{\|B\|^9}det(B,B',B'') \\ + \left(\frac{\|B'\|^2 + \langle B'',B\rangle}{\|B\|^5} - \frac{\langle B,B'\rangle^2}{\|B\|^7}\right)det(B,B',B''') \end{pmatrix}, \begin{pmatrix} \begin{bmatrix} \frac{(\langle B^*,B''\rangle + 2\langle B^{*'},B'\rangle + \langle B,B^{*''}\rangle)}{\|B\|^4} \\ + \frac{6\langle B^*,B\rangle\langle B,B'\rangle^2}{\|B\|^8} \\ - \frac{2\langle B,B'\rangle(\langle B^*,B'\rangle + \langle B^{*'},B\rangle)}{\|B\|^6} \\ - \frac{4\langle B^*,B\rangle(\|B'\|^2 + \langle B'',B\rangle)}{\|B\|^6} \end{bmatrix}B \times B' \\ + \frac{1}{\|B\|^2}B' \times B^{*''} - \frac{\langle B,B'\rangle}{\|B\|^4}B \times B^{*''} \\ + \left(\frac{\langle B,B'\rangle^2}{\|B\|^6} - \frac{(\|B'\|^2 + \langle B'',B\rangle)}{\|B\|^4}\right)B' \times B^* \\ + \left(\frac{\|B'\|^2 + \langle B'',B\rangle}{\|B\|^4} - \frac{\langle B,B'\rangle^2}{\|B\|^6}\right)B \times B^{*'} \\ + \left(\frac{4\langle B,B'\rangle\langle B^*,B\rangle}{\|B\|^6} - \frac{\langle B^*,B'\rangle + \langle B^{*'},B\rangle}{\|B\|^4}\right)B \times B'' \\ - \frac{2\langle B^*,B\rangle}{\|B\|^4}B' \times B'' \\ - \frac{\langle B,B'\rangle}{\|B\|^4}B^* \times B'' + \frac{1}{\|B\|^2}B^{*'} \times B'' \end{pmatrix}, \begin{bmatrix} \frac{1}{\|B\|^2}B' \times B'' + \\ + \left(\frac{\|B'\|^2 + \langle B'',B\rangle}{\|B\|^4}\right)B \times B' \\ - \frac{\langle B,B'\rangle}{\|B\|^4}B \times B'' \\ - \frac{\langle B,B'\rangle^2}{\|B\|^6}B \times B' \end{bmatrix}\right\rangle}{\left\|\frac{1}{\|B\|^2}B' \times B'' + \left(\frac{\|B'\|^2 + \langle B'',B\rangle}{\|B\|^4} - \frac{\langle B,B'\rangle^2}{\|B\|^6}\right)B \times B' - \frac{\langle B,B'\rangle}{\|B\|^4}B \times B''\right\|^3}\right]$$

Example:

Let a dual Bézier curve $\hat{B}(t)$ with control points $\hat{P}_0 = (-1,0,1) + \varepsilon(1,1,-1)$, $\hat{P}_1 = (1,2,0) + \varepsilon(0,-1,2)$, and $\hat{P}_1 = (2,-1,1) + \varepsilon(-1,2,1)$ be considered. So

$$B(t) = (-t^2 + 4t - 1, -5t^2 + 4t, 2t^2 - 2t + 1)$$

$$B^*(t) = (1 - 2t, 5t^2 - 4t + 1, -4t^2 + 6t - 1)$$

can be written. So the dual Bézier curve $\hat{B}(t)$ is formulated as

$$\hat{B}(t) = (-t^2 + 4t - 1, -5t^2 + 4t, 2t^2 - 2t + 1) + \varepsilon(1 - 2t, 5t^2 \\ - 4t + 1, -4t^2 + 6t - 1)$$

In this case the projection curve of $\hat{B}(t)$ on the dual unit sphere is

$$\tilde{B}(t) = \frac{(-t^2 + 4t - 1, -5t^2 + 4t, 2t^2 - 2t + 1)}{\sqrt{30t^4 - 56t^3 + 42t^2 - 12t + 2}} + \\ +\varepsilon \left(\frac{(1 - 2t, 5t^2 - 4t + 1, -4t^2 + 6t - 1)}{\sqrt{30t^4 - 56t^3 + 42t^2 - 12t + 2}} - \frac{(-33t^4 + 62t^3 - 48t^2 + 18t - 2)(-t^2 + 4t - 1, -5t^2 + 4t, 2t^2 - 2t + 1)}{(30t^4 - 56t^3 + 42t^2 - 12t + 2)\sqrt{30t^4 - 56t^3 + 42t^2}} \right)$$

The ruled surface corresponding this spherical projection curve is

$$X(t, \vartheta) = \frac{(30t^4 - 28t^3 + 14t^2 + 2t - 1, 4t^4 + 18t^3 - 23t^2 + 6t, -5t^4 + 14t^3 - 9t^2 + 4t - 1)}{30t^4 - 56t^3 + 42t^2 - 12t + 2} \\ + \vartheta \frac{(-t^2 + 4t - 1, -5t^2 + 4t, 2t^2 - 2t + 1)}{\sqrt{30t^4 - 56t^3 + 42t^2 - 12t + 2}}$$

These curves are sketched in Fig.2. According to E. Study's theorem the projection curve corresponds to a ruled surface in R^3 space. (See Fig.1)
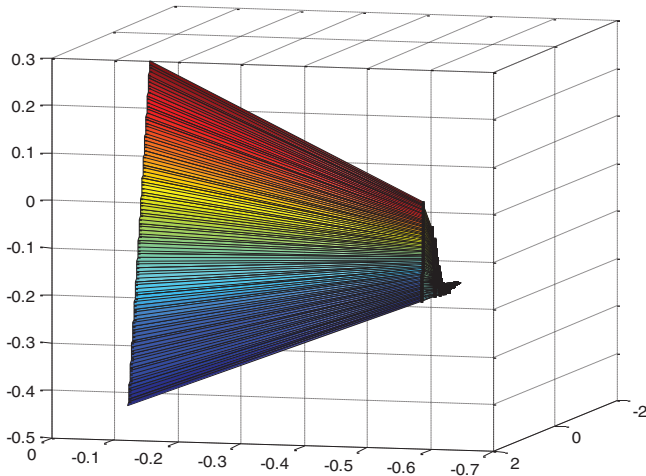

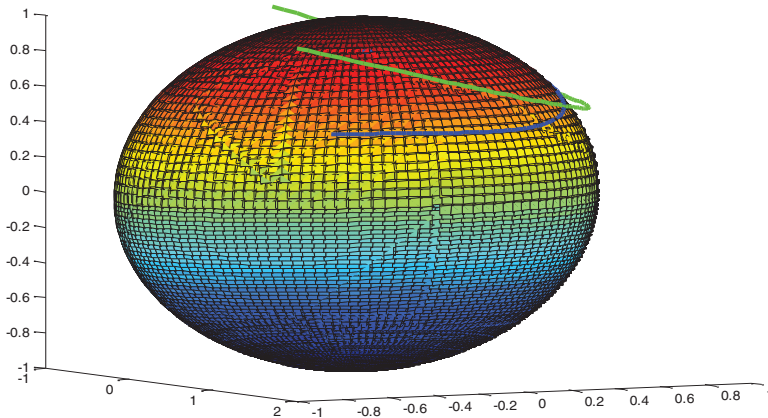Figure 1: The ruled surface corresponding dual spherical curve $\tilde{B}$

Figure 2: The representative graphics of the dual Bézier curve $\hat{B}(t)$ and projection $\tilde{B}$ of it to dual unit sphere

Let the derivatives and Frenet frame be calculated at the point $\tilde{B}(t = 0)$.

$B(t) = (-t^2 + 4t - 1, -5t^2 + 4t, 2t^2 - 2t + 1)$ $B(t = 0) = (-1,0,1)$ $\|B(t = 0)\| = \sqrt{2}$

$B^*(t) = (1 - 2t, 5t^2 - 4t + 1, -4t^2 + 6t - 1)$ $B^*(t = 0) = (1,1,-1)$ $\langle B, B^* \rangle = -2$

$B'(t) = (-2t + 4, -10t + 4, 4t - 2)$ $B'(t = 0) = (0,4,-2)$ $\|B'(t = 0)\| = \sqrt{20}$

$B^{*'}(t) = (2t, 10t - 4, -8t + 6)$ $B^{*'}(t = 0) = (0,-4,6)$ $\langle B, B^{*'} \rangle = 6$ $\langle B, B' \rangle = -2$

$B''(t) = (-2, -10, 4)$ $\langle B, B'' \rangle = 6$

$\langle B', B^{*'} \rangle = -28$ $\langle B^*, B'' \rangle = -16$

$B^{*''}(t) = (2, 10, -8)$ $B^{*''}(t = 0) = (2,10,-8)$

$\langle B, B^{*''} \rangle = -10$ $\langle B^{*''}, B' \rangle = 56$

$B'''(t) = 0$ $\langle B^*, B' \rangle = 6,$ $B \times B'' = (10,2,10)$

$B \times B^{*'} = (4,6,4)$

$B^{*'''}(t) = 0$ $B^{*'} \times B'' = (44, -12, -8)$ $B^* \times B'' = (-6, -2, -8)$ $B \times B' = (-1, 0, -1)$

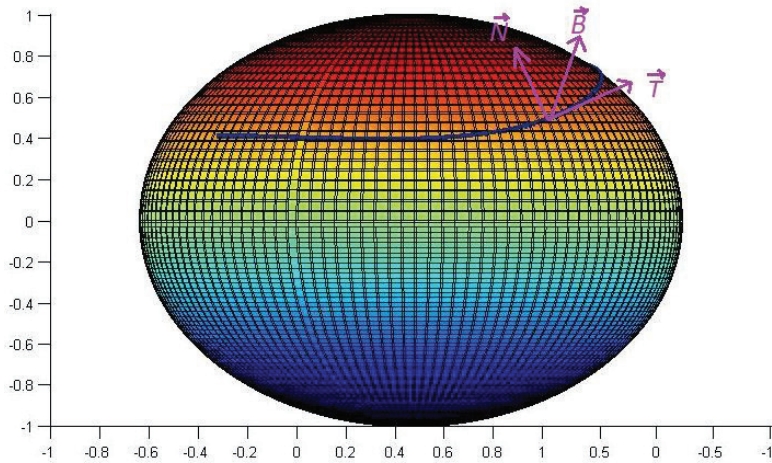$\langle B^{*'}, B'' \rangle = 64,$ $\langle B', B'' \rangle = -48$

Figure 3: The Frenet Frame on the dual spherical projection curve $\tilde{B}$

$$\tilde{B}'(t = 0) = \frac{1}{\sqrt{2}}[(-1,4,-1) + \varepsilon(-2,1,6)]$$

$$\tilde{B}''(t = 0) = \frac{1}{\sqrt{2}}[(8,-2,-10) + \varepsilon(9,-74,11)]$$

$$\tilde{B}' \times \tilde{B}''(t = 0) = (-21,-9,-15) + \varepsilon(-14,15,17)$$

$$\tilde{B}'''(t = 0) = \frac{1}{\sqrt{2}}[(-210,-150,276) + \varepsilon(-57,396,333)]$$

$$\left\|\tilde{B}' \times \tilde{B}''\right\|(t = 0) = 3\sqrt{83} - \varepsilon\frac{32}{\sqrt{83}}$$

$$\left\|\tilde{B}'(t = 0)\right\| = 3 + \varepsilon.0 = 3$$

$$det(\tilde{B}',\tilde{B}'',\tilde{B}''')(t = 0) = \frac{1}{\sqrt{2}}\left(1620 - \varepsilon(1980)\right)$$

The Frenet Frame at the point t=0 is:

$$\boldsymbol{T} = \frac{1}{3\sqrt{2}}[(-1,4,-1) + \varepsilon(-2,1,6)]$$

$$B = \frac{(-21,-9,-15) + \varepsilon(-14,15,17)}{3\sqrt{83} - \varepsilon\dfrac{32}{\sqrt{83}}}$$

$$= \frac{1}{3\sqrt{83}}(-21,-9,-15)$$

$$+ \varepsilon\left[\frac{32}{747\sqrt{83}}(-21,-9,-15) + \frac{1}{3\sqrt{83}}(-14,15,17)\right]$$

$$N = B \times T = \frac{32}{2241\sqrt{166}}(69,-6,-93)$$

$$+ \varepsilon\left[\frac{1}{9\sqrt{166}}(-39,156,-39)\right.$$

$$\left. + \frac{1}{1422\sqrt{166}}(-20059,-8311,-13185)\right]$$

$$\kappa = \frac{3\sqrt{83} - \varepsilon\dfrac{32}{\sqrt{83}}}{27} = \frac{\sqrt{83}}{9} - \varepsilon\frac{32}{27\sqrt{83}}$$

$$\tau = \frac{\dfrac{1}{\sqrt{2}}(1620 - \varepsilon(1980))}{\left(3\sqrt{83} - \varepsilon\dfrac{32}{\sqrt{83}}\right)^2} = \frac{(1620 - \varepsilon(1980))}{\sqrt{2}(747 - \varepsilon192)}$$

$$= \frac{(1620 - \varepsilon(1980))(747 + \varepsilon192)}{558009\sqrt{2}}$$

$$= \frac{1210140}{558009\sqrt{2}} - \varepsilon\frac{1168020}{558009\sqrt{2}}$$

References

Ayyildiz N., Coken A.C., Yucesan A., (2007) A charecterization of Dual Lorentzian Spherical Curves in the Dual Lorentzian Space, Taiwanese Journal of Mathematics, 11(4), 999-1018

Clifford, W. K. (1873) Preliminary sketch of bi-quaternions. Proceedings of the London Mathematical Society, s1–4(1):381–395.

Choi B.K.,(1991) Surface Modeling for CAD/CAM, Elsevier Science Publishers B.V., Amsterdam.

Divjak, Blaženka, and Zcaron Milin-Šipuš. (2002) "Special curves on ruled surfaces in Galilean and pseudo-Galilean spaces." *Acta Mathematica Hungarica* 98.3: 203-215.

Emilija Nešović , Ufuk Öztürk , Esra B. Koç Öztürk , Kazım İlarslan, (2016) On ruled surfaces with pseudo null base curve in Minkowski 3-space, *Int. Electron. J. Geom.* **9**(2) 9–20.

Gray A., (1998) Modern Differential Geometry of curves and surfaces with Mathematica, 2nd edition, CRC Press LCC, Boca Raton, Florida.

GURSOY, O . (1990a), The Dual Angle of A Closed Ruled Surface, Mech. Mach. Theory , 25 (2), 131-1 40.

GURSOY, O. (1990b), On Integral Invariant of A Closed Ruled Surface, Journal of Geometry, vol.39, 80-91.

GURSOY, O. (1992), Some Results on Closed Ruled Surfaces and Closed space Curves Mech. Mach. Theory, 27, 323-330

GURSOY, O., Küçük A. (1999), On the Invariants of Trajectory Surfaces, Mech. Mach. Theory,34, 587-597.

GURSOY ,O., Küçük A., (2004) On the Invariants of Bertrand Trajectory Surfaces Offsets, Applied Mathematics and Computation , 151(3), 763-773.

Guven I.A, Nurkan S.K. and Karacan M.K., (2014) Ruled Weingarten Surfaces Related to Dual Spherical Curves, Gen. Math. Notes, 24 (2), 10-17.

Güler F. and E. Kasap, (2018) A path planning method for robot end effector motion using the curvature theory of the ruled surfaces, *Int. J. Geom. Meth. Mod. Phys.* **15** 1850048.

Hacısaliholu H. H., On the pitch of a ruled surface, *Mech. Mach. Theory*, Great Britain **7** (1972) 291–305, doi: 10.1016/0094-114X(72)90039-0.

Hacısalihoğlu, H. H. (1983). *Hareket geometrisi ve kuaterniyonlar teorisi*. Gazi Üniversitesi.

Hathout F., M. Bekar and Y. Yaylı, (2017) Ruled surfaces and tangent bundle of unit 2-sphere, *Int. J. Geom. Meth. Mod. Phys.* **14** 1750145.

Hoschek J., (1985) Offset curves in the plane, Computer Aided Design, 17, 2 , 77-82.

Incesu, M., Gursoy, O. (2004). Bézier Yüzeylerinde Esas Formlar ve Eğrilikler. *XVII Ulusal Matematik Sempozyumu*, 146-157.

Incesu Muhsin, (2021) The new characterization of Ruled surfaces corresponding Dual Bézier curves, Mathematical Methods in the Applied Sciences, MMA7398, 17038625, doi: https://doi.org/10.1002/mma.7398

Incesu M., Gürsoy O., (2018) On the Bertrand Dual Curve Pairs, INTERNATIONAL CONFERENCE ON MATHEMATICS "An Istanbul Meeting for World Mathematicians" Minisymposium on Approximation Theory & Minisymposium on Math Education 3-6 July 2018, İstanbul, Turkey pp: 149-154

Kazaz M, Özdemir A, Güroğlu T. (2008) On the determination of a developable timelike ruled surface. SDÜ Fen-Edebiyat Fakültesi Fen Dergisi (E-Dergi); 3(1): 72-79

Küçük A. (2004) On the developable timelike trajectory ruled surfaces in Lorentz 3-space 3 1 IR . App Math and Comp; 157: 483-489

Liming R., (1944) Practical Analytic Geometry with Applications to Aircraft*,* Macmillan.

Mavroidis C. and Roth B., (1997) On the Geometry of Spatial Polygons and Screw Polygons, Journal of Mechanical Design Transactions of the ASME, 119, 246-252.

McCarthy J. M. and B. Roth, The curvature theory of line trajectories in spatial kinematics, *J. Mech. Design* **103**(4) (1981) 718–724, doi: 10.1115/1.3254978.

Müller H.R., Spharische Kinematik, VEB Deutscher Verlag der Wissenschaften, Berlin 1962.

Okullu P.B., Kocayigit H., Aydin T.A., (2019) An Explicit Characterization of Spherical curces according to Bishop Frame and Approximately Solutıon, Thermal Science, 23 (1), 361-370.

Potmann H., (1995) Rational curves and surfaces with rational offsets, Computer Aided Geometric Design, 12, 175-192.

Study E. (1891),Von den bewegungen und umlegungen. Mathematische Annalen, 39, 441–566.

Taş F., K. İlarslan (2019) A new approach to design the ruled surface, International Journal of Geometric Methods in Modern Physics Vol. 16, No. 6, 1950093 (16 pages)

Taş F., On the Design and Invariants of a Ruled Surface, https://arxiv.org/ftp/arxiv/papers/1706/1706.00267.pdf

Taş F., (2016) A method of determining dual unit spherical B´ezier curves and line surfaces,*J. Logic Math. Linguistics Appl. Sci.* **1** 1–6.

Taş F. and O. Gürsoy, (2018) On the line congruences, *Int. Electron. J. Geom.* **11**(2) 47–53.

Ting K.-L. and A. H. Soni, Instantaneous kinematics of a plane in spherical motion,*J. Mech. Transmissions, and Automation in Design* **105**(3) (1983) 560–567, doi:10.1115/1.3267395.

Tiller W. and Hanson E., (1984) Offsets of two- dimentional profiles, IEEE Computer Graphics and Applications, 4, 36-46.

Yayli,Y. Saracoglu S.,(2011) Some Notes on Dual Spherical Curves, Journal of Informatics and Mathematical Sciences, 3(2),177-189.

Yayli,Y. Saracoglu S.,(2011) Ruled Surface and Dual Spherical Curves, Acta Universitatis Apulensis, No.30/2012, 337-354.

Zha, X. F. (1997) A new approach to generation of ruled surfaces and its applications in engineering, *Int. J. Adv. Manuf. Technol.* **13** 155–163, doi: 10.1007/BF01305867.